frontiers | Research Topics

New insights into the influences of soil nutrients on plant-fungal symbiosis in agro- and forest ecosystems

Edited by
Kai Sun, Fangdong Zhan, Yu Shi, Jiayu Zhou and Jun Zhou

Published in
Frontiers in Microbiology

ISSN 1664-8714
ISBN 978-2-8325-3140-2
DOI 10.3389/978-2-8325-3140-2

About Frontiers

Frontiers is more than just an open access publisher of scholarly articles: it is a pioneering approach to the world of academia, radically improving the way scholarly research is managed. The grand vision of Frontiers is a world where all people have an equal opportunity to seek, share and generate knowledge. Frontiers provides immediate and permanent online open access to all its publications, but this alone is not enough to realize our grand goals.

Frontiers journal series

The Frontiers journal series is a multi-tier and interdisciplinary set of open-access, online journals, promising a paradigm shift from the current review, selection and dissemination processes in academic publishing. All Frontiers journals are driven by researchers for researchers; therefore, they constitute a service to the scholarly community. At the same time, the *Frontiers journal series* operates on a revolutionary invention, the tiered publishing system, initially addressing specific communities of scholars, and gradually climbing up to broader public understanding, thus serving the interests of the lay society, too.

Dedication to quality

Each Frontiers article is a landmark of the highest quality, thanks to genuinely collaborative interactions between authors and review editors, who include some of the world's best academicians. Research must be certified by peers before entering a stream of knowledge that may eventually reach the public - and shape society; therefore, Frontiers only applies the most rigorous and unbiased reviews. Frontiers revolutionizes research publishing by freely delivering the most outstanding research, evaluated with no bias from both the academic and social point of view. By applying the most advanced information technologies, Frontiers is catapulting scholarly publishing into a new generation.

What are Frontiers Research Topics?

Frontiers Research Topics are very popular trademarks of the *Frontiers journals series*: they are collections of at least ten articles, all centered on a particular subject. With their unique mix of varied contributions from Original Research to Review Articles, Frontiers Research Topics unify the most influential researchers, the latest key findings and historical advances in a hot research area.

Find out more on how to host your own Frontiers Research Topic or contribute to one as an author by contacting the Frontiers editorial office: frontiersin.org/about/contact

New insights into the influences of soil nutrients on plant-fungal symbiosis in agro- and forest ecosystems

Topic editors

Kai Sun — Nanjing Normal University, China

Fangdong Zhan — Yunnan Agricultural University, China

Yu Shi — Henan University, China

Jiayu Zhou — Institute of Botany, Jiangsu Province and Chinese Academy of Sciences, China

Jun Zhou — University of York, United Kingdom

Topic coordinator

Long Peng — Research Institute of Subtropical Forestry, Chinese Academy of Forestry, China

Citation

Sun, K., Zhan, F., Shi, Y., Zhou, J., Zhou, J., eds. (2023). *New insights into the influences of soil nutrients on plant-fungal symbiosis in agro- and forest ecosystems*. Lausanne: Frontiers Media SA. doi: 10.3389/978-2-8325-3140-2

Table of contents

frontiers | Frontiers in Microbiology

TYPE Editorial
PUBLISHED 18 July 2023
DOI 10.3389/fmicb.2023.1237534

OPEN ACCESS

EDITED AND REVIEWED BY
Trevor Carlos Charles,
University of Waterloo, Canada

*CORRESPONDENCE
Kai Sun
✉ sunkainnu@sina.cn

RECEIVED 09 June 2023
ACCEPTED 05 July 2023
PUBLISHED 18 July 2023

CITATION
Sun K, Zhan FD, Shi Y, Zhou JY, Zhou J and Peng L (2023) Editorial: New insights into the influences of soil nutrients on plant-fungal symbiosis in agro- and forest ecosystems. *Front. Microbiol.* 14:1237534.
doi: 10.3389/fmicb.2023.1237534

Editorial: New insights into the influences of soil nutrients on plant-fungal symbiosis in agro- and forest ecosystems

Kai Sun [1]*, Fang-Dong Zhan[2], Yu Shi[3,4,5], Jiayu Zhou[6], Jun Zhou [7] and Long Peng[8]

[1]Jiangsu Key Laboratory for Microbes and Functional Genomics, Jiangsu Engineering and Technology Research Center for Industrialization of Microbial Resources, College of Life Sciences, Nanjing Normal University, Nanjing, Jiangsu, China, [2]College of Resources and Environment, Yunnan Agricultural University, Kunming, China, [3]State Key Laboratory of Crop Stress Adaptation and Improvement, School of Life Sciences, Henan University, Kaifeng, China, [4]Henan Dabieshan National Field Observation and Research Station of Forest Ecosystem, Zhengzhou, China, [5]Xinyang Academy of Ecological Research, Xinyang, China, [6]Institute of Botany, Jiangsu Province and Chinese Academy of Sciences, Nanjing, China, [7]Chrono-Environnement UMR 6249, CNRS, Université Bourgogne Franche-Comté, Besançon, France, [8]Research Institute of Subtropical Forestry, Chinese Academy of Forestry, Hangzhou, China

KEYWORDS

soil nutrient availability, nutrient forms, symbiotic fungi, arbuscular mycorrhizal fungi, fungal endophyte, fungal community, plant-fungal symbiosis, agroecosystem and forest ecosystem

Editorial on the Research Topic
New insights into the influences of soil nutrients on plant-fungal symbiosis in agro- and forest ecosystems

Symbiotic fungi are widely distributed and form associations with over 90% of terrestrial plant species, playing an essential role in global agro- and forest ecosystems (Behie and Bidochka, 2014). These symbionts provide various benefits to host plants, including increased biomass accumulation (Hiruma et al., 2016), enhanced nutrient uptake (Guether et al., 2009; Fochi et al., 2017), and improved environmental adaptation (Sui et al., 2019). In return, host plants offer suitable habitats and accessible photosynthate for fungal survival and reproduction (Siegel et al., 1987; Jiang et al., 2017). However, in natural ecosystems, plant-fungal symbioses often face changing soil conditions, particularly variations in nutrient status (Sun et al., 2020, 2022). Different nutrient availabilities, forms, and compositions can significantly affect plant metabolism, growth, and immunity, which are crucial for maintaining the interplay between plants and fungi (Saikkonen et al., 2004; Sánchez-Bel et al., 2018). Conversely, soil nutrient status can influence the community composition of soil fungi, thereby impacting the establishment of symbionts.

The goal of this Research Topic is to showcase the latest studies focusing on the global effects of soil nutrients on plant-fungi interactions, enhancing our understanding of the mechanisms underlying the colonization and community dynamics of symbiotic fungi during their interaction with host plants across various species/genotypes, soil types, and nutrient levels and forms. The Research Topic covers studies on arbuscular mycorrhizal fungi (AMF), fungal endophytes and the plant-associated fungal community.

Insights into the impact of soil nutrients on AMF symbiosis

Ancient AMF symbioses can be seen as the bridge between plants and soils (Saia and Jansa, 2022; Kuyper and Jansa, 2023). The AMF symbionts are influenced by the forms and levels of nutrients in the soil, including nitrogen (N), phosphorus (P), and potassium (K). Yu et al. pointed out that AMF are sensitive to N addition over short timescales (1 year). Beneficial AMF associations are promoted under N-deficient conditions (Bonfante and Genre, 2010; Sanchez-Bel et al., 2016; Sánchez-Bel et al., 2018). Additionally, ammonium reduced AMF colonization levels in numerous plant species compared to nitrate (Pattinson et al., 2000).

Two noteworthy perspectives highlight the important roles of AMF symbiosis in plant invasion in agro-ecosystems based on greenhouse experiments. Du et al. revealed that the AMF *Septoglomus constrictum* provides host plants with higher N and P accumulation, conferring invasive plants with greater advantages over native congeners. Chen et al., through the analysis of AMF community associated with the invasive species *Solidago canadensis* and its native congener *S. decurrens*, clarified that AMF could confer invasive plants with greater advantages over native congeners, dependent on the forms of P in the soil.

Inorganic orthophosphate (Pi) is the available form of P that plants can acquire and utilize. However, Pi is often insufficient in the field due to its low solubility and relative immobilization (Nagy et al., 2009). Under P starvation, AMF can efficiently promote Pi uptake and homeostasis in host plants (Dierks et al., 2021). In this Research Topic, Zhang et al. identify a HLH domain containing transcription factor, *RiPho4*, from *Rhizophagus irregularis*. Through subcellular localization, yeast one-hybrid experiments, and using virus-induced gene silencing approaches, the authors demonstrated that *RiPho4* acts as a transcriptional activator in AMF to maintain arbuscule development and regulate Pi uptake in host plants during Pi starvation. This study provides new insights into the mechanisms underlying how AMF regulates Pi uptake in host plants under Pi deficiency.

Apart from N and Pi, the AMF-plant interaction is also sensitive to changes in soil K nutrient (Han et al., 2023). In a greenhouse experiment, Yuan et al. investigated sweet potato (*Ipomoea batatas* (L.) Lam.]), a versatile crop with high K requirements for enhanced yield. Their study showed that K application and the presence of AMF *Claroideoglomus etunicatum* exhibited a synergistic effect on the root development and K acquisition of the "Xu28" variety of sweet potato, which has high K use efficiency, resulting in significant yield promotion. These results, combined with previous studies, expand our knowledge of the influences of soil nutrients on plant-AMF symbiosis.

Impact of heavy metal contamination on plant-fungal interactions

Heavy metal contamination in soil is a pressing global issue (Marrugo-Negrete et al., 2017) that affects plant-fungal interactions (Motaharpoor et al., 2019). Dark septate endophytes (DSEs) are ubiquitous colonizers of plant roots in various terrestrial ecosystems, often found in stressful environments, especially heavy metal-polluted soils (Su et al., 2021). Wang et al. highlighted the ability of *Exophiala pisciphila* H93, a beneficial dark septate endophyte which colonizes maize roots, to withstand cadmium exposure without compromising its growth-promotion effect on maize. They found that H93 colonization enhances plant resistance to heavy metal by influencing the expression of genes involved in signal transduction, hormonal pathway, and glutathione metabolism.

Influence of soil nutrients on plant-associated fungal communities

The response of the plant-associated fungal community to global changes plays a crucial role in understanding carbon and N cycling processes in agro- and forest ecosystems (Falkowski et al., 2008). In this Research Topic, Yu et al. demonstrated that the interaction between N addition and rainfall patterns has significant effects on soil fungal diversity in a grassland ecosystem. Similarly, Zhao et al. showed in a forest ecosystem that climate factors, such as temperature and precipitation, significantly influence dominant fungal genera and functional guilds in soil, particularly ectomycorrhizal fungi. Furthermore, fungal diversity and composition are strongly influenced by seasonal variation in soil nutrients, including total N and available P. The effect of vegetation type on rhizosphere microbes is also of great interest across different ecosystems. Liu et al. compared fungal communities in the rhizosphere of three typical vegetation types (herb, shrubs, and arbors). They discovered that the fungal community structure in the rhizosphere can vary across vegetation types and is primarily governed by deterministic processes. Additionally, plant metabolism has a significant impact on the plant-associated microbiome (Trivedi et al., 2020). Zhu et al. demonstrated that by applying exogenous salicylic acid, beneficial rhizosphere microorganisms were selectively enriched to enhance watermelon resistance to *Fusarium* wilt. These community analyses provide insights into the potential of plant-associated fungi in sustainable agriculture.

In this Research Topic, the majority of the studies aimed to elucidate the influences of changing environmental conditions, particularly soil nutrients, on plant-fungal symbiosis. However, more efforts are needed to clarify the molecular mechanisms underlying how nutrient factors drive the maintenance and breakdown of plant-fungi symbionts. Additionally, limited studies have been conducted under field conditions, which could provide better guidance for agricultural production. We anticipate further novel discoveries in the future.

Author contributions

KS wrote the manuscript. All authors reviewed and revised the manuscript.

Funding

KS was funded by the Jiangsu Funding Program for Excellent and Postdoctoral Talent (2022ZB357) and China Postdoctoral Science Foundation (2021M701748). FDZ was funded by the National Natural Science Foundation of China (42177381 and 42267002) and the expert workstation of Longhua Wu in Yunnan Province (202305AF150042). YS was funded by the Natural Science Foundation of Henan (222300420035) and Xinyang Academy of Ecological Research Open Foundation (2023DBS09). JYZ was funded by the Open Fund of Jiangsu Key Laboratory for the Research and Utilization of Plant Resources (JSPKLB201926). JZ was funded by the project of Sustainable Innovations for Regenerative Agriculture in the Mediterranean area-SIRAM (ANR-22-PRIM-0001).

Acknowledgments

The guest editors thank Dr. Madeleine Berger and Dr. Fabian Vaistij (University of York, UK) for proofreading the manuscript. The guest editors are heart fully thanks the reviewers in their aid helping this Research Topic.

Conflict of interest

The authors declare that the research was conducted in the absence of any commercial or financial relationships that could be construed as a potential conflict of interest.

Publisher's note

All claims expressed in this article are solely those of the authors and do not necessarily represent those of their affiliated organizations, or those of the publisher, the editors and the reviewers. Any product that may be evaluated in this article, or claim that may be made by its manufacturer, is not guaranteed or endorsed by the publisher.

References

Behie, S. W., and Bidochka, M. J. (2014). Nutrient transfer in plant-fungal symbioses. *Trends Plant. Sci.* 19, 734–740. doi: 10.1016/j.tplants.2014.06.007

Bonfante, P., and Genre, A. (2010). Mechanisms underlying beneficial plant-fungus interactions in mycorrhizal symbiosis. *Nat. Commun.* 1, 48. doi: 10.1038/ncomms1046

Dierks, J., Blaser-Hart, W. J., Gamper, H. A., Nyoka, I. B., and Six, J. (2021). Trees enhance abundance of arbuscular mycorrhizal fungi, soil structure, and nutrient retention in low-input maize cropping systems. *Agric. Ecosyst. Environ.* 318, 107487. doi: 10.1016/j.agee.2021.107487

Falkowski, P. G., Fenchel, T., and Delong, E. F. (2008). The microbial engines that drive Earth's biogeochemical cycles. *Science.* 320, 1034–1039. doi: 10.1126/science.1153213

Fochi, V., Chitarra, W., Kohler, A., Voyron, S., Singan, V. R., Lindquist, E. A., et al. (2017). Fungal and plant gene expression in the *Tulasnella calospora-Serapias vomeracea* symbiosis provides clues about nitrogen pathways in orchid mycorrhizas. *New Phytol.* 213, 365–379. doi: 10.1111/nph.14279

Guether, M., Balestrini, R., Hannah, M., He, J., Udvardi, M. K., and Bonfante, P. (2009). Genome-wide reprogramming of regulatory networks, transport, cell wall and membrane biogenesis during arbuscular mycorrhizal symbiosis in *Lotus japonicus*. *New Phytol.* 182, 200–212. doi: 10.1111/j.1469-8137.2008.02725.x

Han, S., Wang, X., Cheng, Y., Wu, G., Dong, X., He, X., et al. (2023). Multidimensional analysis reveals environmental factors that affect community dynamics of arbuscular mycorrhizal fungi in poplar roots. *Front. Plant Sci.* 13, 1068527. doi: 10.3389/fpls.2022.1068527

Hiruma, K., Gerlach, N., Sacristán, S., Nakano, R. T., Hacquard, S., Kracher, B., et al. (2016). Root endophyte *Colletotrichum tofieldiae* confers plant fitness benefits that are phosphate status dependent. *Cell* 165, 464–474. doi: 10.1016/j.cell.2016.02.028

Jiang, Y., Wang, W., Xie, Q., Liu, N., Liu, L., Wang, D., et al. (2017). Plants transfer lipids to sustain colonization by mutualistic mycorrhizal and parasitic fungi. *Science* 356, 1172–1175. doi: 10.1126/science.aam9970

Kuyper, T. W., and Jansa, J. (2023). Arbuscular mycorrhiza: advances and retreats in our understanding of the ecological functioning of the mother of all root symbioses. *Plant Soil.* doi: 10.1007/s11104-023-06045-z

Marrugo-Negrete, J., Pinedo-Hernández, J., and Díez, S. (2017). Assessment of heavy metal pollution, spatial distribution and origin in agricultural soils along the Sinú River Basin, Colombia. *Environ. Res.* 154, 380–388. doi: 10.1016/j.envres.2017.01.021

Motaharpoor, Z., Taheri, H., and Nadian, H. (2019). *Rhizophagus irregularis* modulates cadmium uptake, metal transporter, and chelator gene expression in *Medicago sativa*. *Mycorrhiza*. 29, 389–395. doi: 10.1007/s00572-019-00900-7

Nagy, R., Drissner, D., Amrhein, N., Jakobsen, I., and Bucher, M. (2009). Mycorrhizal phosphate uptake pathway in tomato is phosphorus-repressible and transcriptionally regulated. *New Phytol.* 181, 950–959. doi: 10.1111/j.1469-8137.2008.02721.x

Pattinson, G. S., Sutton, B. G., and Mcgee, P. A. (2000). Leachate from a waste disposal centre reduces the initiation of arbuscular mycorrhiza, and spread of hyphae in soil. *Plant Soil.* 227, 35–45. doi: 10.1023/A:1026519527211

Saia, S., and Jansa, J. (2022). Editorial: Arbuscular mycorrhizal fungi: the bridge between plants, soils, and humans. *Front. Plant Sci.* 13, 875958. doi: 10.3389/fpls.2022.875958

Saikkonen, K., Wäli, P., Helander, M., and Faeth, S. H. (2004). Evolution of endophyte-plant symbioses. *Trends Plant Sci.* 9, 275–280. doi: 10.1016/j.tplants.2004.04.005

Sánchez-Bel, P., Sanmartín, N., Pastor, V., Mateu, D., Cerezo, M., Vidal-Albalat, A., et al. (2018). Mycorrhizal tomato plants fine tunes the growth defence balance upon N depleted root environments. *Plant Cell. Environ.* 41, 406–420. doi: 10.1111/pce.13105

Sanchez-Bel, P., Troncho, P., Gamir, J., Pozo, M. J., Camañes, G., Cerezo, M., et al. (2016). the nitrogen availability interferes with mycorrhiza-induced resistance against *Botrytis cinerea* in tomato. *Front. Microbiol.* 7, 1598. doi: 10.3389/fmicb.2016.01598

Siegel, M. R., Latch, G. C. M., and Johnson, M. C. (1987). Fungal endophytes of grasses. *Annu. Rev. Ecol. Evol. Syst.* 15, 462e468. doi: 10.1146/annurev.py.25.090187.001453

Su, Z. Z., Dai, M. D., Zhu, J. N., Liu, X. H., Li, L., Zhu, X. M., et al. (2021). Dark septate endophyte *Falciphora oryzae*-assisted alleviation of cadmium in rice. *J. Hazard. Mater.* 419, 126435. doi: 10.1016/j.jhazmat.2021.126435

Sui, X. L., Zhang, T., Tian, Y. Q., Xue, R. J., and Li, A. R. (2019). A neglected alliance in battles against parasitic plants: arbuscular mycorrhizal and rhizobial symbioses alleviate damage to a legume host by root hemiparaitic *Pedicularis* species. *New Phytol.* 221, 470–481. doi: 10.1111/nph.15379

Sun, K., Lu, F., Huang, P. W., Tang, M. J., Xu, F. J., Zhang, W., et al. (2022). Root endophyte differentially regulates plant response to NO_3^- and NH_4^+ nutrition by modulating N fluxes at the plant-fungal interface. *Plant Cell Environ.* 45, 1813–1828. doi: 10.1111/pce.14304

Sun, K., Zhang, W., Yuan, J., Song, S. L., Wu, H., Tang, M. J., et al. (2020). Nitrogen fertilizer-regulated plant-fungi interaction is related to root invertase-induced hexose generation. *FEMS Microbiol. Ecol.* 96, fiaa139. doi: 10.1093/femsec/fiaa139

Trivedi, P., Leach, J. E., Tringe, S. G., Sa, T., and Singh, B. K. (2020). Plant-microbiome interactions: from community assembly to plant health. *Nat. Rev. Microbiol.* 18, 607–621. doi: 10.1038/s41579-020-0412-1

frontiers | Frontiers in Microbiology

ORIGINAL RESEARCH
published: 28 June 2022
doi: 10.3389/fmicb.2022.906818

The Diversity and Function of Soil Bacteria and Fungi Under Altered Nitrogen and Rainfall Patterns in a Temperate Steppe

Yang Yu[1,2], *Lu Liu*[1,2], *Jianing Zhao*[1,2], *Shuchen Wang*[1,2], *Yijun Zhou*[1,2]* and *Chunwang Xiao*[1,2]*

[1] Key Laboratory of Ecology and Environment in Minority Areas, Minzu University of China, National Ethnic Affairs Commission, Beijing, China, [2] College of Life and Environmental Sciences, Minzu University of China, Beijing, China

The response of soil microorganisms to altered nitrogen (N) and rainfall patterns plays an important role in understanding ecosystem carbon and nitrogen cycling processes under global change. Previous studies have separately focused on the effects of N addition and rainfall on soil microbial diversity and community composition. However, the combined and interactive impact of N addition and rainfall on soil microbial diversity and function mediated by plant and soil processes have been poorly investigated for grassland ecosystems. Here, we conducted a field experiment with simulated N addition (N addition: 10 g N m^{-2} yr^{-1}) and altered rainfall pattern [control, rainfall reduction (compared to control –50%); rainfall addition (compared to control + 50%)] to study their interactive effects on soil microbial diversity and function in a temperate steppe of Inner Mongolia. Our results showed that N addition and rainfall addition significantly increased soil bacterial diversity, and the bacterial diversity was positively correlated with soil microbial biomass nitrogen, inorganic nitrogen, and *Stipa krylovii* root exudate C:N ratio, *Allium polyrhizum* root exudate C and N, and *A. polyrhizum* root exudate C:N ratio. N addition and rainfall reduction significantly reduced fungal diversity, which correlated closely with soil microbial biomass carbon and the C:N ratio of *A. polyrhizum* root exudates. Bacteria were mainly eutrophic r-strategists, and the responses of bacterial function guilds to the interaction between N addition and rainfall pattern were not significant. However, the arbuscular mycorrhizal fungi (AMF), in the functional classification of fungi, were significantly reduced under the condition of N addition and rainfall reduction, and the absolute abundance of the phylum Glomeromycota increased under rainfall addition, suggesting that AMFs are sensitive to altered N and rainfall patterns over short timescales (1 year). Collectively, our results have important implications for understanding the plant–soil–microbe system of grasslands under climate change.

Keywords: nitrogen addition, rainfall addition, rainfall reduction, bacterial diversity, fungal diversity, functional prediction, temperate steppe

OPEN ACCESS

Edited by:
José A. Siles, Center for Edaphology and Applied Biology of Segura (CSIC), Spain

Reviewed by:
Longyu Hou, Institute of Botany (CAS), China
Linna Ma, Institute of Botany (CAS), China

***Correspondence:**
Chunwang Xiao
cwxiao@muc.edu.cn
Yijun Zhou
zhouyijun@muc.edu.cn

Specialty section:
This article was submitted to Terrestrial Microbiology, a section of the journal Frontiers in Microbiology

Received: *29 March 2022*
Accepted: *29 April 2022*
Published: *28 June 2022*

Citation:
Yu Y, Liu L, Zhao J, Wang S, Zhou Y and Xiao C (2022) The Diversity and Function of Soil Bacteria and Fungi Under Altered Nitrogen and Rainfall Patterns in a Temperate Steppe. Front. Microbiol. 13:906818. doi: 10.3389/fmicb.2022.906818

INTRODUCTION

Due to the unreasonable use of resources and the burning of fossil fuels, atmospheric nitrogen (N) deposition has increased by 2–7 fold compared to pre-industrial revolution levels (Galloway et al., 2004). N deposition increased soil nitrogen content, which can affect the growth of plants, quality of grassland forage, and nutrient cycling within ecosystems (Waldrop et al., 2004; Turner and Henry, 2010). Meanwhile, due to natural factors and human activities, global rainfall patterns have also changed at different latitudes (Allen et al., 2018). Previous studies have shown water availability is an important factor limiting the productivity of arid and semi-arid grasslands (Füzy et al., 2008); furthermore, the grassland of Inner Mongolia is an area that is more sensitive to rainfall. Therefore, a better understanding of the impact of climate change on the grassland ecosystem could be gained from studying the interaction between N addition and rainfall.

As decomposers, the diversity, composition, and function of soil microorganisms correlate closely with the biogeochemical cycles and homeostasis of ecosystems (Bardgett and Putten, 2014; Fierer, 2017; Tian et al., 2021). N deposition enhanced the photosynthetic capacity of plants (Wang et al., 2012), leading to an increase in plant biomass and the quantity of plant litter, and then acting as a sufficient nutrient source for soil microorganisms and affecting microbial diversity, community structure, and function. Previous studies have shown that N deposition increased the competition among plant species and decreased plant species diversity, thus affecting the food source and living microenvironments of soil microorganisms and resulting in the variation of soil microbial diversity (Fierer and Jackson, 2006; Fierer et al., 2007; Rousk et al., 2010). The variation of rainfall is an important factor affecting global climate change (Liu et al., 2013; Marvel and Bonfils, 2013). Rainfall addition increases soil moisture and affects the relative abundance of soil fungi and Gram-negative bacteria, resulting in altered bacteria: fungi ratios, which further impact the bacteria and fungi that participate in soil carbon and nitrogen cycling (Williams and Rice, 2007). Also, Jie et al. (2011) have documented that changes in rainfall patterns influence soil N availability. In brief, N and water are two important factors that limit soil microbial activity in the grasslands of northern China (Zhang et al., 2015). A previous study showed that precipitation was an important environmental factor affecting soil microbial carbon utilization profiles based on BIOLOG carbon substrate utilization under N addition (Sun et al., 2015). However, the functional classification of microorganisms involved in carbon cycling is still insufficient. Plants secrete a variety of root exudates during the process of growth, and these exudates act as the interaction medium between plants and microorganisms. The composition of root exudates is known to affect the soil microbial diversity and function (Baudoin et al., 2003). However, the mechanism by which the C:N ratio of root exudates affects soil microbe is still unclear. Understanding the C:N ratio of root exudates lays a foundation for explaining how plant–soil–microbial interactions play significant roles in ecosystem processes, such as carbon and nitrogen nutrient cycling.

Liang et al. (2020) have reported long-term fertilization significantly changed the composition of soil microbial community, which in turn affects the functional characteristics of the community (Fukami, 2015). It was reported that Proteobacteria, Acidobacteria, and Actinobacteria dominated the bacterial communities in the typical steppe of northern China, and that the fungal community was mainly composed of Ascomycota, Basidiomycota, and Glomeromycota (Yu et al., 2021a). Actinobacteria, Proteobacteria, and Bacteroidetes are classified as r-strategists, mainly decomposing labile C, while most Acidobacteria are classified as K-strategists and decompose recalcitrant C (Sun et al., 2021). However, it is not clear whether N addition, rainfall, and their interaction are dominated by r-strategist bacteria and accelerated soil carbon and nitrogen cycling. At present, the effects of fertilization on fungal functional groups mainly focused on arbuscular mycorrhizal fungi (AMF). AMF play important roles in plant growth, by providing multiple nutrients and assisting the host plants to resist pathogen invasion. Chen et al. (2017) have found that fertilization has decreased AMF α-diversity and altered community composition and phylogenetic patterns, suggesting that environmental factors are important driving forces of AMF community assembly. Nevertheless, the effect of interaction between N addition and rainfall on fungal functional classification is still unknown.

In order to understand how microbial diversity and function are affected by altering N and rainfall patterns, we conducted a short-term (1 year) field N addition and rainfall interaction experiment in a temperate steppe of Inner Mongolia. The main objectives of this study were (1) to assess the effects of N addition, rainfall, and their interaction on soil microbial diversity and community composition, and to confirm whether the community composition mainly belongs to r-strategists, and (2) to examine the functions of soil microorganisms in response to N addition, rainfall, and their interaction. Since bacteria are more sensitive to changes in soil moisture than fungi (Gordon et al., 2008), we hypothesized that N and rainfall interaction would (i) increase soil bacterial diversity, while not affecting fungal diversity; (ii) may increase the soil inorganic nitrogen content and soil water content and create sufficient food sources that, in turn, will increase bacterial diversity and affect bacterial community composition, mainly belonging to r-strategies; and (iii) the increased soil nutrient input will accelerate soil bacterial cycling of soil carbon and nitrogen, and enhance the functional classes of microorganisms involved in soil carbon and nitrogen cycling. Thus, the interaction between N and rainfall may increase the relative abundance of the AMF.

MATERIALS AND METHODS

Site Description

We conducted a field experiment in a temperate steppe at the Hulun Lake Reserve in Inner Mongolia (113.21°E, 48.75°N), China. This site is located in a temperate zone with a mean annual temperature of –0.4°C and mean annual precipitation of 283 mm, respectively. The mean temperature was 1.8°C, and the precipitation during the growing season was 169 mm in

2018. The soil is classified as Calcic Luvisols (FAO, 1957). The vegetation is dominated by perennial species, primarily *Stipa krylovii* and *Allium polyrhizum*.

Experimental Design

The experimental design has been described in detail by Li C. et al. (2021). In brief, the experiment used a factorial, nested design with rainfall treatment [control, reduction (–50%), and addition (+ 50%)] and nitrogen (N) treatments (control and addition). Each treatment had five replicate blocks, for a total of thirty 2 m × 2 m plots that were set up on 1 June 2018. The rainfall treatments were covered by transparent rainfall shelters supported on an iron frame roof, the rainfall reduction was collected through a PVC pipe into a barrel, and rainfall addition was applied by respraying the collected rainwater from the bucket onto the treatment area. The N addition rate (in the form of NH_4NO_3) was 10 g N m^{-2} yr^{-1}, which was applied in June, July, and August.

Field Sampling

Soil samples were collected on 10 August 2018. Five soil cores (10 cm in diameter) were randomly collected from 0 to 10 cm topsoil and then mixed to create a composite sample for each plot. The composite soil samples were sieved through a 2.0-mm sieve to remove plant debris and roots. The sieved soil samples were then separated into two parts, with one stored at 4°C for testing of physical and chemical properties and one at –80°C for high-throughput sequencing of microorganisms. The aboveground biomass was measured by cutting living plants at ground level within 0.5 m × 0.5 m quadrat. The belowground biomass was estimated by using the soil cores method (Vogt and Persson, 1991). The root exudation of *S. krylovii* and *A. polyrhizum* was collected by using a modified method in August 2018 (Phillips et al., 2008). The methods of collecting root exudates and measuring the carbon and nitrogen of root exudates were described in detail by Li C. et al. (2021).

Lab Analysis

Soil samples were oven-dried for 48 h at 105°C to obtain soil moisture content. Ten grams of air-dried soil was used to calculate the soil ammonia nitrogen and nitrate nitrogen with 50 ml of 2 M KCl, shaken for 30 min, and the filtered solution was measured by using a continuous flow analyzer (Futura, Alliance Instruments, Frépillon, France). Soil microbial biomass carbon and nitrogen contents (SMBC and SMBN, respectively) were measured using the fumigation extraction method (Vance et al., 1987). Twenty-five grams of fresh soil was extracted with 100 ml of 0.5 M K_2SO_4, and the extracted solutions were analyzed by a TOC analyzer (Analytik, Jena, Germany). Aboveground and belowground biomass samples were oven-dried at 65°C to a constant weight.

DNA Extraction and Polymerase Chain Reaction Amplification and Sequencing

Soil DNA was extracted from 0.5 g of fresh soil using the PowerSoil expand DNA Isolation Kit (MO BIO) according to the manufacturer's instructions. Nanodrop Spectrophotometer (Nano-100, Aosheng Instrument Co Ltd.) assays qualified genomic DNA concentration and polymerase chain reaction (PCR) amplification products. The primers 515F (5′-GTGCCAGCMGCCGCGGTAA-3′) and 806R (5′-GGACTACHVGGGTWTCTAAT-3′) were used to amplify the V4 region of bacteria 16S rRNA gene (Caporaso et al., 2012). In order to distinguish the different samples, a barcode sequence was added to the 5′ – end of the reverse primer. The PCR was performed in a 50-μl reaction mixture containing 20 μl of nuclease-free water, 25 μl of 2 × Primer Taq (Takara, RR902A), 1 μl of forward primer (10 mM), 1 μl of reverse primer (10 mM), and 3 μl of g-DNA. PCR cycling conditions were set for 95°C for 5 min, followed by 40 cycles of denaturation at 94°C for 30 s, annealing at 53°C for 30 s, extension at 72°C for 40 s, with a final extension of 72°C for 8 min. For fungi, the primers ITS3 (5′-GCATCGATGAAGAACGCAGC-3′) and ITS4 (5′-TCCTCCGCTTATTGATATGC-3′) (Ihrmark et al., 2012) were used to amplify the ITS2 region (Gardes and Bruns, 2010). The PCR reaction mixture was the same as that used for the bacterial 16S rRNA gene. PCR cycling conditions were set at 95°C for 5 min, followed by 40 cycles of denaturation at 94°C for 30 s, annealing at 58°C for 30 s, extension at 72°C for 40 s, with a final extension of 72°C for 8 min. The PCR products were purified using the Omega kit following the manufacturer's protocol. The purified PCR products were paired-end sequenced using Illumina HiSeq 2500 platform. We also quantified the absolute abundance of 16S rRNA and ITS genes. The reaction mixture for qPCR included 10 μl of 2 × qPCR mix, 2 μl of g-DNA, 2 μl of 2.5 μM (515F/806R and ITS3/ITS4) primers, and 6 μl of ddH_2O. PCR cycling conditions were set at 95°C for 5 min, followed by 31 cycles of denaturation at 95°C for 30 s, annealing at 53°C for 15 s (16s rRNA) and 58°C for 15 s (ITS RNA), and extension at 72°C for 30 s. The melt curve was set for temperature from 60 to 95°C, and the curve was checked for every increase of 0.3°C.

Sequence Data Processing

Raw sequencing data were processed using an in-house Galaxy Pipeline[1] (Feng et al., 2017). We detected barcodes used Trimmomatic-0.33 to discard the low-quality sequences and obtain high-quality sequences. We use Flash to combine the forward sequences and reverse sequences. Reads were assigned to the same OTU by using the UPARSE method according to the 97% identity threshold. All the analysis is based on the generated OTU table. 16S and ITS OTU representative sequences were taxonomically assigned by using RDP Classifier against the 16S ref. Silva database and ITS Refs database (Zhou et al., 2011). On average, we obtained high-quality sequences with 48,783 16S rRNA sequences and 42,487 ITS sequences per sample across all soil samples. We then resampled 33,371 16S rRNA sequences and 27,731 ITS sequences per sample for further microbial analyses.

Data Analysis

Based on the resampled OTU table, we calculated the bacterial and fungal α-diversity (Shannon index and Inv-Simpson Index).

[1] http://mem.rcees.ac.cn:8080/

We measured the influences of N and rainfall patterns on the α-diversity index of bacteria and fungi by using one-way ANOVA analysis. The relative abundance of species was estimated through the data analysis platform (see text footnote 1) (Louca et al., 2016). Pearson correlation analysis was used to evaluate the relationship between soil physicochemical properties, plant root exudation, and bacteria α-diversity by using ggcorplot and ggthemes packages in RStudio (3.6.2). LefSe analysis was used to test the bacterial and fungal biomarker groups for N addition and altered rainfall patterns. LDA (linear discriminant analysis) measured the relative abundance of bacterial and fungal species (Yu et al., 2021a). We used the FAPROTAX database and FUNGuild pipeline to predict the bacterial and fungal functions by data process platform (see text footnote 1) (Yu et al., 2021b). Mantel and partial Mantel tests were used to examine the relationships between the Glomeromycota community composition and environmental variables.

RESULTS

Plant Biomass and Soil Chemo-Physical Properties

The results of aboveground biomass, belowground biomass, and root C and N exudation rates and C:N ratios of root exudates, soil moisture, soil nitrate, and ammonium were previously published in Li C. et al. (2021). The SMBC significantly increased under nitrogen (N) addition and N addition and rainfall addition interaction (RA + N), and significantly decreased under rainfall reduction (RR) (**Supplementary Table 1**). The SMBN significantly increased under N addition, N addition and rainfall reduction interaction (RR + N), and RA + N (**Supplementary Table 1**). The SMBC:SMBN ratio significantly decreased in response to RR (**Supplementary Table 1**).

Factors Influencing Bacterial and Fungal Diversity

By themselves, N and rainfall did not significantly affect bacterial and fungal Shannon diversity and Inv-Simpson indices (**Figure 1**). Bacterial Shannon diversity and Inv-Simpson diversity indices significantly increased under the condition of RA + N (**Figures 1A,B**), while the fungal Shannon diversity index significantly decreased under rainfall reduction and N addition (RR + N) (**Figures 1C,D**). Pearson's correlation analysis indicated that SMBN, inorganic nitrogen (NO_3^- and NH_4^+), *S. krylovii* root exudate C:N ratio, and *A. polyrhizum* root exudate C, N, and C:N ratio all significantly affected bacterial Shannon diversity index (**Figure 2A**). SMBC and *A. polyrhizum* root exudate C:N ratio significantly affected the fungal Shannon diversity index (**Figure 2B**).

Bacterial and Fungi Community Composition and Biomarkers

At the phylum level, the bacterial community was dominated by Actinobacteria (mean·20%), Acidobacteria (mean 16%), and Proteobacteria (mean 13%) (**Figure 3A**). The fungal community was mainly constituted of Ascomycota (mean 78%), Basidiomycota (mean 10%), and Glomeromycota (mean 0.70%) (**Figure 3B**). LefSe showed that the bacterial biomarkers of RR mainly belonged to the phylum Proteobacteria (genus *Ensifer*, family Rhizobiaceae). The biomarkers of RA included the phyla Gemmatimonadetes (class Longimicrobia), Firmicutes (class Clostridia and order Bacillales), Bacteroidetes (order Cytophagales), and class Deltaproteobacteria. The biomarkers of N addition mainly belonged to the phylum Proteobacteria (order Neisseriales). The biomarker bacteria of RR + N mainly belonged to the phylum Proteobacteria, while the biomarkers of RA + N belonged to the phylum Proteobacteria (genus *Inquilinus*, family Rhodospirillaceae, and order Rhodospirillales) (LDA = 2, **Figure 4A**). The biomarker fungi of RR mainly belonged to the phyla Ascomycota (class Dothideomycetes) and Basidiomycota (genus *Clavulinopsis*, family Clavariaceae, and order Sebacinales). The fungal biomarkers of N treatment mainly belonged to the phylum Basidiomycota (genus *Bovista* and family Lycoperdaceae). The indicator fungi of RR + N treatment mainly belonged to the phylum Ascomycota (genus *Nigrospora*, family Trichosphaeriaceae, and order Trichosphaeriales). The indicator fungi of RA + N treatment belonged to the phylum Ascomycota (class Pezizomycetes, order Botryosphaeriales, genus *Aureobasidium*, family Aureobasidiaceae, and order Dothideales) (LDA = 4, **Figure 4B**).

Functional Prediction of Soil Bacteria and Fungi

There was no significant response by soil bacterial function prediction to N addition and rainfall patterns (**Figure 5A**). For fungal function prediction, only arbuscular mycorrhizal significantly decreased under the RR + N treatment (**Figure 5B**). As the arbuscular mycorrhizal (AM) fungi are dominated by the members of the phylum Glomeromycota, within belowground plant–microbe systems (Johnson et al., 2013), by calculating the absolute abundance of this phylum, it was shown that RA treatment significantly increased the absolute abundance of Glomeromycota as compared to RR + N treatment (**Figure 6**). Mantel test showed that the root C exudation rates of *A. polyrhizum* significantly affected the abundance of Glomeromycota (**Table 1**).

DISCUSSION

Effects of Nitrogen Addition and Rainfall Interaction on Soil Bacterial and Fungal Diversity

Our results showed that nitrogen (N) addition did not affect the diversity of bacteria and fungi, which was consistent with the non-linear response of bacterial diversity to N addition found by Liu et al. (2021a), and supports our first hypothesis. A previous study showed that the diversity of bacteria decreased with N addition when the level of N input was between 16 and 32 g N m^{-2} yr^{-1} (Liu et al., 2021a), while Zhang et al. (2018) found that fungal diversity did not significantly change under N addition

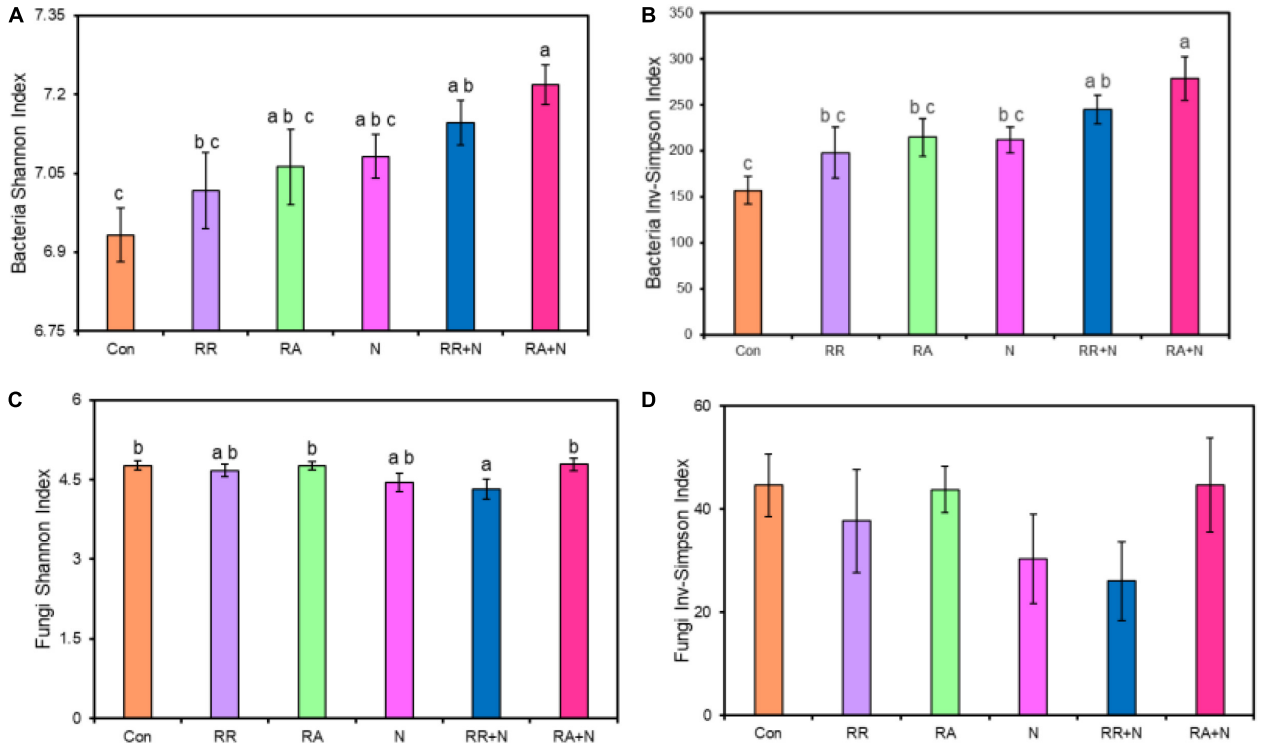

FIGURE 1 | The effects of altered nitrogen addition and rainfall, and their interaction, on bacterial Shannon index **(A)** and Inv-Simpson index **(B)**, fungal Shannon index **(C)** and Inv-Simpson index **(D)** in August 2018. Different treatments: Con: Control; RR: Rainfall reduction; RA: Rainfall addition; N: Nitrogen addition; RR + N: Rainfall reduction and Nitrogen addition; RA + N: Rainfall addition and Nitrogen addition. Values are mean ± SE (n = 5). Different lowercase letters indicate significant differences ($p < 0.05$) according to Duncan's *post hoc* test.

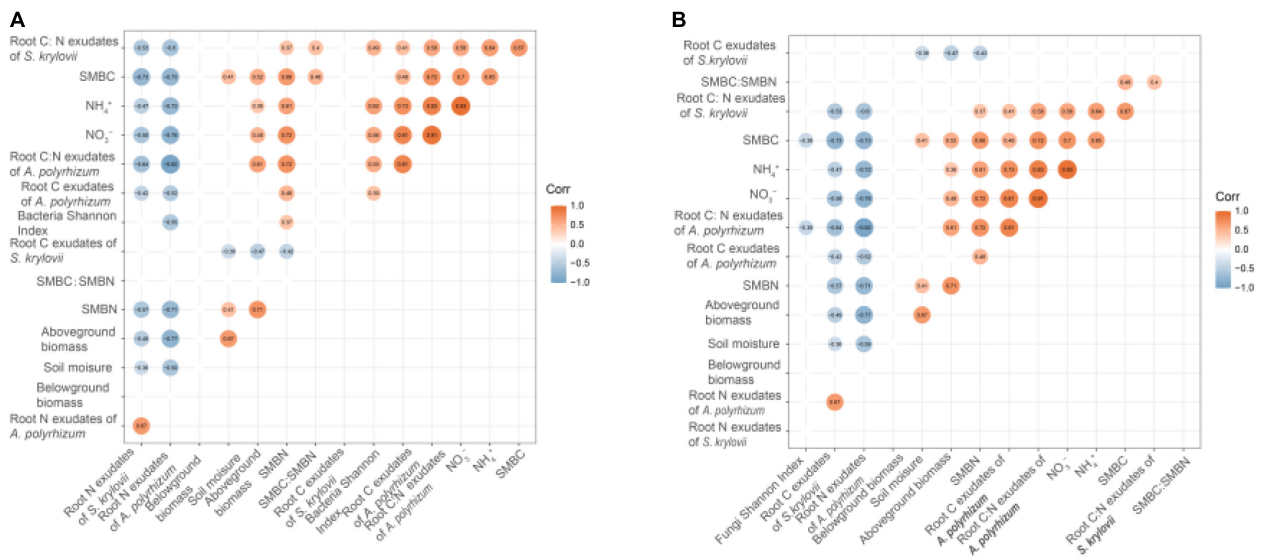

FIGURE 2 | Pearson correlations among bacterial Shannon index **(A)**, fungi Shannon index **(B)**, aboveground biomass, belowground biomass, soil moisture, soil microbial biomass carbon (SMBC), soil microbial biomass nitrogen (SMBN), SMBC:SMBN, NO_3^-, NH_4^+, root C exudates of *Stipa krylovii*, root N exudates of *S. krylovii*, root C: N exudates of *S. krylovii*, root C exudates of *Allium polyrhizum*, root N exudates of A. polyrhizum, and root C: N exudates of *A. polyrhizum*. The number represents the correlation coefficient. Coefficients that are not correlated have been hidden. Different treatments: Con: Control; RR: Rainfall reduction; RA: Rainfall addition; N: Nitrogen addition; RR + N: Rainfall reduction and Nitrogen addition; RA + N: Rainfall addition and Nitrogen addition.

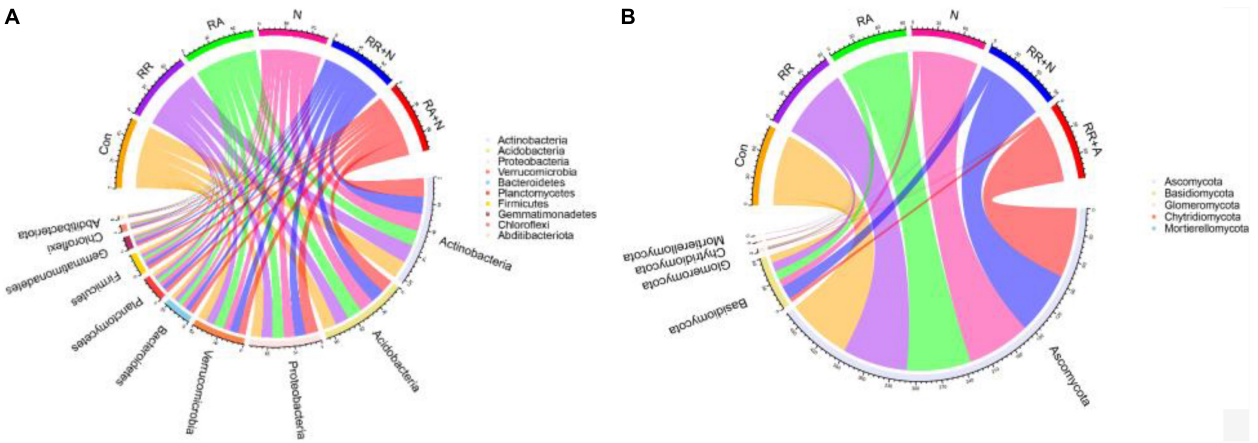

FIGURE 3 | The effects of altered nitrogen addition and rainfall, and their interaction, on the relative abundance of dominant members of the bacterial **(A)** and fungal **(B)** communities in August 2018. Different treatments: Con: Control; RR: Rainfall reduction; RA: Rainfall addition; N: Nitrogen addition; RR + N: Rainfall reduction and Nitrogen addition; RA + N: Rainfall addition and Nitrogen addition.

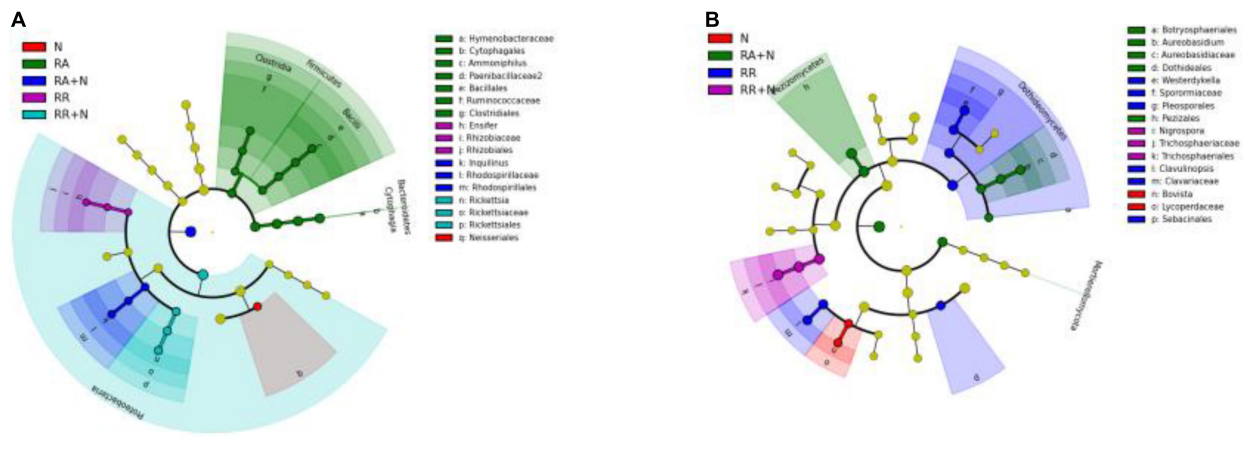

FIGURE 4 | Cladogram indicates the phylogenetic distribution of bacterial lineages (P = 0.05, LDA = 2.0) **(A)** and fungal lineages (P = 0.05, LDA = 4.0) **(B)** under the treatment of altered nitrogen addition and rainfall patterns. Each circle's diameter is proportional to the given taxon's relative abundance (n = 5). Different treatments: Con: Control; RR: Rainfall reduction; RA: Rainfall addition; N: Nitrogen addition; RR + N: Rainfall reduction and Nitrogen addition; RA + N: Rainfall addition and Nitrogen addition.

alone (< 100 kg N·ha^{-1}·yr^{-1}). In our study, N addition was 10 g N m^{-2} yr^{-1}, which was below the threshold level required to affect bacteria and fungi, and therefore the α-diversities of bacteria and fungi were not significantly increased by N addition. However, the treatment of RA + N significantly increased the bacterial Shannon diversity index. The interaction between N and rainfall may provide better conditions for bacterial survival, which may be the main reason for the increased bacterial α-diversity under RA + N (Shade et al., 2012). When water is sufficient, N addition has a positive effect on bacterial diversity (Zhang et al., 2015). Intriguingly, our results revealed that N addition alone did not affect fungal diversity and that RR + N decreased fungal diversity, therefore ignoring the factor that rainfall may influence judgment of the effect of N addition on soil fungal diversity. Consistent with our research, Wang H. et al. (2020). showed that rainfall played a key role in influencing the composition of the fungal community under N addition. Therefore, rainfall can alleviate the effects of N deposition on fungal diversity. Previous research found that N addition increased fungal α-diversity, and that the interaction between N and irrigation did not affect fungal diversity (Zhang et al., 2018). In total, soil fungal diversity might be overestimated if variations in moisture under N deposition are ignored (Zhang et al., 2018). Also, previous research, using PLFA technology, provided evidence that N deposition decreased the relative abundance and biomass of bacteria and fungi (Ma et al., 2016; Tian et al., 2017), and that under a high level of N addition (200 kg N ha^{-1} yr^{-1}) in the absence of water leaching, the growth of fungi was significantly inhibited (Sun et al., 2015). Therefore, under the interaction of RR + N, the α-diversity of fungi was significantly reduced. Moreover, some studies have indicated that the fungal community was more sensitive than bacteria under N deposition

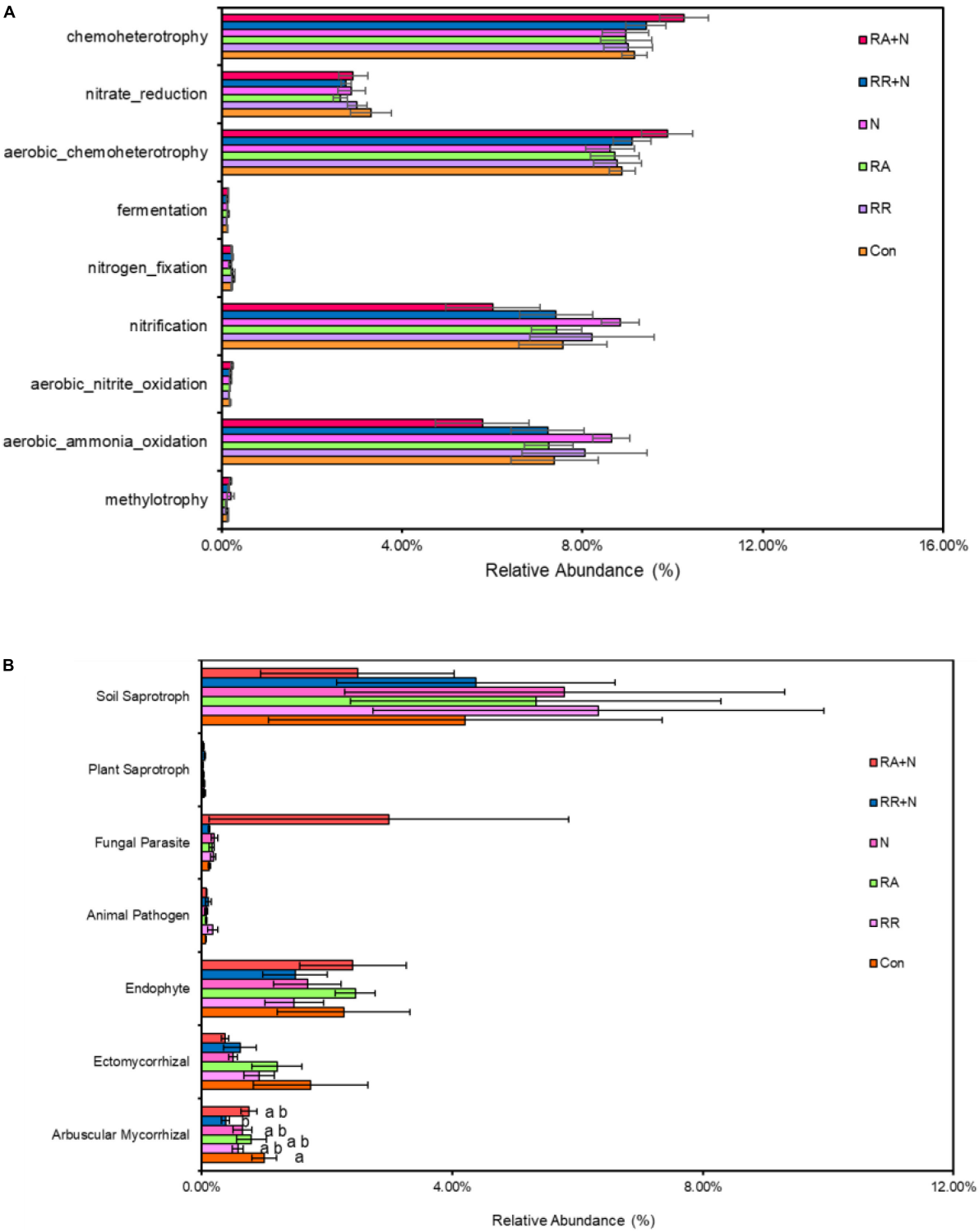

FIGURE 5 | The effects of altered nitrogen addition and rainfall, and their interaction, on the relative abundance of bacterial **(A)** and fungal **(B)** functional groups based on the FAPROTAX tool and FUNGuild pipeline, respectively. Different treatments: Con: Control; RR: Rainfall reduction; RA: Rainfall addition; N: Nitrogen addition; RR + N: Rainfall reduction and Nitrogen addition; RA + N: Rainfall addition and Nitrogen addition. Values are mean ± SE (n = 5). Different lowercase letters indicate the significant differences ($p < 0.05$) according to Duncan's *post hoc* test. Different lowercase letters indicate significant differences ($p < 0.05$) according to Duncan's *post hoc* test.

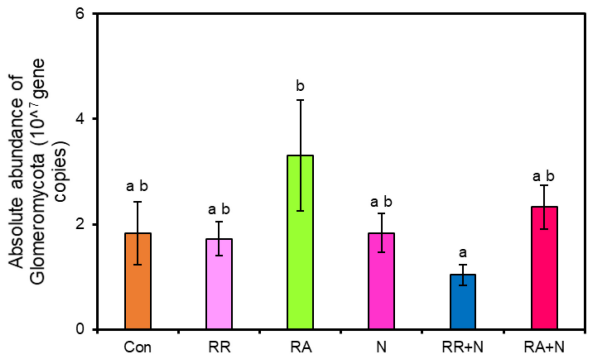

FIGURE 6 | The effects of nitrogen addition and rainfall and their interaction on the absolute abundance of Glomeromycota. Different treatments: Con: Control; RR: Rainfall reduction; RA: Rainfall addition; N: Nitrogen addition; RR + N: Rainfall reduction and Nitrogen addition; RA + N: Rainfall addition and Nitrogen addition. Values are mean ± SE (n = 5). Different lowercase letters indicate significant differences ($p < 0.05$) according to Duncan's *post hoc* test.

(Herold et al., 2012; Wang J. et al., 2020; Liu et al., 2021b). The long-term response of bacterial and fungal diversity to N addition and rainfall interaction requires further experimental verification.

In grassland ecosystems, soil microbial diversity was influenced by biological and abiotic factors, including soil nutrients, aboveground biomass, and litter quality (Contosta et al., 2015). Using meta-analysis, Wang et al. (2018) showed that decreased soil microbial diversity was associated with the decreased microbial biomass under N deposition. Our results showed that there was a significant correlation between the bacterial diversity and SMBN, ammonia nitrogen, and nitrate nitrogen. A possible explanation for the correlation may be that N addition increases ammonia nitrogen and nitrate nitrogen, stimulating the soil bacteria to uptake inorganic nitrogen and increase bacterial biomass and diversity. Due to the carbon–nitrogen coupling mechanism of bacteria, N input accelerates bacterial carbon uptake and increases bacterial activity, which stimulates the ability of bacteria to degrade litter (Schleuss et al., 2019). This may be a possible explanation for the increase in bacterial diversity under RR + N and RA + N conditions. Our results indicated that the main factors affecting fungal diversity were SMBC and the *A. polyrhizum* root exudate C:N ratio. In general, fungal communities are less affected by the external environment in the short term when they are mycelium rich. However, our study results indicated that soil abiotic and biological factors had significant effects on bacterial and fungal diversity under N, rainfall, and their interaction. It also highlights the impact of climate change on plant–soil–microbe interactions.

Effects of Nitrogen Addition and Rainfall Interaction on Biomarker Organisms and the Survival Strategies of Soil Bacteria and Fungi

Actinobacteria and Acidobacteria dominated all of the bacterial communities in our study. Based on Pianka's r/K-selection theory, both Actinobacteria (20%) and Proteobacteria (13%) grow faster and are eutrophic r-strategists (Fierer et al., 2007; Schleuss et al., 2019; Sun et al., 2021), while Acidobacteria (16%) are oligotrophic K-strategists (Sun et al., 2021). The majority of soil bacteria are r-strategists, with a few being K-strategists (Sun et al., 2021). Through Lefse analysis across treatments, we found nitrogen (N) addition mainly increased the relative abundance of the Proteobacteria, which are r-strategists, and therefore, N addition increased the bacterial r-strategist community. A potential explanation for this might be that N addition increased inorganic nitrogen content and stimulated microbial input of nitrogen and labile C (Fontaine et al., 2003; Fierer et al., 2012), resulting in faster microbial growth rates. This is in agreement with Sun et al. (2015) and is consistent with our second hypothesis that copiotrophic groups of bacteria will be mainly observed in a nutrient-rich environment under N addition treatment. Rainfall addition mainly increased the relative abundance of the phyla Gemmatimonadetes, Firmicutes, Bacteroidetes. Gemmatimonadetes, Firmicutes, and Bacteroidetes, all of which are copiotrophic r-strategists (Li H. et al., 2021; Sun et al., 2021). The effect of N and rainfall interaction also increased the relative abundance of the eutrophic bacterial community, which is in agreement with previous research that N and rainfall interaction promoted plant growth, plant litter quantity, dissolved carbon and nitrogen, and root exudate components, therefore accelerated bacterial growth, especially that of copiotrophic r-strategists (Meier and Bowman, 2008; Millard and Singh, 2010). As for fungal community structure, N addition mainly increased the relative abundance of the phylum Basidiomycota, while the effects of N and rainfall interaction increased the relative abundance of Ascomycota and Basidiomycota. These two phyla mainly represent copiotrophic r-strategists and oligotrophic k-strategists, respectively (Yao et al., 2017). The fungal communities in the control soil were also dominated by Ascomycota and Basidiomycota, and N addition and rainfall had little effect on fungi over the short term of our study. In fact, due to the rich mycelium of fungal communities,

TABLE 1 | The phylum Glomermycota relative to OTUs and environmental factors based on Mantel tests.

	R	p
Aboveground biomass	0.0109	0.442
Belowground biomass	–0.0685	0.832
Soil moisture (%)	–0.0035	0.489
SMBC	–0.0643	0.779
SMBN	0.0112	0.407
NO_3^-	0.0181	0.278
NH_4^+	0.0373	0.251
C exudation rates of *Stipa krylovii*	–0.0459	0.679
N exudation rates of *Stipa krylovii*	–0.0765	0.818
C: N exudation rates of *Stipa krylovii*	–0.0997	0.927
C exudation rates of *Allium polyrhizum*	0.142	**0.014***
N exudation rates of *Allium polyrhizum*	–0.057	0.772
C: N exudation rates of *Allium polyrhizum*	0.0095	0.431

** Represent significant differences at $p < 0.05$.*

they are not very sensitive to external environmental stimuli (Berlemont, 2017; Schleuss et al., 2019).

Effects of Nitrogen and Rainfall Interaction on the Functions of Soil Bacteria and Fungi

In this study, the interaction between N addition and rainfall had no significant effect on the bacteria participating in soil carbon and nitrogen cycling. This was inconsistent with our third hypothesis. Our results suggested that although the bacterial community saw an increased copiotrophic r-strategy groups, there was no obvious effect on the degradation of soil organic matter. The reason for this inconsistency may be that the short timescale (only 1 year) of the treatment did not significantly affect soil physical and chemical properties in our study, and bacteria had functional redundancy that they did not affect the soil carbon and nitrogen cycle. Moreover, soil bacteria can flexibly adapt to environmental changes, leading to bacterial functions not being significantly affected (Shade et al., 2012). Previous studies found that long-term fertilization significantly decreased microbial functional guilds involved in carbon fixation, degradation, N fixation, and mineralization. Because changes in soil functional community structure lead to a decrease in stochastic processes in the community assembly, microbial community structure tends to develop in a deterministic manner (Liang et al., 2020). Based on the functions of fungi predicted by using the FUNGuild database, we found that the AMF fungi community functional classification was significantly reduced under RR + N. AMF play an important role in ecosystem functions and regulate ecosystem stability by providing plants with N and P nutrients through symbiotic association with plant roots (Cotton et al., 2015; Yang et al., 2018). Previous studies found that N enrichment negatively affected AMF spore abundance, species richness, and biodiversity (Egerton-Warburton and Allen, 2000; Liu et al., 2013; Chen et al., 2017). A possible explanation for the significant decrease of AMF under RR + N treatment observed in the current study may be that N addition increased the inorganic nitrogen content (ammonia and nitrate nitrogen) of the soil. Plants prefer to utilize inorganic nitrogen in the soil for their own growth, and fertilization would reduce the demand for inorganic nitrogen produced by microbial decomposition and mineralization. Moreover, the AMF are a significant fungal community that participates in soil nitrogen mineralization (Cavagnaro et al., 2012; Bender et al., 2015). The reduction of soil water content also reduces the leaching of soil nutrient elements. Plants would require fewer nutrient elements from AMF community decomposition. Correspondently, the relative abundance of AMF was significantly reduced under RR + N conditions in our study.

The AMF of belowground ecosystem communities is mainly dominated by the phylum Glomeromycota (Johnson et al., 2013). We calculated the absolute abundance of the Glomeromycota through the absolute quantification of the ITS gene, and our results found that the absolute abundance of Glomeromycota did not significantly change between control and RR + N. However, it still exhibited a decreasing tendency, which was somewhat consistent with our fungal function prediction results. Our results further indicated that rainfall addition had positive effects on the phylum Glomeromycota. Rainfall addition increased the leaching of soil nutrients, especially NO_3^-. This would greatly increase plant demand for nitrogen, phosphorus, and other nutrients, and may cause AMF to symbiotically interact with plant roots to provide more of these nutrients to the host plants. Therefore, the absolute abundance of AMF significantly increased under rainfall addition. Mantel test showed that the rates of root exudate C from *A. polyrhizum* significantly affected the relative abundance of Glomeromycota. Because the Glomeromycota may have a symbiotic relationship with *A. polyrhizum* roots, the relative abundance of these fungi may be affected to a greater degree by plant root exudates. In addition, regarding the functional microbial groups involved in the soil carbon and nitrogen cycles, the response of AMF under the interaction of N and rainfall is more sensitive than that of other groups, suggesting that the interaction between these two factors has a significant impact on AMF over short timescales.

CONCLUSION

In this study, we studied how the diversity and function of soil bacteria and fungi responded to the interaction between N addition and rainfall patterns in a temperate steppe of Inner Mongolia. The interaction between N addition and altered rainfall patterns had obvious effects on the diversity of these microbial communities. Additionally, the C:N ratios of root exudates from *A. polyrhizum* affected not only the diversity of soil bacteria, but also the diversity of fungi. The functions of bacteria did not significantly change, while the AMF in fungal function classification was obviously reduced under RR + N, suggesting that plants will first use the inorganic nitrogen in the soil for their growth, reducing the demand for inorganic nitrogen produced by AMF decomposition and mineralization. The absolute abundance of the phylum Glomeromycota significantly increased under the treatment of rainfall addition, potentially illustrating that AMF were more sensitive to changes in nitrogen and rainfall patterns. Our findings suggest that this may provide novel and important insights for understanding and predicting microbial-mediated ecological processes under global climate change. Lastly, our experiment examined the short-term response of bacterial and fungal diversity and functions to changes in soil nitrogen and moisture. However, there is still a need for further research about the long-term response mechanism of bacterial and fungal functions and plant–soil–microbe interactions.

DATA AVAILABILITY STATEMENT

The datasets presented in this study can be found in online repositories. The name of the repository and accession number(s) can be found below: National Center for Biotechnology Information (NCBI) BioProject, https://www.ncbi.nlm.nih.gov/bioproject/, PRJNA826987 and PRJNA826724.

AUTHOR CONTRIBUTIONS

CX designed this study. YY and LL conducted the study. YY, CX, JZ, SW, and YZ drafted the manuscript. All authors contributed to revisions and have read and approved the manuscript.

FUNDING

This study was financially supported by the National Natural Science Foundation of China (31770501) and Key Laboratory of Ecology and Environment in Minority Areas (Minzu University of China), and National Ethnic Affairs Commission (KLEEMA202103).

ACKNOWLEDGMENTS

We are grateful to Lang Zheng for their help in samplings during the field experiment and to Hulun Lake Reserve Grassland Ecology Research Station of Minzu University of China for logistics and permission to access the study sites.

SUPPLEMENTARY MATERIAL

The Supplementary Material for this article can be found online at: https://www.frontiersin.org/articles/10.3389/fmicb.2022.906818/full#supplementary-material

REFERENCES

Allen, M., Babiker, M., Chen, Y., and Zickfeld, K. (2018). "Summary for Policymakers. In: Global warming of 1.5°C," in *An IPCC Special Report on the impacts of global warming 1.5°C*, Vol. 1, (IPCC).

Bardgett, R. D., and Putten, W. (2014). Belowground biodiversity and ecosystem functioning. *Nature* 515, 505–511. doi: 10.1038/nature13855

Baudoin, E., Benizri, E., and Guckert, A. (2003). Impact of artificial root exudates on the bacterial community structure in bulk soil and maize rhizosphere. *Soil Biol. Biochem.* 35, 1183–1192. doi: 10.1016/S0038-0717(03)00179-2

Bender, S. F., Conen, F., and Van, D. (2015). Mycorrhizal effects on nutrient cycling, nutrient leaching and N_2O production in experimental grassland. *Soil Biol. Biochem.* 80, 283–292. doi: 10.1016/j.soilbio.2014.10.016

Berlemont, R. (2017). Distribution and diversity of enzymes for polysaccharide degradation in fungi. *Sci. Rep-UK.* 7:222. doi: 10.1038/s41598-017-00258-w

Caporaso, J. G., Lauber, C. L., Walters, W. A., Berg-Lyons, D., Huntley, J., Fierer, N., et al. (2012). Ultra-high-throughput microbial community analysis on the Illumina HiSeq and MiSeq platforms. *ISME J.* 6, 1621–1624. doi: 10.1038/ismej.2012.8

Cavagnaro, T. R., Barrios-Masias, F. H., and Jackson, L. E. (2012). Arbuscular mycorrhizas and their role in plant growth, nitrogen interception and soil gas efflux in an organic production system. *Plant Soil* 353, 181–194.

Chen, Y. L., Xu, Z. W., Xu, T. L., Veresoglou, S. D., Yang, G. W., and Chen, B. D. (2017). Nitrogen deposition and precipitation induced phylogenetic clustering of arbuscular mycorrhizal fungal communities. *Soil Biol. Biochem.* 115, 233–242. doi: 10.1016/j.soilbio.2017.08.024

Contosta, A. R., Frey, S. D., and Cooper, A. B. (2015). Soil microbial communities vary as much over time as with chronic warming and nitrogen additions. *Soil Biol. Biochem.* 88, 19–24. doi: 10.1016/j.soilbio.2015.04.013

Cotton, T. E. A., Fitter, A. H., Miller, R. M., Dumbrell, A. J., and Helgason, T. (2015). Fungi in the future: interannual variation and effects of atmospheric change on arbuscular mycorrhizal fungal communities. *New Phytol.* 205, 1598–1607. doi: 10.1111/nph.13224

Egerton-Warburton, L. M., and Allen, E. B. (2000). Shifts in arbuscular mycorrhizal communities along an anthropogenic nitrogen deposition gradient. *Ecol. Appl.* 10, 484–496. doi: 10.1890/1051-07612000010[0484:siamca]2.0.co;2

FAO (1957). Soil map of the world. *Nature* 179, 1168–1168. doi: 10.1038/1791168c0

Feng, K., Zhang, Z., Cai, W., Liu, W., Xu, M., Yin, H., et al. (2017). Biodiversity and species competition regulate the resilience of microbial biofilm community. *Mol. Ecol.* 26, 6710–6082. doi: 10.1111/mec.14356

Fierer, N. (2017). Embracing the unknown: disentangling the complexities of the soil microbiome. *Nat. Rev. Microbiol.* 15, 579–590. doi: 10.1038/nrmicro.2017.87

Fierer, N., Bradford, M. A., and Jackson, R. B. (2007). Toward an ecological calssification of soil bacteria. *Ecology* 88, 1354–1364. doi: 10.1890/05-1839

Fierer, N., and Jackson, R. B. (2006). The diversity and biogeography of soil bacterial communities. *P. Natl. A Sci.* 103, 626–631. doi: 10.1073/pnas.0507535103

Fierer, N., Leff, J. W., Adams, B. J., Nielsen, U. N., Bates, S. T., Lauber, C. L., et al. (2012). Cross-biome metagenomic analyses of soil microbial communities and their functional attributes. *P. Natl. A. Sci.* 109:21390. doi: 10.1073/pnas.1215210110

Fontaine, S., Mariotti, A., and Abbadie, L. (2003). The priming effect of organic matter: a question of microbial competition? *Soil Biol. Biochem.* 35, 837–843. doi: 10.1016/S0038-0717(03)00123-8

Fukami, T. (2015). Historical contingency in community assembly: integrating niches, species pools, and priority effects. *Annu. Rev. Ecol. Evol. S.* 46, 1–23. doi: 10.1146/annurev-ecolsys-110411-160340

Füzy, A., Biró, B., Tóth, T., Hildebrandt, U., and Bothe, H. (2008). Drought, but not salinity, determines the apparent effectiveness of halophytes colonized by arbuscular mycorrhizal fungi. *J. Plant Physiol.* 165, 1181–1192. doi: 10.1016/j.jplph.2007.08.010

Galloway, J., Dentener, F., Capone, D., Boyer, E., Howarth, R., Seitzinger, S., et al. (2004). Nitrogen cycles: past, present, and future. *Biogeochemistry* 70, 153–226.

Gardes, M., and Bruns, T. D. (2010). ITS primers with enhanced specificity for basidiomycetes–application to the identification of mycorrhizae and rusts. *Mol. Ecol.* 2, 113–118. doi: 10.1111/j.1365-294X.1993.tb00005.x

Gordon, H., Haygarth, P. M., and Bardgett, R. D. (2008). Drying and rewetting effects on soil microbial community composition and nutrient leaching. *Soil Biol. Biochem.* 40, 302–311. doi: 10.1016/j.soilbio.2007.08.008

Herold, M. B., Baggs, E. M., and Daniell, T. J. (2012). Fungal and bacterial denitrification are differently affected by long-term pH amendment and cultivation of arable soil. *Soil Biol. Biochem.* 54, 25–35. doi: 10.1016/j.soilbio.2012.04.031

Ihrmark, K., Bödeker, I. T. M., Cruz-Martinez, K., Friberg, H., Kubartova, A., Schenck, J., et al. (2012). New primers to amplify the fungal ITS2 region – evaluation by 454-sequencing of artificial and natural communities. *FEMS Microbiol. Ecol.* 82, 666–677. doi: 10.1111/j.1574-6941.2012.01437.x

Jie, B., Zhang, N., Yu, L., Yang, H., and Ma, K. (2011). Interactive effects of water and nitrogen addition on soil microbial communities in a semiarid steppe. *J. Plant Ecol.* 5:3. doi: 10.1093/jpe/rtr046

Johnson, N. C., Angelard, C., Sanders, I. R., and Kiers, E. T. (2013). Predicting community and ecosystem outcomes of mycorrhizal responses to global change. *Ecol. Lett.* 16, 140–153. doi: 10.1111/ele.12085

Li, C., Liu, L., Zheng, L., Yu, Y., Mushinski, R. M., Zhou, Y., et al. (2021). Greater soil water and nitrogen availability increase C: N ratios of root exudates in a temperate steppe. *Soil Biol. Biochem.* 161:108384. doi: 10.1016/j.soilbio.2021.108384

Li, H., Yang, S., Semenov, M. V., Yao, F., Ye, J., Bu, R., et al. (2021). Temperature sensitivity of SOM decomposition is linked with a K-selected microbial community. *Glob. Change Biol.* 27, 2763–2779. doi: 10.1111/gcb.15593

Liang, Y., Ning, D., Lu, Z., Zhang, N., Hale, L., Wu, L., et al. (2020). Century long fertilization reduces stochasticity controlling grassland microbial community succession. *Soil Biol. Biochem.* 151:108023. doi: 10.1016/j.soilbio.2020.108023

Liu, J., Wang, B., Cane, M. A., Yim, S. Y., and Lee, J. Y. (2013). Divergent global precipitation changes induced by natural versus anthropogenic forcing. *Nature* 493, 656–659. doi: 10.1038/nature11784

Liu, W., Jiang, L., Yang, S., Wang, Z., Tian, R., Peng, Z., et al. (2021a). Critical transition of soil bacterial diversity and composition triggered by nitrogen enrichment. *Ecology* 101:e03053. doi: 10.1002/ecy.3053

Liu, W., Liu, L., Yang, X., Deng, M., Wang, Z., Wang, P., et al. (2021b). Long-term nitrogen input alters plant and soil bacterial, but not fungal beta diversity in a semiarid grassland. *Glob. Change Biol.* 27, 3939–3950. doi: 10.1111/gcb.15681

Louca, S., Parfrey, L. W., and Doebeli, M. (2016). Decoupling function and taxonomy in the global ocean microbiome. *Science* 353:1272. doi: 10.1126/science.aaf4507

Ma, H., Bai, G., Sun, Y., Kostenko, O., Zhu, X., Lin, S., et al. (2016). Opposing effects of nitrogen and water addition on soil bacterial and fungal communities in the Inner Mongolia steppe: a field experiment. *Appl. Soil Ecol.* 108, 128–135. doi: 10.1016/j.apsoil.2013.03.006

Marvel, K., and Bonfils, C. (2013). Identifying external influences on global precipitation. *P. Natl. A. Sci.* 110, 19301–19306. doi: 10.1073/pnas.1314382110

Meier, C. L., and Bowman, W. (2008). Links between plant litter chemistry, species diversity, and below-ground ecosystem function. *P. Natl. A. Sci.* 105, 19780–19785. doi: 10.1073/pnas.0805600105

Millard, P., and Singh, B. K. (2010). Does grassland vegetation drive soil microbial diversity? *Nutr. Cycl. Agroecosys*. 88, 147–158. doi: 10.1007/s10705-009-9314-3

Phillips, R. P., Erlitz, Y., Bier, R., and Bernhardt, E. S. (2008). New approach for capturing soluble root exudates in forest soils. *Funct. Ecol.* 22, 990–999. doi: 10.1111/j.1365-2435.2008.01495.x

Rousk, J., Bååth, E., Brookes, P. C., Lauber, C. L., Lozupone, C., Caporaso, J. G., et al. (2010). Soil bacterial and fungal communities across a pH gradient in an arable soil. *ISME J.* 4, 1340–1351. doi: 10.1038/ismej.2010.58

Schleuss, P. M., Widdig, M., Heintz-Buschart, A., Guhr, A., Martin, S., Kirkman, K., et al. (2019). Stoichiometric controls of soil carbon and nitrogen cycling after long-term nitrogen and phosphorus addition in a mesic grassland in South Africa. *Soil Biol. Biochem.* 135, 294–303. doi: 10.1016/j.soilbio.2019.05.018

Shade, A., Peter, H., Allison, S. D., Baho, D. L., Berga, M., Bürgmann, H., et al. (2012). Fundamentals of Microbial Community Resistance and Resilience. *Front. Microbiol.* 3:417. doi: 10.3389/fmicb.2012.00417

Sun, L., Qi, Y., Dong, Y., He, Y., Peng, Q., Liu, X., et al. (2015). Interactions of water and nitrogen addition on soil microbial community composition and functional diversity depending on the inter-annual precipitation in a Chinese steppe. *J. Integr. Agr.* 14, 788–799. doi: 10.1016/S2095-3119(14)60773-5

Sun, Y., Wang, C., Yang, J., Liao, J., Chen, H., and Ruan, H. (2021). Elevated CO_2 shifts soil microbial communities from K- to r-strategists. *Glob. Ecol. Biogeogr.* 30, 961–972. doi: 10.1111/geb.13281

Tian, B., Zhu, M., Pei, Y., Ran, G., Shi, Y., and Ding, J. (2021). Climate warming alters the soil microbial association network and role of keystone taxa in determining wheat quality in the field. *Agr. Ecosyst. Environ.* 326:107817. doi: 10.1016/j.agee.2021.107817

Tian, D., Jiang, L., Ma, S., Fang, W., Schmid, B., Xu, L., et al. (2017). Effects of nitrogen deposition on soil microbial communities in temperate and subtropical forests in China. *Sci. Total Environ.* 607- 608, 1367–1375. doi: 10.1016/j.scitotenv.2017.06.057

Turner, M. M., and Henry, H. A. L. (2010). Interactive effects of warming and increased nitrogen deposition on ^{15}N tracer retention in a temperate old field: seasonal trends. *Glob. Change Biol.* 15, 2885–2893. doi: 10.1111/j.1365-2486.2009.01881.x

Vance, E. D., Brookes, P. C., and Jenkinson, D. S. (1987). An extraction method for measuring soil microbial biomass C. *Soil Biol. Biochem.* 19, 703–707. doi: 10.1016/0038-0717(87)90052-6

Vogt, K. A., and Persson, H. (1991). *Measuring growth and development of roots. Techniques and approaches in forest tree ecophysiology*. Boca Raton: CRC Press, 477–501.

Waldrop, M. P., Zak, D. R., Sinsabaugh, R. L., Gallo, M., and Lauber, C. (2004). Nitrogen deposition modifies soil carbon storage through changes in microbial enzymatic activity. *Ecol. Appl.* 14, 1172–1177. doi: 10.1890/03-5120

Wang, C., Liu, D., and Bai, E. (2018). Decreasing soil microbial diversity is associated with decreasing microbial biomass under nitrogen addition. *Soil Biol. Biochem.* 120, 126–133. doi: 10.1016/j.soilbio.2018.02.003

Wang, H., Na, T., Jin, K., Ji, B., Schellenberg, M., Wei, Z., et al. (2020). Interactive effects of nitrogen fertilizer and altered precipitation on fungal communities in arid grasslands of northern china. *J. Soil Sediment*. 20, 1–13.

Wang, J., Shi, X., Zheng, C., Suter, H., and Huang, Z. (2020). Different responses of soil bacterial and fungal communities to nitrogen deposition in a subtropical forest. *Sci. Total Environ.* 755:142449. doi: 10.1016/j.scitotenv.2020.142449

Wang, M., Shi, S., Lin, F., Hao, Z., Jiang, P., and Dai, G. (2012). Effects of soil water and nitrogen on growth and photosynthetic response of Manchurian ash (Fraxinus mandshurica) seedlings in Northeastern China. *PLoS One*. 7:e30754. doi: 10.1371/journal.pone.0030754

Williams, M. A., and Rice, C. W. (2007). Seven years of enhanced water availability influences the physiological, structural, and functional attributes of a soil microbial community. *Appl. Soil Ecol.* 35, 535–545. doi: 10.1016/j.apsoil.2006.09.014

Yang, G., Wagg, C., Veresoglou, S. D., Hempel, S., and Rillig, M. C. (2018). How soil biota drive ecosystem stability. *Trends Plant Sci.* 23, 1057–1067. doi: 10.1016/j.tplants.2018.09.007

Yao, F., Shan, Y., Wang, Z., Wang, X., Ye, J., Wang, X., et al. (2017). Microbial Taxa Distribution Is Associated with Ecological Trophic Cascades along an Elevation Gradient. *Front. Microbiol.* 8:2071. doi: 10.3389/fmicb.2017.02071

Yu, Y., Zang, L., Zhou, Y., Sang, W., Zhao, J., Liu, L., et al. (2021a). Changes in soil microbial community structure and function following degradation in a temperate grassland. *J. Plant Ecol.* 14, 384–397. doi: 10.1093/jpe/rtaa102

Yu, Y., Liu, L., Wang, J., Zhang, Y., and Xiao, C. (2021b). Effects of warming on the bacterial community and its function in a temperate steppe. *Sci. Total Environ.* 792:148409. doi: 10.1016/j.scitotenv.2021.148409

Zhang, H., Wang, L., Liu, H., Zhao, J., Li, G., Wang, H., et al. (2018). Nitrogen deposition combined with elevated precipitation is conducive to maintaining the stability of the soil fungal diversity on the Stipa baicalensis steppe. *Soil Biol. Biochem.* 117, 135–138. doi: 10.1016/j.soilbio.2017.11.004

Zhang, N., Wan, S., Guo, J., Han, G., Gutknecht, J., Schmid, B., et al. (2015). Precipitation modifies the effects of warming and nitrogen addition on soil microbial communities in northern Chinese grasslands. *Soil Biol. Biochem.* 89, 12–23. doi: 10.1016/j.soilbio.2015.06.022

Zhou, J., Xue, K., Xie, J., Deng, Y., Wu, L., Cheng, X., et al. (2011). Microbial mediation of carbon-cycle feedbacks to climate warming. *Nat. Clim. Change.* 2, 106–110. doi: 10.1038/nclimate1331

Conflict of Interest: The authors declare that the research was conducted in the absence of any commercial or financial relationships that could be construed as a potential conflict of interest.

frontiers | Frontiers in Microbiology

TYPE Original Research
PUBLISHED 23 September 2022
DOI 10.3389/fmicb.2022.1015038

OPEN ACCESS

EDITED BY
Yu Shi,
Henan University,
China

REVIEWED BY
Xingjia Xiang,
Anhui University,
China
Ruibo Sun,
Anhui Agricultural University,
China
Congcong Shen,
Research Center for Eco-environmental Sciences (CAS), China

*CORRESPONDENCE
Ruozhong Wang
wangruozhong@hunau.edu.cn

SPECIALTY SECTION
This article was submitted to Microbe and Virus Interactions with Plants, a section of the journal Frontiers in Microbiology

RECEIVED 09 August 2022
ACCEPTED 08 September 2022
PUBLISHED 23 September 2022

CITATION
Zhu F, Fang Y, Wang Z, Wang P, Yang K, Xiao L and Wang R (2022) Salicylic acid remodeling of the rhizosphere microbiome induces watermelon root resistance against *Fusarium oxysporum* f. sp. *niveum* infection.
Front. Microbiol. 13:1015038.
doi: 10.3389/fmicb.2022.1015038

Salicylic acid remodeling of the rhizosphere microbiome induces watermelon root resistance against *Fusarium oxysporum* f. sp. *niveum* infection

Feiying Zhu[1,2], Yong Fang[1], Zhiwei Wang[1], Pei Wang[1], Kankan Yang[1], Langtao Xiao[2] and Ruozhong Wang[2]*

[1]Hunan Academy of Agricultural Sciences, Changsha, China, [2]Hunan Provincial Key Laboratory of Phytohormones, College of Bioscience and Biotechnology, Hunan Agricultural University, Changsha, China

Fusarium wilt disease poses a severe threat to watermelon cultivation by affecting the yield and quality of the fruit. We had previously found that the rhizosphere microbiome has a significant impact on the ability of watermelon plants to resist *Fusarium* wilt development and that salicylic acid (SA) is closely related to this phenomenon. Therefore, in this study, the role of SA as a mediator between plants and microbes in activating resistance against *Fusarium oxysporum* f. sp. *niveum* (FON) infection was explored through physiological, biochemical, and metagenomic sequencing experiments. We demonstrated that exogenous SA treatment could specifically increase some beneficial rhizosphere species that can confer resistance against FON inoculation, such as *Rhodanobacter*, *Sphingomonas*, and *Micromonospora*. Functional annotation analysis indicated that SA application significantly increased the relative abundance of glycoside hydrolase and polysaccharide lyase genes in the microbiome, which may play an essential role in increasing plant lipids. Moreover, network interaction analysis suggested that the highly expressed *AAC6_IIC* gene may be manipulated through SA signal transduction pathways. In conclusion, these results provide a novel strategy for controlling *Fusarium* wilt in watermelons from the perspective of environmental ecology, that is, by manipulating the rhizosphere microbiome through SA to control Fusarium wilt.

KEYWORDS

salicylic acid, rhizosphere, microbiome, watermelon, *Fusarium* wilt

Introduction

Watermelon (*Citrullus lanatus*) is an important horticultural crop worldwide (Everts and Himmelstein, 2015). However, the commercial cultivation of this fruit is severely threatened by the soil-borne fungus *Fusarium oxysporum* f. sp. *niveum* (FON), which causes *Fusarium* wilt, a disease that leads to a significant decline in crop quality and yield (Xu et al.,

2015; Ren et al., 2016; Li et al., 2019). Salicylic acid (SA), a phytohormone present in plants and some microbes, is reported to be an important signaling molecule that induces plant resistance to diseases (Yang et al., 2015; Zhang and Li, 2019). With the deciphering of the watermelon genome, Lü et al. found *via* gene ChIP transcription analysis that the phenylalanine ammonia lyase (*PAL*) gene plays an important role in the lignin metabolic pathway of resistance to *Fusarium* wilt (Lü et al., 2011). Lv reported that the intercropping of wheat and watermelon with FON induced SA synthesis in the watermelon plant to enhance its resistance to *Fusarium* wilt (Lv et al., 2018). Furthermore, our research demonstrated the important role of SA in regulating watermelon resistance against *Fusarium* wilt, with results indicating that the significantly expressed *C. lanatus PAL* (*ClPAL*) and non-pathogen-related (*NPR*) genes play key roles in SA synthesis and signal transduction in this plant species (Zhu et al., 2022a,b).

Recently, increasing evidence has suggested that the rhizosphere microbiome plays critical roles in promoting plant growth and health, such as enhancing nutrient uptake by the host plant and increasing its resistance against pathogen attack (Levy et al., 2017; Berendsen et al., 2018). The establishment of plant–rhizosphere microbiome interaction is a highly coordinated event influenced by the host plant and soil. For instance, the plant immune system shapes the microbiome, which, in turn, can increase the plant's immune capacity (Heintz and Mair, 2014; Levy et al., 2017; Aleklett et al., 2018). Notably, our previous studies have demonstrated the important role of the soil microbial community structure in controlling the occurrence of *Fusarium* wilt in watermelons (Zhu et al., 2018, 2019). For instance, our results indicated that the presence of beneficial microbes, such as *Rhodanobacter*, *Pseudomonas*, *Sphingomonas*, and *Herbaspirillum*, is important for the prevention of watermelon disease (Zhu et al., 2020).

Consistently, more researchers have begun to notice that rhizosphere microbiome composition is influenced by an array of plant-derived metabolic substances (Trivedi et al., 2020; Liu et al., 2021). Additionally, the essential role of SA in recruiting specific rhizosphere microbiomes has been previously reported. For instance, Trivedi et al. showed that SA affected the abundance of specific bacterial groups in the roots *via* a combination of direct and indirect effects (Trivedi et al., 2020). However, the mechanism by which watermelon plants affect microbiome assembly and the impact of this interconnectedness on plant and microbiota functions remains unclear. Chen et al. found that systemic accumulation of SA could affect microbiome assembly in the rhizosphere of *Arabidopsis* plants after foliar infection by pathogens (Chen et al., 2020). Therefore, through metagenomic sequencing and relevant physiological and biochemical analyses, we aimed to explore the effect of exogenous SA in remodeling the watermelon rhizosphere microbiome to induce resistance against FON infection. Our research findings provide a new strategy for controlling watermelon *Fusarium* wilt from the perspective of environmental ecology and have significant value for promoting sustainable agricultural development.

Abbreviations: ARO, antibiotic resistance ontology; dpi, days post-inoculation; FON, *Fusarium oxysporum* f. sp. *niveum*; hpi, hours post-inoculation; MDA, malondialdehyde; PAL, phenylalanine ammonia lyase; POD, peroxidase; SA, salicylic acid.

Materials and methods

Experimental process and sampling

The experiment was conducted in the city of Changsha (112°58′42″E, 28°11′49″N), Hunan Province, China. The soil used for planting was sandy loam, collected from our field experiment at the Gaoqiao Scientific Research Base of the Hunan Academy of Agricultural Sciences in Changsha (Zhu et al., 2020). Our previous studies found that the high content of pathogens in the soil under a continuous cropping system leads to SA accumulation in the plant (Zhu et al., 2022a,b). Therefore, we sterilized the soil to make them as same background before use (LDZM-80KCS-3 vertical pressure steam sterilizer, ZHONGAN, Shanghai, China) to avoid errors and study how SA can improve watermelon immune resistance at the early stage after FON infection. The watermelon variety used was Zaojia 8,424 (Xinjiang Farmer Seed Technology Co., Ltd., Urumqi, China), which is the main cultivar on the Chinese market. The watermelon seedlings were cultivated in seedling pots containing peat, perlite, and vermiculite (6:3:1) and grown in a biochemical incubator (LRH-300, ZHUJIANG, Taihong, Shaoguan, China) that was set at 25°C during 16 h of light and 18°C during 8 h of darkness. After 30 days, each plant was transplanted into separate pots. When the seedlings were at the two-leaf stage, 5 ml of 100 μM exogenous SA (Sigma-Aldrich LLC., Merck KGaA, Darmstadt, Germany) was incorporated into the root zone of each plant, and another 5 ml was added 24 h later. The Fusarium strain FON was firstly incubated in the dark for 7 days on a PDA plate at 28°C. Then, a bam plug was selected from the PDA plate and placed into 300 ml of potato dextrose broth in a flask, before propagation on a rotary shaker at 200 rpm at 26–30°C. Two days later, 5 ml FON (1×10^6 conidia/mL) was added to the root zone of each plant (Li et al., 2019).

The plants were divided into the following three groups: S, mock-inoculation control (H_2O); SA, 100 μM exogenous SA + FON; and SF, FON only. We set six different sampling times before and after the different treatments: 0 days post-inoculation (dpi) (before treatment), 12 h post-inoculation (hpi), 1 dpi, 3 dpi, 5 dpi, and 7 dpi. Sampling was stopped at 7 dpi when the disease symptoms (yellowing and wilting) started to appear. We selected 10 watermelon plants as one replicate and set three independent replicates (30 plants) for each sample group, at six different sampling times with every three treatments (16 groups). Therefore, 480 plant samples were collected from 480 pots.

The soil samples were designated S0 (mock-inoculation control, before treatment), S3 (mock-inoculation control, 3 dpi), SF3 (FON

treatment, 3 dpi), SA3 (SA + FON treatment, 3 dpi), S7 (mock-inoculation control, 7 dpi), SF7 (FON treatment, 7 dpi), and SA7 (SA + FON treatment, 7 dpi). For each treatment group, the rhizosphere soil sample was pooled from 10 plant roots in one repetition, with three independent replicates, at each sampling time. After removing the plant roots and stones, the rhizosphere soil samples were placed in 5 ml sterile centrifuge tubes and then divided into three parts. In total, 21 samples were collected at the three different sampling times (i.e., 0 dpi, 3 dpi, and 7 dpi) and stored at −80°C for sequencing analysis.

Determination of the watermelon plant root morphology and physiological and biochemical indexes

First, the root morphology of each plant was captured using a digital camera. The roots were then cut with sterilized scissors, and their fresh weights were measured using an electronic balance. Thereafter, the roots were placed in sterilized 5 ml centrifuge tubes to test their peroxidase (POD) and phenylalanine ammonia lyase (PAL) activities and malondialdehyde (MDA) content. The POD and PAL activities were analyzed using a BC0095 peroxidase assay kit and BC0215 PAL test kit (Beijing Solarbio Science & Technology Co., Ltd., Beijing, China), respectively, whereas the MDA content was determined using the thiobarbituric acid method using a BC0025 MDA assay kit (Beijing Solar-bio Science & Technology Co., Ltd.), according to the manufacturer's protocols. A Tecan-SPARK microplate reader (Tecan Trading AG, Männedorf, Switzerland) and Eppendorf 5415R refrigerated centrifuge (Eppendorf AG, Hamburg, Germany) were used for the assays. Three biological replicates per sample were performed, with three technical replicates.

The disease incidence was calculated as follows:

$$\text{Disease incidence}(\%) = (\text{no. of infected plants} / \text{total number of plants surveyed}) \times 100.$$

Soil DNA library preparation

A total of 1 μg DNA per sample was used for sequencing. In brief, DNA sequences 350 bp in size were fragmented by sonication, and the fragments were then end-polished, A-tailed, and ligated with the full-length adaptor for Illumina sequencing followed by PCR amplification. The PCR products were purified (AMPure XP system), and libraries were prepared and analyzed for size distribution using the Agilent2100 Bioanalyzer. Three biological replicates per sample were analyzed. Raw data were obtained using the Illumina NovaSeq 6000 sequencing platform.

Metagenomic sequencing

Readfq V8 was used to acquire the clean data for subsequent analysis against the host database using the Basic Local Alignment Search Tool (BLAST), which uses Bowtie 2.2.4 as default software to filter the reads that are of host origin. After all the reads that were not used in the forward step were combined, SOAPdenovo was used to generate the mixed assembly using the same parameters as those applied for the single assembly. The Scaftigs (≥500 bp) assembled from both the single and mixed assemblies were used to predict the open reading frames (ORFs) using MetaGeneMark software, and sequences shorter than 100 nt were filtered from the predicted result with default parameters. For ORF prediction, sequence redundancy was reduced using the Cluster Database at High Identity with Tolerance software, and a unique initial gene catalog was obtained. The clean data of each sample were mapped to the initial gene catalog using Bowtie 2.2.4 with the following parameter settings: --end-to-end, —-sensitive, -I 200, and -X 400. Genes with two or fewer reads in each sample were filtered, and the gene catalog (UniGene database) obtained was used for subsequent analysis.

The abundance of each gene in each sample was statistically analyzed based on the number of mapped reads and their lengths. The basic information statistics, core- and pan-genomic analyses, correlation analysis of the samples, and Venn diagram analysis of the number of genes were all based on the abundance of each gene in each sample in the gene catalog. DIAMOND software was used to blast the UniGene database to the sequences of bacteria, fungi, archaea, and viruses, which were all extracted from the non-redundant database of the National Center for Biotechnology Information (NCBI). Finally, the clean reads were deposited in the NCBI Sequence Read Archive database (Accession number: PRJNA707127).

Assembly of the Core rhizosphere communities, common functional databases used, and resistance gene annotation

To determine the dynamic changes in the dominant soil microbial communities during all three sampling times in the different treatment groups, we used community bar-plot analysis to identify the 10 most abundant soil microbial communities at both the phylum and genus levels. Moreover, we used multiple *t*-tests to compare significant differences in soil microbial communities at 3 and 7 dpi, both at the phylum and genus levels, after SA application. To elucidate the molecular mechanism by which the rhizosphere microbial community cooperates to induce plant resistance against *Fusarium* wilt, we blasted the unique genes against various functional annotation databases such as the Kyoto Encyclopedia of Genes and Genomes (KEGG), Evolutionary Genealogy of Genes: Non-supervised Orthologous Groups (eggNOG), Carbohydrate-Active Enzymes (CAZy), and the Comprehensive Antibiotic Resistance Database (CARD) to determine their abundance and analyzed them statistically with a visual display.

KEGG, eggNOG, and CAZy databases were used for functional annotation of the resistance genes. The Unigenes were aligned to the CARD database using Resistance Gene Identifier software with default parameter settings. The relative abundance of the antibiotic resistance ontology (ARO) cluster, abundance bar charts, abundance cluster heatmaps, and differences in the number of resistance genes between soil groups were displayed according to the alignment results. Similarly, the distribution of resistance genes in each sample and analyses of the species attribution of those genes and their resistance mechanisms were also investigated.

Statistical analysis

Statistical analysis was performed using GraphPad Prism 9 (GraphPad Software, San Diego, CA, United States). All values are expressed as mean ± standard error ($n = 3$). The differences

FIGURE 1
Comparison of watermelon root phenotypes in different treatment groups S, Mock-inoculation control; SA, SA+FON treatment; SF, FON treatment; FON, *Fusarium oxysporum* f. sp. *niveum*; SA, salicylic acid; hpi, hours post-inoculation; dpi, days post-inoculation.

between the groups were tested using an analysis of similarities. Figures were constructed using Microsoft Office 2010 (Microsoft Corporation, Redmond, WA, United States).

Results

Effectiveness of salicylic acid treatment in controlling *fusarium* wilt of watermelon

To clarify whether exogenous SA treatment can control *Fusarium* wilt disease in watermelon, we first compared the root phenotypes after exposure to exogenous SA + FON or FON alone at five different sampling times. The SA group had more fibrous roots than the SF group did. The roots in the SF group began to turn yellow at 3 dpi, and obvious plant yellowing and wilting symptoms were observed at 7 dpi (Figure 1). Furthermore, there was a significant difference in the fresh weight of the roots between the samples at 1, 3, and 7 dpi. For instance, the root fresh weight of the SA group was 2.5 times heavier than that of the SF group at 7 dpi (Figure 2A). The incidence of *Fusarium* wilt after SA application was significantly lower (by −20%) than that in plants not treated with phytohormones (Figure 2B). Moreover, the MDA content in the SF group first increased from 12 hpi onward, then declined at 3 dpi and finally increased significantly again at 7 dpi. However, we noticed an increase in MDA content at 3 dpi in both SA and S groups (Figure 2C). Similarly, POD activity was significantly increased at 3 dpi in the SA and S groups, which indicated that this sampling time might be a key time point for activating resistance defenses in watermelon plants (Figure 2D). Moreover, there were significant enhancements in PAL activity in the SA group at 3 dpi and 7 dpi, whereas the enzyme activity was significantly lower in the SF group at 7 dpi (Figure 2E), which confirmed the symptoms and disease incidence results. Therefore, the results from plant root physiological and biochemical studies indicate that exogenous SA treatment can effectively reduce the incidence of *Fusarium* wilt in watermelon.

Sequencing and metagenome assembly

We selected three sampling times to compare the dynamic changes in the dominant soil microbial communities between the different treatments. Gene sequencing analysis revealed that the ORFs were approximately 200–600 nt in length (Supplementary Figure S1A). According to the results of the quality control analysis, the evenness of the number of ORFs observed in the samples tended to be consistent (Supplementary Figure S1B). The Venn diagram showed that there were 624,730 overlapping genes among all groups

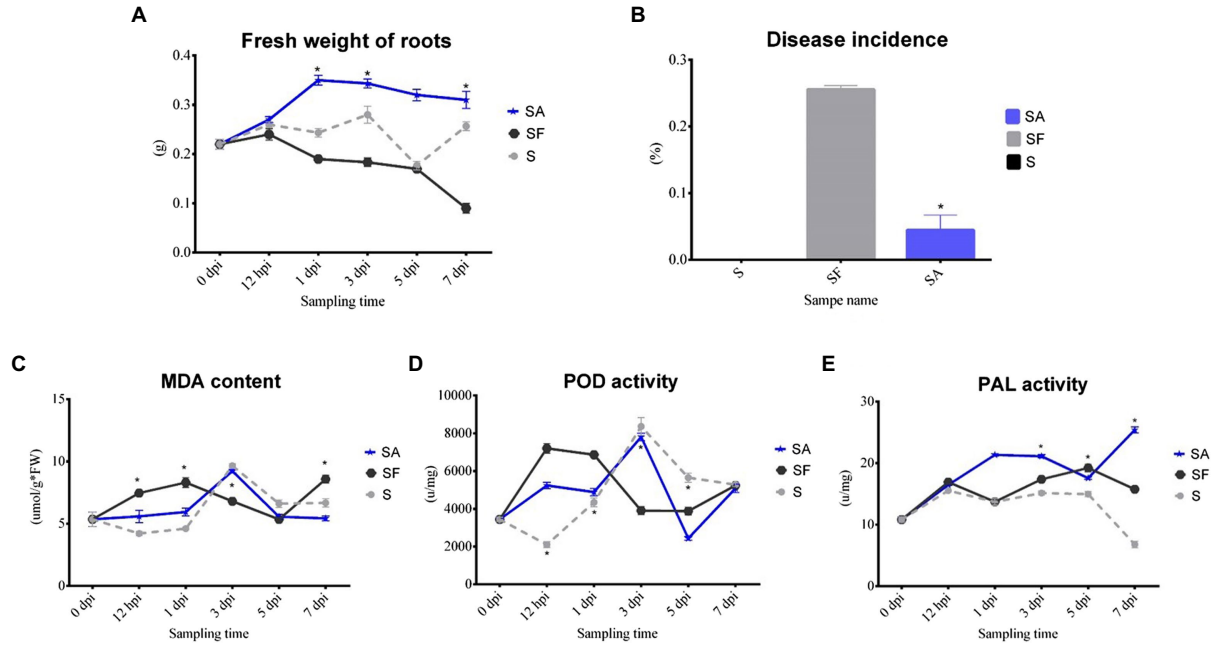

FIGURE 2
Comparison of physiological changes, disease incidence, and biochemical indexes of watermelon plants after exogenous salicylic acid application. **(A)** Comparison of the root fresh weight of different samples. **(B)** Comparison of the disease incidence in different samples. **(C)** Comparison of the malondialdehyde (MDA) content in different samples. **(D)** Comparison of the peroxidase (POD) activity in different samples. **(E)** Comparison of the phenylalanine ammonia lyase (PAL) activity in different samples. S, Mock-inoculation control; SA, SA+FON treatment; SF, FON treatment; FON, *Fusarium oxysporum* f. sp. *niveum*; SA, salicylic acid; hpi, hours post-inoculation; dpi, days post-inoculation; 0 dpi: before treatment. Three biological replicates per sample were analyzed. Data are expressed as mean±SE (n=3). Multiple t-tests of ANOSIM (*$p \leq 0.0001$).

of samples, and there were unique genes in each group (Supplementary Figure S1C).

Dynamic changes in the soil microbial community structure

The top 10 phyla in all samples were Proteobacteria, Actinobacteria, Bacteroidetes, Gemmatimonadetes, Firmicutes, Acidobacteria, Verrucomicrobia, Deinococcus-Thermus, Elusimicrobiota, and Chloroflexi (Figure 3A). The top 10 genera were *Rhodanobacter*, *Micromonospora*, *Massilia*, *Flavobacterium*, *Cellvibrio*, *Frateuria*, *Stenotrophomonas*, *Streptomyces*, *Pseudomonas*, and *Solimonas* (Figure 3B). Additionally, the heatmap showed dynamic changes in the rhizosphere communities among the groups at different sampling times; that is, there was an obvious enrichment of Proteobacteria and Firmicutes in the SA3 sample but a higher accumulation of Actinobacteria, Candidatus Saccharibacteria, Candidatus Woesebacteria, Chlamydiae, and Mucoromycota in the SF3 sample (Figure 4A). In agreement with previous research, our results indicated that Proteobacteria is the second largest phylum

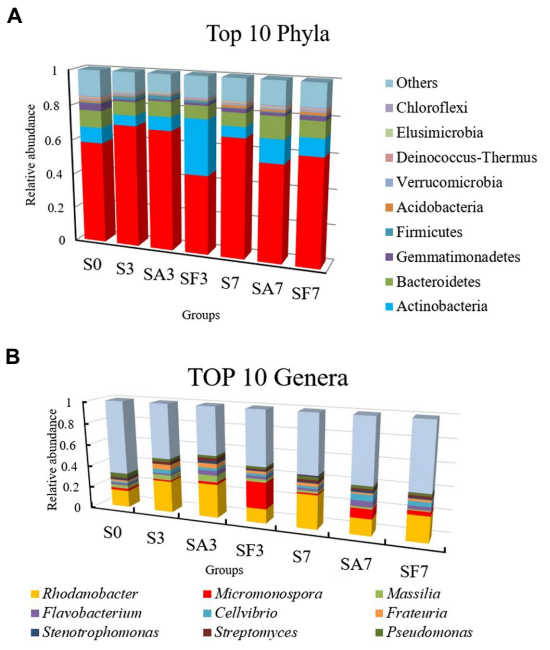

FIGURE 3
Assembly of core rhizosphere microbial communities. **(A)** Community bar-plot analysis of the relative abundance of rhizosphere microbial communities in the different soil groups at the phylum level. **(B)** Community bar-plot analysis of the relative abundance of rhizosphere microbial communities in the different soil groups at the genus level. S0, Mock-inoculation control (before treatment); S3, mock-inoculation control, 3 dpi; S7, mock-inoculation control, 7 dpi; SA3, SA+FON treatment, 3 dpi; SA7, SA+FON treatment, 7 dpi; SF3, FON treatment, 3 dpi; SF7, FON treatment, 7 dpi. FON, *Fusarium oxysporum* f. sp. *niveum*; SA, salicylic acid; dpi, days post inoculation. Three biological replicates per sample were analyzed. Data are expressed as mean±SE (n=3).

of hydrogenogenic CO oxidizers, which may play a significant role in helping plants against FON infection (Badger and Bek, 2008; Wang and Sugiyama, 2020). Overall, our results indicated that the application of SA changed the watermelon rhizosphere soil microbial communities.

For instance, at the phylum level, the abundances of Actinobacteria, Chlamydiae, Chloroflexi, Cyanobacteria, Dictyoglomi, Proteobacteria, Thermotogae, and Thaumarchaeota differed significantly between the SA3 and SF3 samples (Figure 4B). Moreover, the SA3 sample showed a significant abundance of Proteobacteria, whereas the SF3 sample was significantly enriched with Actinobacteria. In contrast, the SA7 sample had a significantly higher abundance of Blastocladiomycota, Dictyoglomi, and Elusimicrobiota, whereas the SF7 sample had a high abundance of Actinobacteria, Dictyoglomi, Gemmatimonadetes, Deinococcus-Thermus, Ascomycota, and Planctomycetes (Figure 4B). At the genus level, the abundance of *Rhodanobacter* increased significantly in the SA3 sample, whereas that of *Actinoplanes*, *Burkholderia*, *Chryseolinea*, *Luteimonas*, *Micromonospora*, *Nitrolancea*, *Ohtaekwangia*, *Sorangium*, *Sphingomonas*, and *Xanthomonas* decreased significantly compared to the levels in the SF3 sample (Figure 4C). However, the abundances of *Stenotrophomonas*, *Sphingomonas*, *Ramlibacter*, *Herbaspirillum*, *Polaromonas*, and *Azospirillum* were significantly higher, whereas those of *Dokdonella*, *Gemmatirosa*, *Castellaniella*, *Gemmatimonas*, *Chitinophaga*, *Myxococcus*, *Mizugakiibacter*, *Trichoderma*, and *Moritella* were significantly lower in the SA7 soil than in the SF7 sample (Figure 4C). Collectively, these results suggest that although the structure of the main soil microbial community did not change, the abundance of specific species was significantly altered at different time points after pathogen injection.

Functional annotations and gene taxonomy predictions for the different rhizosphere microbiomes

For the SA3 sample, KEGG analysis of the cluster at level 1 revealed the significant activation of four major pathways: environmental information processing, cellular processes, metabolism, and human diseases (Figure 5A). Detailed information on the 43 pathways at cluster level 2 is displayed in Figure 5B. The heatmap of the KEGG ortholog groups (Figure 5C) showed that K06042 (precorrin-8X/cobalt-precorrin-8 methyl mutase), K02055 (putative spermidine/putrescine transport system substrate-binding protein), K16164 (acyl pyruvate hydrolase), and K18930 (D-lactate dehydrogenase) were more highly enriched in the SF3 sample than in the SA3 soil. Furthermore, the distribution of linear discriminant analysis scores between the SA3 and SF3 KEGG ortholog groups indicated that K02014 (iron complex outer membrane receptor protein) was increased in SA3, whereas K03088 (RNA polymerase sigma-70 factor, ECF subfamily) was increased in SF3 (Figure 5C).

The heatmap of the eggNOG classification, where the significantly expressed genes were merged into 12 groups, is shown

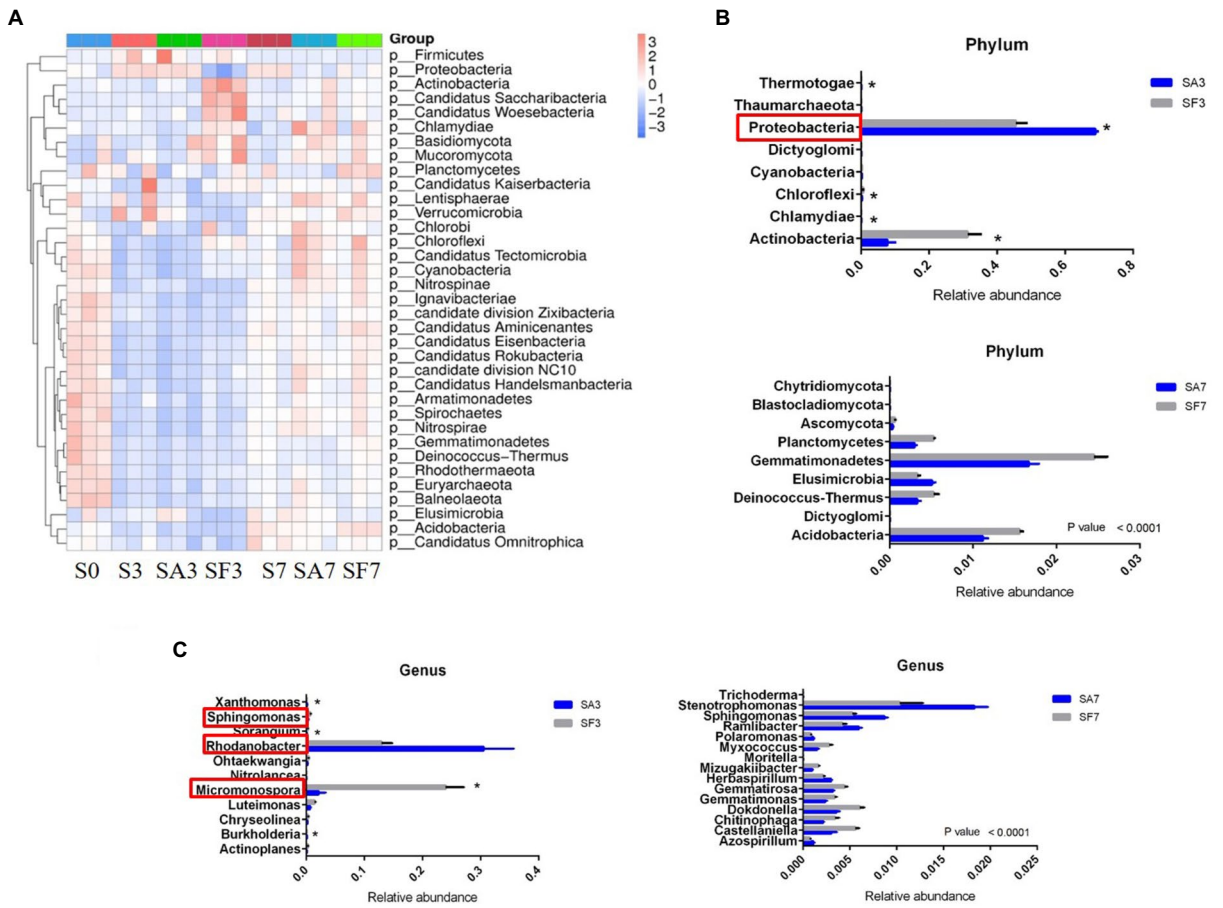

FIGURE 4
Dynamic changes in the significantly abundant rhizosphere microbial communities. **(A)** Heatmap of the dynamic changes in different phyla among the various soil groups. **(B)** Bar plots showing the significant differences in relative abundance of the main phyla. **(C)** Bar plots showing the significant differences in relative abundance of the main genera. Three biological replicates per samples were analyzed. Data are expressed as mean±SE (n=3). Multiple t-tests (*$p \leq 0.01$). S0, Mock-inoculation control, before treatment; S3, mock-inoculation control, 3 dpi; S7, mock-inoculation control, 7 dpi; SA3, SA+FON treatment, 3 dpi; SA7, SA+FON treatment, 7 dpi; SF3, FON treatment, 3 dpi; SF7, FON treatment, 7 dpi; FON, *Fusarium oxysporum* f. sp. *niveum*; SA, salicylic acid; dpi, days post-inoculation.

in Figure 6A. Histograms of the distribution of linear discriminant analysis scores for resistance genes with statistically significant differences between the groups are shown in Figure 6B. For instance, there was a significantly higher expression level of genes related to transcription, carbohydrate transport, and metabolism in SF3 than in S3 plants. The genes significantly expressed in SA3 belonged mainly to post-translational; intracellular trafficking, secretion; cell motility; and cell wall: membrane envelope biogenesis. In contrast, those in SF3 belonged primarily to transcription and secondary metabolite biosynthesis. However, SF7 had a significantly higher number of genes related to translation, ribosomal structure, and biogenesis; cell cycle control and cell division; carbohydrate transport and metabolism; intracellular trafficking, secretion; energy production and conversion; defense mechanisms; and replication, recombination, and repair.

A Venn diagram of the distribution of resistance genes among the five selected samples is shown in Figure 7A. Heatmap analysis of the six CAZy classes indicated that the highly enriched genes in SA3 were in the classes GH: glycoside hydrolases and PL: polysaccharide lyases (Figure 7B). Analysis of the relative abundance of Unigenes showed that the major facilitator superfamily antibiotic efflux pump (*bcr_1*), drug class of aminoglycoside antibiotics, resistance mechanism of antibiotic inactivation (*AAC6_IIC*), and *Serratia* metallo-beta-lactamase (*SMB_1*) genes were highly expressed in SA3, whereas the ATP-binding cassette antibiotic efflux pump (*msrC*), drug class of aminoglycoside antibiotic, resistance mechanism of antibiotic inactivation (*AAC6_IIC*), ATP-binding cassette antibiotic efflux pump, major facilitator superfamily antibiotic efflux pump, resistance-nodulation-cell division antibiotic efflux pump (*Pseudomonas_aeruginosa_soxR*), and defensin-resistant *mprF* (*Listeria_monocytogenes_mprF*) genes were increased in SA7 (Figure 7C). Finally, two-circle graphs (Figure 8) of the main phyla associated with the resistance genes expressed in the soil samples indicated that Proteobacteria were the predominant source in SA3, whereas Chloroflexi, Acidobacteria, and Cyanobacteria expressed most of the resistance genes in SA7. Interestingly, some resistance genes from Ascomycota were observed only in the SF groups and those from Firmicutes only in the SF7 group.

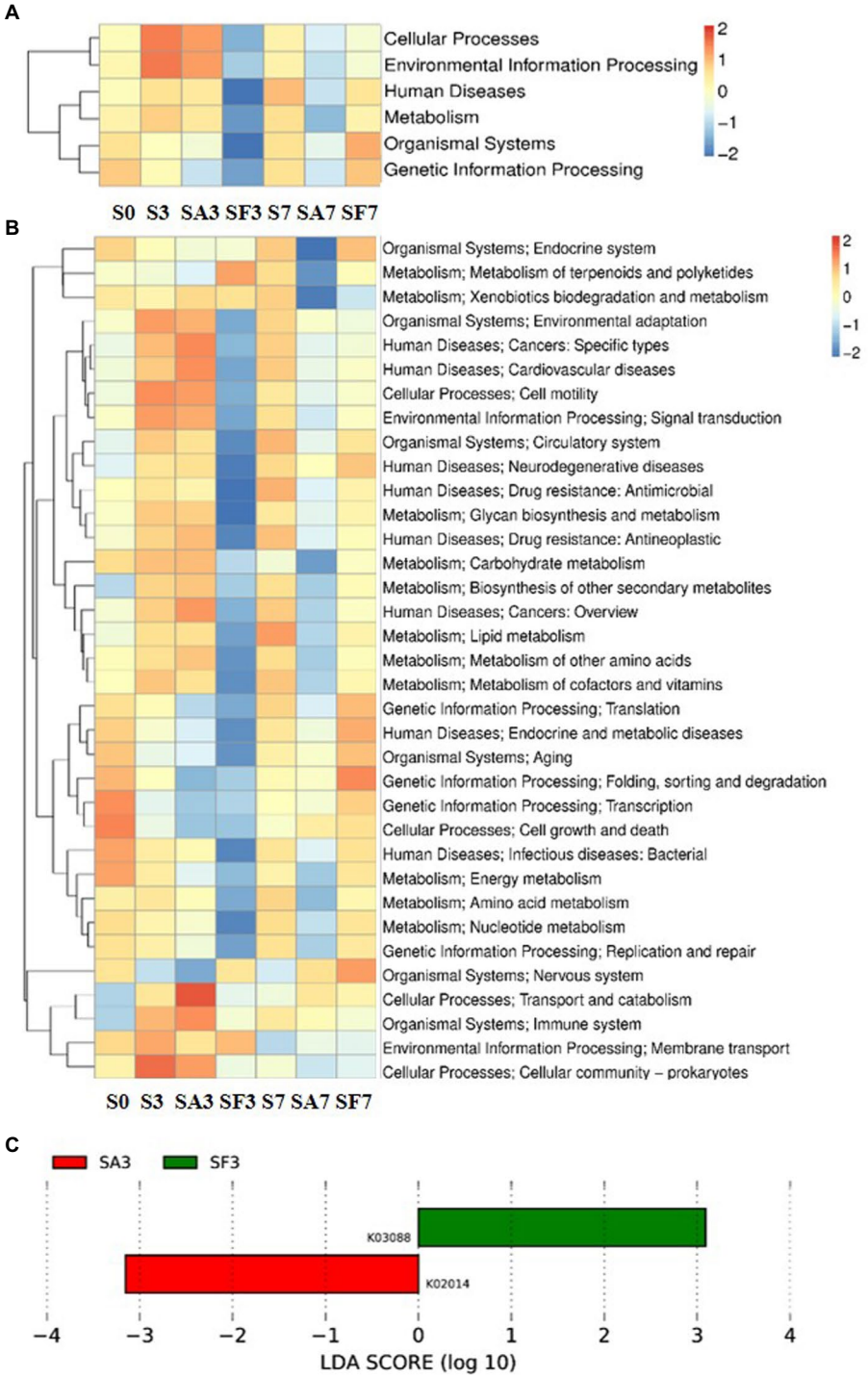

FIGURE 5
Functional diversity of the microbiomes among different soil samples based on KEGG pathways analysis **(A)** Heatmap of enrichment differences in six major metabolic pathways on level 1 among the samples. **(B)** Heatmap of enrichment differences in metabolic pathways on level 2 among the samples. The *X*-axis represents the sample group names; the *Y*-axis represents the KEGG metabolic pathway annotation information.
(C) Distribution of linear discriminant analysis (LDA) scores between the SA3 and SF3 KEGG ortholog groups. S0, Mock-inoculation control, before treatment; S3, mock-inoculation control, 3 dpi; S7, mock-inoculation control, 7 dpi; SA3, SA+FON treatment, 3 dpi; SA7, SA+FON treatment, 7 dpi; SF3, FON treatment, 3 dpi; SF7, FON treatment, 7 dpi; FON, *Fusarium oxysporum* f. sp. *niveum*; SA, salicylic acid; dpi, days post-inoculation.

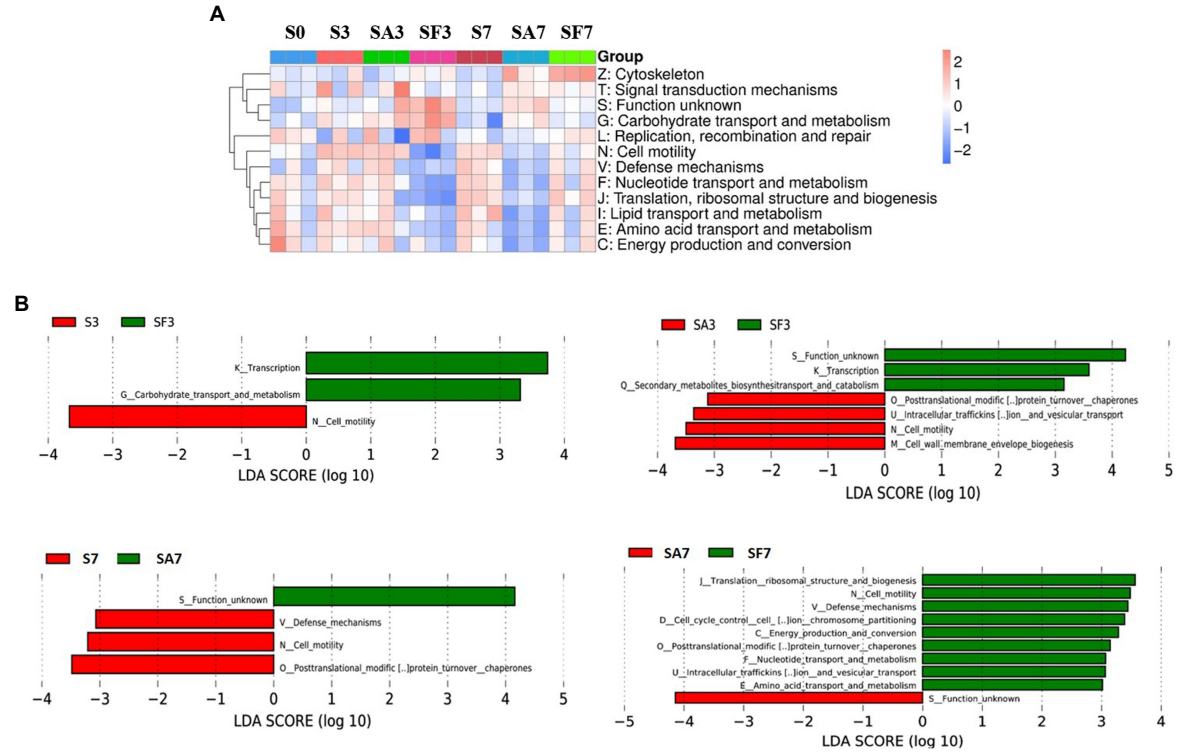

FIGURE 6
Functional diversity of the microbiomes among different soil samples based on eggNOG metabolic pathway analysis **(A)** Heatmap of enrichment differences in metabolic pathways among the samples. The *X*-axis represents the sample group name; the *Y*-axis represents the eggNOG metabolic pathway annotation information. **(B)** Distribution of LDA scores of functional differences between samples. The *X*-axis represents the LDA score; the *Y*-axis represents the eggNOG metabolic pathway annotation information. Three biological replicates per sample were analyzed. Data are expressed as mean±SE (n=3). S0, Mock-inoculation control, before treatment; S3, mock-inoculation control, 3 dpi; S7, mock-inoculation control, 7 dpi; SA3, SA+FON treatment, 3 dpi; SA7, SA+FON treatment, 7dpi; SF3, FON treatment, 3 dpi; SF7, FON treatment, 7 dpi. FON, *Fusarium oxysporum* f. sp. *niveum*; SA, salicylic acid; dpi, days post-inoculation.

Discussion

Exogenous salicylic acid application leads to the enrichment of beneficial microbes in the watermelon rhizosphere

The rhizosphere plays a fundamental role in microbe–microbe and plant–soil–microbe interactions. Microbes and their interactions can extend the capacity of plants for disease resistance and improve their nutrient use efficiency (Berendsen et al., 2018). Emerging evidence indicates that some microbial symbionts communicate with the plant immune system through multiple feedback mechanisms, giving the plant the ability to resist pathogens and to maintain growth and development (Liu et al., 2021). Many studies have emphasized the role of soil microbial communities in enhancing plant growth and health (Aleklett et al., 2018; Toju et al., 2018). For example, Xin et al. found that the plant immune system is required to maintain the normal growth of commensal bacteria in *Arabidopsis* (Xin et al., 2016). Other studies have reported that assemblages of host-specific microbiomes in the rhizosphere are vital for disease resistance. For instance, some disease-resistant crop varieties are enriched in specific sets of bacterial species in the rhizosphere, which contribute to the suppression of pathogens (Delgado-Baquerizo et al., 2018). Another study showed that SA causes changes in the microbiome through allelopathy in wheat (Kong et al., 2020). It is not known how plant roots normally select and maintain a healthy rhizosphere microbiota. SA plays an important role in regulating plant immunity, which is necessary for systemically acquired resistance (Trivedi et al., 2020). In agreement with this theory, our results indicated that although the structure of the main soil microbial community did not change, specific microbes were significantly altered at different time points after pathogen injection. Likewise, we observed that Proteobacteria, the second largest phylum of hydrogenogenic CO oxidizers (Badger and Bek, 2008; Wang and Sugiyama, 2020), accumulated significantly in SA3. Lebeis et al. found that SA could modulate the root microbiome of *A. thaliana*. Specifically, plants with altered SA signaling had root microbiomes that differed from each other in their relative abundance of Proteobacteria as one of the core microbiomes when compared with those of wild-type plants (Lebeis et al., 2015). Furthermore, at the genus level, SA3 had a significantly higher abundance of

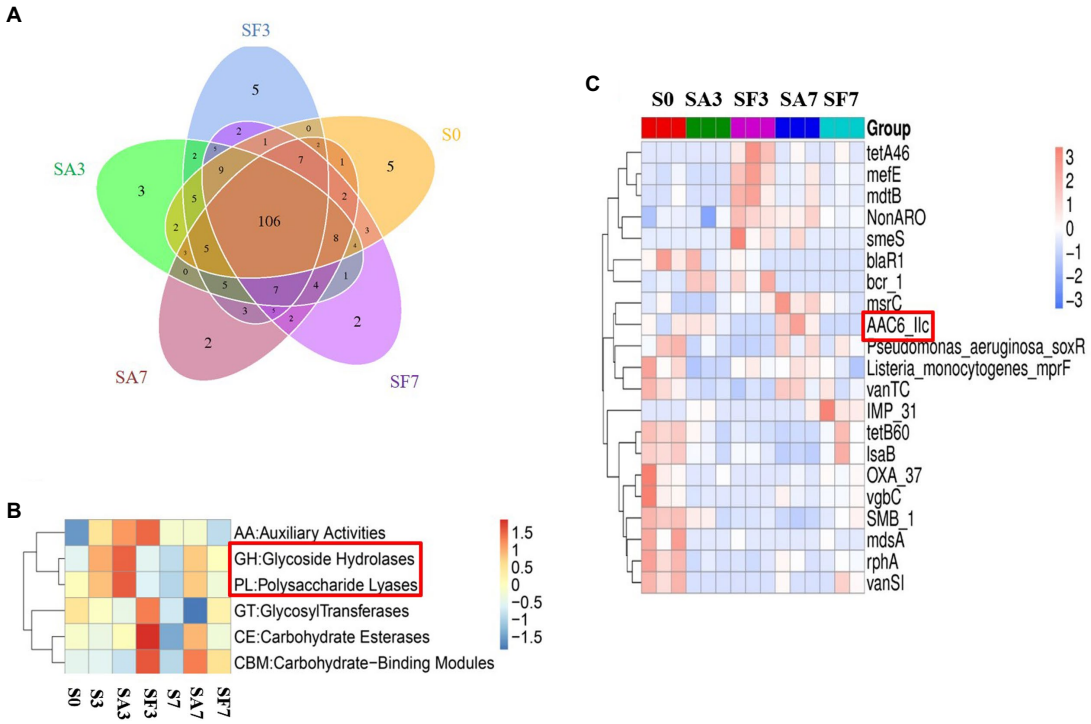

FIGURE 7
Differential abundance of functional resistance genes among different soil samples **(A)** Venn diagram showing the distribution of functional resistance genes among the five selected sample groups. **(B)** Heatmap of the differences in relative abundance of six CAZy classes among the samples. **(C)** Heatmap of the differences in relative abundance of the antibiotic resistance ontology (ARO) cluster among the samples. S0, Mock-inoculation control, before treatment; S3, mock-inoculation control, 3 dpi; S7, mock-inoculation control, 7 dpi; SA3, SA+FON treatment, 3 dpi; SA7, SA+FON treatment, 7 dpi; SF3, FON treatment, 3 dpi; SF7, FON treatment, 7 dpi. FON, *Fusarium oxysporum* f. sp. *niveum*; SA, salicylic acid; dpi, days post-inoculation.

Rhodanobacter than SF3 and SA7 had a higher abundance of *Azospirillum*, *Herbaspirillum*, *Stenotrophomonas*, and *Sphingomonas* than SF7. *Rhodanobacter* is capable of oxidizing ammonia and of denitrification (De Cercq et al., 2006; Huo et al., 2018). Some members of the genus *Azospirillum* exhibit biocontrol activity against phytopathogens and have been used as biofertilizers because of their plant growth-promoting activities, such as biological nitrogen fixation, hormone production, phosphate solubilization, and siderophore production (Mendez-Gomez et al., 2020). *Sphingomonas* is considered an abundant microbial resource for the biodegradation of aromatic compounds, thus showing great potential for environmental protection and industrial production applications because of its high metabolic capacity and multifunctional physiological characteristics (Vorholt et al., 2017). *Stenotrophomonas maltophilia*, which exists widely in water, soil, and animals, is a multidrug-resistant opportunistic pathogen that causes life-threatening infections in immunocompromised individuals (Messiha et al., 2007; Mendes et al., 2013; Hassan and Bano, 2016). *Herbaspirillum* species have been described as closely associated with plants, both endophytically and epiphytically, because their nitrogenase activity promotes plant growth (Wang et al., 2014). For instance, using histochemical analysis, *Herbaspirillum seropedicae* has been shown to colonize the root surfaces and inner tissues of maize, sorghum, wheat, and rice seedlings grown in vermiculite (Ramos et al., 2020).

Therefore, these significantly altered microbial communities confirmed our hypothesis that SA can recruit beneficial microorganisms (such as *Rhodanobacter*, *Sphingomonas*, *and Micromonospora*) in the watermelon rhizosphere. The next question that needs to be answered is whether SA-influenced changes in rhizosphere microflora are beneficial to the antagonism of plants against pathogens, that is, is the increased resistance of plants to pathogens induced directly by SA alone, or by the rhizosphere microbiota, or by both?

Significantly expressed microbiome genes may interact with salicylic acid signaling to regulate watermelon resistance to disease

Many researchers have found that SA and plant-associated beneficial microorganisms are key candidates for systemic acquired resistance (SAR) and induced systemic resistance (ISR), respectively (Berendsen et al., 2018; Teixeira et al., 2019). Therefore, to elucidate the molecular mechanism through which the rhizosphere microbial community cooperates with the watermelon plant to induce

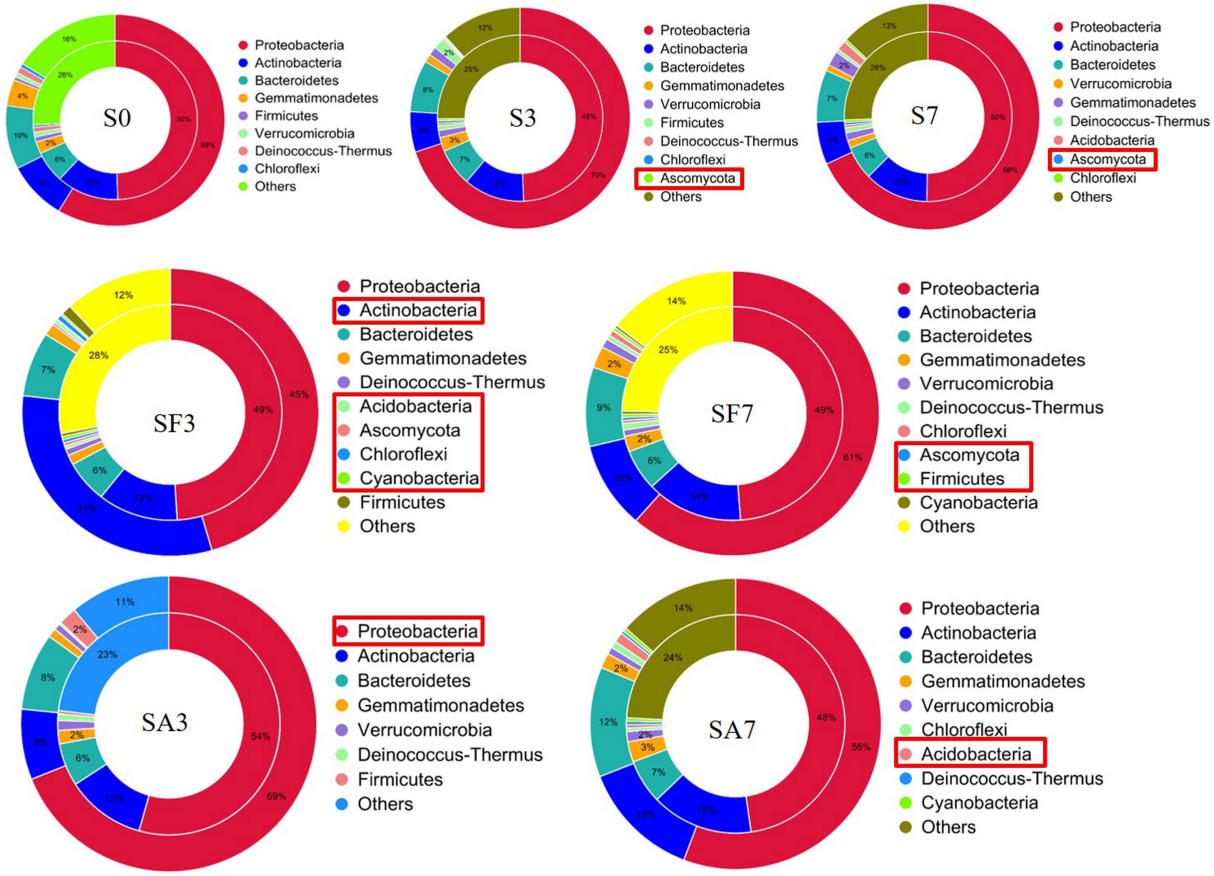

FIGURE 8
Comparison of the relationship between resistance genes and main phyla in the different soil samples S0, Mock-inoculation control, before treatment; S3, mock-inoculation control, 3 dpi; S7, mock-inoculation control, 7 dpi; SA3, SA+FON treatment, 3 dpi; SA7, SA+FON treatment, 7 dpi; SF3: FON treatment, 3 dpi; SF7, FON treatment, 7 dpi. The inner circle is the phylum distribution for the antibiotic resistance ontology (ARO) cluster, and the outer circle is the phylum distribution for all sample genes in the group. FON, *Fusarium oxysporum* f. sp. *niveum*; SA, salicylic acid; dpi, days post inoculation.

resistance against *Fusarium* wilt, we blasted unique genes to annotate their functions. Surprisingly, genes enriched in environmental information processing, cellular processes, and metabolism pathways were significantly more highly expressed in SA3 than in SF3. Furthermore, K02014 (iron complex outer membrane receptor protein) was expressed at significantly higher levels in SA3 than in SF3. Simultaneously, the genes enriched in the process groups of cell motility and cell wall: membrane envelope biogenesis were expressed more significantly in SA3 than in SF3. These results confirm our hypothesis that the rhizosphere microbiome assemblage is affected by SA signal transduction pathways (Mendes et al., 2011; Chaparro et al., 2014; Vorholt et al., 2017; Delgado-Baquerizo et al., 2018). Notably, the resistance genes from GHs and PLs were highly accumulated in SA3 compared with those in the other soil groups. In particular, *AAC6_IIC* was consistently more significantly accumulated in the SA groups, indicating that it may play an important role in interplay with plant lipid membranes. Furthermore, we noticed that the relative abundance of Proteobacteria corresponding to resistance genes was the highest post-inoculation, which means that more of such genes may come from species in this phylum. Our results confirm the conclusions of other studies that plant genetics and agricultural practices can potentially impose selective pressures on specific microbes and microbial communities. Thus, our findings not only show that SA treatment is beneficial to the antagonism of plants against pathogens but also suggest that, during pathogen infection, the rhizosphere microbiome may play a key role in activating a series of defensive feedback mechanisms in the plant through SA signal transduction pathways.

Conclusion

In conclusion, our results indicate that exogenous SA treatment can specifically increase some beneficial rhizosphere species that can confer resistance against FON inoculation. The glycoside hydrolase and polysaccharide lyase genes in the microbiome, specifically from a group of beneficial microbes (such as *Rhodanobacter*, *Sphingomonas*, *and Micromonospora*), may potentially induce activation of the plant immune system against *Fusarium* wilt disease and promote plant growth. Our results provide a novel strategy for controlling *Fusarium* wilt in watermelon by manipulating the

rhizosphere microbiome through phytohormones, such as exogenous SA treatment. Furthermore, we aim to elucidate the mechanisms underlying the interplay between lipid membrane signaling and SA signal transduction pathways in future studies.

Data availability statement

The datasets presented in this study can be found in online repositories. The names of the repository/repositories and accession number(s) can be found in the article/Supplementary material.

Author contributions

FZ and RW: conceptualization. YF, ZW, and FZ: methodology. PW, KY, and FZ: investigation. FZ: writing—original draft preparation. FZ and RW: writing—review and editing and funding acquisition. LX and RW: supervision. All authors contributed to the article and approved the submitted version.

Funding

This study was financially supported by the National Natural Science Foundation of China (nos. 31671777 and 31871714) to RW, the Natural Science Foundation of Hunan Province, China (no. 2022JJ40213), and the Natural Science Foundation of Changsha City, China (no. kq2202335) to FZ.

Conflict of interest

The authors declare that the research was conducted in the absence of any commercial or financial relationships that could be construed as a potential conflict of interest.

Publisher's note

All claims expressed in this article are solely those of the authors and do not necessarily represent those of their affiliated organizations, or those of the publisher, the editors and the reviewers. Any product that may be evaluated in this article, or claim that may be made by its manufacturer, is not guaranteed or endorsed by the publisher.

Supplementary material

The Supplementary material for this article can be found online at: https://www.frontiersin.org/articles/10.3389/fmicb.2022.1015038/full#supplementary-material

References

Aleklett, K., Kiers, E. T., Ohlsson, P., Shimizu, T. S., Caldas, V. E., and Hammer, E. C. (2018). Build your own soil: exploring microfluidics to create microbial habitat structures. *ISME J.* 12, 312–319. doi: 10.1038/ismej.2017.184

Badger, M. R., and Bek, E. J. (2008). Multiple rubisco forms in proteobacteria: their functional significance in relation to co2 acquisition by the cbb cycle. *J. Exp. Bot.* 59, 1525–1541. doi: 10.1093/jxb/erm297

Berendsen, R. L., Vismans, G., Yu, K., Song, Y., de Jonge, R., Burgman, W. P., et al. (2018). Disease-induced assemblage of a plant-beneficial bacterial consortium. *ISME J.* 12, 1496–1507. doi: 10.1038/s41396-018-0093-1

Chaparro, J. M., Badri, D. V., and Vivanco, J. M. (2014). Rhizosphere microbiome assemblage is affected by plant development. *ISME J.* 8, 790–803. doi: 10.1038/ismej.2013.196

Chen, T., Nomura, K., Wang, X., Sohrabi, R., Xu, J., Yao, L., et al. (2020). A plant genetic network for preventing dysbiosis in the phyllosphere. *Nature* 580, 653–657. doi: 10.1038/s41586-020-2185-0

De Cercq, D., Van Tappen, S., Cleenwerck, I., Ceustermans, A., Swings, J., Coosemans, J., et al. (2006). Rhodanobacter spathiphylli sp. nov., a gammaproteobacterium isolated from the roots of Spathiphyllum plants grown in a compost-amended potting mix. *Int. J. Syst. Evol. Microbiol.* 56, 1755–1759. doi: 10.1099/ijs.0.64131-0

Delgado-Baquerizo, M., Oliverio, A. M., Brewer, T. E., Benavent-Gonzalez, A., Eldridge, D. J., Bardgett, R. D., et al. (2018). A global atlas of the dominant bacteria found in soil. *Science* 359, 320–325. doi: 10.1126/science.aap9516

Everts, K. L., and Himmelstein, J. C. (2015). Fusarium wilt of watermelon: towards sustainable management of a re-emerging plant disease. *Crop Prot.* 73, 93–99. doi: 10.1016/j.cropro.2015.02.019

Hassan, T. U., and Bano, A. (2016). Comparitive effects of wild type Stenotrophomonas maltophilia and its IAA deficient mutants on wheat. *Plant Biol.* 18, 835–841. doi: 10.1111/plb.12477

Heintz, C., and Mair, W. (2014). You are what you host: microbiome modulation of the aging process. *Cells* 156, 408–411. doi: 10.1016/j.cell.2014.01.025

Huo, Y., Kang, J. P., Park, J. K., Li, J., Chen, L., and Yang, D. C. (2018). Rhodanobacter ginsengiterrae sp. nov., an antagonistic bacterium against root rot fungal pathogen fusarium solani, isolated from ginseng rhizospheric soil. *Arch. Microbiol.* 200, 1457–1463. doi: 10.1007/s00203-018-1560-9

Kong, H. G., Song, G. C., Sim, H. J., and Ryu, C. M. (2020). Achieving similar root microbiota composition in neighbouring plants through airborne signalling. *ISME J.* 15, 397–408. doi: 10.1038/s41396-020-00759-z

Lebeis, S. L., Paredes, S. H., Lundberg, D. S., Breakfield, N., Gehring, J., McDonald, M., et al. (2015). Salicylic acid modulates colonization of the root microbiome by specific bacterial taxa. *Science* 349, 860–864. doi: 10.1126/SCIENCE.AAA8764

Levy, A., Salas Gonzalez, I., Mittelviefhaus, M., Clingenpeel, S., Herrera Paredes, S., Miao, J., et al. (2017). Genomic features of bacterial adaptation to plants. *Nat. Genet.* 50, 138–150. doi: 10.1038/s41588-017-0012-9

Li, C., Fu, X., Zhou, X., Liu, S., Xia, Y., Li, N., et al. (2019). Treatment with wheat root exudates and soil microorganisms from wheat/watermelon companion cropping can induce watermelon disease resistance against *fusarium oxysporum f. sp. niveum*. *Plant Dis.* 103, 1693–1702. doi: 10.1094/PDIS-08-18-1387-RE

Liu, H., Li, J., Carvalhais, L. C., Percy, C. D., Prakash Verma, J., Schenk, P. M., et al. (2021). Evidence for the plant recruitment of beneficial microbes to suppress soil-borne pathogens. *New Phytol.* 229, 2873–2885. doi: 10.1111/nph.17057

Lü, G., Guo, S., Zhang, H., Geng, L., Song, F., Fei, Z., et al. (2011). Transcriptional profiling of watermelon during its incompatible interaction with fusarium oxysporum f. sp. niveum. *Eur. J. Plant Pathol.* 131, 585–601. doi: 10.1007/s10658-011-9833-z

Lv, H., Cao, H., Nawaz, M. A., Sohail, H., Huang, Y., Cheng, F., et al. (2018). Wheat intercropping enhances the resistance of watermelon to fusarium wilt. *Front. Plant Sci.* 9:696. doi: 10.3389/fpls.2018.00696

Mendes, R., Garbeva, P., and Raaijmakers, J. M. (2013). The rhizosphere microbiome: significance of plant beneficial, plant pathogenic, and human pathogenic microorganisms. *FEMS Microbiol. Rev.* 37, 634–663. doi: 10.1111/1574-6976.12028

Mendes, R., Kruijt, M., de Bruijn, I., Dekkers, E., van der Voort, M., Schneider, J. H., et al. (2011). Deciphering the rhizosphere microbiome for disease-suppressive bacteria. *Science* 332, 1097–1100. doi: 10.1126/science.1203980

Mendez-Gomez, M., Castro-Mercado, E., Pena-Uribe, C. A., L Cruz, H. R., Lopez-Bucio, J., and Garcia-Pineda, E. (2020). Azospirillum brasilense Sp245 lipopolysaccharides induce target of rapamycin signaling and growth in Arabidopsis thaliana. *J. Plant Physiol.* 253:153270. doi: 10.1016/j.jplph.2020.153270

Messiha, N. A. S., Diepeningen, A. D. V., Farag, N. S., Abdallah, S. A., Janse, J. D., and Bruggen, A. H. C. V. (2007). Stenotrophomonas maltophilia: A new potential biocontrol agent *of Ralstonia solanacearum*, causal agent of potato brown rot. *Eur. J. Plant Pathol.* 118, 211–225. doi: 10.1007/s10658-007-9136-6

Ramos, A. C., Melo, J., de Souza, S. B., Bertolazi, A. A., Silva, R. A., Rodrigues, W. P., et al. (2020). Inoculation with the endophytic bacterium Herbaspirillum seropedicae promotes growth, nutrient uptake and photosynthetic efficiency in rice. *Planta* 252:87. doi: 10.1007/s00425-020-03496-x

Ren, L., Huo, H., Zhang, F., Hao, W., Xiao, L., Dong, C., et al. (2016). The components of rice and watermelon root exudates and their effects on pathogenic fungus and watermelon defense. *Plant Signal. Behav.* 11:e1187357. doi: 10.1080/15592324.2016.1187357

Teixeira, P. J. P., Colaianni, N. R., Fitzpatrick, C. R., and Dangl, J. L. (2019). Beyond pathogens: microbiota interactions with the plant immune system. *Curr. Opin. Microbiol.* 49, 7–17. doi: 10.1016/j.mib.2019.08.003

Toju, H., Peay, K. G., Yamamichi, M., Narisawa, K., Hiruma, K., Naito, K., et al. (2018). Core microbiomes for sustainable agroecosystems. *Nat. Plants* 4, 247–257. doi: 10.1038/s41477-018-0139-4

Trivedi, P., Leach, J. E., Tringe, S. G., Sa, T., and Singh, B. K. (2020). Plant-microbiome interactions: from community assembly to plant health. *Nat. Rev. Microbiol.* 18, 607–621. doi: 10.1038/s41579-020-0412-1

Vorholt, J. A., Vogel, C., Carlström, C. I., and Müller, D. B. (2017). Establishing causality: opportunities of synthetic communities for plant microbiome research. *Cell Host Microbe* 22, 142–155. doi: 10.1016/j.chom.2017.07.004

Wang, X., Cao, Y., Tang, X., Ma, X., Gao, J., and Zhang, X. (2014). Rice endogenous nitrogen fixing and growth promoting bacterium Herbaspirillum seropedicae DX35. *Acta Microbiol Sin.* 54, 292–298. doi: 10.13343/j.cnki.wsxb.2014.03.006

Wang, B., and Sugiyama, S. (2020). Phylogenetic signal of host plants in the bacterial and fungal root microbiomes of cultivated angiosperms. *Plant J.* 104, 522–531. doi: 10.1111/tpj.14943

Xin, X. F., Nomura, K., Aung, K., Velasquez, A. C., Yao, J., Boutrot, F., et al. (2016). Bacteria establish an aqueous living space in plants crucial for virulence. *Nature* 539, 524–529. doi: 10.1038/nature20166

Xu, W., Wang, Z., and Wu, F. (2015). Companion cropping with wheat increases resistance to fusarium wilt in watermelon and the roles of root exudates in watermelon root growth. *Physiol. Mol. Plant Pathol.* 90, 12–20. doi: 10.1016/j.pmpp.2015.02.003

Yang, L., Li, B., Zheng, X. Y., Li, J., Yang, M., Dong, X., et al. (2015). Salicylic acid biosynthesis is enhanced and contributes to increased biotrophic pathogen resistance in Arabidopsis hybrids. *Nat. Commun.* 6:7309. doi: 10.1038/ncomms8309

Zhang, Y., and Li, X. (2019). Salicylic acid: biosynthesis, perception, and contributions to plant immunity. *Curr. Opin. Plant Biol.* 50, 29–36. doi: 10.1016/j.pbi.2019.02.004

Zhu, F., Tian, C., Zhang, Y., Xiao, J., Wei, L., and Liang, Z. (2018). Effects of different fertilization treatments on soil microbial community structure and the occurrence of watermelon wilt. *Chin. J. Biol. Control* 34, 589–597. doi: 10.16409/j.cnki.2095-039x.2018.04.014

Zhu, F., Wang, Z., Fang, Y., Tong, J., Xiang, J., Yang, K., et al. (2022a). Study on the role of Phytohormones in resistance to watermelon fusarium wilt. *Plants* 11:156. doi: 10.3390/plants11020156

Zhu, F., Wang, Z., Su, W., Tong, J., Fang, Y., Luo, Z., et al. (2022b). Study on the role of salicylic acid in watermelon-resistant fusarium wilt under different growth conditions. *Plants* 11:293. doi: 10.3390/plants11030293

Zhu, F., Xiao, J., Zhang, Y., Wei, L., and Liang, Z. (2020). Dazomet application suppressed watermelon wilt by the altered soil microbial community. *Sci. Rep.* 10:21668. doi: 10.1038/s41598-020-78839-5

Zhu, F., Zhang, Y., Xiao, J., Wei, L., and Liang, Z. (2019). Regulation of soil microbial community structures and watermelon fusarium wilt by using bio-organic fertilizer. *Acta Microbiol Sin.* 59, 2323–2333. doi: 10.13343/j.cnki.wsxb.20190038

frontiers | Frontiers in Microbiology

TYPE Original Research
PUBLISHED 09 January 2023
DOI 10.3389/fmicb.2022.1075957

OPEN ACCESS

EDITED BY
Yu Shi,
Henan University, China

REVIEWED BY
Yurong Yang,
Northeast Normal University, China
Dilin Liu,
Guangdong Academy of Agricultural Sciences (GDAAS), China

*CORRESPONDENCE
Jidong Wang
jidongwang@jaas.ac.cn

SPECIALTY SECTION
This article was submitted to Microbe and Virus Interactions with Plants, a section of the journal Frontiers in Microbiology

RECEIVED 21 October 2022
ACCEPTED 19 December 2022
PUBLISHED 09 January 2023

CITATION
Yuan J, Shi K, Zhou X, Wang L, Xu C, Zhang H, Zhu G, Si C, Wang J and Zhang Y (2023) Interactive impact of potassium and arbuscular mycorrhizal fungi on the root morphology and nutrient uptake of sweet potato (*Ipomoea batatas* L.). *Front. Microbiol.* 13:1075957. doi: 10.3389/fmicb.2022.1075957

Interactive impact of potassium and arbuscular mycorrhizal fungi on the root morphology and nutrient uptake of sweet potato (*Ipomoea batatas* L.)

Jie Yuan[1,2], Kun Shi[1,2,3], Xiaoyue Zhou[1,2,3], Lei Wang[1,2], Cong Xu[1,2], Hui Zhang[1,2], Guopeng Zhu[3], Chengcheng Si[3], Jidong Wang[1,2]* and Yongchun Zhang[1,2]

[1]Institute of Agricultural Resources and Environment, Jiangsu Academy of Agricultural Sciences, Nanjing, Jiangsu, China, [2]National Agricultural Experimental Station for Agricultural Envrionment, Nanjing, Jiangsu, China, [3]College of Horticulture, Hainan University, Haikou, Hainan, China

Sweet potato is a typical "potassium (K)-favoring" food crop and strongly dependent on arbuscular mycorrhizal fungi (AMF). Recent studies show the importance of K and AMF to morphology optimization and nutrient uptake regulation of sweet potato; meanwhile, the interaction exists between K and K use efficiency (KIUE) in sweet potato. To date, only a few studies have shown that AMF can improve plant K nutrition, and whether the benefits conferred by AMF on plant are related to K remains unclear. In this study, low-KIUE genotype "N1" and high-KIUE genotype "Xu28" were used as experimental sweet potato; *Funneliformis mosseae* (FM) and *Claroideoglomus etunicatum* (CE) were used as experimental AMF. In a pot experiment, plants "N1" and "Xu28" were inoculated with FM or CE, and applied with or without K fertilizer to uncover the effects of K application and AMF inoculation on the root morphology and nutrient absorption of sweet potato during their growing period. Results demonstrated that AMF inoculation-improved root morphology of sweet potato highly relied on K application. With K application, AMF inoculation significantly increased root tip number of "N1" in the swelling stage and optimized multiple root morphological indexes (total root length, root surface area, root volume, root diameter, root branch number, and root tip number) of "Xu28" and CE had the best optimization effect on the root morphology of "Xu28". In addition, CE inoculation significantly promoted root dry matter accumulation of "Xu28" in the swelling and harvesting stages, coordinated aerial part and root growth of "Xu28", reduced the dry matter to leaf and petiole, and was beneficial to dry matter allocation to the root under conditions of K supply. Another promising finding was that CE inoculation could limit K allocation to the aboveground and promote root K accumulation of "Xu28" under the condition with K application. The above results lead to the

conclusion that K and CE displayed a synergistic effect on root development and K acquisition of high-KIUE "Xu28". This study could provide a theoretical basis for more scientific application of AMF in sweet potato cultivation and will help further clarify the outcomes of plant-K–AMF interactions.

KEYWORDS

sweet potato, arbuscular mycorrhizal fungi, potassium, nutrient uptake, root morphology, tuberous root yield

Introduction

Many tuber and storage root crops owing to their high nutritional values offer high potential to overcome food security issues (Kondhare et al., 2021). Sweet potato [*Ipomoea batatas* (L.) Lam.], belongs to the Convolvulaceae family, is widely grown in tropical and subtropical climates worldwide (Minemba et al., 2019), and it is an essential root crop and a high-yield food, which guarantees food security and improves the nutritional status of people (Liu et al., 2019; Wang et al., 2022a). It is worth noting that the root system of sweet potato is involved not only in uptake of water and mineral nutrient but also in storage of photosynthate, and hence root growth and differentiation are closely related to tuberous root yield (Gao et al., 2021). Less root differentiation and low nutrient uptake efficiency are currently the main obstacles limiting the further improvement of sweet potato yield production. As documented, the average root diameter and root volume of sweet potato reflect the root differentiation, and the total root length, root surface area, and root tip number determine the water and nutrient absorption efficiency (Liu et al., 2017). Therefore, it is imperative to seek effective methods for root morphology and nutrient uptake optimization. Previous studies have reported that soil and rhizosphere microbial activities are the major factors that determine the availability of nutrients to plants and consequently have significant influences on root growth and plant productivity (Wang et al., 2017). Recent evidence suggests that fertilization optimization and microbial inoculation were effective tools for sweet potato cultivation (Minemba et al., 2019; Alhadidi et al., 2021).

Sweet potato is a typical versatile crop with higher requirements for K for optimum production throughout the growth period than cereals, oilseeds, and commercial crops (Tang et al., 2015). Over the past few years, studies have proven that K was quite important for root system development and the final tuberous root yield of sweet potato (Gao et al., 2021). As estimated, about 10 kg K was required to produce 1,000 kg (on dry matter [DM] basis) tuberous root of sweet potato (George et al., 2002). The K utilization efficiency (KIUE) was interlinked with K uptake (Wang et al., 2017). Using K-efficient genotypes in combination with appropriate soil fertilization worked as an optimal K nutrient management strategy for sustainable and environmentally protective crop production (Romheld and Kirkby, 2010). In 1993, a study reported the significant interaction between environment and K supply on sweet potato biomass production and KIUE (Woodend and Glass, 1993). Our previous studies have selected 5 out of 108 sweet potato genotypes based on the significant differences in KIUE among the field experiment (Wang et al., 2015). Then, we investigated the interactions between environmental factors and KIUE genotype of sweet potato and found that high-KIUE genotype had a more optimal partitioning of K to economic sink as well as higher K was associated with the resource–sink relationship at different growth stages than did low-KIUE genotype (Wang et al., 2017).

Arbuscular mycorrhizal fungi (AMF) could live in a mutualistic symbiosis with plant roots of the majority (> 80%) of terrestrial plant species (Kalamulla et al., 2022; Seemakram et al., 2022). Sweet potato was easily colonized by mycorrhizal fungi (O'Keefe and Sylvia, 1993; Minemba et al., 2019). AMF varied in their ability to establish after inoculation, and in their effect on the yield and quality of sweet potato tubers (Farmer et al., 2007). Recently, some beneficial effects of AMF on the performance of sweet potato were reported (Tong et al., 2013; Yooyongwech et al., 2016; Alhadidi et al., 2021), such as water-deficit tolerance improvement, β-carotene concentration increase, root morphology regulation, and nutrient acquisition alternation. Therefore, the beneficial interaction of AMF with sweet potato is considered suitable for the cultivation of sweet potato. Typically, AMF develop extraradical mycelia that extend the depletion zone that develops around roots, and facilitate the acquisition of nutrients of low mobility (Seemakram et al., 2022). Consistent with this phenomenon, a meta-analysis about the effects of AMF on plant growth and nutrient uptake reflected that AMF could increase plant nitrogen (N), phosphorus (P), and K uptake by 22.1, 36.3, and

Abbreviations: K, potassium; AMF, Arbuscular Mycorrhizal Fungi; KIUE, K use efficiency; *F. mosseae*, *Funneliformis mosseae*; FM, *Funneliformis mosseae*; *C. etunicatum*, *Claroideoglomus etunicatum*; CE, *Claroideoglomus etunicatum*; N, nitrogen; P, phosphorus; −FM, inoculated with sterilized FM; −CE, inoculated with sterilized CE; +FM, inoculated with FM; +CE, inoculated with CE; DPI, days post inoculation; DM, dry matter; FM, fresh matter; ANOVA, analysis of variance; G, genotype.

18.5%, respectively (Chandrasekaran, 2020). It is important to note that the enhanced nutrient uptake by AMF is ascribed to regulation in root elongation, lateral root and root hair formation, and root surface area and root volume expansion (Chandrasekaran, 2020). However, only a few studies have shown that AMF can improve plant K nutrition (Garcia and Zimmermann, 2014). To date, there is still no report on the effects of AMF inoculation on K uptake of sweet potato, and whether the benefits conferred by AMF on plants are related to K remains unknown. Given the importance of K and AMF to morphology optimization and nutrient uptake regulation of sweet potato (Minemba et al., 2019; Alhadidi et al., 2021), the interaction exists between K and KIUE in sweet potato (Wang et al., 2017); hence, a global understanding of the interactive impact of K and AMF on the tuberous root yield, root morphology, and nutrient uptake of different KIUE genotypes of sweet potato should be considered.

In this study, low KIUE genotype "N1" and high KIUE genotype "Xu28" were used as the experimental varieties of sweet potato based on our previous results (Wang et al., 2015, 2017); *Funneliformis mosseae* (FM) and *Claroideoglomus etunicatum* (CE) were used as the experimental AMF mainly considering the existing studies (Gai et al., 2006; Alhadidi et al., 2021). In a pot experiment, the plants "N1" and "Xu28" were inoculated with FM or CE, and applied with or without K fertilizer to uncover the effects of K application and AMF inoculation on the root morphology and nutrient absorption of sweet potato during their growing period. The following three essential questions were addressed throughout this article: (1) How K application and AMF inoculation differentially affect root morphology and nutrient uptake of low-KIUE and high-KIUE sweet potato? (2) Whether there are interactive effects on the root morphology and nutrient uptake between K application and AMF inoculation? and (3) Which is the best combination of K (with or without K application) and AMF (FM or CE inoculation)?

Materials and methods

Soil, plant, and AMF materials

The soil was sandy loam fluvo-aqic (Eutyic Cambisol) collected from Jiangyan City, Jiangsu Province (Wang et al., 2017). Before the experiment began, plant debris and rocks were removed from the soil. The soil sample used in this study contained (on a DM basis) 52.01 g kg^{-1} alkali-hydrolyzable N; 12.15 mg kg^{-1} Olsen-P; 53 mg kg^{-1} available K (with NH_4OAC extraction); and 15.1 mg kg^{-1} organic matter. The pH of the soil was 7.13 in a 1:2.5 (w/v) soil–water suspension ratio.

The two sweet potato genotypes "N1" and "Xu28" were selected based on K uptake and K-use efficiency in the previous studies (Wang et al., 2015, 2017, 2018), with "N1" bred by the Institute of Food Crops, Jiangsu Academy of Agricultural Sciences, exhibiting low K uptake and K-use efficiency, while "Xu28" bred by the Jiangsu Xuzhou Sweet Potato Research Central, exhibiting high K uptake and K-use efficiency.

The original AMF inoculum FM (BGC XJ02) and CE (BGC XJ03C) were purchased from the Bank of Glomales in China (BGC), Institute of Plant Nutrition and Resources, Beijing Academy of Agriculture and Forestry Sciences (Beijing, China). AMF spores were germinated with *Trifolium repens* as host plant in sterilized fine sand and vermiculite culture in a greenhouse of the Jiangsu Academy of Agricultural Sciences (Nanjing, China, 119°32′21″E, 31°44′ 03″N) over 3 months (Xu et al., 2021). The AMF inoculum for both FM and CE consisted of spores (∼42 spores g^{-1}), external hyphae, infected root in addition to fine sand and vermiculite.

Experimental procedure

A greenhouse experiment was conducted in the greenhouse of the Jiangsu Academy of Agricultural Sciences (Nanjing, China, 119°32'21″E, 31°44' 03″N) over 4 months from August to November 2021. Two different K treatment (0 or 160 mg K_2SO_4 per kg air-dried soil) were applied in the presence or absence of AMF (FM or CE) for two sweet potato genotypes ("N1" or "Xu28"). Each plastic pot (height = 30 cm, diameter = 30 cm) was filled with 7 kg air-dried soil; the soil contained 0.82 g urea, 1.55 g superphosphate, and either without K_2SO_4 (K0) or with 1.12 g K_2SO_4 (K1). In total, 16 (cultivar × K treatment × AMF inoculation) treatments include (1) N1/−K/−FM, (2) N1/−K/+FM, (3) N1/−K/−CE, (4) N1/−K/+CE, (5) N1/+K/−FM, (6) N1/+K/+FM, (7) N1/+K/−CE, (8) N1/+K/+CE, (9) Xu28/−K/−FM, (10) Xu28/−K/+FM, (11) Xu28/−K/−CE, (12) Xu28/−K/+CE, (13) Xu28/+K/−FM, (14) Xu28/+K/+FM, (15) Xu28/+K/−CE, and (16) Xu28/+K/+CE. For +FM or +CE, the AMF inoculum (70 g) of FM or CE was inoculated into each pot at the depth of 10 cm, respectively. For −FM or −CE, the same amount of AMF inoculum (70 g) of FM or CE was sterilized three times (121°C, 20 min) and filtered through a 25-μm membrane, respectively. The obtained microbial filtrate (50 ml) of FM or CE inoculum was inoculated into the pot of −FM or −CE, respectively. Each pot contained one plant, and there were 12 pots of each of the 16 (genotype × K treatment × AMF inoculation) combinations.

Plant sampling and analysis

Three pots for 16 treatments were randomly selected at plantlet stage [S1, 30 days post inoculation (DPI)], swelling stage (S2, 60 DPI), maturing stage (S3, 85 DPI), and harvesting stage (S4, 120 DPI). Three sweet potato plants from three individual pots were destructively sampled and regarded as three independent biological replicates.

Plant samples were separated into leaves, stems, stalks, and roots for fresh matter (FM) measurement, and fresh root samples were used for the evaluation of root morphological characteristics and the analysis of mycorrhizal colonization. Additionally, the root parts were divided into fibrous roots and tuberous roots at harvesting stage. Then, leaves, stem, petiole, and root were oven-dried at 105°C for 1 h and then at 75°C to constant weight for DM measurement, then ground and passed through a 0.5-mm sieve for K concentration analysis.

Root morphology of sweet potato was characterized using an Epson Perfection V850 Pro scanner (Epson, Nagano, Japan) at 300 dpi. Root morphological characteristics, including the root length (RL), total root length (RL), root surface area (RA), average root diameter (RD), root volume (RV), root tip number (RT), root branch number (RB), and root cross number (RC), were estimated using WinRHIZO Pro 2017a Root Analysis System (Regent Instruments Inc., Canada) (Huang et al., 2019).

Mycorrhizal root colonization intensity was assessed. The fresh fine roots (0.5 g) were cleared with 10% KOH for 60 min at 90°C, acidified in 2% HCl for 30 min, and then stained with ink (Sheaffer Pen, Shelton, CT, USA) and the vinegar method at 90°C for 15 min. Then, about 90 root segments were randomly selected from each sample and mounted on the microscope slides. Mycorrhizal colonization of root was determined using a microscope at 40× magnification (SMZ745T Nikon, Japan) (Phillips and Hayman, 1970).

Dried plant samples passed through 0.5-mm sieve (0.5 g) were digested with a mixture of H_2SO_4 and H_2O_2, then the K concentration was determined by flame photometry (Wang et al., 2017). The plant K uptake was calculated as follows:

$$K\ uptake = DM \times K\ concentration \quad (1)$$

Statistical analysis

Means and standard errors (SE) were calculated using SPSS Statistics 20.0 software (SPSS Inc., Chicago, IL, USA) (Wang et al., 2017; Yuan et al., 2019). Values are the means of three independent experiments. Bars represent standard errors. Before the analysis of variance (ANOVA), the normality and homogeneity of variance were checked. For the normality test of variance, Shapiro–Wilk test was conducted when the date is less than 50. When the P value is >0.05, the data have the characteristic of normal distribution. If the absolute value of kurtosis is <10 and the absolute value of skewness is <3, the data can be accepted as normal distribution basically. The normal distribution histogram and regression analysis was observed intuitively to check whether this set of data roughly conforms to the normal distribution. For the homogeneity test of variance, when the P value is >0.05, the data conforms to homogeneity of variance. The statistical evaluation between two treatments was compared using the independent-samples t-test, and asterisks denote significant differences between two treatments (t-test; $^{*}P < 0.05$; $^{**}P < 0.01$; $^{***}P < 0.001$). The statistical evaluation of more than two treatments was compared using one-way ANOVA, followed by Tukey's multiple-comparison test ($P < 0.05$), and different lowercase letters denote significant differences. Two-way ANOVA was used to test the statistical significance of K application (K), FM inoculation (FM), CE inoculation (CE), K application × FM inoculation interaction (K × FM), and K application × CE inoculation interaction (K × CE) using the general linear model (GLM). Three-way ANOVA was used to test the statistical significance of Genotype (G), K application (K), AMF inoculation (AMF), Genotype × K application interaction (G × K), Genotype × AMF inoculation interaction (G × AMF), K application × AMF inoculation interaction (K × AMF), and Genotype × K application × AMF inoculation interaction (G × K × AMF) using the GLM. Pearson's correlation relationship was analyzed using Origin 2021 and displayed as heatmap format.

Results

AMF colonized in the root of sweet potato

Funneliformis mosseae and *Claroideoglomus etunicatum* could establish symbiotic relationship with sweet potato for both "N1" and "Xu28" (**Figure 1** and **Supplementary Figure 1**). ANOVA revealed that genotype significantly affects the colonization rate of FM and CE at harvesting stage and seeding stage, respectively. K application significantly affects AMF colonization rate in root of "N1" at harvesting stage, and K × AMF significantly affects AMF colonization rate in root of "Xu28" at swelling stage. No significant differences were observed in FM and CE colonization rate in the root of "N1" and "Xu28" from seeding stage to harvesting stage, except that FM exhibited significant higher colonization rate in the root of "N1" than that of "Xu28" at the harvesting stage (**Supplementary Figure 1**). K application had no significant effects on FM or CE colonization rate in the root of "N1" or "Xu28", except that K application significantly increased FM colonization rate in the root of "N1" at the harvesting stage. Therefore, FM preferred to colonize in the root of "N1" rather than of "Xu28" at the harvesting stage, and K application contributed to colonization of FM in the root of "N1" at the harvesting stage.

K and AMF improved the tuberous root yield of sweet potato

Potassium application had no significant effects on the tuberous root yield of "N1", while K application significantly increased the tuberous root yield of "Xu28" (**Figure 2**). No significant differences were observed in the tuberous root

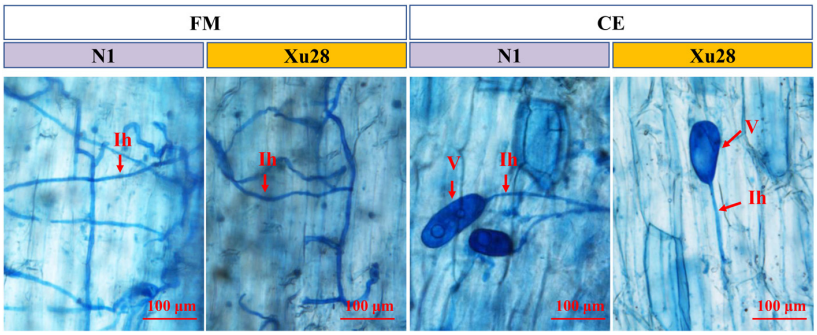

FIGURE 1
Microscopic visualization of arbuscular mycorrhizal fungi structures in root of sweet potato at seeding stage. "N1" and "Xu28" indicate "sweet potato "N1"" and "sweet potato "Xu28"", respectively. "FM" and "CE" indicate "*Funneliformis mosseae*" and "*Claroideoglomus etunicatum*", respectively. Red arrows indicate different arbuscular mycorrhizal fungi (AMF) structures. Ih, intraradical hyphae; V, vesicle.

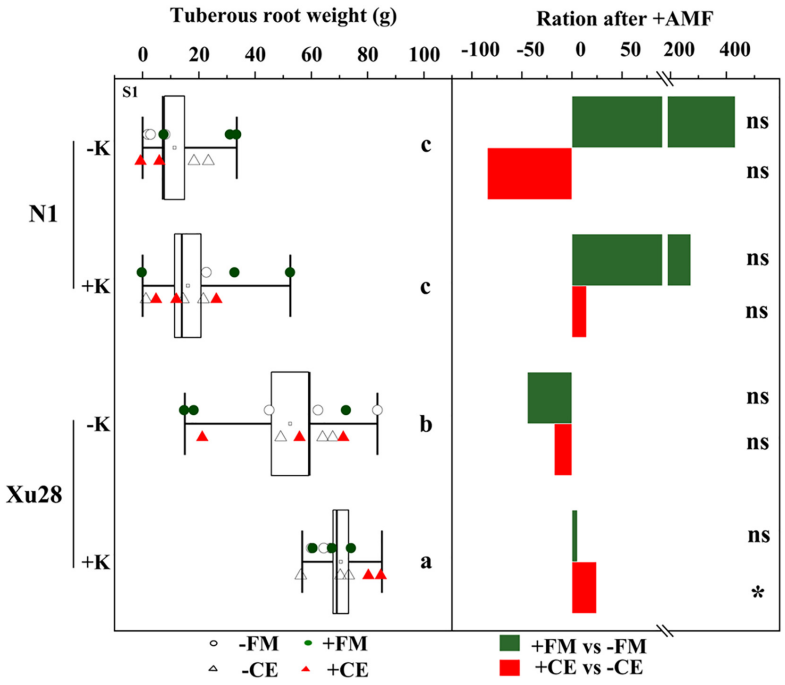

FIGURE 2
The effects of arbuscular mycorrhizal fungi inoculation on tuberous root yield of sweet potato. Different lowercase letters indicate significant differences between different groups ($P < 0.05$). Asterisks denote significant differences after arbuscular mycorrhizal fungi (AMF) inoculation (*t*-test; $^*P < 0.05$), while "ns" indicates nonsignificant difference.

yield of "N1" after FM or CE inoculation, and no significant differences were observed in the tuberous root yield of "Xu28" after FM inoculation, while CE inoculation significantly increased the tuberous root yield of "Xu28" under K application condition. Therefore, FM or CE inoculation did not have a significant effect on improving the tuberous root yield of "N1", while CE inoculation could effectively improve the tuberous root yield of "Xu28" under the condition with K application, and K application and CE inoculation exhibited a synergistic effect on the tuberous root yield of "Xu28". K application and CE inoculation combination increased tuberous root yield of "Xu28" by 37.66% compared with the condition without K application and uninoculated with CE.

K and AMF optimized root morphology of sweet potato

Analysis of variance revealed that K application significantly affects total root length and root branch number of "N1" in

the swelling stage (Figure 3). For "Xu28", K significantly affects root surface area and root volume in the seeding stage, root tip number in the swelling stage, and root diameter in the harvesting stage. Thus, K application differentially regulated the root architecture of "N1" and "Xu28", and K application showed greater effects on root architecture optimization of "Xu28". ANOVA showed that FM significantly regulated the root tip number of "N1" in the seeding and maturing stages, while CE had no significant effects on the root morphology of "N1". For "Xu28", FM had no significant effects on the root morphology, while CE significantly affects root surface area, root diameter, root volume in the seeding stage, and root total root length, root diameter, root tip number, root branch number and root cross number in the swelling stage, and root tip number in the maturing stage. Therefore, FM and CE inoculation were more inclined to optimize root morphology of "N1" and "Xu28", respectively. In particular, FM inoculation only affected "N1" root tip number, while CE inoculation affected several indexes of "Xu28" root morphology.

As shown in Figure 4 and Supplementary Figure 2, FM and K × FM significantly affected root tip number at seeding stage of "N1", and K, CE, and K × CE significantly affected root volume at seeding stage and root tip number at maturing stage of "Xu28". Meanwhile, we analyze the effects of FM and CE inoculation on the root morphology of "N1" and "Xu28" without K application (Figure 4). For "N1", FM inoculation had no significant effects on the root morphology, while CE inoculation significantly decreased root diameter in the seeding stage and root tip number in the maturing stage, and increased root tip number in the harvesting stage. For "Xu28", FM inoculation had no significant effects on the root morphology, and CE inoculation significantly decreased root tip number in the maturing stage. Subsequently, we further analyze the effects of FM and CE inoculation on the root morphology of "N1" and "Xu28" with K application (Figure 4). For "N1", FM inoculation significantly decreased root tip number in the seeding stage and increased root tip number in the swelling stage, CE inoculation significantly increased root tip number in the swelling stage. For "Xu28", FM inoculation significantly increased total root length in the seeding stage and root diameter in the harvesting stage, CE inoculation significantly increased root surface area, root volume, root diameter, and root branch number in the seeding stage, and increased total root length, root surface area, root tip number, and root branch number in the swelling stage. As a result, FM or CE inoculation had little effect on the root morphology of sweet potato and tended to have a negative effect without K application, while FM and CE inoculation significantly increased root tip number of "N1" in the swelling stage and optimized multiple indexes of root morphology of "Xu28" during the whole growth stage under the condition with K application, indicating that K application and AMF inoculation exhibited a considerable synergistic effect on the root morphology of "Xu28".

In addition, CE had the best optimization effect on the root morphology of "Xu28" among the whole growth period under the condition with K application. The longer the total root length and the larger the root surface area, the more effective the plant roots to absorb water and nutrients. The more the root branch number, the more the root tip number. Root tip was the main organ of root nutrient absorption, and root branch number was positively correlated with nutrient absorption capacity. Accordingly, CE inoculation under the

Index	Total root length				Root surface area				Root diameter				Root volume				Total tip number				Total branch number				Total cross number			
Growth stage	S1	S2	S3	S4	S1	S2	S3	S4	S1	S2	S3	S4	S1	S2	S3	S4	S1	S2	S3	S4	S1	S2	S3	S4	S1	S2	S3	S4
Two-way ANOVA for N1																												
K																						*				**		
FM																	**		*									
CE																												
K × FM																	**											
K × CE																		*										
Two-way ANOVA for Xu28																												
K					*							**	*						*									
FM																												
CE		*			*				*	*			*					**	*			*				*		
K × FM																												
K × CE													*						**									

FIGURE 3
Two-way ANOVA for the effects potassium (K) and *F. mosseae* (FM) or *C. etunicatum* (CE) inoculation on root morphological traits of sweet potato. Asterisks denote significant differences (*t*-test; $*P < 0.05$; $**P < 0.01$).

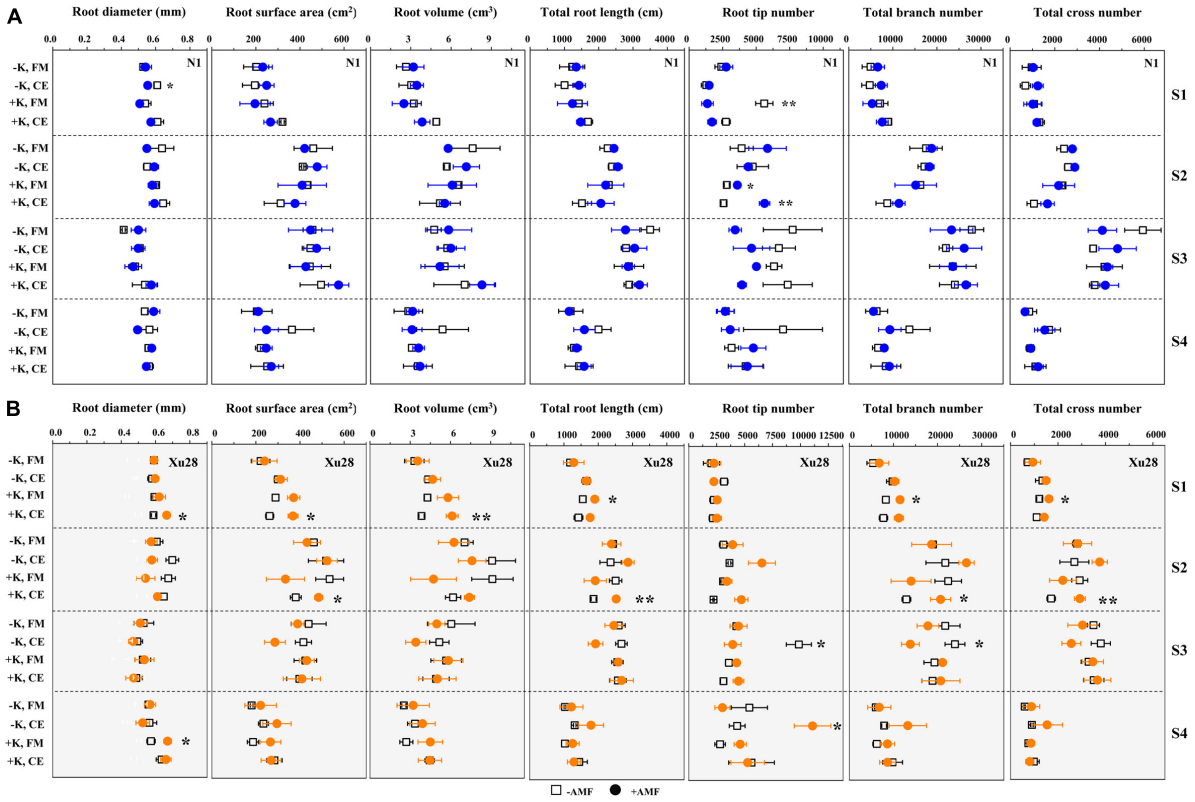

FIGURE 4
The effects of potassium application and arbuscular mycorrhizal fungi (AMF) inoculation on the root morphology of N1 **(A)** and Xu28 **(B)**. For different groups, asterisks denote significant differences after AMF inoculation (*t*-test; $*P < 0.05$; $**P < 0.01$).

condition with K application has the potential to promote root nutrient absorption of "Xu28" at seedling and swelling stages.

K and AMF regulated plant growth parameters of sweet potato

Potassium application had no significant effect on total DM of "N1" from seeding stage to harvesting stage (**Supplementary Figure 3**). For "Xu28", K application had no significant effect on total DM from swelling stage to harvesting stage, while significantly increased total DM at the seeding stage. In addition, no significant differences were observed in total DM of "N1" or "Xu28" after FM or CE inoculation. ANOVA revealed that FM, CE, K × FM, and K × CE had no significant effect on total DM of "N1" or "Xu28" (**Supplementary Figure 4**). Thus, K application favored total DM accumulation of "Xu28" at the seeding stage, while FM and CE had no inspiration effect on total DM of "N1" and "Xu28" with or without K application.

Dry matter accumulation of different organs of sweet potato were analyzed. ANOVA revealed that K, FM, CE, K × FM, and K × CE had no significant effect on root, stem, petiole, or leaf DM of "N1" from seeding stage to harvesting stage, except that K significantly affected leaf DM at swelling stage (**Supplementary Figure 4**). For "Xu28", K, CE, and K × CE significantly affected root DM of "Xu28" at seeding stage, and K significantly affected stem, petiole, leaf DM of "Xu28" at seeding and harvesting stage (**Supplementary Figure 4**). As shown in **Figure 5**, no significant differences were observed in root, stem, petiole, or leaf DM of "N1" or "Xu28" after FM inoculation with or without K application, and no significant differences were observed in root, stem, petiole, or leaf DM of "N1" or "Xu28" after CE inoculation without K application. With K application, CE significantly decreased petiole DM of "N1" in the seeding stage, and significantly promoted root DM accumulation of "Xu28" in the swelling and harvesting stages (**Figure 5**). As a result, K application and CE inoculation exerted a synergistic effect on root DM of "Xu28" at seeding stage.

Furthermore, we further analyze DM proportion of different organs. For "N1", CE inoculation resulted in significantly higher DM proportion of leaf in the seeding and maturing stages without K application, FM inoculation resulted in significantly higher DM proportion of stem in the swelling stage without K application (**Figure 6**). For "Xu28", FM inoculation resulted in significantly lower DM proportion of leaf in the seeding stage with K application, CE inoculation resulted in significantly

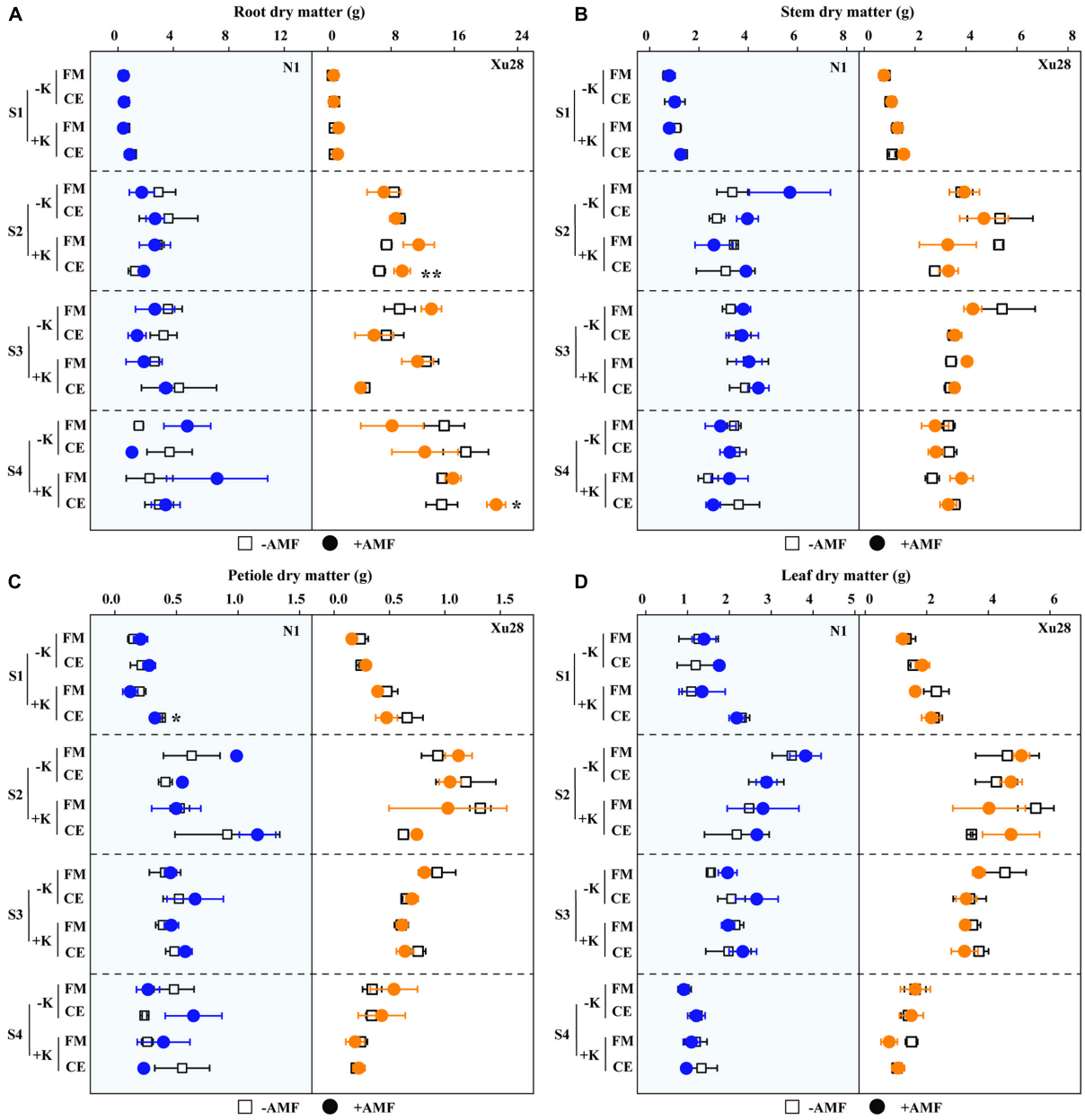

FIGURE 5
The effects of potassium application and arbuscular mycorrhizal fungi (AMF) inoculation on dry matter accumulation of root **(A)**, stem **(B)**, petiole **(C)**, and leaf **(D)** of sweet potato. For different groups, asterisks denote significant differences after AMF inoculation (*t*-test; $*P < 0.05$; $**P < 0.01$).

higher DM proportion of root and lower DM proportion of stem in the harvesting stage with K application (Figure 6). ANOVA revealed that K × CE significantly affected root and aboveground DM proportion (Supplementary Figure 5). The above results indicated that CE inoculation under the condition of K application significantly coordinated the aerial part and root growth of "Xu28" at seeding stage, reduced the DM to leaf and petiole at harvesting stage, and be beneficial to DM allocation to the root at seeding and swelling stages.

K and AMF coordinated plant K uptake and allocation

As shown in Figure 7, K application significantly increased K concentration and K accumulation of "N1" and "Xu28" at seeding stage, swelling stage, and harvesting stage. No significant differences were observed in K concentration and K accumulation of "N1" or "Xu28" after AMF inoculation with or without K application, except that FM significantly

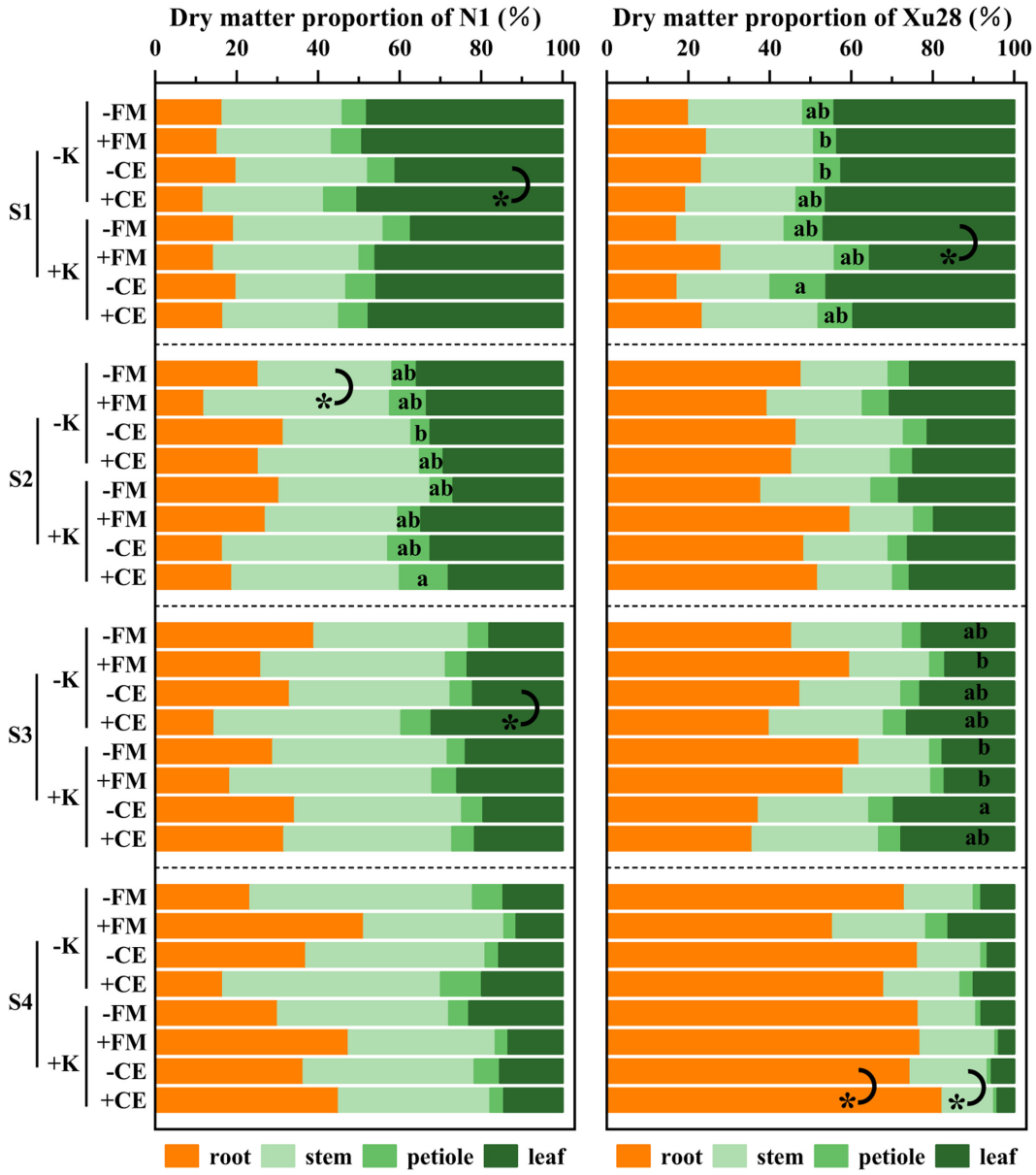

FIGURE 6
The effects of potassium application and arbuscular mycorrhizal fungi inoculation on dry matter proportion of different organs of sweet potato. For each growth stage, different lowercase letters indicate significant differences between different groups ($P < 0.05$). For different groups, asterisks denote significant differences after arbuscular mycorrhizal fungi (AMF) inoculation (t-test; $^*P < 0.05$).

reduced K concentration at maturing stage of "Xu28" under the condition with K application and FM significantly increased K accumulation at maturing stage of "Xu28" under the condition without K application.

Potassium accumulation in different organs of sweet potato was analyzed (Table 1). For "N1", FM inoculation significantly increased petiole K accumulation at swelling and maturing stages and leaf K accumulation at maturing stage under the condition without K application, while significantly decreased leaf K accumulation at maturing stage under the condition with K application. While CE inoculation had no significant effect on K accumulation in different organs of "N1" under the condition with or without K application. Thus, compared with K application, FM inoculation was more conducive to aerial part K accumulation of "N1" under the condition without K application. For "Xu28", FM and CE had no significant effect on K accumulation in different organs under the condition without K application, while FM inoculation significantly increased leaf K accumulation at maturing stage and CE inoculation significantly increased root K accumulation at seeding stage

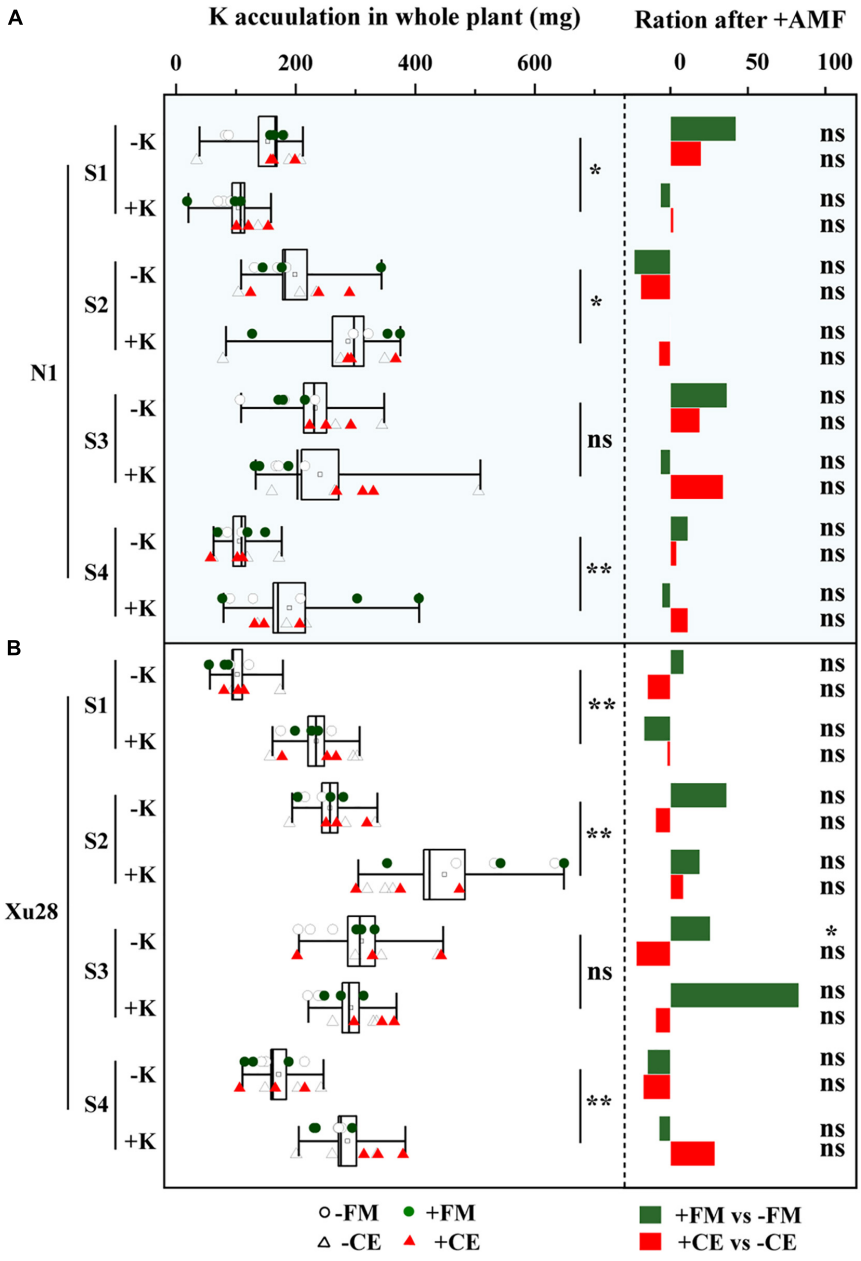

FIGURE 7
The effects of potassium application and arbuscular mycorrhizal fungi inoculation on K concentration **(A)** and K accumulation **(B)** of sweet potato. For each growth stage, different lowercase letters indicate significant differences between different groups ($P < 0.05$). For different groups, asterisks denote significant differences after arbuscular mycorrhizal fungi (AMF) inoculation (*t*-test; $*P < 0.05$; $**P < 0.01$), while "ns" indicates nonsignificant difference.

under the condition with K application, showing that CE-increased root K accumulation at seeding stage and FM-increased leaf K accumulation at maturing stage of "Xu28" were both dependent on K application.

Furthermore, we analyzed the proportion of K accumulation in different organs (Table 2). Either FM or CE inoculation had no significant effect on K proportion in different organs of "N1" and "Xu28" under the condition without K application. With K application, FM inoculation significantly decreased petiole K proportion at seeding stage of "N1" and stem K proportion at swelling of "Xu28". ANOVA revealed that K, CE, and K × CE significantly affected petiole K proportion at seeding stage of "Xu28", and the opposite effects on petiole K proportion of CE inoculation under the condition with and without K application, and CE inoculation significantly decreased petiole K proportion, showing that CE-decreased

petiole K proportion of "Xu28" at seeding stage was highly dependent on K application. In addition, with K application, CE inoculation significantly decreased K proportion in leaf and stem at harvesting stage, and meanwhile significantly increased root K proportion at harvesting stage, indicating that K application and CE inoculation displayed a synergistic effect on K allocation in different organs of "Xu28", and in particular: CE inoculation could limit K allocation to the arial part and be beneficial to K allocation to the root of "Xu28" at harvesting stage under the condition with K application.

Correlation analysis with root morphological index and the K uptake of sweet potato

The above results showed that K and CE displayed a synergistic effect on root development and K acquisition especially for "Xu28". Pearson's correlations revealed that root morphological index showed positive correlations with root DM and root K accumulation of "N1" only at seeding stage (**Figure 8A**), while root morphological index showed positive correlations with root DM and K accumulation of "Xu28" from seeding stage to harvesting stage (**Figure 8B**). No significant positive correlations were observed between root morphological index and K concentration of "N1" or "Xu28" from seeding to harvesting stage, except that root diameter showed significant positive correlation relationships with root K concentration at harvesting stage of "N1" and at maturing stage of "Xu28" (**Figures 8A, B**). In addition, root K accumulation showed significant positive correlation relationship with root DM rather than root K concentration for both "N1" and "Xu28" (**Figures 8C, D**). Therefore, the increased root DM was explained by the optimized morphology of sweet potato for N1 (particularly at seeding stage) and Xu28 (from seeding to harvesting stage), and the increased root K accumulation was attributed to the increased root DM rather than root K concentration of sweet potato.

Discussion

Sweet potato has higher requirements for K for optimum production (Tang et al., 2015), and is easily colonized by AMF (O'Keefe and Sylvia, 1993; Minemba et al., 2019). Meanwhile, optimal K nutrient management strategy for sustainable and environmentally protective crop production was using KIUE genotypes in combination with appropriate soil fertilization (Romheld and Kirkby, 2010). It is acknowledged that root architecture plays a fundamental role for water and nutrients uptake from soil and in turn, yield production (Alhadidi et al., 2021; Caruso et al., 2021). Optimizing root morphology of sweet potato are effective methods guaranteeing yield production of sweet potato. Previously, K application and AMF inoculation have been proven to exert great effects on the root morphology regulation and nutrient acquisition alternation of sweet potato (Alhadidi et al., 2021; Gao et al., 2021), and the interaction exists between K and KIUE in sweet potato (Wang et al., 2017). In the present study, K application differentially regulated the root architecture of "N1" and "Xu28", and K application showed greater effect on root architecture optimization of high-KIUE genotype "Xu28" (**Figure 3**). The defined impact of AMF on plant growth is not stable considering the interaction with AMF and the environmental conditions. It is worth noting that either FM or CE inoculation had little effect on the root morphology of sweet potato and tended to have negative effect without K application, while FM and CE inoculation significantly optimized root morphology under the condition with K application (**Figure 4**), indicating that AMF inoculation-improved root morphology of sweet potato highly relied on K application. Similarly, both K application and AMF inoculation promote root growth and K accumulation of wolfberry, and a synergistic interaction existed between K and AMF (Wang, 2020). Likewise, plant K concentration modified the effects of AMF on root hydraulic properties in maize roots (El-Mesbahi et al., 2012). Therefore, we deduced K application and AMF inoculation exhibited a considerable synergistic effect on the root morphology of sweet potato both low- and high-KIUE genotypes.

Genetic and environmental factors collectively determine plant growth and yield (Wang et al., 2022b). Similarly, sweet sorghum genotypes were selectively associated with AMF inoculations species (FM, *Claroideoglomus claroideum* and CE) for plant root parameters and nutrient uptake (Ortas and Bilgili, 2022). The interaction amongst AMF species may differ between sweet potato varieties (Yooyongwech et al., 2016). On the one hand, plant genotypes were considered in this study. Root morphological indexes (root DM, total root length, root surface area, root volume, root diameter, root branch number, and root tip number) should be analyzed when checking root growth state (Alhadidi et al., 2021; Caruso et al., 2021). As shown in the recent study, *Glomus intraradices* induced different root architecture models (length, surface area, average diameter, and biomass) in relation to the cultivars of *Ficus carica*, suggesting diverse root strategies for exploiting the soil resources (Caruso et al., 2021). In this study, FM and CE inoculation increased root tip number of "N1" in the swelling stage and optimized multiple indexes of root morphology of "Xu28" during the whole growth stage under the condition with K application (**Figure 4**), indicating that AMF differentially regulated root morphology of low-KIUE and high-KIUE sweet potato. On the other hand, AMF species were considered in this study. Three different AMF species (i.e., *C. claroideum*, *Rhizoglomus*

TABLE 1 The effects of K application and arbuscular mycorrhizal fungi (AMF) inoculation on K accumulation in different organs of sweet potato.

G	K	AMF	Root K accumulation (mg)				Stem K accumulation (mg)				Petiole K accumulation (mg)				Leaf K accumulation (mg)			
			S1	S2	S3	S4	S1	S2	S3	S4	S1	S2	S3	S4	S1	S2	S3	S4
N1	−K	−FM	10.03a	47.68a	60.52a	16.99a	47.57a	39.70a	61.17b	40.17a	12.02a	16.52a	14.23b	13.77a	48.49a	59.13a	38.84a	19.87a
		+FM	11.11a	28.39a	44.23a	57.52a	50.05a	81.76a	68.26ab	31.38a	19.58a	33.90a**	23.66ab*	6.75a	87.25a	78.58a	53.68a*	18.53a
		−CE	14.66a	56.21a	73.12a	39.51a	53.79a	49.06a	136.35a	46.20a	19.55a	16.67a	35.46ab	6.50a	60.07a	64.32a	59.93a	29.79a
		+CE	9.51a	45.54a	22.34a	11.58a	61.46a	67.99a	126.05ab	36.52a	26.27a	22.46a	43.66a	18.90a	80.22a	85.81a	67.68a	28.01a
	+K	−FM	5.80a	65.86a	47.01a	42.16a	34.48a	127.06a	65.70ab	58.67a	12.30a	34.68a	13.59b	10.76a	29.49a	78.19a	59.64a	32.18a
		+FM	5.92a	57.87a	24.91a	120.55a	29.68a	104.35a	65.86ab	91.64a	5.81a	30.05a	16.14ab	21.88a	35.32a	93.82a	47.35a*	28.97a
		−CE	16.49a	20.55a	95.19a	47.16a	36.24a	87.73a	132.06ab	84.62a	16.63a	52.13a	31.16ab	19.32a	57.86a	77.84a	55.77a	32.62a
		+CE	16.13a	35.78a	77.7a	61.18a	43.84a	129.33a	125.92ab	67.66a	17.27a	66.10a	36.79ab	11.54a	52.64a	88.43a	66.85a	25.69a
Xu28	−K	−FM	8.64B	114.99B	119.86A	125.78B	20.75B	22.16B	28.30B	11.22B	13.72B	11.53B	13.80B	7.27A	56.27A	74.34B	69.34A	26.49A
		+FM	8.70B	110.35B	210.00A	95.89B	15.63B	24.67B	26.66B	12.35B	7.61B	16.50B	17.88B	11.06A	44.21A	96.64AB	60.81A	25.98A
		−CE	11.26AB	132.37B	164.76A	153.03B	24.18B	34.39B	68.24A	13.91B	11.75B	20.18B	45.14A	8.96A	81.24A	85.68B	85.78A	26.55A
		+CE	9.94B	127.42B	108.35A	117.65B	20.82B	27.19B	78.87A	11.33B	14.57B	36.83AB	56.12A	8.61A	58.32A	92.04AB	85.15A	29.30A
	+K	−FM	16.77AB	154.81AB	282.72A	190.73AB	60.92A	98.10A	15.48B	33.24AB	41.77B	84.76A	9.11B	12.98A	102.59A	207.08A	46.03A	37.35A
		+FM	35.71A	243.49A	181.20A	181.81AB	59.01A	51.57AB	24.41B	47.16A	34.62B	66.41AB	14.11B	6.19A	92.72A	153.41AB	60.24A*	18.82A
		−CE	19.64AB	140.41B	117.80A	203.75AB	52.55A	47.82AB	65.11A	34.22AB	88.15A	34.68AB	49.59A	6.68A	95.64A	124.79AB	80.56A	25.19A
		+CE	28.75AB*	168.98AB	105.00A	295.62A	59.10A	45.51B	76.75A	27.13AB	40.54B	35.69AB	47.67A	5.23A	108.16A	136.61AB	109.83A	19.53A
N1	K		Ns	Ns	Ns	Ns	*	***	Ns	***	Ns	**	Ns	Ns	**	Ns	Ns	Ns
	FM		Ns	Ns	Ns	Ns	Ns	Ns	Ns	Ns	Ns	Ns	*	Ns	Ns	Ns	Ns	Ns
	CE		Ns	Ns	Ns	Ns	Ns	Ns	Ns	Ns	Ns	Ns	Ns	Ns	Ns	Ns	Ns	Ns
	K × FM		Ns	Ns	Ns	Ns	Ns	Ns	Ns	Ns	Ns	Ns	Ns	Ns	Ns	Ns	**	Ns
	K × CE		Ns	Ns	Ns	Ns	Ns	Ns	Ns	Ns	Ns	Ns	Ns	Ns	Ns	Ns	Ns	Ns
Xu28	K		***	**	Ns	***	***	***	Ns	***	***	**	Ns	Ns	**	**	Ns	Ns
	FM		Ns	Ns	Ns	Ns	Ns	Ns	Ns	Ns	Ns	Ns	*	Ns	Ns	Ns	Ns	Ns
	CE		Ns	Ns	Ns	Ns	Ns	Ns	Ns	Ns	Ns	Ns	Ns	Ns	Ns	Ns	Ns	Ns
	K × FM		Ns	Ns	Ns	Ns	Ns	Ns	Ns	Ns	Ns	Ns	Ns	Ns	Ns	Ns	Ns	Ns
	K × CE		*	Ns	Ns	Ns	Ns	Ns	Ns	Ns	Ns	Ns	Ns	Ns	Ns	Ns	Ns	Ns

Different lowercase letters in the same column indicate significant differences between different groups ($P < 0.05$) for "N1" or "Xu28". Asterisks denote significant differences after AMF inoculation (t-test; *$P < 0.05$; **$P < 0.01$; ***$P < 0.001$). Ns denotes not significant using Tukey's test.

10.3389/fmicb.2022.1075957

TABLE 2 The effects of K application and arbuscular mycorrhizal fungi (AMF) inoculation on the proportion of K accumulation in different organs of sweet potato.

G	K	AMF	Root K proportion (%)				Stem K proportion (%)				Petiole K proportion (%)				Leaf K proportion (%)			
			S1	S2	S3	S4	S1	S2	S3	S4	S1	S2	S3	S4	S1	S2	S3	S4
N1	−K	−FM	8.59a	27.25a	31.75a	18.58a	41.71a	25.06a	35.42a	44.53a	10.02a	10.39a	9.23a	15.44a	39.67a	37.30a	23.60ab	21.44a
		+FM	6.66a	10.28a	21.83a	46.99a	29.49a	35.11a	36.89a	29.67a	11.61a	17.53a	12.52a	6.02a	52.24a	37.08a	28.76ab	17.32a
		−CE	12.40a	26.15a	23.94a	28.05a	33.19a	29.24a	45.18a	39.74a	11.85a	9.72a	11.42a	6.07a	42.57a	34.88a	19.46ab	26.14a
		+CE	5.24a	20.11a	8.12a	12.03a	34.67a	30.30a	49.53a	39.95a	14.97a	11.27a	16.32a	19.27a	45.12a	38.32a	26.03ab	28.75a
	+K	−FM	7.32a	21.41a	25.09a	22.39a	42.26a	41.65a	35.15a	42.14a	14.81a	11.29a	7.47a	8.17a	35.61a	25.65a	32.29a	27.31a
		+FM	6.26a	17.04a	13.83a	37.07a	43.70a	37.85a	43.70a	41.26a	5.99a*	10.26a	10.97a	6.88a	44.05a	34.85a	31.50ab	14.79a
		−CE	13.15a	7.63a	25.25a	28.80a	28.09a	36.57a	44.96a	44.57a	13.05a	18.76a	11.17a	9.65a	45.71a	37.03a	18.61b	16.99a
		+CE	12.83a	10.96a	25.11a	35.16a	33.69a	40.70a	41.10a	41.95a	13.36a	20.66a	12.22a	6.82a	40.12a	27.68a	21.58ab	16.07a
Xu28	−K	−FM	8.99A	52.21A	50.18ABC	73.43A	21.41A	9.87A	12.74AB	6.66A	13.52B	5.06A	6.15BC	4.41A	56.09A	32.86A	30.94A	15.50A
		+FM	10.86A	43.50A	66.45AB	60.92A	20.30A	10.21A	8.53B	9.72A	10.13B	6.75A	5.70BC	8.82A	58.70A	39.54A	19.31A	20.53A
		−CE	9.09A	49.35A	43.75ABC	73.22A	19.47A	12.64A	19.43AB	7.47A	9.54B	7.34A	12.94ABC	4.96A	61.89A	30.66A	23.88A	14.35A
		+CE	9.43A	45.79A	30.59C	66.58A	20.08A	9.49A	27.02A	7.42A	13.91B	12.45A	19.57A	6.53A	56.57A	32.27A	22.81A	19.46A
	+K	−FM	7.67A	28.80A	74.64A	69.48A	27.85A	17.80A	5.91B	12.15A	18.41B	15.58A	3.17C	4.74A	46.07AB	37.82A	16.27A	13.63A
		+FM	15.63A	50.76A	64.47AB	72.01A	26.64A	9.32A*	8.74B	18.28A	15.54B	11.60A	5.15BC	2.44A	42.19AB	28.33A	21.64A	7.27A
		−CE	8.27A	40.40A	37.59BC	75.70A	22.97A	13.69A	21.00AB	12.67A	34.62A	9.95A	16.03AB	2.41A	34.14B	35.97A	25.37A	9.22A
		+CE	12.59A	44.02A	31.13C	85.03A*	24.79A	11.80A	22.50AB	7.90A*	16.86B*	9.46A	13.98ABC	1.48A	45.76AB	34.73A	32.39A	5.58A*
N1	K		Ns	Ns	Ns	Ns	Ns	**	Ns	Ns	Ns	Ns	Ns	Ns	Ns	Ns	Ns	Ns
	FM		Ns	Ns	Ns	Ns	Ns	Ns	Ns	Ns	Ns	Ns	Ns	Ns	*	Ns	Ns	Ns
	CE		Ns	Ns	Ns	Ns	Ns	Ns	Ns	Ns	Ns	Ns	Ns	Ns	Ns	Ns	*	Ns
	K × FM		Ns	Ns	Ns	Ns	Ns	Ns	Ns	Ns	*	Ns	Ns	Ns	Ns	Ns	Ns	Ns
	K × CE		Ns	Ns	Ns	Ns	Ns	Ns	Ns	Ns	Ns	Ns	Ns	Ns	Ns	Ns	Ns	Ns
Xu28	K		Ns	Ns	Ns	Ns	*	Ns	Ns	*	**	*	Ns	*	***	Ns	Ns	**
	FM		Ns	Ns	Ns	Ns	Ns	*	Ns	Ns	Ns	Ns	Ns	Ns	Ns	Ns	Ns	Ns
	CE		Ns	Ns	Ns	Ns	Ns	Ns	Ns	Ns	*	Ns	Ns	Ns	Ns	Ns	Ns	Ns
	K × FM		Ns	Ns	Ns	Ns	Ns	*	Ns	Ns	Ns	Ns	Ns	Ns	Ns	Ns	Ns	Ns
	K × CE		Ns	Ns	Ns	Ns	Ns	Ns	Ns	Ns	**	Ns	Ns	Ns	Ns	Ns	Ns	Ns

Different lowercase letters in the same column indicate significant differences between different groups ($P < 0.05$) for "N1" or "Xu28". Asterisks denote significant differences after AMF inoculation (t-test; *$P < 0.05$; **$P < 0.01$; ***$P < 0.001$). Ns denotes not significant using Tukey's test.

10.3389/fmicb.2022.1075957

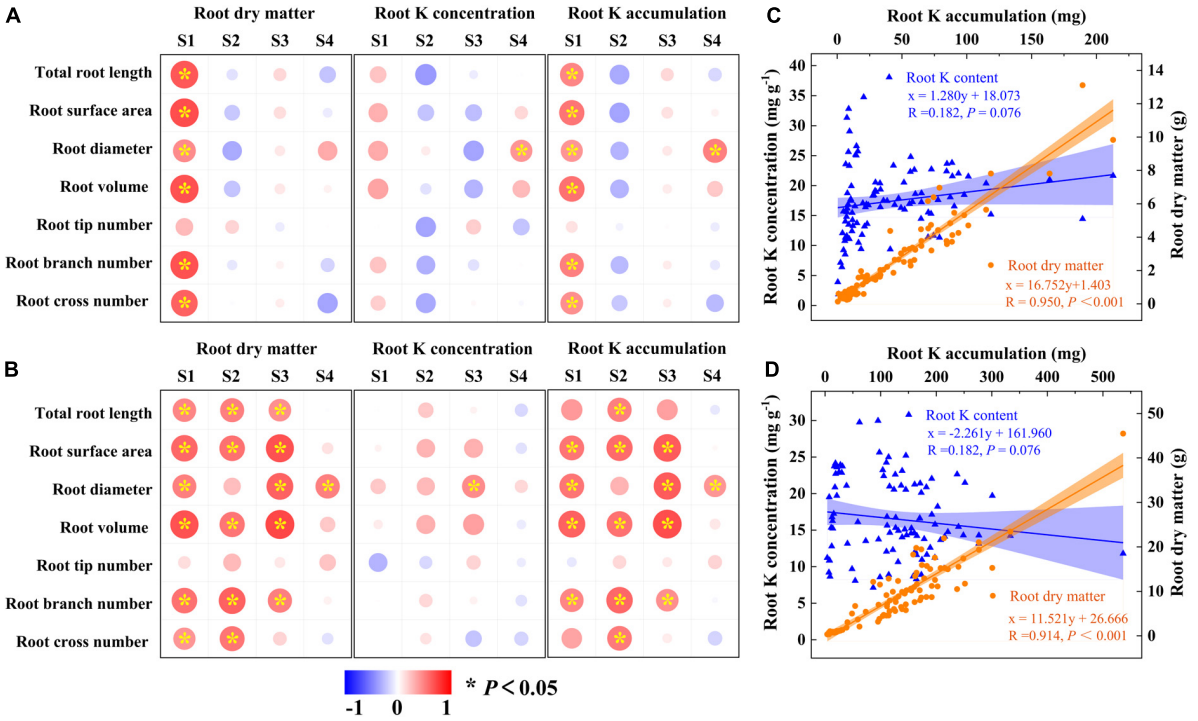

FIGURE 8
Pearson's correlation coefficients between root morphological index, root dry matter, root K concentration, and root K accumulation of N1 **(A)** and Xu28 **(B)**. Relationship between root K concentration or root dry matter and root K accumulation of N1 **(C)** and Xu28 **(D)**. Asterisks denote significant differences (*$P < 0.05$). The value of R and P given in each figure to exhibit the significant level ($P < 0.05$, significant; $P \geq 0.05$, nonsignificant).

irregulare, and FM) varied in their effects on plant biomass and nutrient acquisition of different host plant (Köhl and van der Heijden, 2016). In this study, FM and CE were more favorable to optimize root morphology of "N1" and "Xu28", respectively (Figure 4), CE rather than FM had the best optimization effect on the root morphology of "Xu28" under the condition with K application (Figure 4 and Supplementary Figure 2), indicating that AMF species greatly affected root morphology of sweet potato. Therefore, we speculated that both sweet potato genotypes and AMF species affected the outcome of benefits that AMF conferred to sweet potato to a great extent.

Consistent with the optimized root morphology of "Xu28" (Figure 4 and Supplementary Figure 2), CE inoculation significantly promoted root DM accumulation of "Xu28" in the swelling and harvesting stages (Figure 5), and coordinated of aerial part and root growth of "Xu28", reduced the DM to leaf and petiole, be beneficial to DM allocation to the root under conditions of K supply (Figure 6). Likewise, CE inoculation could limit K allocation to the aboveground and promote root K accumulation of "Xu28" under the condition with K application (Tables 1, 2). The above results lead to the interesting finding that K and CE displayed a synergistic effect on root development and K acquisition of high-KIUE genotype "Xu28". Moreover, CE inoculation, and K application and CE inoculation interaction significantly increased tuberous root yield of "Xu28" rather than "N1" (Figure 2), indicating that K application and CE inoculation exhibited a synergistic effect on tuberous root yield of "Xu28". Therefore, CE inoculation under the condition of K application is an effective strategy to improve the yield production of high-KIUE genotype "Xu28". Thus, we proposed that K application and CE inoculation synergistically optimized root morphology, improved root DM and root K accumulation, coordinated the aerial part and root growth and K allocation, and increased tuberous root production of high-KIUE genotype "Xu28" (Figure 9). In this study, −FM or −CE was set as the control of +FM or +CE, respectively, to replenish the interference from other factors such as mineral and non-mycorrhizal microbial components in the living inoculums. It's worth noting that there are some differences between −FM and −CE in the same genotype and same K level (Table 1). For −FM or −CE, AMF inoculum (70 g) of FM or CE was sterilized and filtered through a 25-μm membrane, respectively. And, to replenish the mineral and non-mycorrhizal microbial components in the living inoculums, the obtained microbial filtrate of unsterilized FM or CE inoculum was inoculated into the pot of −FM or −CE, respectively. Thus, the −FM treatment and −CE treatment were not the same treatment, and some

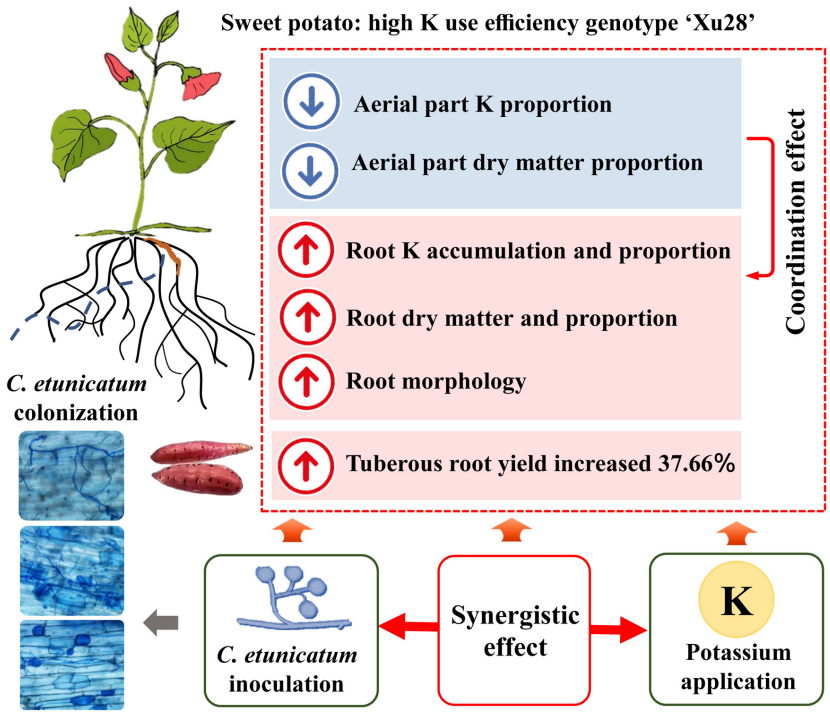

FIGURE 9
Conceptual diagram depicting the synergistic effect of K and arbuscular mycorrhizal fungi (AMF) on root development and K acquisition of high K use efficiency genotype "Xu28".

metabolite may also mediate these differences. Considering more complex and uncertain environmental factor existing in field, and environmental factor (soil types, soil acidity, carbon: nitrogen: phosphorus ratio in soil, climate, etc.) could affect the functional effect of AMF in the agricultural field (Kalamulla et al., 2022), further studies will be conducted to investigate whether K application and CE inoculation improve root morphology and yield production in field experiments, which will contribute to more scientific application of AMF in sweet potato cultivation.

Conclusion

This study showed that K application differentially regulated the root architecture of low-KIUE genotype "N1" and high-KIUE genotype "Xu28", FM and CE inoculation were more inclined to optimize root morphology of "N1" and "Xu28", respectively. AMF inoculation-improved root morphology of sweet potato highly relied on K application. Particularly, K application and CE inoculation displayed a synergistic effect on root development and K acquisition of high-KIUE genotype "Xu28". This study provides a theoretical basis for more scientific application of AMF in sweet potato cultivation and helps to further clarify plant–nutrient–AMF interactions.

Data availability statement

The original contributions presented in this study are included in this article/**Supplementary material**, further inquiries can be directed to the corresponding author.

Author contributions

JY and JW: conceptualization. JY, LW, CX, HZ, and CS: methodology. JY, KS, and XZ: investigation. JY: writing—original draft preparation. JY, YZ, and JW: writing—review and editing and funding acquisition. GZ, YZ, and JW: supervision. All authors contributed to the article and approved the submitted version.

Funding

This study was financially supported by the earmarked fund for CARS-10-Sweetpotato, the Jiangsu Agriculture Science and Technology Innovation Fund [CX (21)1009], the Key Research and Development Project of Jiangsu Province (BE2019378 and BE2021378), and Youth Joint Innovation Project 2022, Institute of Agricultural Resources and Environment, Jiangsu Academy of Agricultural Sciences [ZCX (2022) 21].

Conflict of interest

The authors declare that the research was conducted in the absence of any commercial or financial relationships that could be construed as a potential conflict of interest.

Publisher's note

All claims expressed in this article are solely those of the authors and do not necessarily represent those of their affiliated organizations, or those of the publisher, the editors and the reviewers. Any product that may be evaluated in this article, or claim that may be made by its manufacturer, is not guaranteed or endorsed by the publisher.

Supplementary material

The Supplementary Material for this article can be found online at: https://www.frontiersin.org/articles/10.3389/fmicb.2022.1075957/full#supplementary-material

References

Alhadidi, N., Pap, Z., Ladányi, M., Szentpéteri, V., and Kappel, N. (2021). Mycorrhizal inoculation effect on sweet potato (*Ipomoea batatas* (L.) Lam) seedlings. *Agronomy* 11:2019. doi: 10.3390/agronomy11102019

Caruso, T., Mafrica, R., Bruno, M., Vescio, R., and Sorgonà, A. (2021). Root architectural traits of rooted cuttings of two fig cultivars: Treatments with arbuscular mycorrhizal fungi formulation. *Sci. Hortic.* 283:110083. doi: 10.1016/j.scienta.2021.110083

Chandrasekaran, M. (2020). A meta-analytical approach on arbuscular mycorrhizal fungi inoculation efficiency on plant growth and nutrient uptake. *Agriculture* 10:370. doi: 10.3390/agriculture10090370

El-Mesbahi, M. N., Azcon, R., Ruiz-Lozano, J. M., and Aroca, R. (2012). Plant potassium content modifies the effects of arbuscular mycorrhizal symbiosis on root hydraulic properties in maize plants. *Mycorrhiza* 22, 555–564. doi: 10.1007/s00572-012-0433-3

Farmer, M. J., Li, X., Feng, G., Zhao, B., Chatagnier, O., Gianinazzi, S., et al. (2007). Molecular monitoring of field-inoculated AMF to evaluate persistence in sweet potato crops in China. *Appl. Soil Ecol.* 35, 599–609. doi: 10.1016/j.apsoil.2006.09.012

Gai, J. P., Feng, G., Christie, P., and Li, X. L. (2006). Screening of arbuscular mycorrhizal fungi for symbiotic efficiency with sweet potato. *J. Plant Nutr.* 29, 1085–1094. doi: 10.1080/01904160600689225

Gao, Y., Tang, Z. H., Xia, H. Q., Sheng, M. F., Liu, M., Pan, S. Y., et al. (2021). Potassium fertilization stimulates sucrose-to-starch conversion and root formation in sweet potato (*Ipomoea batatas* (L.) Lam.). *Int. J. Mol. Sci.* 22:4826. doi: 10.3390/ijms22094826

Garcia, K., and Zimmermann, S. D. (2014). The role of mycorrhizal associations in plant potassium nutrition. *Front. Plant Sci.* 5:337. doi: 10.3389/fpls.2014.00337

George, M. S., Lu, G. Q., and Zhou, W. J. (2002). Genotypic variation for potassium uptake and utilization efficiency in sweet potato (*Ipomoea batatas* L.). *Field Crops Res.* 77, 7–15. doi: 10.1016/S0378-4290(02)00043-6

Huang, L., Chen, D., Zhang, H., Song, Y., Chen, H., and Tang, M. (2019). *Funneliformis mosseae* enhances root development and pb phytostabilization in *Robinia pseudoacacia* in Pb-contaminated soil. *Front. Microbiol.* 10:2591. doi: 10.3389/fmicb.2019.02591

Kalamulla, R., Karunarathna, S. C., Tibpromma, S., Galappaththi, M. C. A., Suwannarach, N., Stephenson, S. L., et al. (2022). Arbuscular mycorrhizal fungi in sustainable agriculture. *Sustainability* 14:12250. doi: 10.3390/su141912250

Köhl, L., and van der Heijden, M. G. A. (2016). Arbuscular mycorrhizal fungal species differ in their effect on nutrient leaching. *Soil Biol. Biochem.* 94, 191–199. doi: 10.1016/j.soilbio.2015.11.019

Kondhare, K. R., Patil, A. B., and Giri, A. P. (2021). Auxin: An emerging regulator of tuber and storage root development. *Plant Sci.* 306:110854. doi: 10.1016/j.plantsci.2021.110854

Liu, M., Zhang, A., Chen, X., Jin, R., Li, H., and Tang, Z. (2017). The effect of potassium deficiency on growth and physiology in sweetpotato [*Ipomoea batatas* (L.) Lam.] during early growth. *HortScience* 52, 1020–1028. doi: 10.21273/hortsci12005-17

Liu, M., Zhang, A., Chen, X., Sun, H., Jin, R., Li, H., et al. (2019). Regulation of leaf and root physiology of sweet potato (*Ipomoea batatas* [L.] Lam.) with exogenous hormones under potassium deficiency stress. *Arch. Agron. Soil Sci.* 66, 600–613. doi: 10.1080/03650340.2019.1628346

Minemba, D., Gleeson, D. B., Veneklaas, E., and Ryan, M. H. (2019). Variation in morphological and physiological root traits and organic acid exudation of three sweet potato (*Ipomoea batatas*) cultivars under seven phosphorus levels. *Sci. Hortic.* 256:108572. doi: 10.1016/j.scienta.2019.108572

O'Keefe, D. M., and Sylvia, D. M. (1993). Seasonal dynamics of the association between sweet potato and vesicular-arbuscular mycorrhizal fungi. *Mycorrhiza* 3, 115–122.

Ortas, I., and Bilgili, G. (2022). Mycorrhizal species selectivity of sweet sorghum genotypes and their effect on nutrients uptake. *Acta Agricult. Scand. B Soil Plant Sci.* 72, 733–743. doi: 10.1080/09064710.2022.2063167

Phillips, J. M., and Hayman, D. S. (1970). Improved procedures for clearing roots and staining parasitic and vesicular-arbuscular mycorrhizal fungi for rapid assessment of infection. *Trans. Br. Mycol. Soc.* 55, 158–161. doi: 10.1016/S0007-1536(70)80110-3

Romheld, V., and Kirkby, E. A. (2010). Research on potassium in agriculture: Needs and prospects. *Plant Soil* 335, 155–180. doi: 10.1007/s11104-010-0520-1

Seemakram, W., Paluka, J., Suebrasri, T., Lapjit, C., Kanokmedhakul, S., Kuyper, T. W., et al. (2022). Enhancement of growth and Cannabinoids content of hemp (*Cannabis sativa*) using arbuscular mycorrhizal fungi. *Front. Plant Sci.* 13:845794. doi: 10.3389/fpls.2022.845794

Tang, Z.-H., Zhang, A.-J., Wei, M., Chen, X.-G., Liu, Z.-H., Li, H.-M., et al. (2015). Physiological response to potassium deficiency in three sweet potato (*Ipomoea batatas* [L.] Lam.) genotypes differing in potassium utilization efficiency. *Acta Physiol. Plant* 37:184. doi: 10.1007/s11738-015-1901-0

Tong, Y., Gabriel-Neumann, E., Ngwene, B., Krumbein, A., Baldermann, S., Schreiner, M., et al. (2013). Effects of single and mixed inoculation with two arbuscular mycorrhizal fungi in two different levels of phosphorus supply on β-carotene concentrations in sweet potato (*Ipomoea batatas* L.) tubers. *Plant Soil* 372, 361–374. doi: 10.1007/s11104-013-1708-y

Wang, J. D., Wang, H. Y., Zhang, Y. C., Zhou, J. M., and Chen, X. Q. (2015). Intraspecific variation in potassium uptake and utilization among sweet potato (*Ipomoea batatas* L.) genotypes. *Field Crops Res.* 170, 76–82. doi: 10.1016/j.fcr.2014.10.007

Wang, J., Zhu, G., Dong, Y., Zhang, H., Rengel, Z., Ai, Y., et al. (2018). Potassium starvation affects biomass partitioning and sink–source responses in three sweet potato genotypes with contrasting potassium-use efficiency. *Crop Pasture Sci.* 69, 506–514. doi: 10.1071/cp17328

Wang, J.d, Hou, P., Zhu, G.p, Dong, Y., Hui, Z., Ma, H., et al. (2017). Potassium partitioning and redistribution as a function of K-use efficiency under K deficiency in sweet potato (*Ipomoea batatas* L.). *Field Crops Res.* 211, 147–154. doi: 10.1016/j.fcr.2017.06.021

Wang, L., Zhang, H., Wang, J., Wang, J., and Zhang, Y. (2022a). Long-term fertilization with high nitrogen rates decreased diversity and stability of diazotroph communities in soils of sweet potato. *Appl. Soil Ecol.* 170:104266. doi: 10.1016/j.apsoil.2021.104266

Wang, Y., Wang, X., Sun, S., Jin, C., Su, J., Wei, J., et al. (2022b). GWAS, MWAS and mGWAS provide insights into precision agriculture based on genotype-dependent microbial effects in foxtail millet. *Nat. Commun.* 13:5913. doi: 10.1038/s41467-022-33238-4

Wang, Y. (2020). *The mechanism of arbuscular mycorrhizal fungi and potassium regulating salt tolerance and potassium absorption of Lycium barbarum*. Shaanxi: Northwest A & F University. doi: 10.27409/d.cnki.gxbnu.2020.000588

Woodend, J. J., and Glass, A. D. M. (1993). Genotype-environment interaction and correlation between vegetative and grain production measures of potassium use-efficiency in wheat (T. *aestivum* L.) grown under potassium stress. *Plant Soil* 151, 39–44.

Xu, F. J., Zhang, A. Y., Yu, Y. Y., Sun, K., Tang, M. J., Zhang, W., et al. (2021). Soil legacy of arbuscular mycorrhizal fungus *Gigaspora margarita*: The potassium-sequestering glomalin improves peanut (*Arachis hypogaea*) drought resistance and pod yield. *Microbiol. Res.* 249:126774. doi: 10.1016/j.micres.2021.126774

Yooyongwech, S., Samphumphuang, T., Tisarum, R., Theerawitaya, C., and Cha-um, S. (2016). Arbuscular mycorrhizal fungi (AMF) improved water deficit tolerance in two different sweet potato genotypes involves osmotic adjustments via soluble sugar and free proline. *Sci. Hortic.* 198, 107–117.

Yuan, J., Zhang, W., Sun, K., Tang, M. J., Chen, P. X., Li, X., et al. (2019). Comparative transcriptomics and proteomics of atractylodes lancea in response to endophytic fungus Gilmaniella sp. AL12 reveals regulation in plant metabolism. *Front. Microbiol.* 10:1208. doi: 10.3389/fmicb.2019.01208

frontiers | Frontiers in Microbiology

TYPE Original Research
PUBLISHED 20 January 2023
DOI 10.3389/fmicb.2022.1114089

OPEN ACCESS

EDITED BY
Kai Sun,
Nanjing Normal University,
China

REVIEWED BY
Zhiyong Pan,
Huazhong Agricultural University,
China
Lin Zhang,
China Agricultural University,
China

*CORRESPONDENCE
Xianan Xie
✉ xiexianan8834203@126.com
Ming Tang
✉ tangmingyl@163.com

SPECIALTY SECTION
This article was submitted to Microbe and Virus Interactions With Plants, a section of the journal Frontiers in Microbiology

RECEIVED 02 December 2022
ACCEPTED 28 December 2022
PUBLISHED 20 January 2023

CITATION
Zhang S, Nie Y, Fan X, Wei W, Chen H, Xie X and Tang M (2023) A transcriptional activator from *Rhizophagus irregularis* regulates phosphate uptake and homeostasis in AM symbiosis during phosphorous starvation. *Front. Microbiol.* 13:1114089. doi: 10.3389/fmicb.2022.1114089

A transcriptional activator from *Rhizophagus irregularis* regulates phosphate uptake and homeostasis in AM symbiosis during phosphorous starvation

Shuyuan Zhang, Yuying Nie, Xiaoning Fan, Wei Wei, Hui Chen, Xianan Xie* and Ming Tang*

State Key Laboratory of Conservation and Utilization of Subtropical Agro-Bioresources, Guangdong Laboratory for Lingnan Modern Agriculture, Guangdong Key Laboratory for Innovative Development and Utilization of Forest Plant Germplasm, College of Forestry and Landscape Architecture, South China Agricultural University, Guangzhou, China

Introduction: Phosphorus (P) is one of the most important nutrient elements for plant growth and development. Under P starvation, arbuscular mycorrhizal (AM) fungi can promote phosphate (Pi) uptake and homeostasis within host plants. However, the underlying mechanisms by which AM fungal symbiont regulates the AM symbiotic Pi acquisition from soil under P starvation are largely unknown. Here, we identify a HLH domain containing transcription factor RiPho4 from *Rhizophagus irregularis*.

Methods: To investigate the biological functions of the RiPho4, we combined the subcellular localization and Yeast One-Hybrid (Y1H) experiments in yeasts with gene expression and virus-induced gene silencing approach during AM symbiosis.

Results: The approach during AM symbiosis. The results indicated that *RiPho4* encodes a conserved transcription factor among different fungi and is induced during the *in planta* phase. The transcription of *RiPho4* is significantly up-regulated by P starvation. The subcellular localization analysis revealed that RiPho4 is located in the nuclei of yeast cells during P starvation. Moreover, knock-down of *RiPho4* inhibits the arbuscule development and mycorrhizal Pi uptake under low Pi conditions. Importantly, RiPho4 can positively regulate the downstream components of the phosphate (PHO) pathway in *R. irregularis*.

Discussion: In summary, these new findings reveal that RiPho4 acts as a transcriptional activator in AM fungus to maintain arbuscule development and regulate Pi uptake and homeostasis in the AM symbiosis during Pi starvation.

KEYWORDS

arbuscular mycorrhizal fungi, P starvation, P uptake, RiPho4, transcription factor, yeast one-hybrid, virus-induced gene silencing

Introduction

Arbuscular mycorrhizal fungi (AMF) belong to the Glomeromycotina in the Mucoromycota, and are a kind of the obligate soilborne fungi which can form the AM symbioses with more than 70% of land plants (Brundrett and Tedersoo, 2019; Bonfante and Venice, 2020; Genre et al., 2020; Rich et al., 2021). AMF have been shown to benefit plant productivity and they can absorb water and mineral nutrients such as phosphorus (P), nitrogen (N), iron, sulfur and zinc from soils, then transfer them to the host plants *via* the symbiotic interfaces (Watts-Williams and Cavagnaro, 2018; Kobae, 2019; Rahman et al., 2020; Ma et al., 2022). In return, host plants can transport fatty acids and sugars to AMF as the carbon and energy sources (Campos-Soriano and Segundo, 2011; Jiang et al., 2017; Luginbuehl and Oldroyd, 2017; An et al., 2019). These bidirectional processes effectively regulate the nutrient balance between the host plants and their AM fungal symbionts, and thus these associations are capable of promoting plant development and fitness (Pozo and Azcón-Aguilar, 2007; Hajong et al., 2013; Fellbaum et al., 2014).

Soil available P can be acquired at the root periphery and utilized by plants in the form of inorganic orthophosphate (Pi), however, Pi is always insufficient in the fields due to its low solubility and relative immobilization in soils (Vance et al., 2003; Hirsch et al., 2006; Nagy et al., 2009). The formation of AM symbiosis is an effective strategy for land plants to cope with low Pi availability (Cibichakravarthy et al., 2015; Dierks et al., 2021). During colonization, the branch hyphae of spores produce swellings called appressoria on the surface of the root epidermal cells after the perception of host plant-derived strigolactones (Giovannetti et al., 1993; Akiyama et al., 2005). Subsequently, the appressoria penetrate the epidermal cells to grow the intraradical hyphae assembled within the prepenetration apparatus (Genre et al., 2005, 2008, 2012; Russo et al., 2019); the developing intraradical mycelium (IRM) then run across the root cortical cells and form the tree-like structures called arbuscules in these cortical cells, where the nutrient transport and unloading (such as Pi and N) occurs (Parniske, 2008; Gutjahr and Parniske, 2013; Luginbuehl and Oldroyd, 2017; Hui et al., 2022). Meanwhile, arbuscules are surrounded by the extension of plant plasma membrane called the periarbuscular membrane (PAM) (Harrison et al., 2002; Pumplin et al., 2012). It is also considered to be the main nutrient exchange site of AM symbiosis (Balestrini and Bonfante, 2014; Ivanov and Harrison, 2014; Roth et al., 2019). During AM symbiosis, the extraradical mycelium (ERM) of AMF can reach up to 100 times length of root hairs (Javot et al., 2007) and form the large external hyphal networks to expand more area for Pi absorption beyond the rhizospheres, and also increase the phosphatase activities at the rhizospheres (Wang et al., 2016; Hu et al., 2019). Therefore, the AM symbioses can enhance plant Pi uptake and utilization during P starvation (Smith, 2009; Cibichakravarthy et al., 2015; Dierks et al., 2021).

Earlier radiotracer studies have demonstrated that Pi travels from soils through the AM fungal hyphae to the host plants (Pearson and Jakobsen, 1993; Smith et al., 2003). In past two decades, the high-affinity transporter genes belonging to the PHT1 (PHOSPHATE TRANSPORTER 1) family that are expressed in the ERM and IRM have been identified and characterized from some AMF species, for example, *GmosPT*, *GigmPT*, *GvPT*, and *RiPT* from *Glomus mosseae, Gigaspora margarita*, *Glomus versiforme* (currently *Diversispora epigaea*), and *Rhizophagus irregularis* (Harrison and van Buuren, 1995; Maldonado-Mendoza et al., 2001; Benedetto et al., 2005; Fiorilli et al., 2013; Xie et al., 2016; Sun et al., 2019; Venice et al., 2020). AMF can absorb Pi from soil by ERM, and polymerize Pi into polyphosphate (Poly-P) by vacuolar transporter chaperone (VTC) complex; the Poly-P was accumulated in the vacuoles, and then transferred to the IRM associating with water transport process (Kikuchi et al., 2016). The Poly-P phosphatases Ppn1 and Ppx1 in IRM can hydrolyze the Poly-P into Pi, and export it from vacuoles to the cytoplasm through the unknown P transporters located in the vacuole membrane (Solaiman et al., 1999; Ezawa and Saito, 2018; Xie et al., 2022).

It has been shown that there is a specialized Pi export system in the arbuscules, where free Pi is transported and unloaded into the periarbuscular space (PAS) (Ezawa and Saito, 2018; Zhou et al., 2021; Xie et al., 2022). After the Poly-P hydrolyzation in the IRM and arbuscules, the Pi transporters containing SPX (SYG1/Pho81/XPR1) domains participate in the Pi export process at the symbiotic interface, releasing Pi into the PAS (Ezawa and Saito, 2018; Plassard et al., 2019; Xie et al., 2022). Pi in the PAS cross the PAM to root cortical cells relies on the mycorrhiza-induced phosphate transporters belonging to the plant PHT1 gene family (Javot et al., 2007; Yang et al., 2012; Xie et al., 2013; Volpe et al., 2016). On the other hand, it has been found that AMF also possesses the low-affinity Pi transport system (such as Pho87/90/91) and phosphatases (Tisserant et al., 2012; Lin et al., 2014; Venice et al., 2020). The Pi transport systems in AMF is very similar to that of *Saccharomyces cerevisiae*, which is well-known to contain the high-affinity system Pho84p and Pho89p and the low-affinity system Pho87p, Pho90p, and Pho91p (Auesukaree et al., 2003). This suggests that there exists a conserved PHOSPHATE (PHO) signaling pathway between AMF and yeasts (Aono et al., 2004; Olsson et al., 2006; Kikuchi et al., 2014; Zhou et al., 2021).

Transcription factors (TFs) play crucial roles in the regulation of gene expression in fungal cells and determine the functions of eukaryotic cells (Shelest, 2008). Recent advances have been made in identifying several hub TFs in mycorrhizal plants functioning in the control of AM symbiosis nutrient uptake and exchange (Pimprikar and Gutjahr, 2018; Shi et al., 2021; Das et al., 2022; Ho-Plágaro and García-Garrido, 2022). By contrast, the studies on AM fungal TFs are very limited. In two previous studies, only a few TFs, such as RiMsn2 from *R. irregularis* and GintSTE from *Glomus intraradices* (currently *R. irregularis*) are preliminarily investigated (Tollot et al., 2009; Sun et al., 2018), while the key transcriptional regulators engaged in Pi absorption and homeostasis have not been explored in AMF. Some recent studies

have shown that there exists the bHLH domain-containing transcription factors encoding genes involved in the PHO pathway in response to low Pi conditions in *G. margarita*, *Gigaspora rosea* and *R. irregularis* (Tang et al., 2016; Xie et al., 2016, 2022; Zhou et al., 2021). It is well-known that in *S. cerevisiae*, the AMF bHLH ortholog ScPho4 is the transcription factor regulating the PHO pathway to control Pi absorption and homeostasis (Lenburg and O'Shea, 1996; Auesukaree et al., 2004; Wykoff et al., 2007). Although several studies have revealed that some important genes are involved in the Pi signaling and metabolism pathways in AM fungal symbionts (Balestrini et al., 2007; Xie et al., 2016, 2022), the underlying molecular mechanisms on the regulation of Pi uptake and homeostasis in AMF during symbiosis remain elusive.

Eucalyptus species is the most valuable and widely planted hardwood in the world (Qin et al., 2021). It has many advantages such as fast growth and strong adaptability to drought, fire, insect pest, soil acidity and low fertility (Rockwood et al., 2008). *Eucalyptus* wood can be used as an important raw material for industrial pulp and paper making, fuel and charcoal production because of its high-density property (Rockwood et al., 2008; Kato and Hibino, 2009). Because of its economic and ecological values, it is important to enhance the productivity of *Eucalyptus* limited by environmental factors such as P and N (Santos et al., 2016; Yao et al., 2021; Che et al., 2022). AM symbiosis is an environmentally friendly strategy to promote the *Eucalyptus* plants nutrient absorption when compared with fertilizer excessive use (Smethurst, 2010). Recently, there are many researches on physiological roles of AMF and ectomycorrhizal fungi on the *Eucalyptus* plants (Pagano and Scotti, 2008; Santos et al., 2021), but little studies focus on the regulatory mechanisms of Pi uptake and exchange processes in AM fungal symbiont during AM fungus-*Eucalyptus* symbiosis.

After the investigation of Pi uptake and transport processes during AMF and plant interaction, to further understand the regulatory mechanisms of the Pi uptake and homeostasis at the symbiotic interface, we start to search the regulators (TFs) in *R. irregularis* expressed during the *in planta* phase. Here, we show a new transcription factor from *R. irregularis* (RiPho4), which contains a C-terminal bHLH domain, and provide experimental evidence for roles in the regulation of Pi uptake and homeostasis during AMF-*Eucalyptus* symbiosis. Moreover, our findings offer new insights into the control of Pi uptake and metabolism in the AM fungal symbionts at the symbiotic interfaces.

Materials and methods

AM fungus and plant materials and growth conditions

AM fungus used in this study was *R. irregularis* DAOM 197198, which was propagated in the pot cultures with maize (*Zea mays*). Spores of *R. irregularis* were collected from *Z. mays* root segments. The plant material used in this study was *Eucalyptus grandis* (The seeds was from the Research Institute of Tropical Forestry, Chinese Academy of Forestry). The surface-sterilization of *E. grandis* seeds was performed as the described previously (Plasencia et al., 2016). The seedlings germinated were transferred from solid medium to the pots, and then inoculated with *R. irregularis* (about 200 spores per plant). After inoculation, *E. grandis* plants are cultivated in a growth chamber under 16 h: 8 h, 24°C: 19°C, light: dark conditions (light intensity, 100–200 Wm^{-2}; relative humidity, 55%).

Phosphate treatment

Eucalyptus grandis plants were cultivated in pots under AMF inoculation (AM) and uninoculated control (NM) treatments. Each treatment was carried out with three Pi concentrations including 30, 300 and 1,000 μM K_2HPO_4 (Sugimura and Saito, 2017; Fan et al., 2020). The plants were fertilized once a week using the modified Long-Ashton (mLA) solutions (Hewitt, 1966) containing the indicated Pi concentrations. After 45 days treatments, NM and AM plants were collected and stored at-80°C for subsequent experiments. And plant roots colonized with AMF in the pot experiment were collected to extract DNA and RNA from *R. irregularis*.

For RiPho4 subcellular localization analysis, yeast cells were cultured in YNB medium without uracil (Ura) for 24 h. And the yeast cells were cultured in YNB/-Ura medium for 12 h, supplemented with different Pi concentrations (the final Pi concentrations in each were 600 μM, 1 mM, 10 mM KH_2PO_4, respectively) (O'Neill et al., 1996; Komeili and O'Shea, 1999; Zhou and O'Shea, 2011).

Genomic and RNA-seq data analysis

To identify the candidate genes of the PHO pathway in *R. irregularis*, the genes of PHO signaling pathway in *S. cerevisiae* was used as the queries to search for the homologues genes in the genome of *R. irregularis* DAOM 197198 (Supplementary Table S2). Through genome BLAST in NCBI and GEO databases, tBLASTn and BLASTp searches were carried out to search the target genes in *R. irregularis*, and the best matching sequence ranking first from BLASTp results is used for subsequent analysis. The homologous amino acid sequences were collected from the NCBI database.

To analyze the expression profiles of the target genes in different fungal tissues of *R. irregularis*, the original RNA-seq sequences of non-symbiotic tissues (germinating spores) and symbiotic tissues (mycorrhizal roots) of *R. irregularis* download from DDBJ database. The accession numbers of RNA-seq reads are as follows: germinating spores harvested at a week after inoculation (DRA002591), germinating spores collected at 7 days after induction (GSE67913), laser microdissected cells contain

IRM and arbuscules collected from *Medicago truncatula* mycorrhizal roots (GSE99655), mycorrhizal roots of *M. truncatula* (GSE99655, GSE67926), ERM collected from carrot root culture (GSE99655) (Zeng et al., 2018, 2020).

Gene expression analysis

The extraction of the genomic DNA from *R. irregularis* was referred to the method of Zézé et al. (1994) for amplification of gene fragments containing non-coding regions. Besides, total RNA was extracted by Trizol (Invitrogen) method, and the concentration and purity of total RNA were detected by NanoDrop 2000 (Thermo Scientific, United States). First-strand cDNA was produced from total RNA by a Hiscript III reverse transcriptase kit with gDNA wiper (Vazyme Biotech, Nanjing, China) following the manufacturer's instructions. The qRT-PCR experiments were performed in a 96-well Real time PCR system instrument (BioRed, Hercules, CA, United States) (Xie et al., 2022). *RiEF1α* gene from *R. irregularis* was used as an internal control for qRT-PCR analysis. Relative expression levels were calculated using $2^{-\Delta\Delta Ct}$ method. The list of gene-specific primers used for qRT-PCR analysis is given in Supplementary Table S3.

Yeast manipulations

The full-length of *RiPho4* was amplified by gene-specific primers containing the *BamH*I site (Primer sequences are listed in Supplementary Table S4). One step cloning Kit (Vazyme Biotech, Nanjing, China) was used to recombine the *RiPho4* cDNA into the pUG36 vector, and the resulting plasmid pUG36-GFP-RiPho4 was transformed into the yeast EY57 strain using the LiOAc/PEG-based method described previously (Gietz and Schiestl, 2007). Positive transformants were grown in YNB liquid medium lacking Ura for oscillation culture at 28°C for 24 h.

The ORF of *RiPho4* was cloned from cDNA of *R. irregularis* using the primers ADRiPho4-F/R, and then cloned into the pGADT7 (Chien et al., 1991). To construct bait-specific pAbAi vector, *cis*-acting elements with their flanking nucleotides from the promoters of target genes (Tomar and Sinha, 2014) (listed in Supplementary Table S4) were synthesized and cloned into the *Sal*I site of the pAbAi vector (Clontech Laboratories, United States). Then the constructed vectors were transformed into the Y1HGold yeast strain, and grown on YNB/-Ura solid medium with Aureobasidin A (AbA) concentration (100 mM) for testing the minimal inhibitory concentration of AbA for bait-specific pAbAi plasmids. We transformed the bait-specific pAbAi fragments and pGADT7-RiPho4 were co-transformed into yeast cells, and screened using the SD medium lacking Leucine. The yeast cells (OD_{600} = 0.2) containing both RiPho4-pGADT7 and promoter fragments were inoculated on SD medium lacking Leucine with different AbA concentrations (100–800 ng/ml). The yeast cells carrying pAbAi-p53 and pGADT7-SV40 were used as the positive control, whereas the yeast cells containing pGADT7-RiPho4 and promoter fragments lacking the *cis*-element served as the negative control. In addition, the inhibitory effect was adjusted based on the growth of yeast (Zhan et al., 2017; Sun et al., 2018; Yang et al., 2019).

Virus-induced gene silencing

Tobacco (*Nicotiana benthamiana*) is used for this virus-induced gene silencing (VIGS) experiment (Zhang and Liu, 2014; Kikuchi et al., 2016; Xie et al., 2022). Two specific cDNA fragments of *RiPho4* from the-9 to +226 regions (*RiPho4-RNAi-1*) and + 1,200 to +1,429 regions (*RiPho4-RNAi-2*) relative to the start codon ATG (Supplementary Figure S5) were amplified by PCR following the method described by Senthil-Kumar and Mysore (2014). The cloned gene fragments (the primers VigsRiPho4-F1/R1 and VigsRiPho4-F2/R2 were listed in Supplementary Table S4) were ligated to the pTRV2 vector. And the resulting plasmids *pTRV2-RiPho4-1* and *pTRV2-RiPho4-2* were separately transformed into *Agrobacterium tumefaciens* GV3101 (Grønlund et al., 2013; Zhang and Liu, 2014). *A. tumefaciens* culture (OD_{600} = 1.0) with pTRV1 and that with pTRV2 or pTRV2-RiPho4 were mixed together and activated by adding 10 mM Acetosyringone, then stood in darkness for 2 h. The inoculums were injected into the leaves of *N. benthamiana*, whose roots had been inoculated with *R. irregularis* for 4 weeks as described by Kikuchi et al. (2016). Tobacco plants treated with three Pi concentrations (30 μM, 100 μM, 300 μM) were cultured in a small chamber for 2 weeks.

AM phenotypical analysis

The collected *E. grandis* roots were digested in 10% KOH solution at 90°C for 40 min for 3 times, and washed with distilled water, then neutralized in 2% HCI solution for 20 min. After washing with sterile water for 3 times, AM roots were stained with 5 μg/ml wheat germ agglutinin 488 (WGA488, Invitrogen) at 37°C for 30 min (Phillips and Hayman, 1970; Ivashuta et al., 2005). The enzyme activities of succinate dehydrogenase (SDH), alkaline phosphatase (ALP) and acid phosphatase (ACP) were performed as described previously (Zhao et al., 1997). Mycorrhizal colonization was estimated according to Trouvelot et al. (1986).

Microscopy

The fluorescent signals in yeast cells and AM roots were observed by a fluorescence microscope (Y-TV55; Nikon, Tokyo, Japan). The colonization levels of SDH, ACP and ALP enzyme activity staining was calculated under the light microscope (Y-TV55; Nikon, Tokyo, Japan).

Total P concentration analysis

Fresh samples of *E. grandis* were lyophilized for 6 h. To grind dried samples into powder, we added magnetic beads to them and grinded them with a grinder (35 Hz) for 2 min. 0.3 g of sample powders were digested by 6 M nitric acid under the water bath at 90°C for 1 h (Fan et al., 2020). The digested samples were filtered with filter membranes and diluted with 5% nitric acid to 10 ml. Total P concentrations in the *E. grandis* digests were measured by the inductively coupled plasma optical emission spectrometry (ICP-OES; Varian, United States). Total P concentrations of *N. benthamiana* were detected by the tissue total P content detection Kit (Cat. NO. BC2855, Solarbio, China) and measured with the Microplate Reader (Vaioskan, Thermo Scientific, United States).

Bioinformatics

The BLASTP[1] was used to search homologs of RiPho4 protein in the fungi species. The characteristics of the secondary structure of RiPho4 were analyzed by the SMART program.[2] The SWISS-MODEL website[3] was employed to build the three-dimensional model of RiPho4. The conserved regions of RiPho4 and its homologous proteins were analyzed by Meme.[4] The heat diagram for PHO pathway gene expression levels in different fungal tissues was made by the TBtools (Chen et al., 2020). The existence of *cis*-acting element by searching for 1.5 kb promoter sequences of the target gene coding regions through the NCBI database and PlantCARE software.[5]

Phylogenetic analysis

The unrooted phylogenetic tree of RiPho4 protein and other amino acid sequences in different fungi species were constructed with MEGA7.0 (Kumar et al., 2016) using the neighbor-joining method. Accession numbers of all the fungal proteins are shown in Supplementary Table S2.

Statistical analysis

Data are preliminarily accounted by Microsoft EXCEL 2016, and statistical significances between treatments were analyzed by analysis of variance (ANOVA) using SPSS software (Version 26.0, SPSS Inc., United States). The Duncan's multiple range test were used for comparing more than two datasets. A value of $p < 0.05$ was considered to be statistically significant. The different letters indicate significant differences among phenotypes or treatments. Huang and Freiser (1993, Origin Lab, United States) to plot and illustrate diagram for changing curves of different treatments.

Accession numbers

Sequence data from this article can be found in the AM fungal genome and GenBank libraries under the following accession numbers: RiPho4 (XP_025175129.1), RdPho4 (RGB28534.1), RcPho4 (GBB98521.1), GcPho4 (RIA86088.1), GmPho4 (KAF0357978.1), GrPho4 (RIB17793.1), DePho4 (RHZ83467.1). Other accession numbers of fungal Pho4 proteins were provided in Supplementary Table S2.

Results

Effects of AMF on the growth and Pi uptake of *Eucalyptus grandis* in roots under Pi-deficient conditions

To study the effects of AMF inoculation on the growth and Pi uptake of *E. grandis* subjected to different Pi conditions, we treated mycorrhizal (AM) *E. grandis* with three phosphate concentrations when compared with non-mycorrhizal (NM) *E. grandis*. After 7 weeks inoculation, the growth performance of AM *E. grandis* was better than NM plants under medium and low phosphate conditions (30 and 300 μM) (Supplementary Figure S1). Overall growth (such as plant height, root length, and biomass) also showed such a trend (Figures 1A–D). Compared with NM plants, the total P concentrations of both roots and shoots showed significant increases in AM plants under low and medium phosphate concentrations (30 and 300 μM), while there were no significant differences between AM and NM plants under high Pi conditions (Figure 1E). In addition, it was found that the colonization levels of *E. grandis* exposed to low Pi (30 μM) were significantly higher than those grown under the medium and high Pi treatments (300 and 1,000 μM) (Figure 1F). Moreover, we also detected the activities of ACP, ALP and SDH involved in AM fungal function and mycorrhizal Pi utilization efficiency (Guillemin et al., 1995; Vivas et al., 2003; Kouas et al., 2009; Li et al., 2017). Activities of these three enzymes in roots exposed to 30 μM Pi were significantly higher than that subjected to 300 μM and 1,000 μM Pi (Figures 1G–I; Supplementary Table S1). Taken together, these results revealed that, during AM symbiosis, AM fungus *R. irregularis* can promote the *E. grandis* Pi uptake and utilization efficiency to improve the plant growth under Pi-deficient conditions.

1 http://blast.ncbi.nlm.nih.gov/Blast.cgi
2 http://smart.embl.de/
3 https://swissmodel.expasy.org/
4 https://meme-suite.org/meme/tools/meme
5 http://bioinformatics.psb.ugent.be/webtools/plantcare/html/

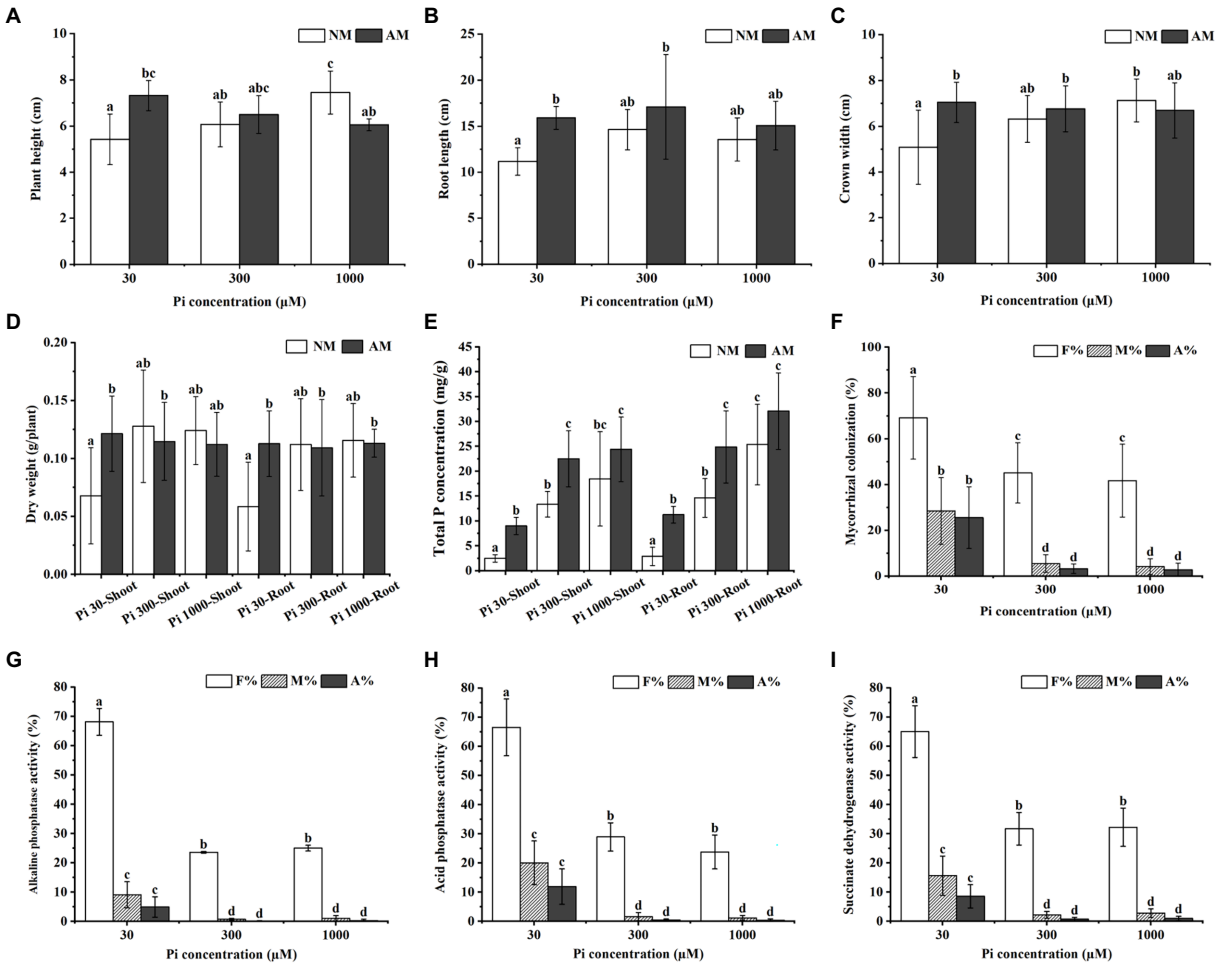

FIGURE 1
Impact of different Pi concentrations and AMF colonization on *Eucalyptus grandis* growth and enzyme activities within mycorrhizal roots. **(A–D)** The growth performances of NM and AM *E. grandis* plants under different phosphate concentrations. **(E)** Total P concentrations of shoots and roots of NM and AM *E. grandis* with *R. irregularis* grown at different Pi levels. **(F)** Mycorrhizal colonization levels among different phosphate concentrations were determined in roots after the WGA488 staining. **(G–J)** Impact of phosphate concentrations on three enzymes activities, including alkaline phosphatase (ALP), acid phosphatase (ACP) and succinate dehydrogenase (SDH), which are involved in AM fungal metabolism and Pi homeostasis during symbiosis. Data on the pictures are obtained by the ALP **(G)**, ACP **(H)**, and SDH **(I)** activities staining, respectively. (F–I) F%, the total colonization frequency; M%, the percentage of mycorrhizal intensity; A%, the percentage of arbuscule abundance. Error bars represent the mean of five biological replicates ± SD. Averages with the different letters on the top of the column mean significantly differences at $p<0.05$ level, based on Duncan's new multiple range test.

Transcription levels of PHO pathway genes in *Rhizophagus irregularis* are dependent on Pi availability

To investigate the effect of external phosphate concentrations on the transcription levels of AM fungal genes involved in Pi uptake and metabolism, we examined the expression profiles of 12 genes in the PHO pathway of *R. irregularis* in mycorrhizal *E. grandis* roots during different Pi conditions. As shown in Figure 2A, relative to medium and high P concentrations (300 and 1,000 μM) conditions, the transcript of *RiPho2*, which was predicted to be a cofactor for RiPho4 (Chen et al., 2018; Xie et al., 2022), was significantly higher in mycorrhizal roots under low Pi (30 μM) conditions. Similarly, the expression levels of *RiPT1*, *RiPT2*, *RiPT3* and *RiPT6*, which encode the potential phosphate transporters responsible for Pi uptake, were much higher in mycorrhizal roots during low Pi concentration when compared with high Pi treatments (Figures 2B–E). Moreover, the *RiACP1* and *RiALP1* involved in Pi and Poly-P metabolisms were expressed in response to the low Pi application (Figures 2F,G). Besides, the expressions of key genes in response to Pi starvation signaling, such as *RiPho81* and *RiPho85* were also detected in mycorrhizal roots under such conditions. *RiPho81* was significantly induced at low Pi concentration, while transcripts of *RiPho85* were slightly but not significantly reduced at high Pi treatments (Figures 2H,I). On the other hand, the expressions of Poly-P accumulation-related genes *RiVTC1* and *RiVTC4* were

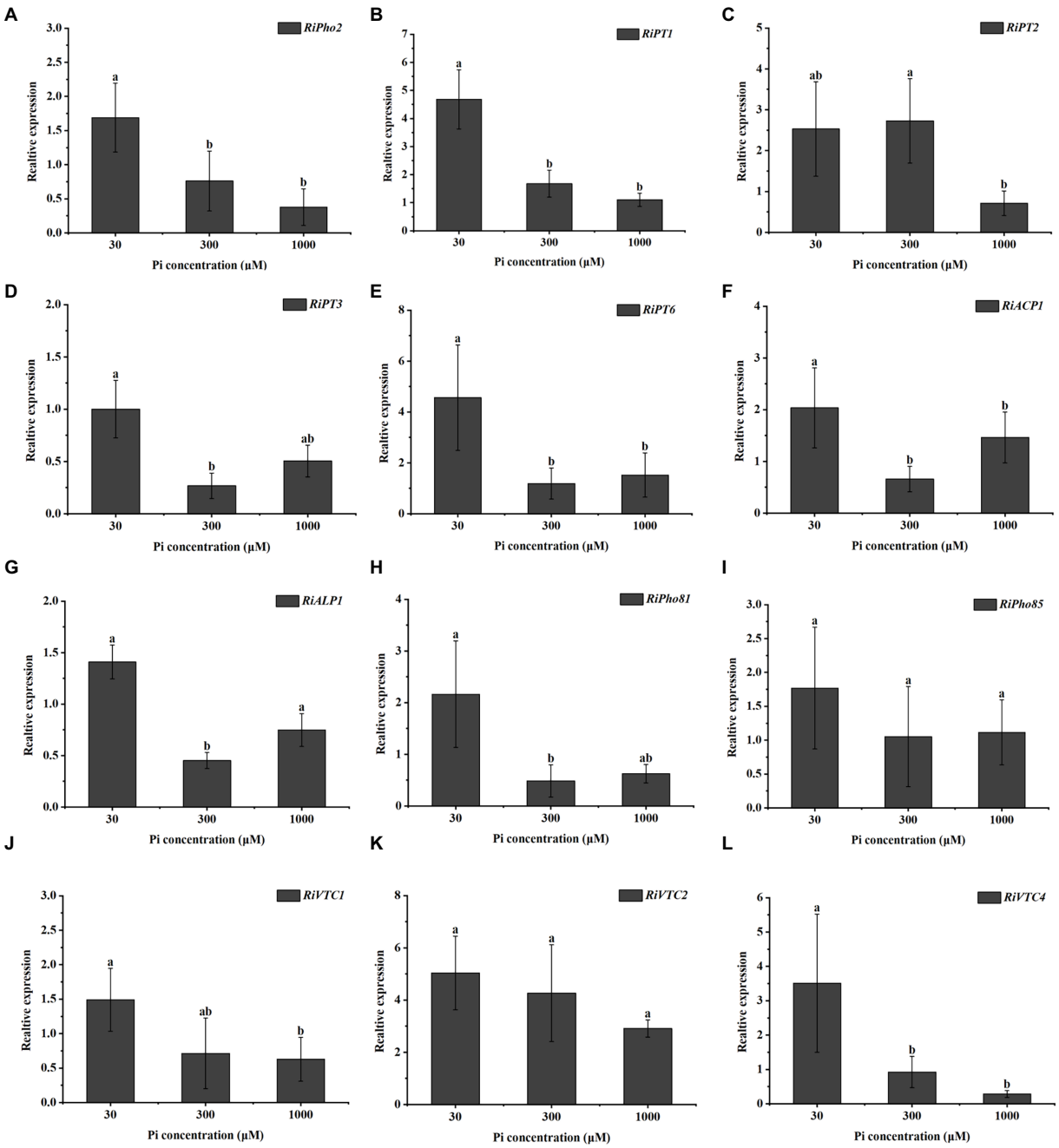

FIGURE 2
Expression profiles of the genes involved in the phosphate (PHO) signaling pathway from *R. irregularis* in mycorrhizal *E. grandis* roots at different phosphate concentrations. **(A–L)** Expression levels of genes of PHO pathway under different phosphate concentrations, including **(A)** transcription cofactor, **(B–E)** Pi transporters, **(F,G)** phosphatase related genes, **(H,I)** cyclin-protein genes and **(J–L)** vacuolar transporters, suggesting that the expressions of PHO pathway genes are affected by phosphate concentrations. AM fungal *RiEF1α* is set as the reference gene. The data represent the means of three biological replicates with standard deviations. Different letters indicate the Duncan's multiple comparison results. Significance, $p<0.05$.

significantly higher at 30 μM Pi than medium and high Pi concentrations (300 and 1,000 μM), whereas *RiVTC2* expression was not significantly enhanced in roots exposed to low Pi concentration (Figures 2J–L). Overall, these gene expression profiles revealed that the Pi sensing and transport/metabolism genes are regulated in response to Pi starvation in *R. irregularis* during AM symbiosis.

Identification of RiPho4, which encodes a HLH domain-containing transcription factor

The above results (see Figure 2) indicate that the downstream genes of the PHO pathway in *R. irregularis* are transcriptionally dependent on the Pi availability. In order to identify the key

transcription factor regulating the expression of downstream PHO genes in response to phosphate starvation, we searched for the sequences that correspond to the TFs in PHO pathway of *S. cerevisiae* using the genome sequencing projects of *R. irregularis* DAOM 197198 (Tisserant et al., 2013; Chen et al., 2018), and found a transcription factor called RiPho4. According to the GenBank annotation, *RiPho4* contains 5 exons and 4 introns, a total length of 2052 bp with 1710 bp of ORF (Figure 3A). Using Smart program, it is predicted that *RiPho4* encoding protein has 6 domains, 5 of which are low complex domains (LCDs), while the region from +436 to +515 is a HLH (helix loop helix) domain (Figure 3B), which is one of the specific domains of TFs (Ferré-D'Amaré et al., 1993; Kiribuchi et al., 2004; Carretero-Paulet et al., 2010; Zhu and Huq, 2011). Further the three-dimensional conformation of RiPho4 (Figure 3C) showed that RiPho4 is a typical HLH domain containing protein. Therefore, it is predicted that RiPho4 may serve as a key transcription factor containing a HLH domain in *R. irregularis*.

RiPho4 is conserved across fungi species

To determine the evolutionary relationships of Pho4 proteins between *R. irregularis* and other different fungi species, we performed the phylogenetic analysis and conserved motif identification. The result shows that RiPho4 is related to AM fungal TFs GmPho4, GcPho4, FgPho4 and FmPho4, and has closely relative to the RdPho4 and RcPho4 from *Rhizophagus diaphanous* and *Rhizophagus clarus* (Figure 3D). RiPho4 protein is >98% identical to Pho4 from *R. diaphanous*, 41% to LtPho4 from the filamentous fungi *Lobosporangium transversale* and 38% to ScPho4 of *S. cerevisiae* which has been reported to be a typical HLH-type transcription factor (Oshima, 1997; Tomar and Sinha, 2014). In addition, we identified RiPho4 functional orthologs with Pho4 from other AMF (Supplementary Figure S2). These *in silico* results suggest that *R. irregularis* RiPho4 is highly conserved across fungi species.

RiPho4 is induced in mycorrhizal roots

To determine the spatiotemporal expression patterns of *RiPho4* from *R. irregularis*, the transcriptional analysis of *RiPho4* and relevant PHO genes were performed in different tissues of *R. irregularis* using the RNA-sequencing data (Zeng et al., 2018, 2020). As shown in Figure 4A, the transcription of *RiPho2, RiPT1, RiPho81, RiPho80,* and *RiPho91* (equally RiPT7, Xie et al., 2022) were up-regulated in mycorrhizal roots when compared with other fungal tissues, while the transcriptional levels of *RiPho4* were induced in both mycorrhizal roots and arbuscules of *R. irregularis*, and *RiPho85* were constitutively expressed in these six different fungal tissues. To confirm the transcriptomic data, we further conducted the qRT-PCR experiments with roots of *E. grandis*

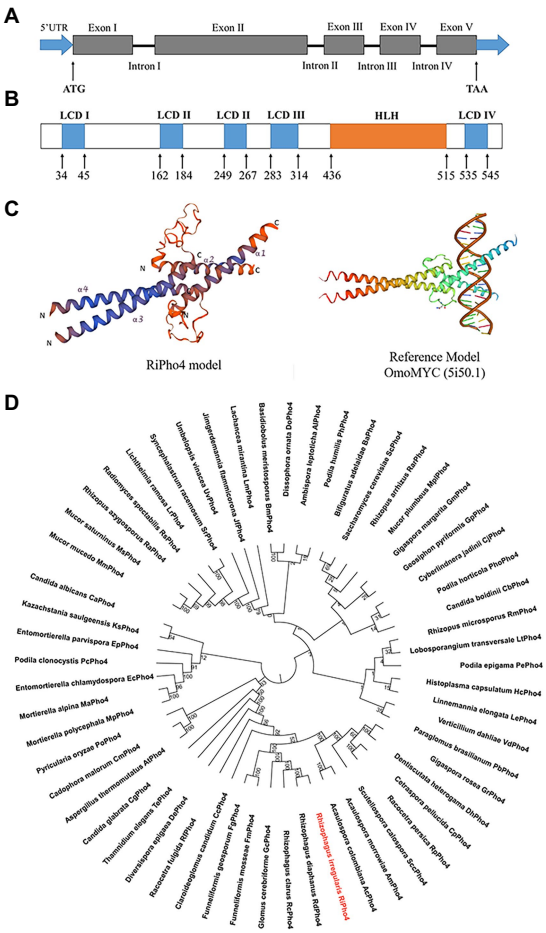

FIGURE 3
Gene and protein structures of *RiPho4* in *R. irregularis* and the evolutionary relationships with Pho4 proteins in various fungi species. **(A)** The *RiPho4* gene contains five exons and four introns, corresponding to gene ID 36869193. The untranslated regions (UTRs) are shown in the figure, ATG and TAA represent the translation start site and translation termination site, respectively. **(B)** Inferred protein domain of RiPho4. RiPho4 protein contains 570 amino acids and consists of one HLH domain and four low complex domains (LCDs) (http://smart.embl.de/). **(C)** Predicted three-dimensional structure of RiPho4 model by SWISS-MODEL. It was predicted that the 3D structure of RiPho4 is similar to that of OmoMYC (5i50.1), a protein encoded by MYC dominant-negative allele in *Mus musculus* (Jung et al., 2017). **(D)** The unrooted phylogenetic tree was constructed with the neighbor-joining method, based on multiple sequence alignments of RiPho4 (red color) and other Pho4 proteins from different fungi species using MEGA v7.0 software. Bootstrap tests were performed using 1,000 replicates. The accession numbers of all Pho4 proteins are provided in the Supplementary Table S2.

colonized with *R. irregularis*. The time-course analysis indicated that *RiPho4* expression was still high in the later stage of mycorrhizal symbiosis, and its transcript reached the highest level at 56 days post inoculation (Figure 4B), this pattern was correlated with the colonization and development processes of *R. irregularis* within *E. grandis* roots (Supplementary Figure S3). Additionally, transcriptional

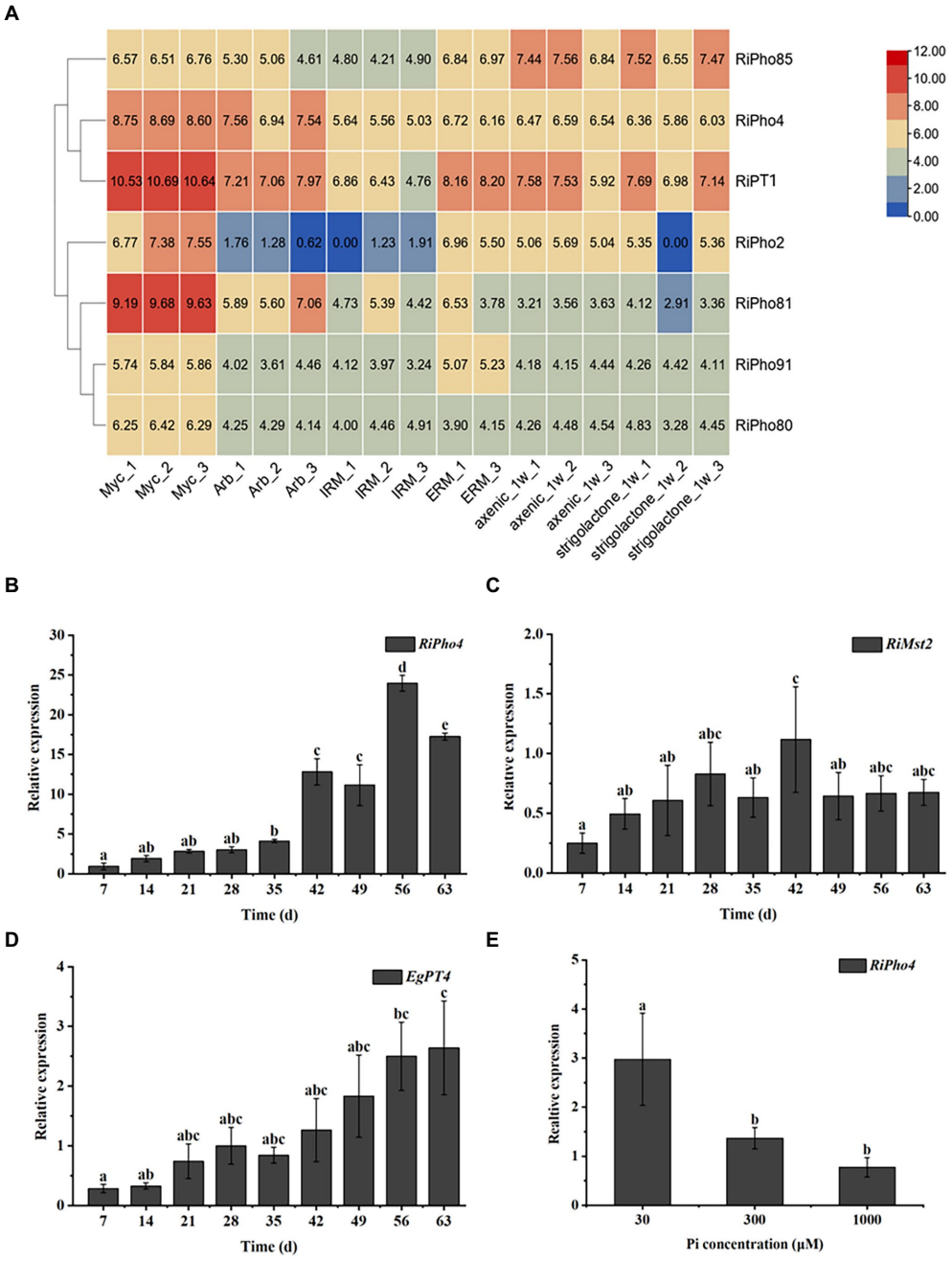

FIGURE 4
Spatiotemporal expression patterns of *RiPho4* from the AM fungus *R. irregularis*. **(A)** Analysis of the heat diagram for transcriptional levels of *RiPho4* and some PHO pathway genes in different fungal tissues: mycorrhizal roots of *Medicago truncatula* (Myc), arbuscules from *M. truncatula* mycorrhizal roots (Arb), intraradical mycelium (IRM), extraradical mycelium (ERM), axenic germinating spores harvested at a week after inoculation (axenic_1w) and germinating spores at 7days after GR24 induction (strigolactone_1w). The heatmap of identities was visualized by the TBtools (Chen et al., 2020). **(B–D)** Time-course assay of the expression of *RiPho4*, *RiMst2* and *EgPT4* in *E. grandis* mycorrhizal roots after 7, 14, 21, 28, 35, 42, 49, 56 and 63days (d) inoculation with *R. irregularis*. *RiEF1α* and *EgUBI3* were used as the reference genes for *R. irregularis* and *E. grandis* gene normalization, respectively. **(E)** Expression analysis of *RiPho4* in mycorrhizal roots of *E. grandis* grown under different phosphate concentrations. The error bars are the means with standard errors of three biological replications. Treatments with the same letters do not differ from others by the Duncan's test at 5% probability.

patterns of the monosaccharide transporter gene *RiMst2* and Pi transporter gene *EgPT4*, which are thought to be the AM marker genes (Helber et al., 2011; Che et al., 2022), were also similar to that of *RiPho4* during symbiosis (Figures 4C,D). Therefore, these results indicated that *RiPho4* is induced in the arbuscles of mycorrhizal roots.

RiPho4 is expressed in response to Pi starvation

To further determine the effect of external Pi concentrations on the transcription of *RiPho4* during the *in planta* phase, *E. grandis* plants inoculated with *R. irregularis* were cultured in the pots supplemented with different phosphate concentrations (30, 300 or 1,000 μM). The qRT-PCR experiment was then performed on the mycorrhizal roots of *E. grandis* subjected to different Pi concentrations as mentioned above. As a result, the expression levels of *RiPho4* were significantly inhibited in roots during high Pi concentrations (300, 1,000 μM) (Figure 4E). This result is consistent with the above findings on PHO gene expression profiles (see Figure 2), suggesting that *RiPho4* is induced during mycorrhizal symbiosis in response to Pi starvation.

RiPho4 encodes a transcription factor and localizes in nucleus at low phosphate concentrations

Previous studies have found that ScPho4 protein in *S. cerevisiae* imports into the nucleus under low phosphorus supply, whereas the Pho4 exports into the cytoplasm nucleus of yeast cells exposed to high phosphorus conditions (Kaffman et al., 1994; Byrne et al., 2004; Urrialde et al., 2015). To investigate whether RiPho4 has a similar function to ScPho4 from *S. cerevisiae*, we carried out the subcellular localization experiments in yeast cells. As expected, GFP-RiPho4 fusion protein was localized in the nuclei of yeast strain EY57 cells during low Pi treatment (600 μM), while this fusion protein was found in the cytoplasm of yeast cells exposed to high P concentration (10 mM) (Figure 5A). To further verify the localization results as mentioned above, we used a labeling dye DAPI, which can bind to DNA to label the nuclei of yeast cells. The co-localization analysis indicated that the expression of GFP-RiPho4 fusion protein in yeast cells was confirmed to be correctly localized in the nuclei of yeast cells under Pi-limited (600 μM and 1 mM) conditions (Figure 5B). In conclusion, these results reveal that RiPho4 protein locates in the nucleus under low Pi conditions and may serve as a transcription factor in fungal cells.

RiPho4 is required for arbuscule development

In order to further study the roles of *RiPho4* in AM symbiosis, we knocked down *RiPho4* expression by the VIGS method. We designed two RNAi regions to target the corresponding specific regions of *RiPho4* that was very divergent from the other genes containing bHLH domains in *R. irregularis* to avoid off-target silencing (see Supplementary Figure S5). First, we detected the transcriptional levels of *RiPho4* in mycorrhizal roots of *N. benthamiana* under three different Pi concentrations

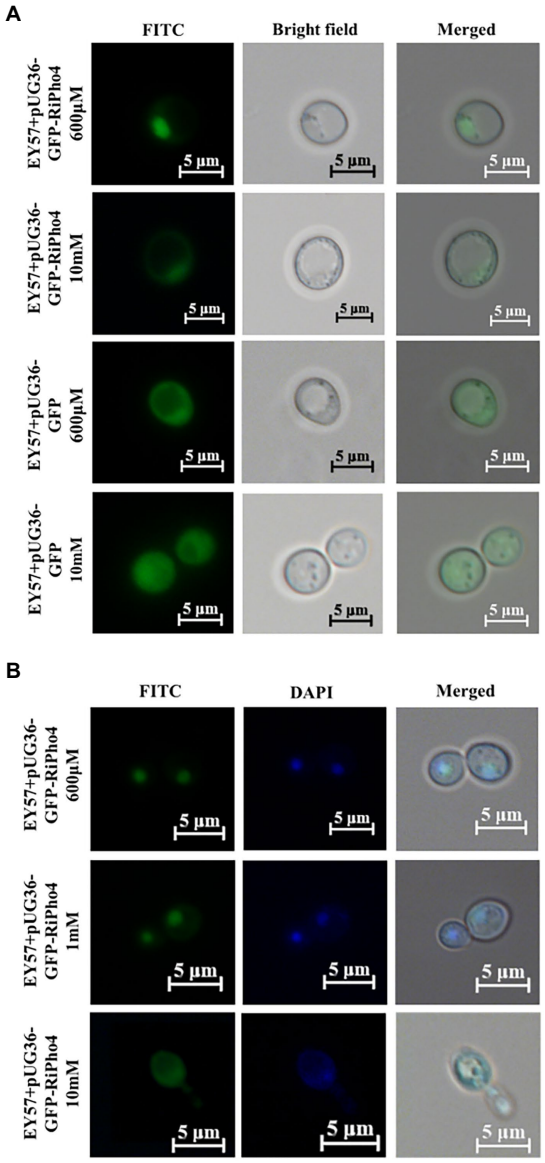

FIGURE 5
Subcellular localization of RiPho4 in *Saccharomyces cerevisiae* grown under different phosphate conditions. Fluorescence microscope images of *S. cerevisiae* EY57 cells expressing pUG36-GFP or pUG36-GFP-RiPho4. **(A)** Localization of RiPho4 was captured by fluorescence microscopy, the pUG36 containing the GFP reporter gene was used as the control, showing the fluorescence signal in the cytoplasm. The yeast cells were grown in YNB liquid medium with different Pi (600μM, 10mM KH_2PO_4) treatments for 12h. **(B)** The transformed cells were grown in YNB medium under different Pi (600μM, 1mM, 10mM K_2HPO_4) conditions for 12h. FITC showed the green fluorescence channel; DAPI presented transformed yeast cells stained with DAPI dye. Scale bars, 5μm.

(30, 100, or 300 μM). The results showed that the transcriptional levels of *RiPho4* in the *VIGS-RiPho4* roots were significantly reduced by more than 60%, when compared with the control roots, indicating that expression of *RiPho4* was effectively knocked down (Figure 6A). Expressions of the monosaccharide transporter

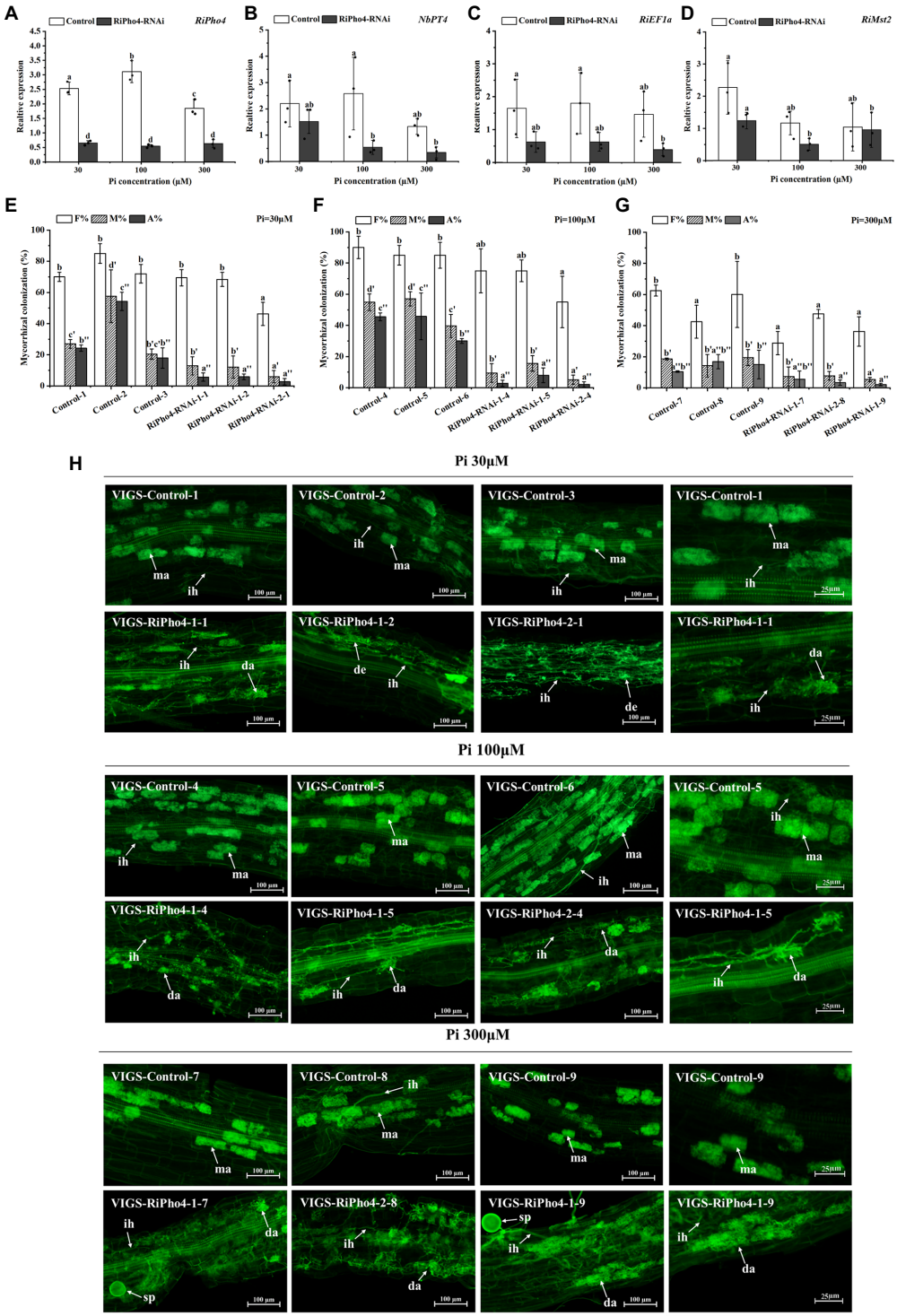

FIGURE 6
Molecular and arbuscular mycorrhizal phenotypes of virus-induced gene silencing (VIGS) of *RiPho4* in tobacco (*Nicotiana benthamiana*) roots colonized by *R. irregularis* grown under different Pi conditions. **(A–D)** Expression levels of *RiPho4*, *NbPT4*, *RiEF1α* and *RiMst2* in mycorrhizal tobacco *RiPho4-RNAi* roots under different phosphate conditions, estimated by quantitative RT-PCR. *R. irregularis RiEF1a* and *N. benthamiana NbTEF1a* were used as the endogenous genes for normalization of *RiPho4*, *RiMst2*, *NbPT4* and *RiEF1α* expression, respectively. The data represented the means of three biological replicates. Bars indicated the standard errors of means. Means designated with the same letters are not significantly different ($p \geq 0.05$) according to Duncan's multiple range test. **(E–G)** Mycorrhizal colonization levels between the control and *RiPho4-RNAi* roots exposed to different Pi (30μM, 100μM and 300μM K_2HPO_4) concentrations were determined after the WGA488 staining. F%, the total colonization frequency; M%, the percentage of mycorrhizal intensity; A%, the percentage of arbuscule abundance. **(H)** Fluorescence microscopic images of *R. irregularis* arbuscules in control and *RiPho4-RNAi* roots grown under different Pi conditions. The arrows and letters in the figure represent different structures of *R. irregularis*: ma, mature arbuscules; da, degraded arbuscules; de, dead arbuscules; ih, intraradical hyphae; sp., spores. Scale bars, 100μm (1–3 columns), 25μm (the 4th column).

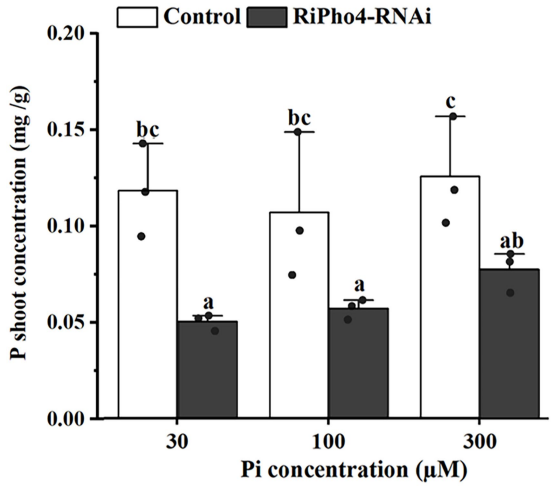

FIGURE 7
Phosphate concentrations in the tobacco (*N. benthamiana*) shoots of the control and VIGS of *RiPho4* treatments under different Pi conditions. The data represented the means with SE. Different letters indicated the significant differences which statistically analyzed by Duncan's multiple range test at the alpha=0.05 level.

gene *RiMst2*, AM fungal reference gene *RiEF1α* and Pi transporter gene of *N. benthamiana NbPT4*, which are considered as symbiotic marker genes (Helber et al., 2011; Kikuchi et al., 2016; Xie et al., 2022), were significantly decreased in *RiPho4-RNAi* roots under different Pi concentrations (Figures 6B–D).

Further observation of the mycorrhizal colonization uncovered the distinguishable AM phenotype between the *RiPho4-RNAi* and control roots during AM symbiosis under different Pi concentrations. Relative to the controls, the total AMF colonization in most of *RiPho4-RNAi* roots showed a slightly but not significantly decrease, while silencing of *RiPho4* obviously decreased the mycorrhizal intensity and arbuscule abundance in roots (Figures 6E–G). Moreover, more arbuscules in the *RiPho4-RNAi* roots were abnormal, or degenerating under different Pi conditions (Figure 6H). Collectively, these findings reveal that *RiPho4* is essential for arbuscule development.

RiPho4 plays an important role in regulating the symbiotic Pi absorption during AM symbiosis

To determine whether RiPho4 regulates the symbiotic Pi transport in AM symbiosis of *N. benthamiana*, we examined the total P concentration of AM tobacco shoots of control and *RiPho4-RNAi* plants grown under three different Pi (30, 100, or 300 μM) conditions. As a result, the P concentration in AM plants of RiPho4-silenced lines were significantly reduced compared with control plants (Figure 7). This result indicated that RiPho4 may regulate Pi transport at the symbiotic interface of arbuscular mycorrhizas.

Knock-down of RiPho4 affects the expression of PHO pathway genes in *Rhizophagus irregularis* during AM symbiosis

To confirm the function of RiPho4 in the PHO pathway of *R. irregularis*, qRT-PCR was used to explore the effect of *RiPho4* knock-down on the PHO pathway genes in mycorrhizal *N. benthamiana* roots exposed to different Pi concentrations. The results showed that *RiPho2, RiPT1*, *RiPT2* and *RiPT3* were significantly decreased in RiPho4-silenced roots under low Pi conditions (30–100 μM) when compared with control roots (Figures 8A–D). Furthermore, the expression levels of genes involved in Pi and Poly-P metabolism in *R. irregularis*, such as *RiALP1*, *RiACP1, RiPPX1* and *RiPPN1* (Xie et al., 2022), were also inhibited in the *RiPho4-RNAi* roots when compared to the controls (Figures 8E–H), suggesting that loss of *RiPho4* function results in a reduction of Pi and Poly-P metabolisms under Pi-limited conditions. Therefore, these results indicate that *RiPho4* may positively regulate the transcriptional levels of the downstream genes of PHO pathway in *R. irregularis* during AM symbiosis under Pi-deficient conditions.

RiPho4 directly regulates the Pi transporter genes of PHO pathway from *Rhizophagus irregularis*

To confirm that *RiPho4* encodes a transcription factor to regulate PHO genes, we tested its ability to interact with Pi transporters of *R. irregularis* by the yeast one-hybrid (Y1H) assay. It is known that the common binding motif of Pho4 transcription factor is CACGTG/T (Secco et al., 2012; Tomar and Sinha, 2014), we therefore selected the same CREs (*cis*-regulatory elements) in the promoters of three Pi transporter genes *RiPT1, RiPT2,* and *RiPT3* for further studies (see Supplementary Table S5).

As a result, the Y1HGold yeast cells containing pAbAi vector with P_{RiPT1}, P_{RiPT2}, or P_{RiPT3} were significantly inhibited at 400, 600, and 800 ng/ml AbA, respectively (see Supplementary Figure S4). In the Y1H assay, the yeast cells containing AD-RiPho4 plasmid and wild-type promoter P_{RiPT1}, P_{RiPT2}, or P_{RiPT3} still grew well on medium supplemented with 700 ng/ml, 800 ng/ml, or 900 ng/ml AbA, while the yeasts containing mutant promoters without Pho4-binding sites (CACGTG/T) were strongly inhibited under such conditions (Figure 8I). These data showed that RiPho4 protein interacts with the promoters of *RiPT1*, *RiPT2*, and *RiPT3* through the Pho4-binding sites (CACGTG/T). Therefore, the transcription factor RiPho4 can directly regulate the Pi transporter genes *RiPT1*, *RiPT2* and *RiPT3* in PHO pathway. Collectively, the Y1H results implicate that RiPho4 may act as a transcriptional activator in the PHO pathway in *R. irregularis*.

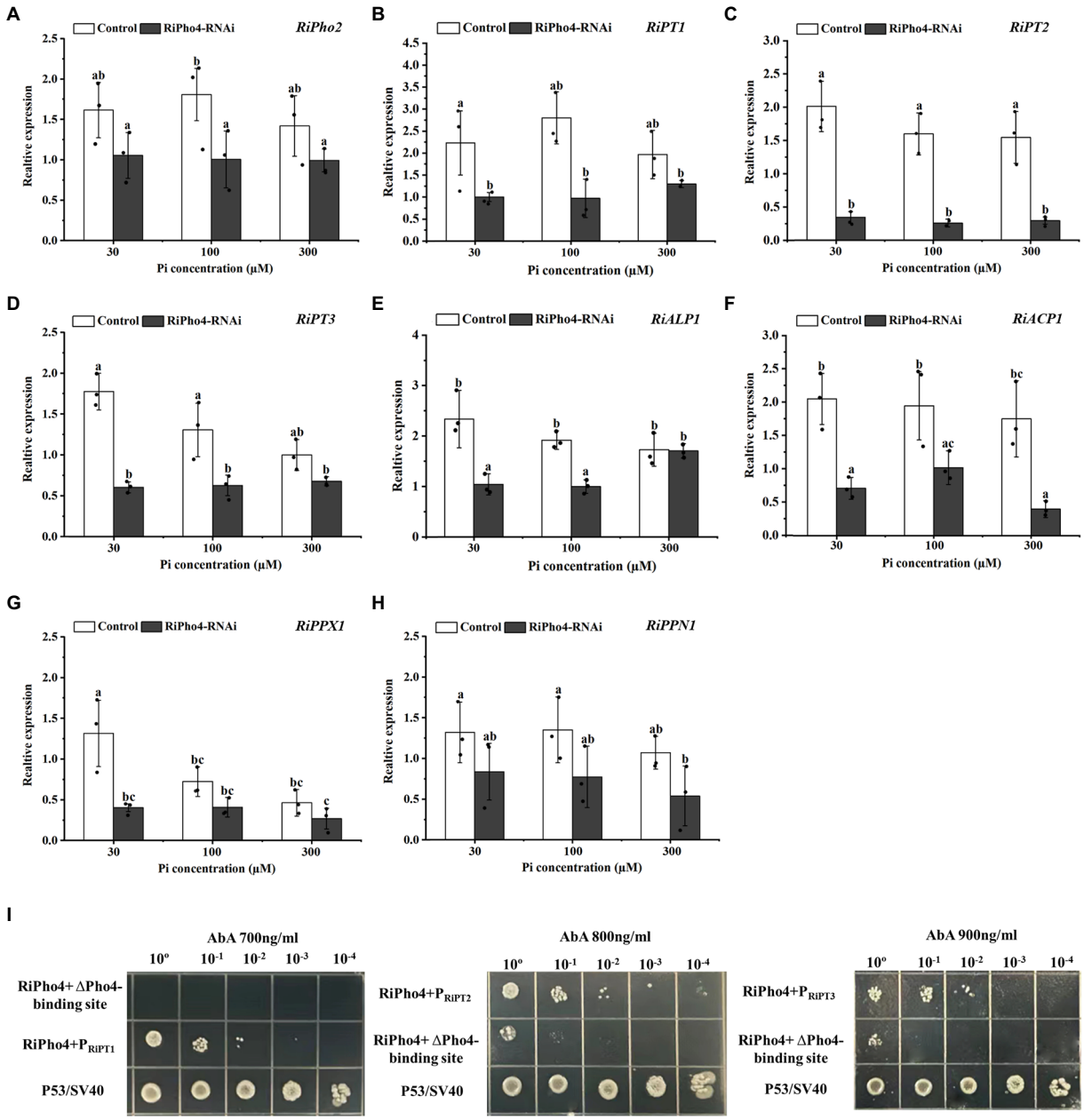

FIGURE 8
RiPho4 regulates the expression of downstream genes involved in Pi transport and metabolism processes in *R. irregularis*. **(A–H)** Expression analysis of *R. irregularis* genes engaged in PHO pathway between *RiPho4-RNAi* and control roots under different phosphate concentrations. Expression levels of *RiPho2* **(A)**, Pi transport genes *RiPT1, RiPT2, RiPT3* **(B–D)**, phosphatase related genes *RiALP1, RiACP1* (E-F), *RiPPX1* and *RiPPN1* related to Poly-P metabolism **(G,H)** in response to different phosphate concentrations were estimated by real-time qRT-PCR analysis. Different letters indicated significant differences between control and RNAi lines. The differences between samples were analyzed using Duncan's new multi-range test at the alpha=0.05 level. **(I)** Yeast one-hybrid analysis of the interaction between RiPho4 with promoters of *RiPT1*, *RiPT2*, and *RiPT3*. The promoter regions of *RiPT1*, *RiPT2* and *RiPT3* containing the *cis*-acting elements CACGTG/T named P_{RiPT1}, P_{RiPT2}, and P_{RiPT3}. The identification of interaction between RiPho4 and the promoter of *RiPT1*, *RiPT2*, or *RiPT3* under the screened even higher AbA inhibition concentration indicated in Fig. S4. Yeast cells carrying both pGBKT7-P53 and pGADT7-SV40 grown on SD/−Leu were used as the positive control, P_{RiPT1}, P_{RiPT2}, P_{RiPT3}-ΔPho4-binding sites with pGADT7-RiPho4 were used as the negative controls. ΔPho4-binding site indicates the deletion of the Pho4 binding site (CACGTG/T) elements located in P_{RiPT1}, P_{RiPT2}, P_{RiPT3} promoters. 10-fold serial dilutions of yeast cells were spotted on plates, and the initial yeast concentration was OD_{600}=0.2.

Discussion

Recent years, more researchers have reported the physiological responses of Eucalyptus species to low Pi stress (Wu et al., 2014; Niu et al., 2015; Bahar et al., 2018), and focused on the effects of different P levels on plant biomass and P content (Xu et al., 2001; Standish et al., 2007; Bichara et al., 2021), but little study on the molecular mechanisms of

the interaction between AMF and Eucalyptus plants. Although the PHO pathway responsible for Pi absorption, transport and metabolism has been described in several fungi species (Kerwin and Wykoff, 2009; Zheng et al., 2020; Ahmed et al., 2022), the regulatory mechanisms of Pi nutrient exchange between AMF and host plants through PHO pathway is still partially understood so far (Xie et al., 2016, 2022). In this study, we focus on the AM fungus *R. irregularis* mediating Pi uptake and homeostasis in AM symbiosis of *E. grandis* by investigating the expression, localization and function of RiPho4, a transcription factor of the PHO pathway.

The PHO pathway of AM fungus plays a Key role in phosphate absorption during AM symbiosis

It has been reported that AMF can significantly promote Pi uptake and Pi stress adaptation abilities of host plants in both field and laboratory conditions (Abdel-Fattah, 2001; Kobae, 2019; Wang et al., 2019). Accordingly, a large number of studies have shown that the growth indices of AM plants, such as plant height, stem diameter, leaf area, root volume, shoot, root dry weight and P content, were significantly higher than those of NM plants under phosphorus limitation (Pumplin and Harrison, 2009; Frosi et al., 2016; Tian et al., 2017; Carballar-Hernandez et al., 2018; Wang et al., 2019). Especially at low Pi concentration, the host plants have high dependence to AMF (Chu et al., 2013). The results and data of the overall growth and physiological status of *R. irregularis-E. grandis* interaction in this study (Supplementary Figure S1; Figures 1A–E) are consistent with the previous results. AMF are sensitive to P supply and a low to moderate supply is required (Ezawa et al., 2002), the intensities of fungal ALP, ACP and SDH activities reflecting the metabolic activity and function of AMF also decreased with the increasing P input (Hamel et al., 1990; Saito, 1995; Vivas et al., 2003; Li et al., 2017; Wang et al., 2017). Similarly, high Pi supply strongly suppressed the AMF colonization and arbuscule formation (see Figure 1F) as well as the intensities of AM fungal ALP, ACP, and SDH activities (see Figures 1G–I; Supplementary Table S1) in this study. Because ACP and ALP are involved in the hydrolysis of Poly-P in the AMF (Ezawa et al., 2002), it can be considered that AMF greatly improved P nutrient of host plants by Poly-P hydrolysis in the IRM and apoplast when phosphate concentration was limited. The previous studies have found that the Pi uptake of mycorrhizal plants includes the direct uptake pathway and mycorrhizal uptake pathway (Smith and Smith, 2011). When Pi concentration was limited, Pi absorption of symbiotic plants is mainly through the mycorrhizal pathway (Zhang et al., 2021). However, when the phosphorus supply is sufficient, the direct pathway is activated within host plants to uptake from root surface, and the AMF has few Pi contribution (Chu et al., 2020). This is consistent with the results that the AMF colonization decreased and the phosphatase activities were decreased in mycorrhizal roots when Pi concentration was high (see Figure 1). In conclusion, plants absorb Pi mainly *via* the mycorrhizal pathway under low P environments, and AMF plays an important role in the growth of *E. grandis*.

Until now, molecular mechanisms by which AMF regulate Pi efflux from the IRM to symbiotic interface are partially understood (Wang et al., 2017; Nguyen and Saito, 2021; Xie et al., 2022). In yeast, several studies have implicated that transcription of PHO pathway genes are closely related to the Poly-P metabolism and cytosolic Pi transportation (Vardi et al., 2014; Desfougeres et al., 2016). The PHO pathway has been extensively characterized in yeast but less in AMF (Tisserant et al., 2012; Xie et al., 2016, 2022). In the case of yeasts and AMF, the homeobox transcription factor Pho2, Pi transporter genes, VTC complex VTC1/2/4, cyclin Pho80, CDK inhibitor Pho81, Cyclin-dependent kinase Pho85 are all controlled in the PHO pathway and in response to Pi deficiency (Lenburg and O'Shea, 1996; Ezawa et al., 2002; Tomar and Sinha, 2014; Xie et al., 2022). Similar identification was conducted on these homologous genes in *Neurospora crassa* (Gras et al., 2013). Through qRT-PCR analysis, it was found that the PHO pathway genes in *R. irregularis* were generally more active at low Pi levels than at medium and high Pi levels (see Figure 2). Besides, the transcriptional levels of *RiALP1* and *RiACP1* were influenced by high Pi supply (see Figures 2F,G) were consistent with the ALP and ACP staining results (see Figures 1G–I; Supplementary Table S1). Therefore, it is predicted that the PHO pathway genes of *R. irregularis* may play important roles in promoting plant Pi absorption during AM symbiosis under low Pi conditions, and the regulon which control the transcription of PHO pathway genes during Pi starvation is worthy to be further investigated.

RiPho4 acts as a key transcription factor of the PHO pathway in *Rhizophagus irregularis*

Very recently, it has been found that the core components of PHO pathway are evolutionarily conserved among AMF and yeast species (Zhou et al., 2021). In *S. cerevisiae*, Pho4 is known as a helical loop–helix (HLH) transcription factor to activate the expression of PHO downstream genes in response to Pi limitation (Vogel et al., 1989; Komeili and O'Shea, 1999; Urrialde et al., 2015). ScPho4 is a Pi-sensitive core regulation factor (Tomar and Sinha, 2014). Here, RiPho4, the homologous protein of ScPho4 in *R. irregularis*, is highly conserved in fungi species containing the HLH domain to bind to DNA (see Figure 3; Supplementary Figure S2). Therefore, RiPho4 can be considered as an important transcription factor of the PHO pathway in *R. irregularis*.

From expression patterns of *RiPho4* (see Figure 4), it is more active in mycorrhizal roots and arbuscules during

symbiosis, indicating that RiPho4 may function in the Pi nutrient exchange at the symbiotic interface, especially in arbuscules (Smith and Smith, 1997; Karandashov et al., 2004; Harrison, 2012; Luginbuehl and Oldroyd, 2017). Moreover, the transcription of *RiPho4* is dependent on the Pi availability, this is similar to *Pho4* in filamentous fungi (Peleg et al., 1996; Gras et al., 2013; Tomar and Sinha, 2014). The RiPho4 protein location in the nuclei of yeast cells is also dependent on Pi availability. When facing to the high phosphate concentrations, RiPho4 can be moved to the cytoplasm (see Figure 5). This finding is similar to Pho4 location patterns of yeasts and filamentous fungi (Peleg et al., 1996; Byrne et al., 2004; Urrialde et al., 2015). It is well-known that one of the mechanisms regulating the activation of TFs is cytoplasmic retention and subsequent translocation into the nucleus due to external stimuli (Reich and Liu, 2006; Hao and O'Shea, 2012). And for RiPho4, the transcription factor in the cytoplasm subsequently translocates into the nucleus in response to low Pi stimulus, like ScPho4. Therefore, our findings reveal that the transcription factor RiPho4 in *R. irregularis* is induced during P starvation, and may play a key role in the regulation of Pi uptake and homeostasis during AM symbiosis.

RiPho4 regulates arbuscule development and Pi concentration of mycorrhizal plants through modulating the PHO genes in *Rhizophagus irregularis*

Up to date, few Pi transporter genes of PHO pathway in AMF, such as *GigmPT* and *RiPT7*, have been functionally described by gene silencing, and knock-down of *GigmPT* or *RiPT7* leads to fungal growth arrest and impaired arbuscule development (Xie et al., 2016, 2022). Correspondingly, in our study, *RiPho4* silencing also results in the obvious phenotype of arbuscule degradation (see Figure 6). The previous studies have shown that the process of AMF Pi delivery to plant cells serve as a signal to maintain the arbuscule development (Javot et al., 2007; Xie et al., 2016, 2022). However, Pi levels of mycorrhizal tobacco were significantly reduced in the *RiPho4-RNAi* lines when compared with the control lines (see Figure 7), suggesting that the loss of *RiPho4* function results in the hinder of Pi transportation from the arbuscules to host plants. Therefore, RiPho4 functions in maintaining the arbuscule development, resulting from its role in promoting Pi exchange at the symbiotic interface of mycorrhizas. Indeed, this regulatory roles of fungal Pho4 proteins in Pi uptake and homeostasis have been demonstrated. Previous studies showed that *NUC-1* (*Pho4* homologous gene) from *N. crassa* is considered to be a factor to activate the transcription of Pi transporter genes (Kang and Metzenberg, 1990; Gras et al., 2013), and in AMF, Pho4 is predicted to have a regulatory role on the PHO responsive genes (Xie et al., 2016; Zhou et al., 2021). As expected, in *R. irregularis*, the knock-down of *RiPho4* by VIGS resulted in the significant decrease in expression levels of Pi transporter genes, Pi and Poly-P metabolism genes under Pi limited conditions (see Figures 8A–H). From this result, it is suggested that RiPho4 regulates Pi transport and homeostasis at the symbiotic interface through controlling the PHO gene expression.

Next, question is how RiPho4 regulates the transcription of PHO genes in *R. irregularis*. We used the Y1H assay to preliminarily address this issue. As shown in Figure 8I, the RiPho4 protein interacted with the promoters of Pi transporter genes *RiPT1*, *RiPT2* and *RiPT3* in *R. irregularis* through binding to the CACGTG/T sites. On the basis of the results, it is concluded that RiPho4 is able to directly regulate Pi transporter genes of PHO pathway. Since other downstream genes of PHO pathway, such as *RiVTC1, RiVTC2* and *RiALP1*, also contain the Pho4-binding sites (CACGTG/T), it is predicted that RiPho4 may also have regulatory functions on these Pi and Poly-P metabolism genes (see Supplementary Table S5). In filamentous fungi, Pi responsive genes containing the Pho4-binding sites, including phosphate permeases and repressible alkaline phosphatase genes, help the cell to survive in the prevailing low Pi environment (Lenburg and O'Shea, 1996; Gras et al., 2007; Leal et al., 2007; Tomar and Sinha, 2014). These evidences indicate that RiPho4 can directly regulate the downstream genes of PHO pathway to control Pi uptake and homeostasis during AM symbiosis. However, whether RiPho4 binds to a large number of Pi responsive genes involved in the PHO pathway of *R. irregularis* need to be further identified in future. Taken together, it is proposed that RiPho4 as a transcription factor regulates arbuscule development and symbiotic Pi homeostasis through controlling the downstream genes in the PHO Pathway of *R. irregularis*.

A model of the key regulon RiPho4, which functions in the control of PHO genes in AM fungus during symbiosis

According to our results and previous studies (Oshima, 1997; Tomar and Sinha, 2014; Zhou et al., 2016; Ahmed et al., 2022), we proposed a working model in which RiPho4 acts as a transcription factor controlling the PHO genes to regulate Pi transport and homeostasis at the symbiotic interface (Figure 9). In this model, under low Pi conditions (Figure 9A), in arbuscules, the level of inositol heptakisphosphate (IP7), an evolutionary conserved metabolite (Lee et al., 2007), may increase. This induces the expression increasement of CDK inhibitor RiPho81 function (Lee et al., 2008; York and Lew, 2008), thereby preventing the formation of RiPho85 and RiPho80 complex (Schneider et al., 1994; Huang et al., 2007; Lee et al., 2008). The non-formation of the RiPho85 and RiPho80 complex results in hypo-phosphorylate of RiPho4, which is accumulated in the nucleus and activated with cofactor RiPho2 (Urrialde et al., 2015). Subsequently, RiPho4 binds to the CACGTG/T sites to

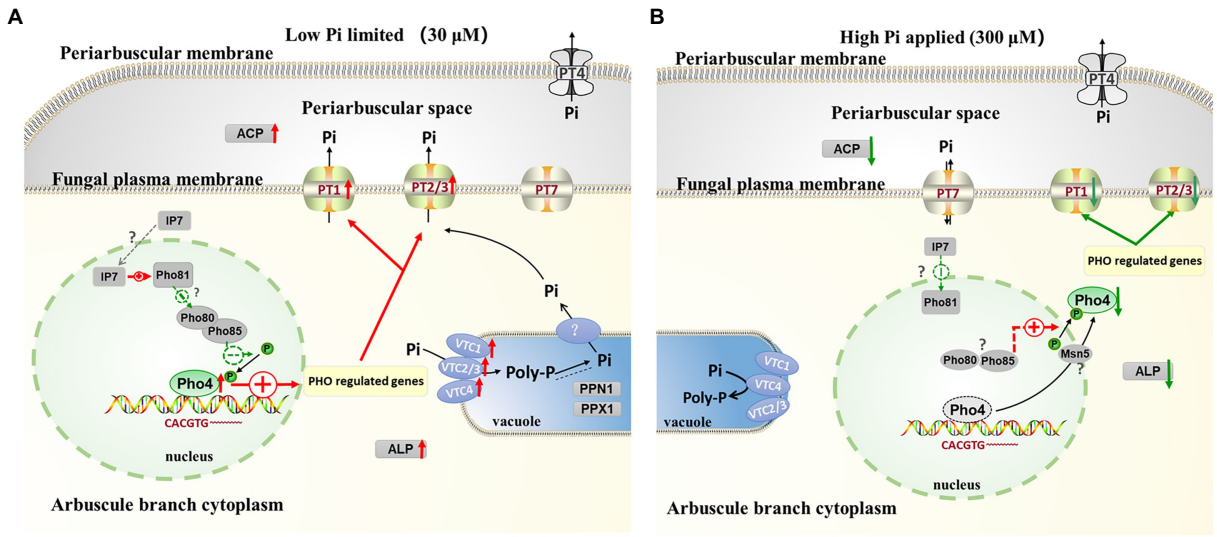

FIGURE 9
Schematic representation of the function of RiPho4 protein regulating phosphate transport and homeostasis in *R. irregularis* during AM symbiosis. **(A)** Under Pi limiting conditions, it is predicted that RiPho4 may be hypo-phosphorylated by RiPho80-RiPho85 complex (Jeffery et al., 2001), and Pho4 locates in nucleus to activate the transcription of downstream genes involved in the PHO pathway, such as *PT1/2/3*, *ACP*, *ALP*, *PPN1* and *PPX1*. **(B)** Under high Pi conditions, the SPX domain-containing Pi transporter RiPT7 is responsible for Pi transport at the symbiotic interface (Xie et al., 2022), whereas the IP7 signal is predicted to be inhibited and the Pho85-Pho80 complex may phosphorylate Pho4 protein (Lee et al., 2008), which is exported from nucleus to cytoplasm, then switches off the PHO pathway. Negative and positive regulatory effects were indicated by green and red arrows, respectively. The relationships between the well-known genes and those not yet determined were shown by the solid and dashed heads, respectively. IP7, inositol heptakisphosphate; Poly-P, polyphosphate; Pi, inorganic phosphate. The green up and red down arrows next to genes indicated that transcript levels of genes were increased and decreased, respectively.

activate the transcriptions of PHO pathway genes in arbuscules, such as the Pi transporter genes *RiPT1/2/3* and Pi metabolism genes *RiALP1* and *RiACP1*. Moreover, *RiPPN1* and *RiPPX1* are also induced to function in the Poly-P metabolism in vacuoles (Xie et al., 2016; Ezawa and Saito, 2018; Zhou et al., 2021). Therefore, during Pi deficiency, RiPho4 regulates the PHO-related genes to enhance the hydrolyzation of Poly-P in arbuscules, and these free Pi are transported into the PAS *via* the Pi transporters (Xie et al., 2022), then the PAM-located PT4 carriers transport Pi to the plant cells (Harrison et al., 2002; Javot et al., 2007; Che et al., 2022). Conversely, under Pi-sufficient conditions (Figure 9B), the IP7 may be lacking in arbuscules and prevent RiPho81 from inhibiting the kinase activity of RiPho85-RiPho80, thus enabling the phosphorylation of RiPho4 (Jeffery et al., 2001; Huang et al., 2007). However, the phosphorylated RiPho4 is exported from the nucleus into the cytoplasm where it cannot activate the transcription of PHO pathway genes (Oshima, 1997; Kaffman et al., 1998; Ghillebert et al., 2011). Under such conditions, the SPX domain-containing transporter RiPT7 can export Pi into the PAS, and AM-specific PT4 can acquire Pi from PAS (Tomar and Sinha, 2014; Che et al., 2022; Xie et al., 2022).

Conclusion

In conclusion, this study presented the expression, localization and functions of *RiPho4* from *R. irregularis*. RiPho4 is a transcription factor containing a HLH domain, and is located in the nucleus of yeast cells under low Pi conditions. Further studies revealed that RiPho4 is a key regulatory factor in AM fungus to maintain arbuscule development through regulating the expression levels of the PHO pathway downstream genes in order to handle Pi transport and homeostasis at the symbiotic interface. Our findings provide new insights into the underlying mechanisms by which AMF control phosphate uptake and homeostasis during symbiosis.

Data availability statement

The original contributions presented in the study are included in the article/Supplementary material, further inquiries can be directed to the corresponding author/s.

Author contributions

XX and MT designed the experiments and managed the projects. SZ and XF performed the experiments. YN and WW performed data analysis. XF and XX provided advice and guidance on the idea of bioinformatics analysis. SZ, XX, and MT wrote the manuscript. HC assisted with the interpretation of the results. All authors contributed to the manuscript read, edited, and approved the current version.

Funding

This research was funded by the National Natural Science Foundation of China (32170116 and 32071639), the Key Projects of Guangzhou of Science and Technology Plan (grant no. 201904020022), and the Laboratory of Lingnan Modern Agriculture Project (NZ2021025), the Guangdong Basic and Applied Basic Research Foundation (grant no. 2022A1515012013).

Acknowledgments

We are grateful to Jianyong An (Huazhong Agricultural University, Wuhan, China) for kindly providing for kindly providing the spores of *R. irregularis* DAOM 197198 for this study. We would like to thank Nianwu Tang (UMR Interactions Arbres/Microorganismes, Centre INRA-Grand Est-Nancy, Champenoux, France) for his help in analysis of transcriptional levels of PHO pathway genes in different fungal tissues. We are grateful to Honghui Zhu (South China Agricultural University, Guangzhou, China) for kindly providing the pAbAi vector for yeast one-hybrid experiment.

Conflict of interest

The authors declare that the research was conducted in the absence of any commercial or financial relationships that could be construed as a potential conflict of interest.

Publisher's note

All claims expressed in this article are solely those of the authors and do not necessarily represent those of their affiliated organizations, or those of the publisher, the editors and the reviewers. Any product that may be evaluated in this article, or claim that may be made by its manufacturer, is not guaranteed or endorsed by the publisher.

Supplementary material

The Supplementary material for this article can be found online at: https://www.frontiersin.org/articles/10.3389/fmicb.2022.1114089/full#supplementary-material

References

Abdel-Fattah, G. M. (2001). Measurement of the viability of arbuscular-mycorrhizal fungi using three different stains; relation to growth and metabolic activities of soybean plants. *Microbiol. Res.* 156, 359–367. doi: 10.1078/0944-5013-00121

Ahmed, Y., Ikeh, M. A. C., MacCallum, D. M., Day, A. M., Waldron, K., and Quinn, J. (2022). Blocking polyphosphate mobilization inhibits Pho4 activation and virulence in the pathogen *Candida albicans*. *MBio* 13:e0034222. doi: 10.1128/mbio.00342-22

Akiyama, K., Matsuzaki, K., and Hayashi, H. (2005). Plant sesquiterpenes induce hyphal branching in arbuscular mycorrhizal fungi. *Nature* 435, 824–827. doi: 10.1038/nature03608

An, J. Y., Zeng, T., Ji, C. Y., de Graaf, S., Zheng, Z. J., Xiao, T. T., et al. (2019). A *Medicago truncatula* SWEET transporter implicated in arbuscule maintenance during arbuscular mycorrhizal symbiosis. *New Phytol.* 224, 396–408. doi: 10.1111/nph.15975

Aono, T., Maldonado-Mendoza, I. E., Dewbre, G. R., and Saito, H. M. (2004). Expression of alkaline phosphatase genes in arbuscular mycorrhizas. *New Phytol.* 162, 525–534. doi: 10.1111/j.1469-8137.2004.01041.x

Auesukaree, C., Homma, T., Kaneko, Y., and Harashima, S. (2003). Transcriptional regulation of phosphate-responsive genes in low-affinity phosphate-transporter-defective mutants in *Saccharomyces cerevisiae*. *Biochem. Biophys. Res. Commun.* 306, 843–850. doi: 10.1016/S0006-291X(03)01068-4

Auesukaree, C., Homma, T., Tochio, H., Shirakawa, M., Kaneko, Y., and Harashima, S. (2004). Intracellular phosphate serves as a signal for the regulation of the PHO pathway in *Saccharomyces cerevisiae*. *J. Biol. Chem.* 279, 17289–17294. doi: 10.1074/jbc.M312202200

Bahar, N. H. A., Gauthier, P. P. G., O'Sullivan, O. S., Brereton, T., Evans, J. R., and Atkin, O. K. (2018). Phosphorus deficiency alters scaling relationships between leaf gas exchange and associated traits in a wide range of contrasting eucalyptus species. *Funct. Plant Biol.* 45, 813–826. doi: 10.1071/fp17134

Balestrini, R., and Bonfante, P. (2014). Cell wall remodeling in mycorrhizal symbiosis: a way towards biotrophism. *Front. Plant Sci.* 5:237. doi: 10.3389/fpls.2014.00237

Balestrini, R., Gómez-Ariza, J., Lanfranco, L., and Bonfante, P. (2007). Laser microdissection reveals that transcripts for five plant and one fungal phosphate transporter genes are contemporaneously present in arbusculated cells. *Mol. Plant-Microbe Interact.* 20, 1055–1062. doi: 10.1094/mpmi-20-9-1055

Benedetto, A., Magurno, F., Bonfante, P., and Lanfranco, L. (2005). Expression profiles of a phosphate transporter gene (*GmosPT*) from the endomycorrhizal fungus *glomus mosseae*. *Mycorrhiza* 15, 620–627. doi: 10.1007/s00572-005-0006-9

Bichara, S., Mazzafera, P., and de Andrade, S. A. L. (2021). Root morphological changes in response to low phosphorus concentration in eucalypt species. *Trees* 35, 1933–1943. doi: 10.1007/s00468-021-02161-4

Bonfante, P., and Venice, F. (2020). Mucoromycota: going to the roots of plant-interacting fungi. *Fungal Biol. Rev.* 34, 100–113. doi: 10.1016/j.fbr.2019.12.003

Brundrett, M., and Tedersoo, L. (2019). Misdiagnosis of mycorrhizas and inappropriate recycling of data can lead to false conclusions. *New Phytol.* 221, 18–24. doi: 10.1111/nph.15440

Byrne, M., Miller, N., Springer, M., and O'Shea, E. K. (2004). A distal, high-affinity binding site on the cyclin-CDK substrate Pho4 is important for its phosphorylation and regulation. *J. Mol. Biol.* 335, 57–70. doi: 10.1016/j.jmb.2003.10.035

Campos-Soriano, L., and Segundo, B. S. (2011). New insights into the signaling pathways controlling defense gene expression in rice roots during the arbuscular mycorrhizal symbiosis. *Plant Signal. Behav.* 6, 553–557. doi: 10.4161/psb.6.4.14914

Carballar-Hernandez, S., Hernandez-Cuevas, L. V., Montano, N. M., Ferrera-Cerrato, R., and Alarcon, A. (2018). Species composition of native arbuscular mycorrhizal fungal consortia influences growth and nutrition of poblano pepper plants (*Capsicum annuum L.*). *Appl. Soil Ecol.* 130, 50–58. doi: 10.1016/j.apsoil.2018.05.022

Carretero-Paulet, L., Galstyan, A., Roig-Villanova, I., Martínez-García, J. F., Bilbao-Castro, J. R., and Robertson, D. L. (2010). Genome-wide classification and evolutionary analysis of the bHLH family of transcription factors in Arabidopsis, poplar, rice, moss, and algae. *Plant Physiol.* 153, 1398–1412. doi: 10.1104/pp.110.153593

Che, X. R., Lai, W. Z., Wang, S. J., Wang, X. Y., Hu, W. T., Chen, H., et al. (2022). Multiple PHT1 family phosphate transporters are recruited for mycorrhizal symbiosis in *Eucalyptus grandis* and conserved PHT1; 4 is a requirement for the arbuscular mycorrhizal symbiosis. *Tree Physiol.* 42, 2020–2039. doi: 10.1093/treephys/tpac050

Chen, C., Chen, H., Zhang, Y., Thomas, H. R., Frank, M. H., He, Y., et al. (2020). TBtools: An integrative toolkit developed for interactive analyses of big biological data. *Mol. Plant* 13, 1194–1202. doi: 10.1016/j.molp.2020.06.009

Chen, E. C. H., Morin, E., Beaudet, D., Noel, J., Yildirir, G., Ndikumana, S., et al. (2018). High intraspecific genome diversity in the model arbuscular mycorrhizal symbiont *Rhizophagus irregularis*. *New Phytol.* 220, 1161–1171. doi: 10.1111/nph.14989

Chien, C. T., Bartel, P. L., Sternglanz, R., and Fields, S. (1991). The two-hybrid system: a method to identify and clone genes for proteins that interact with a protein of interest. *Proc. Natl. Acad. Sci. U. S. A.* 88, 9578–9582. doi: 10.1073/pnas.88.21.9578

Chu, Q., Wang, X., Yang, Y., Chen, F., Zhang, F., and Feng, G. (2013). Mycorrhizal responsiveness of maize (*Zea mays L.*) genotypes as related to releasing date and available P content in soil. *Mycorrhiza* 23, 497–505. doi: 10.1007/s00572-013-0492-0

Chu, Q., Zhang, L., Zhou, J. W., Yuan, L. X., Chen, F. J., Zhang, F. S., et al. (2020). Soil plant-available phosphorus levels and maize genotypes determine the phosphorus acquisition efficiency and contribution of mycorrhizal pathway. *Plant Soil* 449, 357–371. doi: 10.1007/s11104-020-04494-4

Cibichakravarthy, B., Kumutha, K., and Balachandar, D. (2015). Arbuscular mycorrhizal fungal diversity in phosphorus-deficient Alfisols of a dry north-western agro-ecosystem of Tamil Nadu, India. *Ann. Microbiol.* 65, 143–153. doi: 10.1007/s13213-014-0845-8

Das, D., Paries, M., Hobecker, K., Gigl, M., Dawid, C., Lam, H. M., et al. (2022). Phosphate starvation response transcription factors enable arbuscular mycorrhiza symbiosis. *Nat. Commun.* 13:477. doi: 10.1038/s41467-022-27976-8

Desfougeres, Y., Gerasimaite, R., Jessen, H. J., and Mayer, A. (2016). Vtc5, a novel subunit of the vacuolar transporter chaperone complex, regulates polyphosphate synthesis and phosphate homeostasis in yeast. *J. Biol. Chem.* 291, 22262–22275. doi: 10.1074/jbc.M116.746784

Dierks, J., Blaser-Hart, W. J., Gamper, H. A., Nyoka, I. B., and Six, J. (2021). Trees enhance abundance of arbuscular mycorrhizal fungi, soil structure, and nutrient retention in low-input maize cropping systems. *Agric. Ecosyst. Environ.* 318:107487. doi: 10.1016/j.agee.2021.107487

Ezawa, T., and Saito, K. (2018). How do arbuscular mycorrhizal fungi handle phosphate? New insight into fine-tuning of phosphate metabolism. *New Phytol.* 220, 1116–1121. doi: 10.1111/nph.15187

Ezawa, T., Smith, S. E., and Smith, F. A. (2002). P metabolism and transport in AM fungi. *Plant Soil* 244, 221–230. doi: 10.1023/A:1020258325010

Fan, X., Che, X., Lai, W., Wang, S., Hu, W., Chen, H., et al. (2020). The auxin-inducible phosphate transporter AsPT5 mediates phosphate transport and is indispensable for arbuscule formation in Chinese milk vetch at moderately high phosphate supply. *Environ. Microbiol.* 22, 2053–2079. doi: 10.1111/1462-2920.14952

Fellbaum, C. R., Mensah, J. A., Cloos, A. J., Strahan, G. E., Pfeffer, P. E., Kiers, E. T., et al. (2014). Fungal nutrient allocation in common mycorrhizal networks is regulated by the carbon source strength of individual host plants. *New Phytol.* 203, 646–656. doi: 10.1111/nph.12827

Ferré-D'Amaré, A. R., Prendergast, G. C., Ziff, E. B., and Burley, S. K. (1993). Recognition by max of its cognate DNA through a dimeric b/HLH/Z domain. *Nature* 363, 38–45. doi: 10.1038/363038a0

Fiorilli, V., Lanfranco, L., and Bonfante, P. (2013). The expression of GintPT, the phosphate transporter of *Rhizophagus irregularis*, depends on the symbiotic status and phosphate availability. *Planta* 237, 1267–1277. doi: 10.1007/s00425-013-1842-z

Frosi, G., Barros, V. A., Oliveira, M. T., Cavalcante, U. M. T., Maia, L. C., and Santos, M. G. (2016). Increase in biomass of two woody species from a seasonal dry tropical forest in association with AMF with different phosphorus levels. *Appl. Soil Ecol.* 102, 46–52. doi: 10.1016/j.apsoil.2016.02.009

Genre, A., Chabaud, M., Faccio, A., Barker, D. G., and Bonfante, P. (2008). Prepenetration apparatus assembly precedes and predicts the colonization patterns of arbuscular mycorrhizal fungi within the root cortex of both *Medicago truncatula* and *Daucus carota*. *Plant Cell* 20, 1407–1420. doi: 10.1105/tpc.108.059014

Genre, A., Chabaud, M., Timmers, T., Bonfante, P., and Barker, D. G. (2005). Arbuscular mycorrhizal fungi elicit a novel intracellular apparatus in *Medicago truncatula* root epidermal cells before infection. *Plant Cell* 17, 3489–3499. doi: 10.1105/tpc.105.035410

Genre, A., Ivanov, S., Fendrych, M., Faccio, A., Zársky, V., Bisseling, T., et al. (2012). Multiple exocytotic markers accumulate at the sites of perifungal membrane biogenesis in arbuscular mycorrhizas. *Plant Cell Physiol.* 53, 244–255. doi: 10.1093/pcp/pcr170

Genre, A., Lanfranco, L., Perotto, S., and Bonfante, P. (2020). Unique and common traits in mycorrhizal symbioses. *Nat. Rev. Microbiol.* 18, 649–660. doi: 10.1038/s41579-020-0402-3

Ghillebert, R., Swinnen, E., De Snijder, P., Smets, B., and Winderickx, J. (2011). Differential roles for the low-affinity phosphate transporters Pho87 and Pho90 in *Saccharomyces cerevisiae*. *Biochem. J.* 434, 243–251. doi: 10.1042/bj20101118

Gietz, R. D., and Schiestl, R. H. (2007). High-efficiency yeast transformation using the LiAc/SS carrier DNA/PEG method. *Nat. Protoc.* 2, 31–34. doi: 10.1038/nprot.2007.13

Giovannetti, M., Sbrana, C., Avio, L., Citernesi, A. S., and Logi, C. (1993). Differential hyphal morphogenesis in arbuscular mycorrhizal fungi during pre-infection stages. *New Phytol.* 125, 587–593. doi: 10.1111/j.1469-8137.1993.tb03907.x

Gras, D. E., Persinoti, G. F., Peres, N. T. A., Martinez-Rossi, N. M., Tahira, A. C., Reis, E. M., et al. (2013). Transcriptional profiling of *Neurospora crassa* Delta mak-2 reveals that mitogen-activated protein kinase MAK-2 participates in the phosphate signaling pathway. *Fungal Genet. Biol.* 60, 140–149. doi: 10.1016/j.fgb.2013.05.007

Gras, D. E., Silveira, H. C., Martinez-Rossi, N. M., and Rossi, A. (2007). Identification of genes displaying differential expression in the *nuc-2* mutant strain of the mold *Neurospora crassa* grown under phosphate starvation. *FEMS Microbiol. Lett.* 269, 196–200. doi: 10.1111/j.1574-6968.2006.00613.x

Grønlund, M., Albrechtsen, M., Johansen, I. E., Hammer, E. C., Nielsen, T. H., and Jakobsen, I. (2013). The interplay between P uptake pathways in mycorrhizal peas: a combined physiological and gene-silencing approach. *Physiol. Plant.* 149, 234–248. doi: 10.1111/ppl.12030

Guillemin, J. P., Orozco, M. O., Gianinazzi-Pearson, V., and Gianinazzi, S. (1995). Influence of phosphate fertilization on fungal alkaline phosphatase and succinate dehydrogenase activities in arbuscular mycorrhiza of soybean and pineapple. *Agric. Ecosyst. Environ.* 53, 63–69. doi: 10.1016/0167-8809(94)00555-S

Gutjahr, C., and Parniske, M. (2013). Cell and developmental biology of arbuscular mycorrhiza symbiosis. *Annu. Rev. Cell Dev. Biol.* 29, 593–617. doi: 10.1146/annurev-cellbio-101512-122413

Hajong, S., Kumaria, S., and Tandon, P. (2013). Comparative study of key phosphorus and nitrogen metabolizing enzymes in mycorrhizal and non-mycorrhizal plants of *Dendrobium chrysanthum wall. Ex Lindl. Acta Physiol. Plant.* 35, 2311–2322. doi: 10.1007/s11738-013-1268-z

Hamel, C., Fyles, H., and Smith, D. L. (1990). Measurement of development of endomycorrhizal mycelium using three different vital stains. *New Phytol.* 115, 297–302. doi: 10.1111/j.1469-8137.1990.tb00455.x

Hao, N., and O'Shea, E. K. (2012). Signal-dependent dynamics of transcription factor translocation controls gene expression. *Nat. Struct. Mol. Biol.* 19, 31–39. doi: 10.1038/nsmb.2192

Harrison, M. J. (2012). Cellular programs for arbuscular mycorrhizal symbiosis. *Curr. Opin. Plant Biol.* 15, 691–698. doi: 10.1016/j.pbi.2012.08.010

Harrison, M. J., Dewbre, G. R., and Liu, J. (2002). A phosphate transporter from *Medicago truncatula* involved in the acquisition of phosphate released by arbuscular mycorrhizal fungi. *Plant Cell* 14, 2413–2429. doi: 10.1105/tpc.004861

Harrison, M. J., and van Buuren, M. L. (1995). A phosphate transporter from the mycorrhizal fungus *glomus versiforme*. *Nature* 378, 626–629. doi: 10.1038/378626a0

Helber, N., Wippel, K., Sauer, N., Schaarschmidt, S., Hause, B., and Requena, N. (2011). A versatile monosaccharide transporter that operates in the arbuscular mycorrhizal fungus *glomus* sp is crucial for the symbiotic relationship with plants. *Plant Cell* 23, 3812–3823. doi: 10.1105/tpc.111.089813

Hewitt, E. J. (1966). *Sand and Water Culture Methods used in the Study of Plant Nutrition*. Farnham Royal, UK: Commonwealth Agricultural Bureaux.

Hirsch, J., Marin, E., Floriani, M., Chiarenza, S., Richaud, P., Nussaume, L., et al. (2006). Phosphate deficiency promotes modification of iron distribution in Arabidopsis plants. *Biochimie* 88, 1767–1771. doi: 10.1016/j.biochi.2006.05.007

Ho-Plágaro, T., and García-Garrido, J. M. (2022). Multifarious and interactive roles of GRAS transcription factors during arbuscular mycorrhiza development. *Front. Plant Sci.* 13:836213. doi: 10.3389/fpls.2022.836213

Hu, J., Cui, X., Wang, J., and Lin, X. (2019). The non-simultaneous enhancement of phosphorus acquisition and mobilization respond to enhanced arbuscular mycorrhization on maize (*Zea mays L.*). *Microorganisms* 7:651. doi: 10.3390/microorganisms7120651

Huang, K., Ferrin-O'Connell, I., Zhang, W., Leonard, G. A., O'Shea, E. K., and Quiocho, F. A. (2007). Structure of the Pho85-Pho80 CDK-cyclin complex of the phosphate-responsive signal transduction pathway. *Mol. Cell* 28, 614–623. doi: 10.1016/j.molcel.2007.09.013

Huang, Y., and Freiser, B. S. (1993). Multiphoton infrared photoinduced ion-molecule reactions in the gas phase. *J. Am. Chem. Soc.* 115, 737–742. doi: 10.1021/ja00055a051

Hui, J., An, X., Li, Z., Neuhäuser, B., Ludewig, U., Wu, X., et al. (2022). The mycorrhiza-specific ammonium transporter ZmAMT3;1 mediates mycorrhiza-dependent nitrogen uptake in maize roots. *Plant Cell* 34, 4066–4087. doi: 10.1093/plcell/koac225

Ivanov, S., and Harrison, M. J. (2014). A set of fluorescent protein-based markers expressed from constitutive and arbuscular mycorrhiza-inducible promoters to label organelles, membranes and cytoskeletal elements in *Medicago truncatula*. *Plant J.* 80, 1151–1163. doi: 10.1111/tpj.12706

Ivashuta, S., Liu, J., Liu, J., Lohar, D. P., Haridas, S., Bucciarelli, B., et al. (2005). RNA interference identifies a calcium-dependent protein kinase involved in *Medicago truncatula* root development. *Plant Cell* 17, 2911–2921. doi: 10.1105/tpc.105.035394

Javot, H., Pumplin, N., and Harrison, M. J. (2007). Phosphate in the arbuscular mycorrhizal symbiosis: transport properties and regulatory roles. *Plant Cell Environ.* 30, 310–322. doi: 10.1111/j.1365-3040.2006.01617.x

Jeffery, D. A., Springer, M., King, D. S., and O'Shea, E. K. (2001). Multi-site phosphorylation of Pho4 by the cyclin-CDK Pho80-Pho85 is semi-processive with site preference. *J. Mol. Biol.* 306, 997–1010. doi: 10.1006/jmbi.2000.4417

Jiang, Y., Wang, W., Xie, Q., Liu, N., Liu, L., Wang, D., et al. (2017). Plants transfer lipids to sustain colonization by mutualistic mycorrhizal and parasitic fungi. *Science* 356, 1172–1175. doi: 10.1126/science.aam9970

Jung, L. A., Gebhardt, A., Koelmel, W., Ade, C. P., Walz, S., Kuper, J., et al. (2017). OmoMYC blunts promoter invasion by oncogenic MYC to inhibit gene expression characteristic of MYC-dependent tumors. *Oncogene* 36, 1911–1924. doi: 10.1038/onc.2016.354

Kaffman, A., Herskowitz, I., Tjian, R., and O'Shea, E. K. (1994). Phosphorylation of the transcription factor PHO4 by a cyclin-CDK complex, PHO80-PHO85. *Science* 263, 1153–1156. doi: 10.1126/science.8108735

Kaffman, A., Rank, N. M., O'Neill, E. M., Huang, L. S., and O'Shea, E. K. (1998). The receptor Msn5 exports the phosphorylated transcription factor Pho4 out of the nucleus. *Nature* 396, 482–486. doi: 10.1038/24898

Kang, S., and Metzenberg, R. L. (1990). Molecular analysis of *nuc-1+*, a gene controlling phosphorus acquisition in *Neurospora crassa*. *Mol. Cell. Biol.* 10, 5839–5848. doi: 10.1128/mcb.10.11.5839-5848.1990

Karandashov, V., Nagy, R., Wegmuller, S., Amrhein, N., and Bucher, M. (2004). Evolutionary conservation of a phosphate transporter in the arbuscular mycorrhizal symbiosis. *Proc. Natl. Acad. Sci. U. S. A.* 101, 6285–6290. doi: 10.1073/pnas.0306074101

Kato, T., and Hibino, T. (2009). Isolation and expression analysis of AGAMOUS-like genes from *Eucalyptus grandis*. *Plant Biotechnol.* 26, 121–124. doi: 10.5511/plantbiotechnology.26.121

Kerwin, C. L., and Wykoff, D. D. (2009). *Candida glabrata* PHO4 is necessary and sufficient for Pho2-independent transcription of phosphate starvation genes. *Genetics* 182, 471–479. doi: 10.1534/genetics.109.101063

Kikuchi, Y., Hijikata, N., Ohtomo, R., Handa, Y., Kawaguchi, M., Saito, K., et al. (2016). Aquaporin-mediated long-distance polyphosphate translocation directed towards the host in arbuscular mycorrhizal symbiosis: application of virus-induced gene silencing. *New Phytol.* 211, 1202–1208. doi: 10.1111/nph.14016

Kikuchi, Y., Hijikata, N., Yokoyama, K., Ohtomo, R., Handa, Y., Kawaguchi, M., et al. (2014). Polyphosphate accumulation is driven by transcriptome alterations that lead to near-synchronous and near-equivalent uptake of inorganic cations in an arbuscular mycorrhizal fungus. *New Phytol.* 204, 638–649. doi: 10.1111/nph.12937

Kiribuchi, K., Sugimori, M., Takeda, M., Otani, T., Okada, K., Onodera, H., et al. (2004). *RERJ1*, a jasmonic acid-responsive gene from rice, encodes a basic helix-loop-helix protein. *Biochem. Biophys. Res. Commun.* 325, 857–863. doi: 10.1016/j.bbrc.2004.10.126

Kobae, Y. (2019). Dynamic phosphate uptake in arbuscular mycorrhizal roots under field conditions. *Front. Environ. Sci.* 6:159. doi: 10.3389/fenvs.2018.00159

Komeili, A., and O'Shea, E. K. (1999). Roles of phosphorylation sites in regulating activity of the transcription factor Pho4. *Science* 284, 977–980. doi: 10.1126/science.284.5416.977

Kouas, S., Debez, A., Slatni, T., Labidi, N., Drevon, J. J., and Abdelly, C. (2009). Root proliferation, proton efflux, and acid phosphatase activity in common bean (*Phaseolus vulgaris*) under phosphorus shortage. *J. Plant Biol.* 52, 395–402. doi: 10.1007/s12374-009-9050-x

Kumar, S., Stecher, G., and Tamura, K. (2016). MEGA7: molecular evolutionary genetics analysis version 7.0 for bigger datasets. *Mol. Biol. Evol.* 33, 1870–1874. doi: 10.1093/molbev/msw054

Leal, J., Squina, F. M., Martinez-Rossi, N. M., and Rossi, A. (2007). The transcription of the gene for iso-orotate decarboxylase (IDCase), an enzyme of the thymidine salvage pathway, is downregulated in the pregc mutant strain of *Neurospora crassa* grown under phosphate starvation. *Can. J. Microbiol.* 53, 1011–1015. doi: 10.1139/w07-064

Lee, Y. S., Huang, K. X., Quiocho, F. A., and O'Shea, E. K. (2008). Molecular basis of cyclin-CDK-CKI regulation by reversible binding of an inositol pyrophosphate. *Nat. Chem. Biol.* 4, 25–32. doi: 10.1038/nchembio.2007.52

Lee, Y. S., Mulugu, S., York, J. D., and O'Shea, E. K. (2007). Regulation of a cyclin-CDK-CDK inhibitor complex by inositol pyrophosphates. *Science* 316, 109–112. doi: 10.1126/science.1139080

Lenburg, M. E., and O'Shea, E. K. (1996). Signaling phosphate starvation. *Trends Biochem. Sci.* 21, 383–387. doi: 10.1016/S0968-0004(96)10048-7

Li, C., Li, C., Zhang, H., Liao, H., and Wang, X. (2017). The purple acid phosphatase GmPAP21 enhances internal phosphorus utilization and possibly plays a role in symbiosis with rhizobia in soybean. *Physiol. Plant.* 159, 215–227. doi: 10.1111/ppl.12524

Lin, K., Limpens, E., Zhang, Z., Ivanov, S., Saunders, D. G., Mu, D., et al. (2014). Single nucleus genome sequencing reveals high similarity among nuclei of an endomycorrhizal fungus. *PLoS Genet.* 10:e1004078. doi: 10.1371/journal.pgen.1004078

Luginbuehl, L. H., and Oldroyd, G. E. D. (2017). Understanding the arbuscule at the heart of endomycorrhizal symbioses in plants. *Curr. Biol.* 27, R952–R963. doi: 10.1016/j.cub.2017.06.042

Ma, Q., Chadwick, D. R., Wu, L., and Jones, D. L. (2022). Arbuscular mycorrhiza fungi colonisation stimulates uptake of inorganic nitrogen and Sulphur but reduces utilisation of organic forms in tomato. *Soil Biol. Biochem.* 172:108719. doi: 10.1016/j.soilbio.2022.108719

Maldonado-Mendoza, I. E., Dewbre, G. R., and Harrison, M. J. (2001). A phosphate transporter gene from the extra-radical mycelium of an arbuscular mycorrhizal fungus *glomus intraradices* is regulated in response to phosphate in the environment. *Mol. Plant-Microbe Interact.* 14, 1140–1148. doi: 10.1094/mpmi.2001.14.10.1140

Nagy, R., Drissner, D., Amrhein, N., Jakobsen, I., and Bucher, M. (2009). Mycorrhizal phosphate uptake pathway in tomato is phosphorus-repressible and transcriptionally regulated. *New Phytol.* 181, 950–959. doi: 10.1111/j.1469-8137.2008.02721.x

Nguyen, C. T., and Saito, K. (2021). Role of cell wall polyphosphates in phosphorus transfer at the arbuscular interface in mycorrhizas. *Front. Plant Sci.* 12:725939. doi: 10.3389/fpls.2021.725939

Niu, F., Zhang, D., Li, Z., Iersel, M. V., and Alem, P. (2015). Morphological response of eucalypts seedlings to phosphorus supply through hydroponic system. *Sci. Hortic.* 194, 295–303. doi: 10.1016/j.scienta.2015.08.029

Olsson, P. A., Hansson, M. C., and Burleigh, S. H. (2006). Effect of P availability on temporal dynamics of carbon allocation and glomus intraradices high-affinity P transporter gene induction in arbuscular mycorrhiza. *Appl. Environ. Microbiol.* 72, 4115–4120. doi: 10.1128/aem.02154-05

O'Neill, E. M., Kaffman, A., Jolly, E. R., and O'Shea, E. K. (1996). Regulation of PHO4 nuclear localization by the PHO80-PHO85 cyclin-CDK complex. *Science* 271, 209–212. doi: 10.1126/science.271.5246.209

Oshima, Y. (1997). The phosphatase system in *Saccharomyces cerevisiae*. *Genes Genet. Syst.* 72, 323–334. doi: 10.1266/ggs.72.323

Pagano, M. C., and Scotti, M. R. (2008). Arbuscular and ectomycorrhizal colonization of two eucalyptus species in semiarid Brazil. *Mycoscience* 49, 379–384. doi: 10.1007/s10267-008-0435-3

Parniske, M. (2008). Arbuscular mycorrhiza: the mother of plant root endosymbioses. *Nat. Rev. Microbiol.* 6, 763–775. doi: 10.1038/nrmicro1987

Pearson, J. N., and Jakobsen, I. (1993). The relative contribution of hyphae and roots to phosphorus uptake by arbuscular mycorrhizal plants, measured by dual labelling with ^{32}P and ^{33}P. *New Phytol.* 124, 489–494. doi: 10.1111/j.1469-8137.1993.tb03840.x

Peleg, Y., Addison, R., Aramayo, R., and Metzenberg, R. L. (1996). Translocation of *Neurospora crassa* transcription factor NUC-1 into the nucleus is induced by phosphorus limitation. *Fungal Genet. Biol.* 20, 185–191. doi: 10.1006/fgbi.1996.0034

Phillips, J. M., and Hayman, D. S. (1970). Improved procedures for cleaning and staining parasitic and vesicular arbuscular mycorrhizal fungi for rapid assessment of infection. *Trans. Br. Mycol. Soc.* 55, 158–IN18. doi: 10.1016/S0007-1536(70)80110-3

Pimprikar, P., and Gutjahr, C. (2018). Transcriptional regulation of arbuscular mycorrhiza development. *Plant Cell Physiol.* 59, 678–695. doi: 10.1093/pcp/pcy024

Plasencia, A., Soler, M., Dupas, A., Ladouce, N., Silva-Martins, G., Martinez, Y., et al. (2016). Eucalyptus hairy roots, a fast, efficient and versatile tool to explore function and expression of genes involved in wood formation. *Plant Biotechnol. J.* 14, 1381–1393. doi: 10.1111/pbi.12502

Plassard, C., Becquer, A., and Garcia, K. (2019). Phosphorus transport in mycorrhiza: how far are we? *Trends Plant Sci.* 24, 794–801. doi: 10.1016/j.tplants.2019.06.004

Pozo, M. J., and Azcón-Aguilar, C. (2007). Unraveling mycorrhiza-induced resistance. *Curr. Opin. Plant Biol.* 10, 393–398. doi: 10.1016/j.pbi.2007.05.004

Pumplin, N., and Harrison, M. J. (2009). Live-cell imaging reveals periarbuscular membrane domains and organelle location in *Medicago truncatula* roots during arbuscular mycorrhizal symbiosis. *Plant Physiol.* 151, 809–819. doi: 10.1104/pp.109.141879

Pumplin, N., Zhang, X., Noar, R. D., and Harrison, M. J. (2012). Polar localization of a symbiosis-specific phosphate transporter is mediated by a transient reorientation of secretion. *Proc. Natl. Acad. Sci. U. S. A.* 109, E665–E672. doi: 10.1073/pnas.1110215109

Qin, Z., Li, J., Zhang, Y., Xiao, Y., Zhang, X., Zhong, L., et al. (2021). Genome-wide identification of microRNAs involved in the somatic embryogenesis of eucalyptus. *G3-genes genomes. Genetics* 11:jkab070. doi: 10.1093/g3journal/jkab070

Rahman, M. A., Parvin, M., Das, U., Ela, E. J., Lee, S. H., Lee, K. W., et al. (2020). Arbuscular mycorrhizal symbiosis mitigates iron (Fe)-deficiency retardation in alfalfa (*Medicago sativa L.*) through the enhancement of Fe accumulation and sulfur-assisted antioxidant defense. *Int. J. Mol. Sci.* 21:2219. doi: 10.3390/ijms21062219

Reich, N. C., and Liu, L. (2006). Tracking STAT nuclear traffic. *Nat. Rev. Immunol.* 6, 602–612. doi: 10.1038/nri1885

Rich, M. K., Vigneron, N., Libourel, C., Keller, J., Xue, L., Hajheidari, M., et al. (2021). Lipid exchanges drove the evolution of mutualism during plant terrestrialization. *Science* 372, 864–868. doi: 10.1126/science.abg0929

Rockwood, D. L., Rudie, A. W., Ralph, S. A., Zhu, J. Y., and Winandy, J. E. (2008). Energy product options for eucalyptus species grown as short rotation woody crops. *Int. J. Mol. Sci.* 9, 1361–1378. doi: 10.3390/ijms9081361

Roth, R., Hillmer, S., Funaya, C., Chiapello, M., Schumacher, K., Lo Presti, L., et al. (2019). Arbuscular cell invasion coincides with extracellular vesicles and membrane tubules. *Nat. Plants* 5, 204–211. doi: 10.1038/s41477-019-0365-4

Russo, G., Carotenuto, G., Fiorilli, V., Volpe, V., Faccio, A., Bonfante, P., et al. (2019). TPLATE recruitment reveals endocytic dynamics at sites of symbiotic interface assembly in arbuscular mycorrhizal interactions. *Front. Plant Sci.* 10:1628. doi: 10.3389/fpls.2019.01628

Saito, M. (1995). Enzyme activities of the internal hyphae and germinated spores of an arbuscular mycorrhizal fungus, *Gigaspora margarita Becker & Hall*. *New Phytol.* 129, 425–431. doi: 10.1111/j.1469-8137.1995.tb04313.x

Santos, F. M., Balieiro, F. D., Ataide, D. H. D., Diniz, A. R., and Chaer, G. M. (2016). Dynamics of aboveground biomass accumulation in monospecific and mixed-species plantations of eucalyptus and acacia on a Brazilian sandy soil. *For. Ecol. Manag.* 363, 86–97. doi: 10.1016/j.foreco.2015.12.028

Santos, L. H. D., Madi, J. P. S., Diaz, L., Ramirez, G. M., De Souza, E. C., Nunes, G. M., et al. (2021). Relationship between spectral variables with RapidEye images and dendrometric variables in teak plantations using principal component analysis. *Sci. Forestalis.* 49. doi: 10.18671/scifor.v49n132.09

Schneider, K. R., Smith, R. L., and O'Shea, E. K. (1994). Phosphate-regulated inactivation of the kinase PHO80-PHO85 by the CDK inhibitor PHO81. *Science* 266, 122–126. doi: 10.1126/science.7939631

Secco, D., Wang, C., Shou, H., and Whelan, J. (2012). Phosphate homeostasis in the yeast *Saccharomyces cerevisiae*, the key role of the SPX domain-containing proteins. *FEBS Lett.* 586, 289–295. doi: 10.1016/j.febslet.2012.01.036

Senthil-Kumar, M., and Mysore, K. S. (2014). Tobacco rattle virus-based virus-induced gene silencing in *Nicotiana benthamiana*. *Nat. Protoc.* 9, 1549–1562. doi: 10.1038/nprot.2014.092

Shelest, E. (2008). Transcription factors in fungi. *FEMS Microbiol. Lett.* 286, 145–151. doi: 10.1111/j.1574-6968.2008.01293.x

Shi, J., Zhao, B., Zheng, S., Zhang, X., Wang, X., Dong, W., et al. (2021). A phosphate starvation response-centered network regulates mycorrhizal symbiosis. *Cells* 184, 5527–5540.e18. doi: 10.1016/j.cell.2021.09.030

Smethurst, P. J. (2010). Forest fertilization: trends in knowledge and practice compared to agriculture. *Plant Soil* 335, 83–100. doi: 10.1007/s11104-010-0316-3

Smith, J. (2009). Mycorrhizal symbiosis (third edition). *Proc. Soil Sci. Soc. Am.* 73. doi: 10.2136/sssaj2008.0015br

Smith, F. A., and Smith, S. E. (1997). Structural diversity in (vesicular)-arbuscular mycorrhizal symbioses. *New Phytol.* 137, 373–388. doi: 10.1046/j.1469-8137.1997.00848.x

Smith, S. E., and Smith, F. A. (2011). Roles of arbuscular mycorrhizas in plant nutrition and growth: new paradigms from cellular to ecosystem scales. *Annu. Rev. Plant Biol.* 62, 227–250. doi: 10.1146/annurev-arplant-042110-103846

Smith, S. E., Smith, F. A., and Jakobsen, I. (2003). Mycorrhizal fungi can dominate phosphate supply to plants irrespective of growth responses. *Plant Physiol.* 133, 16–20. doi: 10.1104/pp.103.024380

Solaiman, M. Z., Ezawa, T., Kojima, T., and Saito, M. (1999). Polyphosphates in Intraradical and Extraradical hyphae of an arbuscular mycorrhizal Fungus,Gigaspora margarita. *Appl. Environ. Microbiol.* 65, 5604–5606. doi: 10.1128/AEM.65.12.5604-5606.1999

Standish, R. J., Stokes, B. A., Tibbett, M., and Hobbs, R. J. (2007). Seedling response to phosphate addition and inoculation with arbuscular mycorrhizas and the implications for old-field restoration in Western Australia. *Environ. Exp. Bot.* 61, 58–65. doi: 10.1016/j.envexpbot.2007.03.004

Sugimura, Y., and Saito, K. (2017). Transcriptional profiling of arbuscular mycorrhizal roots exposed to high levels of phosphate reveals the repression of cell cycle-related genes and secreted protein genes in *Rhizophagus irregularis*. *Mycorrhiza* 27, 139–146. doi: 10.1007/s00572-016-0735-y

Sun, X., Chen, W., Ivanov, S., MacLean, A. M., Wight, H., Ramaraj, T., et al. (2019). Genome and evolution of the arbuscular mycorrhizal fungus *Diversispora epigaea* (formerly *glomus versiforme*) and its bacterial endosymbionts. *New Phytol.* 221, 1556–1573. doi: 10.1111/nph.15472

Sun, Z., Song, J., Xin, X., Xie, X., and Zhao, B. (2018). Arbuscular mycorrhizal fungal 14-3-3 proteins are involved in arbuscule formation and responses to abiotic stresses during AM symbiosis. *Front. Microbiol.* 9:91. doi: 10.3389/fmicb.2018.00091

Tang, N., San Clemente, H., Roy, S., Bécard, G., Zhao, B., and Roux, C. (2016). A survey of the gene repertoire of *Gigaspora rosea* unravels conserved features among Glomeromycota for obligate biotrophy. *Front. Microbiol.* 7:233. doi: 10.3389/fmicb.2016.00233

Tian, L., Nasrullah, H., and Wu, Q. S. (2017). Nitric oxide accelerates mycorrhizal effects on plant growth and root development of trifoliate orange. *Sains Malaysiana* 46, 1687–1691. doi: 10.17576/jsm-2017-4610-03

Tisserant, E., Kohler, A., Dozolme-Seddas, P., Balestrini, R., Benabdellah, K., Colard, A., et al. (2012). The transcriptome of the arbuscular mycorrhizal fungus *glomus intraradices* (DAOM 197198) reveals functional tradeoffs in an obligate symbiont. *New Phytol.* 193, 755–769. doi: 10.1111/j.1469-8137.2011.03948.x

Tisserant, E., Malbreil, M., Kuo, A., Kohler, A., Symeonidi, A., Balestrini, R., et al. (2013). Genome of an arbuscular mycorrhizal fungus provides insight into the oldest plant symbiosis. *Proc. Natl. Acad. Sci. U. S. A.* 110, 20117–20122. doi: 10.1073/pnas.1313452110

Tollot, M., Wong Sak Hoi, J., van Tuinen, D., Arnould, C., Chatagnier, O., Dumas, B., et al. (2009). An *STE12* gene identified in the mycorrhizal fungus *glomus intraradices* restores infectivity of a hemibiotrophic plant pathogen. *New Phytol.* 181, 693–707. doi: 10.1111/j.1469-8137.2008.02696.x

Tomar, P., and Sinha, H. (2014). Conservation of PHO pathway in ascomycetes and the role of Pho84. *J. Biosci.* 39, 525–536. doi: 10.1007/s12038-014-9435-y

Trouvelot, A., Kough, J. L., and Gianinazzi-Pearson, V. (1986). "Mesure du taux de mycorhization VA d'un systeme radiculaire. Recherche de methodes d'estimation ayant une signification fonctionnelle" in *Physiological and Genetical Aspects of Mycorrhizae. Proceedings of the 1st European Symposium on Mycorrhizae*. eds. V. Gianinazzi-Pearson and S. Gianinazzi (Paris: Institut National de la Recherche Agronomique), 217–221.

Urrialde, V., Prieto, D., Pla, J., and Alonso-Monge, R. (2015). The Pho4 transcription factor mediates the response to arsenate and arsenite in *Candida albicans*. *Front. Microbiol.* 6:118. doi: 10.3389/fmicb.2015.00118

Vance, C. P., Uhde-Stone, C., and Allan, D. L. (2003). Phosphorus acquisition and use: critical adaptations by plants for securing a nonrenewable resource. *New Phytol.* 157, 423–447. doi: 10.1046/j.1469-8137.2003.00695.x

Vardi, N., Levy, S., Gurvich, Y., Polacheck, T., Carmi, M., Jaitin, D., et al. (2014). Sequential feedback induction stabilizes the phosphate starvation response in budding yeast. *Cell Rep.* 9, 1122–1134. doi: 10.1016/j.celrep.2014.10.002

Venice, F., Ghignone, S., Salvioli di Fossalunga, A., Amselem, J., Novero, M., Xianan, X., et al. (2020). At the nexus of three kingdoms: the genome of the mycorrhizal fungus *Gigaspora margarita* provides insights into plant, endobacterial and fungal interactions. *Environ. Microbiol.* 22, 122–141. doi: 10.1111/1462-2920.14827

Vivas, A., Marulanda, A., Gómez, M., Barea, J. M., and Azcón, R. (2003). Physiological characteristics (SDH and ALP activities) of arbuscular mycorrhizal colonization as affected by *bacillus thuringiensis* inoculation under two phosphorus levels. *Soil Biol. Biochem.* 35, 987–996. doi: 10.1016/S0038-0717(03)00161-5

Vogel, K., Hörz, W., and Hinnen, A. (1989). The two positively acting regulatory proteins PHO2 and PHO4 physically interact with PHO5 upstream activation regions. *Mol. Cell. Biol.* 9, 2050–2057. doi: 10.1128/mcb.9.5.2050-2057.1989

Volpe, V., Giovannetti, M., Sun, X. G., Fiorilli, V., and Bonfante, P. (2016). The phosphate transporters LjPT4 and MtPT4 mediate early root responses to phosphate status in non-mycorrhizal roots. *Plant Cell Environ.* 39, 660–671. doi: 10.1111/pce.12659

Wang, C., White, P. J., and Li, C. J. (2017). Colonization and community structure of arbuscular mycorrhizal fungi in maize roots at different depths in the soil profile respond differently to phosphorus inputs on a long-term experimental site. *Mycorrhiza* 27, 369–381. doi: 10.1007/s00572-016-0757-5

Wang, G. Z., Ye, C. C., Zhang, J. L., Koziol, L., Bever, J. D., and Li, X. L. (2019). Asymmetric facilitation induced by inoculation with arbuscular mycorrhizal fungi leads to overyielding in maize/faba bean intercropping. *J. Plant Interact.* 14, 10–20. doi: 10.1080/17429145.2018.1550218

Wang, X., Zhao, S., and Bücking, H. (2016). Arbuscular mycorrhizal growth responses are fungal specific but do not differ between soybean genotypes with different phosphate efficiency. *Ann. Bot.* 118, 11–21. doi: 10.1093/aob/mcw074

Wang, J. P., Zhong, H. N., Zhu, L. J., Yuan, Y. D., Xu, L. H., Wang, G. G., et al. (2019). Arbuscular mycorrhizal fungi effectively enhances the growth of Gleditsia sinensis Lam. Seedlings under greenhouse conditions. *Forests* 10:567. doi: 10.3390/f10070567

Watts-Williams, S. J., and Cavagnaro, T. R. (2018). Arbuscular mycorrhizal fungi increase grain zinc concentration and modify the expression of root ZIP transporter genes in a modern barley (*Hordeum vulgare*) cultivar. *Plant Sci.* 274, 163–170. doi: 10.1016/j.plantsci.2018.05.015

Wu, P. F., Ma, X. Q., Tigabu, M., Huang, Y., Zhou, L. L., Cai, L., et al. (2014). Comparative growth, dry matter accumulation and photosynthetic rate of seven species of eucalypt in response to phosphorus supply. *J. For. Res.* 25, 377–383. doi: 10.1007/s11676-014-0465-y

Wykoff, D. D., Rizvi, A. H., Raser, J. M., Margolin, B., and O'Shea, E. K. (2007). Positive feedback regulates switching of phosphate transporters in *S. cerevisiae*. *Mol. Cell* 27, 1005–1013. doi: 10.1016/j.molcel.2007.07.022

Xie, X., Huang, W., Liu, F., Tang, N., Liu, Y., Lin, H., et al. (2013). Functional analysis of the novel mycorrhiza-specific phosphate transporter AsPT1 and PHT1 family from *Astragalus sinicus* during the arbuscular mycorrhizal symbiosis. *New Phytol.* 198, 836–852. doi: 10.1111/nph.12188

Xie, X., Lai, W., Che, X., Wang, S., Ren, Y., Hu, W., et al. (2022). A SPX domain-containing phosphate transporter from *Rhizophagus irregularis* handles phosphate homeostasis at symbiotic interface of arbuscular mycorrhizas. *New Phytol.* 234, 650–671. doi: 10.1111/nph.17973

Xie, X., Lin, H., Peng, X., Xu, C., Sun, Z., Jiang, K., et al. (2016). Arbuscular mycorrhizal symbiosis requires a phosphate transceptor in the *Gigaspora margarita* fungal symbiont. *Mol. Plant* 9, 1583–1608. doi: 10.1016/j.molp.2016.08.011

Xu, D., Dell, B., Malajczuk, N., and Gong, M. (2001). Effects of P fertilisation and ectomycorrhizal fungal inoculation on early growth of eucalypt plantations in southern China. *Plant Soil* 233, 47–57. doi: 10.1023/A:1010355620452

Yang, G., Chao, D., Ming, Z., and Xia, J. (2019). A simple method to detect the inhibition of transcription factor-DNA binding due to protein-protein interactions in vivo. *Genes* 10:684. doi: 10.3390/genes10090684

Yang, S. Y., Grønlund, M., Jakobsen, I., Grotemeyer, M. S., Rentsch, D., Miyao, A., et al. (2012). Nonredundant regulation of rice arbuscular mycorrhizal symbiosis by two members of the phosphate transporter1 gene family. *Plant Cell* 24, 4236–4251. doi: 10.1105/tpc.112.104901

Yao, X. Y., Zhang, Q. C., Zhou, H. J., Nong, Z., Ye, S. M., and Deng, Q. (2021). Introduction of *Dalbergia odorifera* enhances nitrogen absorption on eucalyptus through stimulating microbially mediated soil nitrogen-cycling. *For. Ecosyst.* 8:59. doi: 10.1186/s40663-021-00339-3

York, J. D., and Lew, D. J. (2008). IP7 guards the CDK gate. *Nat. Chem. Biol.* 4, 16–17. doi: 10.1038/nchembio0108-16

Zeng, T., Holmer, R., Hontelez, J., Te Lintel-Hekkert, B., Marufu, L., de Zeeuw, T., et al. (2018). Host-and stage-dependent secretome of the arbuscular mycorrhizal fungus *Rhizophagus irregularis*. *Plant J.* 94, 411–425. doi: 10.1111/tpj.13908

Zeng, T., Rodriguez-Moreno, L., Mansurkhodzaev, A., Wang, P., van den Berg, W., Gasciolli, V., et al. (2020). A lysin motif effector subverts chitin-triggered immunity to facilitate arbuscular mycorrhizal symbiosis. *New Phytol.* 225, 448–460. doi: 10.1111/nph.16245

Zézé, A., Dulieu, H., and Gianinazzi-Pearson, V. (1994). DNA cloning and screening of a partial genomic library from an arbuscular mycorrhizal fungus, *Scutellospora castanea*. *Mycorrhiza* 4, 251–254. doi: 10.1007/BF00206773

Zhan, Y., Sun, X., Rong, G., Hou, C., Huang, Y., Jiang, D., et al. (2017). Identification of two transcription factors activating the expression of *OsXIP* in rice defence response. *BMC Biotechnol.* 17:26. doi: 10.1186/s12896-017-0344-7

Zhang, L., Chu, Q., Zhou, J. W., Rengel, Z., and Feng, G. (2021). Soil phosphorus availability determines the preference for direct or mycorrhizal phosphorus uptake pathway in maize. *Geoderma* 403:115261. doi: 10.1016/j.geoderma.2021.115261

Zhang, H., and Liu, Y. (2014). VIGS Assays. *Bio-Protocol.* 4:5. doi: 10.21769/BioProtoc.1057

Zhao, B., Trouvelot, A., Gianinazzi, S., and Gianinazzi-Pearson, V. (1997). Influence of two legume species on hyphal production and activity of two arbuscular mycorrhizal fungi. *Mycorrhiza* 7, 179–185. doi: 10.1007/s005720050179

Zheng, Q., Guan, G., Cao, C., Li, Q., and Huang, G. (2020). The PHO pathway regulates white-opaque switching and sexual mating in the human fungal pathogen *Candida albicans*. *Curr. Genet.* 66, 1155–1162. doi: 10.1007/s00294-020-01100-z

Zhou, X., Li, J., Tang, N., Xie, H., Fan, X., Chen, H., et al. (2021). Genome-wide analysis of nutrient signaling pathways conserved in arbuscular mycorrhizal fungi. *Microorganisms* 9:1557. doi: 10.3390/microorganisms9081557

Zhou, X., and O'Shea, E. K. (2011). Integrated approaches reveal determinants of genome-wide binding and function of the transcription factor Pho4. *Mol. Cell* 42, 826–836. doi: 10.1016/j.molcel.2011.05.025

Zhou, Y., Yuikawa, N., Nakatsuka, H., Maekawa, H., Harashima, S., Nakanishi, Y., et al. (2016). Core regulatory components of the PHO pathway are conserved in the methylotrophic yeast *Hansenula polymorpha*. *Curr. Genet.* 62, 595–605. doi: 10.1007/s00294-016-0565-7

Zhu, L., and Huq, E. (2011). Mapping functional domains of transcription factors. *Methods Mol. Biol.* 754, 167–184. doi: 10.1007/978-1-61779-154-3_9

frontiers | Frontiers in Microbiology

TYPE Original Research
PUBLISHED 14 March 2023
DOI 10.3389/fmicb.2023.1129471

OPEN ACCESS

EDITED BY
Khondoker M. G. Dastogeer,
University of California,
Berkeley,
United States

REVIEWED BY
Xingang Zhou,
Northeast Agricultural University,
China
Yan Zhang,
Hefei Normal University,
China
Sergio Guajardo-Leiva,
University of Talca,
Chile

*CORRESPONDENCE
Yu Shi
✉ yshi@henu.edu.cn

†These authors have contributed equally to this work

SPECIALTY SECTION
This article was submitted to Microbe and Virus Interactions with Plants, a section of the journal Frontiers in Microbiology

RECEIVED 22 December 2022
ACCEPTED 24 February 2023
PUBLISHED 14 March 2023

CITATION
Liu L, Ma L, Zhu M, Liu B, Liu X and Shi Y (2023) Rhizosphere microbial community assembly and association networks strongly differ based on vegetation type at a local environment scale.
Front. Microbiol. 14:1129471.
doi: 10.3389/fmicb.2023.1129471

Rhizosphere microbial community assembly and association networks strongly differ based on vegetation type at a local environment scale

Luxian Liu[1†], Liya Ma[1†], Mengmeng Zhu[1], Bo Liu[1], Xu Liu[2] and Yu Shi[1*]

[1]State Key Laboratory of Crop Stress Adaptation and Improvement, School of Life Sciences, Henan University, Kaifeng, Henan, China, [2]State Key Laboratory of Soil and Sustainable Agriculture, Institute of Soil Science, Chinese Academy of Sciences, Nanjing, China

Introduction: Rhizosphere microbes perform critical functions for their hosts, and their structure is strongly influenced by vegetation type. Although studies on the effects of vegetation on rhizosphere microbial community structure have been conducted at large and global environment scales, studies at local environment scales would eliminate numerous external factors such as climate and soil type, while highlighting the potential influence of local vegetation type.

Methods: Here, we compared rhizosphere microbial communities using 54 samples under three vegetation types (herb, shrubs, and arbors, with bulk soil as the control) at the campus of Henan University. 16S rRNA and ITS amplicons were sequenced using Illumina high throughput sequencing.

Results and Discussion: Rhizosphere bacterial and fungal community structures were influenced considerably by vegetation type. Bacterial alpha diversity under herbs was significantly different from that under arbors and shrubs. The abundance of phyla such as Actinobacteria was extremely higher in bulk soil than in the rhizosphere soils. Herb rhizosphere harbored more unique species than other vegetation type soils. Furthermore, bacterial community assembly in bulk soil was more dominated by deterministic process, whereas the rhizosphere bacterial community assembly was dominated by stochasticity and the construction of fungal communities was all dominated by deterministic processes. In addition, rhizosphere microbial networks were less complex than bulk soil networks, and their keystone species differed based on vegetation type. Notably, bacterial community dissimilarities were strongly correlated with plant phylogenetic distance. Exploring rhizosphere microbial community patterns under different vegetation types could enhance our understanding of the role of rhizosphere microbes in ecosystem function and service provision, as well as basic information that could facilitate plant and microbial diversity conservation at the local environment scale.

KEYWORDS

vegetation type, rhizosphere microbes, microbial networks, local scale, bacteria and fungi

Highlights

- Rhizosphere microbial community structure influenced significantly by vegetation type.
- Contrasting bacterial and fungal assembly processes in bulk and rhizosphere soil.
- Rhizosphere communities harbor less complex networks than bulk soil.
- Rhizosphere bacterial communities significantly correlated with plant phylogeny.

1. Introduction

The rhizosphere is a hotspot of interactions between plant root and soil (Lundberg et al., 2012; Korenblum et al., 2020) It is a complex ecosystem that can be influenced considerably by the composition of the aboveground plants (Liu et al., 2020). Recently, the influence of plants on rhizosphere microbes has been studied extensively (Schmid et al., 2019; Escudero-Martinez et al., 2022) across different ecosystems, including forest (Chen et al., 2018), grassland (Birgander et al., 2017), and cropland (Simonin et al., 2020). The rhizosphere ecosystem is highly complex, and under the influence of various plant species. Therefore, the influence of vegetation type on the rhizosphere microbial community structure should be taken into account.

Recently, researchers have begun focusing on the effect of vegetation type on rhizosphere. In addition, some researchers have explored the structure and function of the global rhizosphere microbiome (Davison et al., 2015; Xu et al., 2018; Ling et al., 2022); however, the researchers mainly focused on certain plant types, or plants in multiple ecosystems. Therefore, the effects of associated factors, such as climate and soil type, on the rhizosphere microbiome cannot be eliminated at large scales.

Rhizosphere microbes, which mainly include bacteria and fungi, are essential for plant growth and development (Huang et al., 2014). Some of the microbes enhance the capacity of plants to obtain nutrients from soil, and resistance to various biotic and abiotic stress factors, such as disease (Song et al., 2021), high salinity (Schmitz et al., 2022), and drought (de Vries et al., 2020) and adaptation to changing environments (Berendsen et al., 2012; Trivedi et al., 2020). In return, the microbes get certain benefits from plants, including nutrients such as carbon (Bais et al., 2006). Consequently, vegetation type can influence rhizosphere community diversity and composition. For example, arbuscular mycorrhizal fungal colonization is higher in forbs than in grass (Bunn et al., 2015). Furthermore, in natural mountain forests of eastern China, Yang et al. (2019) observed dissimilarities in rhizosphere microbial community structure under different vegetation types, which increased significantly with an increase in plant phylogenetic distance, highlighting the role of plant phylogeny in rhizosphere community structure.

In addition to exhibiting high diversity, rhizosphere microbes establish complex ecological networks, which can also be affected by vegetation type. For instance, the rhizosphere bacterial network structure in rubber forest soils is simpler than that in tropical rainforests, whereas the rhizosphere fungal network structure in rubber forest soils is more complex (Lan et al., 2022). However, microbial community structure is the product of interactions among multiple factors, including plant factors and environmental factors (Jiang et al., 2020; Yang et al., 2021b). Consequently, large-scale studies involve too many abiotic and abiotic factors. Generally speaking, plant species is one of the key factors affecting the rhizosphere bacterial species, that is, different plant species should have different rhizosphere bacterial communities (Fitzpatrick et al., 2018). However, recent common garden experiments had found that species identity could only explain a small part of the difference in rhizosphere bacterial community (Leff et al., 2018). And the differences in rhizosphere bacterial communities of the same plant species growing in different soils are generally greater than those observed between different plant species growing in the same soil (Vieira et al., 2020). Guajardo-Leiva et al. (2022) found that soil is the main source of microorganisms, which leads to the homogeneity of community composition of different plant species growing at the same sampling point. While it remains unclear whether the same plants can exert the effects on rhizosphere community structure in different localities with highly similar climate and soil conditions frequently affected by human activities. Besides, considering community complexity would affect community dynamics, in the present study, we have adopted a metric called "Cohesion" for quantifying the degree of connectivity in microbial communities (Herren and McMahon, 2017).

Understanding the microbial assembly process is a key issue in microbial ecology, and can enhance our understanding of the mechanisms of regulation of microbial community structure (Stegen et al., 2013a; Dini-Andreote et al., 2015). Microbial community assembly occurs *via* two key processes, including stochastic processes, which mainly includes dispersal limitation, shift, and other random community changes (Hubbell and Borda-De-Agua, 2004), and deterministic processes, which is largely selection by environmental factors (Stegen et al., 2012, 2013b, 2015). Recently, numerous studies have quantified the relative importance of the two processes in community structuring (Aad et al., 2014; Feng et al., 2018b; Yang et al., 2021a; Liu et al., 2023). For example, Fan et al. (2018) investigated microbial community assembly processes in the rhizosphere soils of wheat fields. Furthermore, some researchers have explored the microbial community assembly processes in the vadose zone (Sheng et al., 2021).

The two dominant processes, stochasticity and determinism, have been further disentangled into five plausible scenarios (Shi et al., 2020a), including heterogeneous selection (HeS) and homogeneous selection (HoS), which belong to determinism (Dini-Andreote et al., 2015), and homogeneous dispersal (HD; van der Plas et al., 2018), dispersal limitation (DL; Whitaker et al., 2003; Zhou et al., 2008), and undominated (UD) cases, which belong to stochastic processes (Jiao et al., 2020). Exploration of microbial community assembly based on the five key processes above could enhance the understanding of rhizosphere microbial community structure across different vegetation types.

City parks or university campuses, which exhibit high plant species diversity, are ideal platforms for investigating the influence of vegetation type on rhizosphere microbes at relatively small spatial scales. In the present study, we collected 54 samples from two locations at Henan University to analyze rhizosphere microbial community structure across three vegetation types.

We hypothesized that microbial community structure in bulk and rhizosphere soils is controlled by different assembly process, and the responses of bacteria and fungi vary based on vegetation type and phylogeny, with markedly different community assembly patterns. We constructed the microbial community networks under different vegetation types to determine whether their topological characteristics and core species, and the underlying factors. The results of the present study could provide novel insights on rhizosphere microbial community structure under different vegetation types at the local environment scale.

2. Materials and methods

2.1. Study site

This study was conducted using soil obtained from the park of Jinming campus of Henan University (longitude: 114.35°E, latitude: 34.80°N) in Kaifeng, China. Kaifeng has a temperate monsoon

climate, with an annual average temperature of 14°C and an annual average precipitation of 650 mm. Rainfall mainly occurs in July and August every summer. The soil types mainly include fluvo-aquic soils, saline soil, aeolian sandy soil, and alluvial soils.

2.2. Soil sampling and testing

We selected two gardens to collect soil samples. One location is in the south of the campus and another is in the north (Supplementary Figure S1). In each garden, we collected samples of 9 species of plants. Only four species (*Ligustrum lucidum, Forsythia viridissima, Oxalis corniculate, Veronica persica*) were collected in both sampling locations. Finally, they were grouped into four vegetation types (arbors, shrubs, herbs, and bulk soil. For the detail information, please see Supplementary Table S1). No specific permissions were required for sample collection and the filed study did not involve endangered or protected species. The distance between two sampling points was more than 3 m. At first, the top litter layer was removed. Before sampling, the sampling tools were wiped with the original soil in the area near the collection location to minimize external interference as much as possible. Subsequently, while wearing disposable gloves, the soil was gently dug with a shovel and the fresh soil sorted to remove stones and to find fine roots (diameter ≤ 2 mm). Taking ginkgo as an example, 0–1 m away from the trunk is the area where fine roots are predominantly distributed, and the range for arbors and shrubs is within 5–20 cm underground. When herbaceous plant samples were collected, the whole plant was taken out as completely as possible to look for fine roots. After shaking off the loose soil, the soil adhering to the fine roots over a 1-mm layer was brushed off and collected as the rhizosphere soil sample. All the soil samples were put in sterile bags (stored in dry ice boxes), transported back to the laboratory within 2 h, and then stored at −80°C until DNA extraction. Bulk soil with no plant roots collected in the adjacent area, at a distance more than 5 m from the nearest sampling point was collected as the control soil sample.

2.3. DNA extraction and PCR amplification

A Power Soil DNA kit (MO BIO, Carlsbad, CA, United States) was used to extract the total DNA from soil samples. Afterward, a NanoDrop ND-1000 spectrophotometer (Thermo Scientific, Waltham, MA, United States) was used to quantify the DNA concentrations of samples. The extracted DNA was diluted to approximately 25 ng/μL with distilled water and stored at −20°C until use.

Rhizosphere and bulk soil bacterial and fungal community were tested by high-throughput sequencing techniques at IlluminaNovaSeq platform of MAGIGENE Company, Guangdong, China.[1] The V3–V4 hypervariable regions of bacterial 16S rRNA genes were amplified with the 338F and 806R primer set (Xu et al., 2016). And the ITS2 region of fungi was amplified using the ITS3F and ITS4R primer set (Toju et al., 2012; Supplementary Table S2). The Polymerase Chain Reactions (PCR) were implemented as follows: 3 min of denaturation at 95°C, followed by 30 cycles of 30 s at 95°C, 30 s at 55°C for annealing, and 45 s at 72°C for elongation, with a final extension at 72°C for 10 min. The reactions were carried out in 20-μL triplicate mixtures, each containing 4 μL of 5× FastPfu Buffer, 2 μL of 2.5 mM dNTPs, 0.8 μL of each primer (5 μM), 0.4 μL of FastPfu Polymerase, and 10 ng of template DNA (Toju et al., 2012; Xu et al., 2016).

2.4. Statistical analysis

The raw data sequences were processed and analyzed using QIIME2 (Bolyen et al., 2019) based on the workflow at https://qiime2.org. Briefly, to obtain the Amplicon Sequence Variant (ASV) table, quality control of the raw sequencing data was performed using the Deblur tool (Amir et al., 2017) and clustered based on 100% shared identity. The taxonomy of each bacterial phylotype was identified using the Greengenes release database (DeSantis et al., 2006) and the fungal taxonomy assignment was performed using the Sklearn-based taxonomy classifier with the dynamic Unite database from 10 October 2017.[2] Finally, we obtained 12,730,609 bacterial sequences in and 9,153,794 fungal sequences, with 98.5% classified into 104,824 distinct ASVs in bacteria and 13,233 in fungal distinct ASVs. To rarify all datasets for each sample to the same degree, 1,122,000 and 3,089,100 bacterial and fungal sequences, respectively, were selected randomly.

2.5. Rhizosphere soil fungal and bacterial community structure analyses

In order to measure the difference between groups, the relative abundance of the top 10 microorganisms were logarithm transformed and then we used the LSD method of "agricolae" package for post-hoc test. To assess the abundance and diversity of microbial communities, the Shannon, Simpson, Chao1, and Observed species indices were calculated at the ASV level using QIIME2. The vegan package was used to calculate the β-diversity (Bray-Curtis and Jaccard distance) of bacterial and fungal communities in the arbor, shrub, and herbage rhizosphere soils, and bulk soil (Oksanen et al., 2020). Differences in diversity among the samples were analyzed using the Wilcoxon rank-sum test. Nonmetric multidimensional scaling (NMDS) ordinations was generated to distinguish the distribution of the samples based on Jensen-Shannon divergence (JSD), using the vegan package (Oksanen et al., 2020). Differences between communities were evaluated using Permutational Multivariate Analysis of Variance using the "Adonis" function in the vegan package.

2.6. Phylogenetic network construction and distance estimation

To construct the phylogenetic networks of the 14 plant species, plastome sequences were downloaded from the GenBank database (Supplementary Table S3). Maximum Likelihood (ML) analysis was

1 http://www.magigene.com/

2 https://unite.ut.ee/

performed using CIPRES Science Gateway v3.3 (Miller et al., 2010) and RAxML v8.1.11(Stamatakis et al., 2008), with GTR + T + G as the optimal substitution model. The default parameter settings were used, except for the bootstrap iterations being set to 1,000. The phylogenetic distance between each species was calculated in the PAML program (Yang, 2007).

2.7. Analyzing the rhizosphere soil bacteria assembly processes

According to Stegen et al. (2013b, 2015), the ß-NTI and Bray-Curtis-based Raup-Crick metrics (RC-Bray) methods were jointly used assess the community assembly processes. β-NTI measures the deviation of the β-mean nearest taxon distance (β-MNTD) and the β-MNTD of the null model, and both were calculated using Phylocom v42 (Webb et al., 2008).

Traits regulating community assembly processes should be phylogenetically conserved (Stegen et al., 2012). Therefore, a phylogenetic signal analysis is required before calculating β-NTI. The relationship between phylogenetic distances of pairwise ASVs and the corresponding environmental conditions was evaluated using "mantelcorrelog" (Stegen et al., 2012), based on the phylogenetic distances calculated using the "cophenetic" function in the "picante" package in R v4.1.3 (R Foundation for Statistical Computing, Vienna, Austria). The Euclidean distance of each soil variable of pairwise ASVs was calculated and the abundance-weighted mean value obtained. Significant relationships within a short phylogenetic distance indicate that phylogenetic signals are also significant. | β-NTI | > 2 indicates a community that is dominated by deterministic processes (Stegen et al., 2012). Conversely, | β- NTI | < 2 indicates that stochastic processes, including DL, HD, and UD, are dominant in the community (Stegen et al., 2015; Tripathi et al., 2018; Feng et al., 2018b).

In the present study, the bacterial ASVs with relatively high abundances (i.e., > 0001%) were selected (3,000 ASVs in our study) for use in calculating the β-NTI and RCbray values (Shi et al., 2018; Feng et al., 2018a).

2.8. Analyzing rhizosphere soil fungal and bacterial stability

Co-occurrence network analyses were conducted based on a SparCC correlation matrix using the SpiecEasi package in R (Friedman and Alm, 2012; Kurtz et al., 2015). To enhance the reliability of the networks, the ASV table was filtered. We constructed four networks corresponding to the four types of samples, including the rhizosphere arbor, shrub, and herb soil, and bulk soil. We only retained ASVs present in more than 20% of the bacterial samples and more than 30% of the fungal samples for each sample type. For each group, the selected fungal and bacterial ASVs were used to jointly construct the microbial network, with 533, 401, 393, and 754 ASVs retained in the herb, shrub, and arbor rhizosphere soil, and bulk soil, respectively, for network construction.

According to Banerjee et al. (2018), network hubs, module hubs, and connectors were defined as keystone species in the present study (Shi et al., 2020b). In addition, according to Guimerà and Nunes Amaral (2005), the z-scores (within-module degree) and c-scores (participation coefficient) of each node in the networks were calculated to identify the hubs and connectors. Based on the threshold values of the within-module degree (z-score) and participation coefficients (c-score) of nodes, nodes with a z-score > 2.5 and c-score > 0.6 were defined as network hubs. Nodes with a z-score > 2.5 and c-score < 0.6 were defined as module hubs, whereas nodes with a z-score < 2.5 and c-score > 0.6 were considered as connectors. Furthermore, nodes with a z-score < 2.5 and c-score < 0.6 were classified as peripherals. Shi et al. (2020b) has expounded in detail the particular role of each type of node in community networks.

3. Results

3.1. Effect of vegetation type on soil microbial community composition

Using the high throughput sequencing platform, 21,884,403 quality sequences were obtained from the 54 soil samples of four types; among them, 86,366 were identified at 100% similarity, being mostly bacteria and 11,188 were identified at 100% similarity, being mostly fungi. At the bacterial phylum level, Proteobacteria (28.8%), Actinobacteria (16.7%), Cyanobacteria (13.1%), Bacteroidetes (12.7%), Chloroflexi (9.7%), and Acidobacteria (5.8%) were dominant, accounting for more than 80% of all sequences (Figure 1) Ascomycota was the most common fungal phylum among the samples (Figure 1). At the fungal class level, Sordariomycetes (21.9%), Dothideomycetes (13.0%), Agaricomycetes (10.8%), Pezizomycetes (7.5%), and Leotiomycete (6.1%) were dominant. Dothideomycetes abundance was the highest in the herb rhizosphere (Figure 1).

In the case of bacteria, compare to those in all the rhizosphere soils, most high abundance microbiomes were significantly enriched in bulk soil, whereas Cyanobacteria and Bacteroidetes abundances in bulk soil were significantly lower (Figure 1; Supplementary Table S4). The abundances of phylum Cyanobacteria in the herbs' rhizosphere soil were also significantly lower than that in arbors' rhizosphere soil, but herbs had the most Bacteroidetes than the others (Figure 1; Supplementary Table S4). And in the case of fungi, the abundance of classes Leotiomycetes in arbor rhizosphere was significantly higher than those in the other soils. The abundances of Sordariomycetes, Pezizomycetes and Mortierellomycetes in bulk soils were the highest while the abundances of class Dothideomycetes and Leotiomycetes in bulk soils were the lowest among the different groups (Figure 1; Supplementary Table S5).

3.2. Effect of vegetation type on soil microbial community structure

Although there were no obvious differences in fungal α diversity among the groups, there were significant differences in bacterial α diversity. The bacterial α diversity of herbs and bulk soils were significantly higher than those of shrubs and arbors. And there is no obvious difference in bacterial diversity between herbs and bulk soils, nor between shrubs and arbors (Supplementary Figures S2, S3).

According to the results of VPA, the explanation of plant type (1.1% for bacteria and 3.4% for fungi) for the differences between groups was higher than that of location (0.5% for bacteria and 1.7%

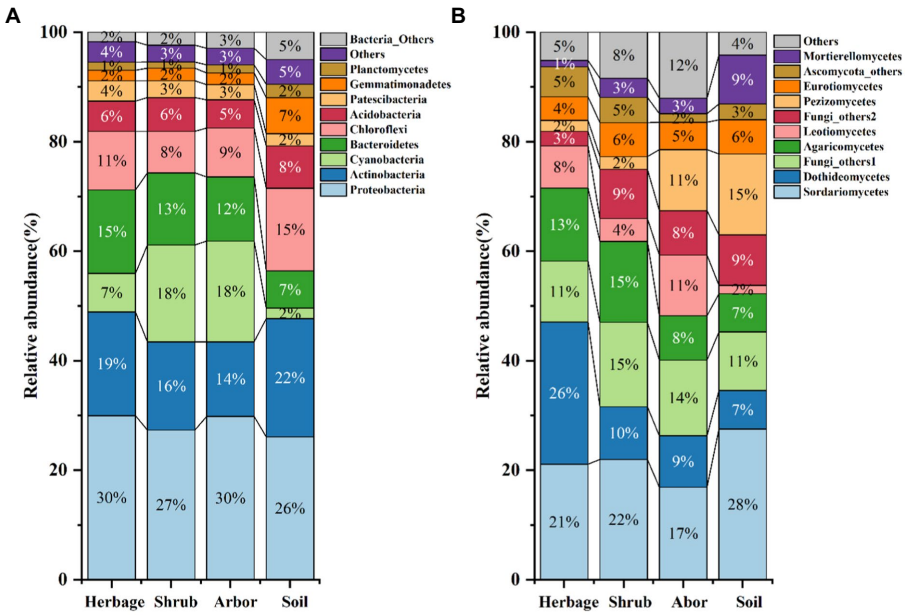

FIGURE 1
Relative abundance of the dominant bacteria phyla **(A)** and dominant fungus classes **(B)** across all soils. Soils are grouped by plant types. The "Bacteria_Others" refers to the sum of bacteria which has very low relative abundance, while "Others" refers to the unidentified sequences.

for fungi; Supplementary Table S7). In addition, both the NMDS and Multivariate Welch ANOVA showed obvious differences between bacteria and fungus (Figure 2; Supplementary Tables S8, S9). According to the results of Multivariate Welch ANOVA, except for some comparisons (S. Herbage vs. N. Herbage, N. Bulk soil vs. N. Shrub, S. Bulk soil vs. N. Shrub, S. Bulk soil vs. N. Arbor, S. Bulk soil vs. N. Bulk soil, S. Bulk soil vs. S. Arbor and S. Arbor vs. S. Shrub), the bacteria in most comparisons had significant differences between groups (Figure 2A; Supplementary Table S8). While the majority of the differences of fungi among groups were significant, except for the differences between the bulk soil, the rhizosphere soil of shrubs and arbors in the south and between the bulk soil in the south and in the north (Figure 2B; Supplementary Table S9). Furthermore, Mantel test results showed that plant phylogeny had a strong influence on bacterial community structure, and not on fungal community structure, while plant vegetation types have a significant impact on the difference between groups of both bacteria and fungi (Supplementary Table S6).

Among bacteria, Cyanobacteria and Firmicutes were significantly higher in the rhizosphere soil of arbor. Bacteroidetes were significantly higher in herbaceous plants, while bulk soil had the largest number of endemic bacterial phyla (Figure 3A). In particular, the bulk soil contains a variety of archaea that are less abundant in the rhizosphere of plants.

For fungus (Figure 3B), Archaeorhizomycetes and Mortierellomycetes were significantly higher in soil than in rhizosphere soil of all plants. Leotiomycetes, Glomeromycota, Tremellomycetes, Rozellomycota and Mucoromycota were significantly higher in arbor soil. The Rhizophydiomycetes, Basidiomycota and Glomeromycota in the rhizosphere soil of shrub were significantly higher. Rhizophlyctidomycetes, Ascomycota and Orbiliomycetes were significantly higher in the rhizosphere soil of herbage.

According to the Venn plot (Figures 3C, D), although the number of bacteria involved in the analysis was much higher than the number of fungi, the number of common fungi in the four samples was still much higher than the number of common bacteria. In addition, the shrub rhizosphere soil had a higher number of common bacteria with arbor rhizosphere soil than with herbage rhizosphere soil, with an opposite trend observed in the case of fungi. In general, the shrub rhizosphere soil had the fewest specialized microbes.

3.3. Soil bacterial and fungal assembly in the four plant types

Bacterial community assembly in rhizosphere was dominated by stochasticity processes, and dispersal limitation was more prevalent in the rhizosphere than in the bulk soil, especially in the herb rhizosphere soil (Figure 4A). Both arbor and shrub rhizosphere soils were partially dominated by stochasticity processes. And in bulk soil, bacterial community assembly was more dominated by deterministic process (Figure 4B). In addition, deterministic processes dominated fungal community assembly processes across all samples. Among them, the assembly processes of shrub rhizosphere were the closest to those of the bulk soil, with relatively similar Normalized Stochasticity Ratio values (Figure 4B).

3.4. Effect of vegetation type on molecular ecological networks of microbial communities

Individual networks were constructed for each of the four sample types (Figure 5A; Table 1). Compared with rhizosphere soil, bulk soil had a more complex microbial network, with the most positive and

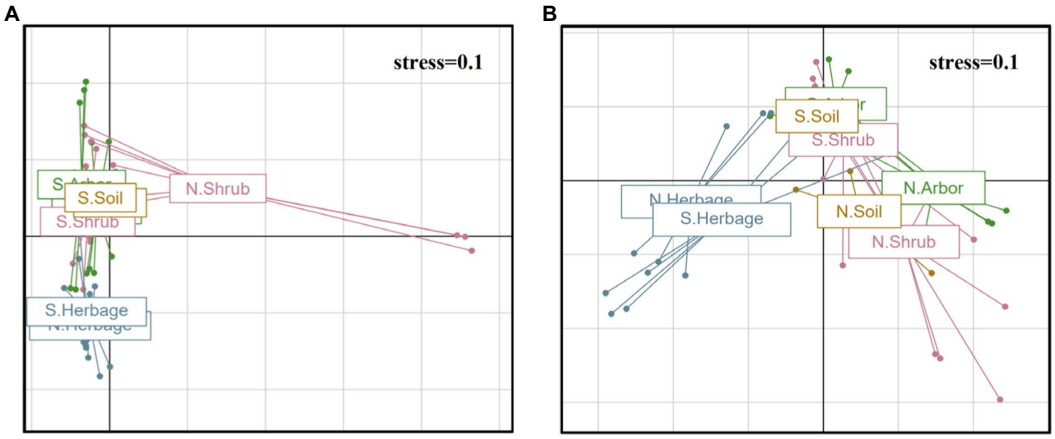

FIGURE 2
Non-metric multidimensional scaling (NMDS) of the bacterial **(A)** and fungal **(B)** community among the samples.

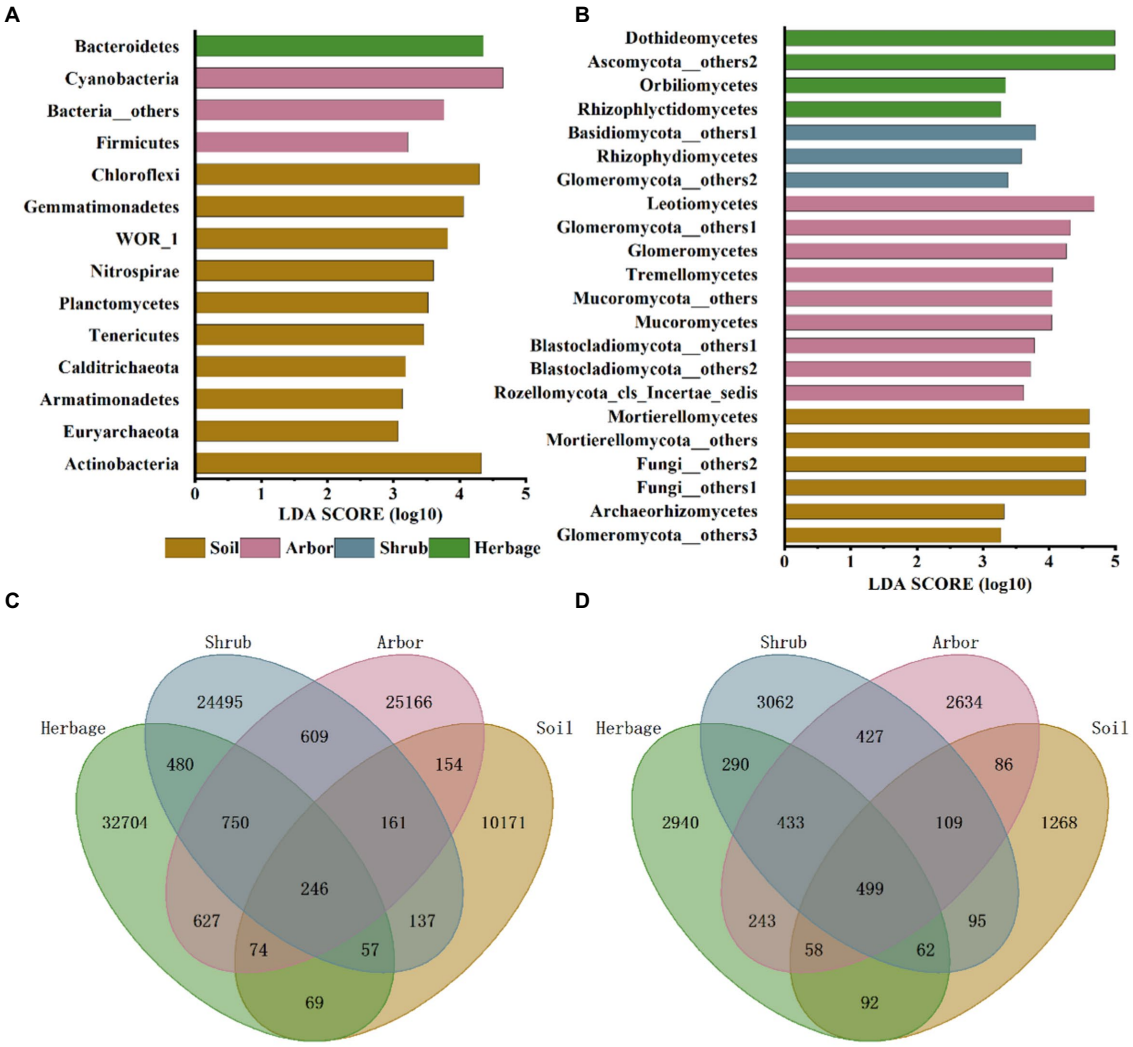

FIGURE 3
Microbial community composition in different soil samples. Linear discriminant analysis effect size (LEfSe) of bacteria phyla/ phylum **(A)** and fungus phyla/ classes **(B)** of four plant types. Venn diagrams of bacteria **(C)** and fungi **(D)** of four plant types.

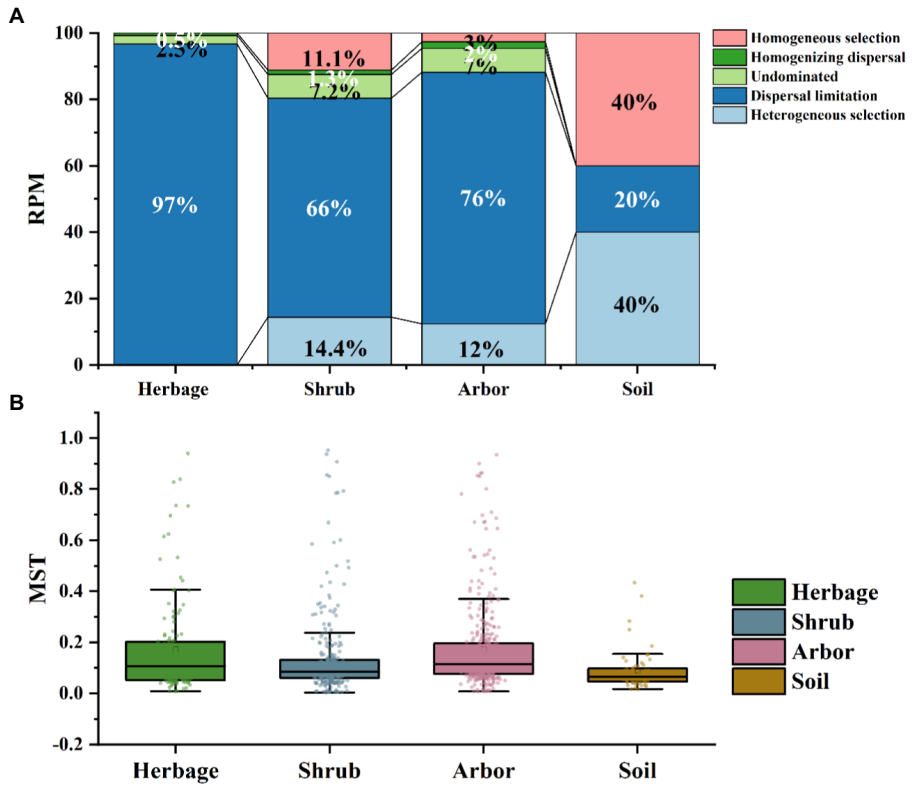

FIGURE 4
Assembly processes of soil microbiome in the four plant types. **(A)** Assembly processes of soil bacteria based on the combined method of ß-NTI. **(B)** Normalized stochasticity ratio (NST) of soil fungal in the four types of samples.

negative connections. The rhizosphere soils of different vegetation types had different core flora. There were 7, 5, 6 and 6 keystone species in the herb, shrub, and arbor rhizosphere soils, and bulk soils, respectively (Table 2). Among them, shrub had the fewest core bacteria. The node and edge numbers in the networks decreased in the order of bulk soil, and herbage, shrub, and arbor rhizosphere soils. Similar trends were observed in the number of positive correlations and negative correlations, and average connectivity (avgK). However, with regard to the ratio of positive to negative correlations and average clustering coefficient (avgCC), shrub rhizosphere had the largest values, excluding bulk soil. In addition, shrub rhizosphere has the lowest average path distance (GD), the lowest number of modules, and the highest Graph density. In addition, the network modularity increased in the order of herbs, shrub, and arbor rhizosphere soils, and bulk soil.

Network robustness was also examined. The results indicated a more stable microbial network in the bulk soil than in the rhizosphere soils. Nodes and edges were discarded in declining order of node betweenness. Therefore, we observed that the natural connectivity of networks in all vegetation types exhibited sharp slopes in all the samples excluding in the bulk soil, suggesting poor stability (Figure 5B). Furthermore, for each group, z-scores and c-scores were calculated for the nodes in the network to identify the keystone species.

Additionally, the shrub has the highest positive cohesion and the lowest negative cohesion (Figure 5C), indicating more cooperation and less competition between microbes in the shrub rhizosphere than in those of other vegetation types.

4. Discussion

Considering the significant effects of human activities on soil environments and vegetation diversity, it is necessary to explore the influence of vegetation type on microbial communities, and whether bacteria and fungi respond differently, at local environment scales. Such a study could provide a scientific basis for understanding microbial function over small spatial scales. In the present study, the influence of vegetation type on soil microbial community structure was glaringly obvious, especially in the case of rhizosphere microbes. Our results showed that rhizosphere microbial community structure could differ considerably across different vegetation types (arbor, shrub, and herbs), which are frequently disturbed by human activities.

4.1. Rhizosphere bacterial and fungal community were significantly different across vegetation types

Arbor, shrub, and herbs are the most common vegetation assemblages in city parks or campuses; therefore, city parks and campuses are ideal sites for investigating the impact of aboveground

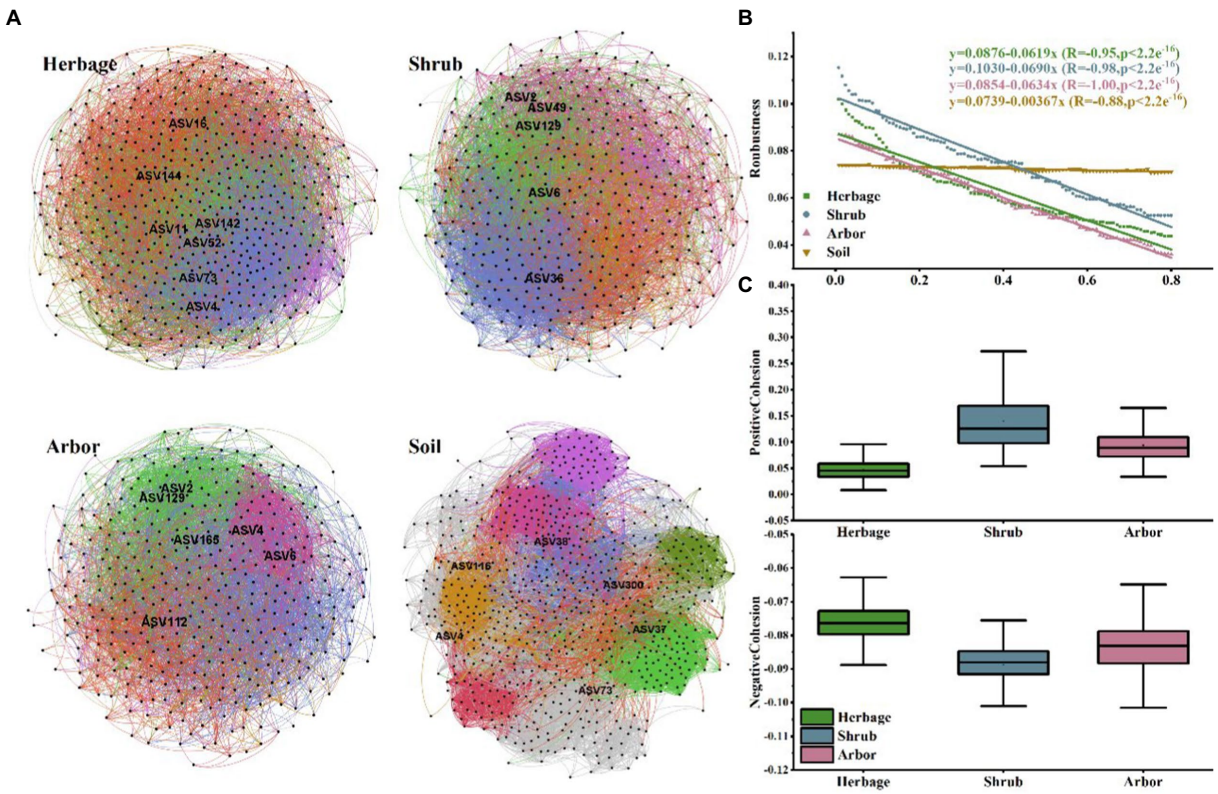

FIGURE 5
(A) Plant rhizosphere networks in the four sample types. Networks represent random matrix theory co-occurrence models, where nodes represent ASVs, and the edges between the nodes indicate significant correlations. In each panel, the size of each node is proportional to the number of connections (i.e., node degree) and the edge color indicates that the node belongs to a different module. **(B)** Robustness of microbial community in the rhizosphere of three types of plants. **(C)** Cohesion of microbial community in the rhizosphere of three types of plants.

vegetation type on belowground soil microbial community structure, while eliminating the effect of climate and soil type. Arbors refer to trees with an upright trunk, usually 6–10 m high, with a trunk independent from the root, and a clear distinction between the trunk and the crown. Arbors also have strong vitality and are widely distributed. At present, arbors are basically found in all terrestrial biomes, including desert, Arctic, and other harsh environments (McBride and Douhovnikoff, 2012; Zhang et al., 2022). Conversely, shrubs are short plants (usually <6 m) with no obvious trunk and numerous branches near the ground, most of which are clustered. Shrubs are generally broad-leaved plants, and some coniferous plants, such as juniper, are shrubs (Lenard, 2008). Shrubs are widely distributed globally, mostly in the tropics and subtropics, and can also be found in arid regions (Xu et al., 2020). In China, shrubs are mainly spread in Zhejiang, Jiangsu, Anhui, Henan, etc., covering about 20% of the land area (Piao et al., 2009). Although there are many differences between arbors and shrubs, they have many similarities with regard to growth habit (Jingui et al., 2023). They are both perennial plants and can survive more than 3 years. Moreover, arbors and shrubs have large numbers of lignified cells, which are obviously different from herbs (Crivellaro et al., 2022). Herbs are usually short with stems that are soft and that break easily. In addition, many herbs are annuals, biennials or triennials, and their xylems are not developed and the vascular bundles do not have cambiums, so that they cannot grow continuously (Evans and Ortega, 2019). Herbs are generally adapted to warm and humid environments. However, herbaceous plants are very resilient, and can be found in hot and humid areas, as well as cold and dry areas. On the whole, the most obvious differences among trees, shrubs, and herbs are based on their physiological traits, biomass, and life span (Yuan et al., 2020).

In the present study, *Pinus massoniana, Gingko biloba, Solanum nigrum, Ligustrum lucidum, Forsythia viridissima, Veronica persica, Punica granatum, Cercis chinensis, Bischofia polycarpa, Oxalis corniculata, Eriobotrya japonica, Euonymus japonicus, Lonicera maackii* and *Ophiopogon japonicus* are grouped into arbors, shrubs, and herbs.

Due to differences in individual size, life history, or physiological function, bacteria and fungus exhibit distinct responses to aboveground plants. In the present study, we observed that soil bacterial α diversity was more sensitive to vegetation type than fungal α diversity. Bacteria are minute, propagate rapidly, and form spores, so that they are ubiquitous and easily dispersed (Foissner, 2006). Conversely, fungi proliferate mainly through budding and spore reproduction. Fungus can also form mycelia, with diverse functions (Cairney and Burke, 1996; Hodge, 2000). Fungal communities jointly form complex belowground networks, which drive the establishment of plant populations and communities, as well as soil nutrient turnover (Yang et al., 2022). According to Sheldrake (2020), fungi are regenerators, recyclers, and network builders that connect the world. Therefore, one or similar fungal species can be observed in different

TABLE 1 Topological properties of the empirical molecular ecological networks of microbial communities in groups.

Network metrics	Type			
	Herbage	Shrub	Arbor	Soil
Number of nodes	533	401	393	754
Number of edges	10,088	6,815	5,233	16,743
Number of positive correlations	5,350	3,738	2,764	11,213
Number of negative correlations	4,738	3,077	2,469	5,530
Ratio of positive to negative correlations	1.129	1.215	1.119	2.028
Average connectivity (avgK)	18.927	16.995	13.316	22.206
Average path distance (GD)	2.224	2.206	2.309	2.640
Average clustering coefficient (avgCC)	0.278	0.311	0.262	0.546
Graph density	0.071	0.085	0.068	0.059
Number of modules[a]	9	9	12	17
Modularity	0.285	0.318	0.352	0.648

[a]Number of modules with ≥ 5 nodes in the networks.

vegetation rhizosphere soils, so that we did not investigate the significant effect of vegetation type on fungal α diversity.

In the β diversity analysis, the results of VPA showed that the explanation of vegetation type for the difference is greater than that of location, which is partially different from the findings of Vieira et al. (2020). In addition, Yang et al. (2019) found that the influence of plant factors on rhizosphere microbial community was greater than spatial factors in the forests of eastern China. In our study, the campus garden is subject to periodic management and frequent human activities, and this will reduce the difference of soil between the two gardens. On the other hand, with the strong effect of host plants, plants exhibited stronger effect than the locations. Additionally, given the low percentage of the variance between samples that explain both the type of plant and the sampling location, possibly, other unaccounted factors can help explain the differences between the samples. According to the results of Multivariate Welch ANOVA, we found that the differences between rhizosphere soils of different vegetation types were generally significant. Consistent with Fitzpatrick et al.'s (2018) study, which found the plant species showed strong effect on the rhizospheric communities. This is also partly similar to the findings in the study of the low Arctic tundra (Shi et al., 2015) which found the soil microbial community could be differed by vegetation types. This may be due to the fact that shrubs and herbs are often closely interlaced, and these interactions would reduce the difference between groups.

4.2. Contrasting bacterial and fungal community assembly processes between bulk and rhizosphere soil

In the present study, bulk soil and rhizosphere soil bacterial communities showed contrasting assembly processes, even under different vegetation types. Bacterial community assembly in bulk soil was more dominated by deterministic process, whereas the rhizosphere bacterial community assembly was dominated by stochasticity and the construction of fungal communities was all dominated by deterministic processes (Figure 4). Similar phenomena were observed in a wheat field ecosystem, with deterministic factors playing a greater role in the assembly of nitrogen fixing bacteria communities in the bulk soil than in the rhizosphere soil (Fan et al., 2018). While Yang et al. (2018) reported a contrary phenomenon that deterministic processes played a more important role than stochastic processes in bacterial community assembly processes in Chinese grassland ecosystem. This may be because environmental filtration has a greater impact on the biogeographic pattern of bacteria. The Anna Karenina principle could explain why we observed that rhizosphere bacterial community assembly was dominated by stochastic process. According to the principle, healthy hosts have relatively stable microbial communities, which form close clusters in an orderly space, while various external stress factors undermine such stability, leading to more dispersed microbial communities (Zaneveld et al., 2017). Therefore, the rhizosphere filtering effect would lead to the cultivation of specific species and be accompanied by the Anna Karenina principal effect, so that a random process occurs.

4.3. Rhizosphere soil harbor less complex networks than bulk soil

Due to the strong filtering effect of plant roots, they harbor simpler communities than bulk soil, and in turn, less complex association networks. Consistent with our study, in farmland, Fan et al. (2018) observed that the network structure of nitrogen fixing microbial communities in rhizosphere soil was less competitive and more stable than that in bulk soil. In grasses, researchers found that rhizosphere networks had less nodes and edges, lower density, but had higher modularity, and greater positive links than bulk soil networks (Li et al., 2021). In a forest ecosystem, co-occurrence network analysis detected relatively higher network complexity and node connectivity in bulk soil than in the rhizosphere community (Jing et al., 2022; Wang et al., 2022). These studies indicated that less complex association networks were prevalent in rhizosphere. In addition, Ling et al. (2022) analyzed 557 pairs of published 16S rDNA amplification sequences from non-rhizosphere soil and rhizosphere soil of different ecosystems globally, and found that the

TABLE 2 Microbial community composition of the keystone species.

Group	ASVID	Category	Kingdom	Phylum	Class
Herbage	ASV4	Provincial hubs	k__Plantae	p__unidentified	c__unidentified
	ASV11	Provincial hubs	k__Fungi	p__Ascomycota	c__Sordariomycetes
	ASV16	Provincial hubs	k__Fungi	p__Ascomycota	c__Sordariomycetes
	ASV52	Provincial hubs	k__Fungi	p__Ascomycota	c__Sordariomycetes
	ASV73	Provincial hubs	k__Fungi	p__Ascomycota	c__Dothideomycetes
	ASV142	Provincial hubs	k__Fungi	p__Ascomycota	c__Dothideomycetes
	ASV144	Provincial hubs	k__Fungi	p__Ascomycota	c__Dothideomycetes
Shrub	ASV2	Provincial hubs	Unassigned		
	ASV6	Provincial hubs	k__Fungi	p__Ascomycota	c__Sordariomycetes
	ASV36	Provincial hubs	k__Plantae	p__unidentified	c__unidentified
	ASV49	Provincial hubs	k__Fungi	p__unidentified	c__unidentified
	ASV129	Provincial hubs	k__Fungi		
Arbor	ASV2	Provincial hubs	Unassigned		
	ASV4	Provincial hubs	k__Plantae	p__unidentified	c__unidentified
	ASV6	Provincial hubs	k__Fungi	p__Ascomycota	c__Sordariomycetes
	ASV112	Provincial hubs	k__Fungi	p__Ascomycota	c__Leotiomycetes
	ASV129	Provincial hubs	k__Fungi		
	ASV165	Provincial hubs	k__Fungi	p__unidentified	c__unidentified
Soil	ASV4	Provincial hubs	k__Plantae	p__unidentified	c__unidentified
	ASV37	Provincial hubs	k__Fungi	p__Ascomycota	c__Pezizomycetes
	ASV38	Provincial hubs	k__Fungi	p__Basidiomycota	c__Tremellomycetes
	ASV73	Provincial hubs	k__Fungi	p__Ascomycota	c__Dothideomycetes
	ASV116	Provincial hubs	k__Plantae		
	ASV300	Provincial hubs	k__Fungi	p__Ascomycota	c__Sordariomycetes

rhizosphere had relatively reduced microbial diversity due to the selection of corresponding microbial populations from soil seed banks, thus forming a highly modular but unstable bacterial network in the rhizosphere. This indicate that less complex networks are not related to the community stability, it might be depending on the ecosystem type.

4.4. Rhizosphere bacterial community structure significantly correlated with plant phylogeny

Yang et al. (2019) observed soil fungal communities could be strongly influenced by plant phylogenetic distance in forest ecosystems across Eastern China. In the present study, we also observed that rhizosphere bacterial communities were significantly correlated with plant phylogeny. In addition, in root microbiomes of multiple plant phyla (Yeoh et al., 2017), researchers observed that soil bacterial communities could be strongly affected by plant phylogeny at the small scale. The reason could be that, at very small scales, plants exert very strong effects on bacteria due to their lower interrelationships, and fungi, because of their hyphae, build highly connected networks at the local scale, so that plant phylogeny did not exhibit strong effects with regard to fungal community structure. Beside this, the effect of specific sampling quantity (Hermans et al., 2019) and soil depth (Chu et al., 2016) on the rhizosphere community were also reported, these two potential impacting factors will be tested in the future.

5. Conclusion

Overall, our results showed that rhizosphere bacterial and fungal community structure could vary across vegetation types in a small scale, and that bacterial assembly was dominated by stochasticity while deterministic processes dominated fungal community assembly processes. Rhizosphere associated networks showed less complexity than bulk soil networks, and their keystone species varied across vegetation types. Community dissimilarities of total bacteria could be influenced by plant phylogenetic distance, while fungi showed no significant correlation. The results of the present study provide insights on belowground microbial structure at the local environment scale under different vegetation types, and might facilitate the knowledge of conservation of belowground microbial biodiversity at a local environment scale.

Data availability statement

The original contributions presented in the study are publicly available. This data can be found at: NCBI, PRJNA898095.

Author contributions

YS and LL designed the study. YS, XL, LM, MZ, BL, and LL performed the research and analyzed the data. LL, LM, MZ, and YS wrote, edited, and finalized the manuscript. All authors contributed to the article and approved the submitted version.

Funding

This work was supported by grants from the Natural Science Foundation of Henan (grant numbers 222300420035, 212300410112) and the National Natural Science Foundation of China (grant number 42077053).

Conflict of interest

The authors declare that the research was conducted in the absence of any commercial or financial relationships that could be construed as a potential conflict of interest.

Publisher's note

Supplementary material

The Supplementary material for this article can be found online at: https://www.frontiersin.org/articles/10.3389/fmicb.2023.1129471/full#supplementary-material

References

Aad, G., Abbott, B., Abdallah, J., Khalek, S. A., Abdinov, O., Aben, R., et al. (2014). Measurements of four-lepton production at the Z resonance in pp collisions at root s=7 and 8 TeV with ATLAS. *Phys. Rev. Lett.* 112:1806. doi: 10.1103/PhysRevLett.112.231806

Amir, A., McDonald, D., Navas-Molina, J. A., Kopylova, E., Morton, J. T., Xu, Z. Z., et al. (2017). Deblur rapidly resolves single-nucleotide community sequence patterns. *mSystems* 2, e00191–e00116. doi: 10.1128/mSystems.00191-16

Bais, H. P., Weir, T. L., Perry, L. G., Gilroy, S., and Vivanco, J. M. (2006). The role of root exudates in rhizosphere interactions with plants and other organisms. *Annu. Rev. Plant Biol.* 57, 233–266. doi: 10.1146/annurev.arplant.57.032905.105159

Banerjee, S., Schlaeppi, K., and van der Heijden, M. G. A. (2018). Keystone taxa as drivers of microbiome structure and functioning. *Nat. Rev. Microbiol.* 16, 567–576. doi: 10.1038/s41579-018-0024-1

Berendsen, R. L., Pieterse, C. M. J., and Bakker, P. (2012). The rhizosphere microbiome and plant health. *Trends Plant Sci.* 17, 478–486. doi: 10.1016/j.tplants.2012.04.001

Birgander, J., Rousk, J., and Olsson, P. A. (2017). Warmer winters increase the rhizosphere carbon flow to mycorrhizal fungi more than to other microorganisms in a temperate grassland. *Glob. Chang. Biol.* 23, 5372–5382. doi: 10.1111/gcb.13803

Bolyen, E., Rideout, J. R., Dillon, M. R., Bokulich, N. A., Abnet, C. C., Al-Ghalith, G. A., et al. (2019). Reproducible, interactive, scalable and extensible microbiome data science using QIIME 2. *Nat. Biotechnol.* 37, 852–857. doi: 10.1038/s41587-019-0209-9

Bunn, R. A., Ramsey, P. W., and Lekberg, Y. (2015). Do native and invasive plants differ in their interactions with arbuscular mycorrhizal fungi? A meta-analysis. *J. Ecol.* 103, 1547–1556. doi: 10.1111/1365-2745.12456

Cairney, J. W. G., and Burke, R. M. (1996). Physiological heterogeneity within fungal mycelia: an important concept for a functional understanding of the ectomycorrhizal symbiosis. *New Phytol.* 134, 685–695. doi: 10.1111/j.1469-8137.1996.tb04934.x

Chen, X., Ding, Z. J., Tang, M., and Zhu, B. A. (2018). Greater variations of rhizosphere effects within mycorrhizal group than between mycorrhizal group in a temperate forest. *Soil Biol. Biochem.* 126, 237–246. doi: 10.1016/j.soilbio.2018.08.026

Chu, H., Sun, H., Tripathi, B. M., Adams, J. M., Huang, R., Zhang, Y., et al. (2016). Bacterial community dissimilarity between the surface and subsurface soils equals horizontal differences over several kilometers in the western Tibetan plateau. *Environ. Microbiol.* 18, 1523–1533. doi: 10.1111/1462-2920.13236

Crivellaro, A., Piermattei, A., Dolezal, J., Dupree, P., and Buntgen, U. (2022). Biogeographic implication of temperature-induced plant cell wall lignification. *Commun. Biol.* 5:767. doi: 10.1038/s42003-022-03732-y

Davison, J., Moora, M., Opik, M., Adholeya, A., Ainsaar, L., Ba, A., et al. (2015). Global assessment of arbuscular mycorrhizal fungus diversity reveals very low endemism. *Science* 349, 970–973. doi: 10.1126/science.aab1161

de Vries, F. T., Griffiths, R. I., Knight, C. G., Nicolitch, O., and Williams, A. (2020). Harnessing rhizosphere microbiomes for drought-resilient crop production. *Science* 368:270. doi: 10.1126/science.aaz5192

DeSantis, T. Z., Hugenholtz, P., Larsen, N., Rojas, M., Brodie, E. L., Keller, K., et al. (2006). Greengenes, a chimera-checked 16S rRNA gene database and workbench compatible with ARB. *Appl. Environ. Microbiol.* 72, 5069–5072. doi: 10.1128/AEM.03006-05

Dini-Andreote, F., Stegen, J. C., van Elsas, J. D., and Salles, J. F. (2015). Disentangling mechanisms that mediate the balance between stochastic and deterministic processes in microbial succession. *P. Natl. Acad. Sci. USA* 112, E1326–E1332. doi: 10.1073/pnas.1414261112

Escudero-Martinez, C., Coulter, M., Terrazas, R. A., Foito, A., Kapadia, R., Pietrangelo, L., et al. (2022). Identifying plant genes shaping microbiota composition in the barley rhizosphere. Nature. *Communications* 13:1022. doi: 10.1038/s41467-022-31022-y

Evans, L. S., and Ortega, H. (2019). Xylem conductivities in grasses. *Flora* 257:151420. doi: 10.1016/j.flora.2019.151420

Fan, K. K., Weisenhorn, P., Gilbert, J. A., Shi, Y., Bai, Y., and Chu, H. Y. (2018). Soil pH correlates with the co-occurrence and assemblage process of diazotrophic communities in rhizosphere and bulk soils of wheat fields. *Soil Biol. Biochem.* 121, 185–192. doi: 10.1016/j.soilbio.2018.03.017

Feng, M., Adams, J. M., Fan, K., Shi, Y., Sun, R., Wang, D., et al. (2018a). Long-term fertilization influences community assembly processes of soil diazotrophs. *Soil Biol. Biochem.* 126, 151–158. doi: 10.1016/j.soilbio.2018.08.021

Feng, Y., Chen, R., Stegen, J. C., Guo, Z., Zhang, J., Li, Z., et al. (2018b). Two key features influencing community assembly processes at regional scale: Initial state and degree of change in environmental conditions. *Mol. Ecol.* 27, 5238–5251. doi: 10.1111/mec.14914

Fitzpatrick, C. R., Copeland, J., Wang, P. W., Guttman, D. S., Kotanen, P. M., and Johnson, M. T. J. (2018). Assembly and ecological function of the root microbiome across angiosperm plant species. *Proc. Natl. Acad. Sci.* 115:7115. doi: 10.1073/pnas.1717617115

Foissner, W. (2006). Biogeography and dispersal of micro-organisms: a review emphasizing protists. *Acta Protozool.* 45, 111–136.

Friedman, J., and Alm, E. J. (2012). Inferring correlation networks from genomic survey data. *PLoS Comput. Biol.* 8:e1002687. doi: 10.1371/journal.pcbi.1002687

Guajardo-Leiva, S., Alarcón, J., Gutzwiller, F., Gallardo-Cerda, J., Acuña-Rodríguez, I. S., Molina-Montenegro, M., et al. (2022). Source and acquisition of rhizosphere microbes in Antarctic vascular plants. *Front. Microbiol.* 13:6210. doi: 10.3389/fmicb.2022.916210

Guimerà, R., and Nunes Amaral, L. A. (2005). Functional cartography of complex metabolic networks. *Nature* 433, 895–900. doi: 10.1038/nature03288

Hermans, S. M., Buckley, H. L., and Lear, G. (2019). Perspectives on the impact of sampling design and intensity on soil microbial diversity estimates. *Front. Microbiol.* 10:1820. doi: 10.3389/fmicb.2019.01820

Herren, C. M., and McMahon, K. D. (2017). Cohesion: a method for quantifying the connectivity of microbial communities. *ISME J.* 11, 2426–2438. doi: 10.1038/ismej.2017.91

Hodge, A. (2000). Microbial ecology of the arbuscular mycorrhiza. *FEMS Microbiol. Ecol.* 32, 91–96. doi: 10.1111/j.1574-6941.2000.tb00702.x

Huang, X. F., Chaparro, J. M., Reardon, K. F., Zhang, R. F., Shen, Q. R., and Vivanco, J. M. (2014). Rhizosphere interactions: root exudates, microbes, and microbial communities. *Botany* 92, 267–275. doi: 10.1139/cjb-2013-0225

Hubbell, S. P., and Borda-De-Agua, L. (2004). The unified neutral theory of biodiversity and biogeography: reply. *Ecology* 85, 3175–3178. doi: 10.1890/04-0808

Jiang, X. L., Liu, W. Z., Yao, L. G., Liu, G. H., and Yang, Y. Y. (2020). The roles of environmental variation and spatial distance in explaining diversity and biogeography of soil denitrifying communities in remote Tibetan wetlands. *FEMS Microbiol. Ecol.* 96:63. doi: 10.1093/femsec/fiaa063

Jiao, S., Yang, Y. F., Xu, Y. Q., Zhang, J., and Lu, Y. H. (2020). Balance between community assembly processes mediates species coexistence in agricultural soil microbiomes across eastern China. *ISME J.* 14, 202–216. doi: 10.1038/s41396-019-0522-9

Jing, L., Jia-min, A., Xiao-dong, L., Ying-ying, J., Chao-chao, Z., Rui-hua, Z., et al. (2022). Environmental filtering drives the establishment of the distinctive rhizosphere, bulk, and root nodule bacterial communities of Sophora davidii in hilly and gully regions of the loess plateau of China. *Front. Microbiol.* 13:5127. doi: 10.3389/fmicb.2022.945127

Jingui, D., Yi, F., Ruirui, F., Mengke, S., Quanlin, Z., Dandan, H., et al. (2023). Convergence of main bark functional traits of tree and shrub twigs in evergreen broad-leaved forest of the Wuyi Mountain. *Acta Ecol. Sin.*, 3, 1–11.

Korenblum, E., Dong, Y. H., Szymanski, J., Panda, S., Jozwiak, A., Massalha, H., et al. (2020). Rhizosphere microbiome mediates systemic root metabolite exudation by root-to-root signaling. *Proc. Natl. Acad. Sci. U. S. A.* 117, 3874–3883. doi: 10.1073/pnas.1912130117

Kurtz, Z. D., Muller, C. L., Miraldi, E. R., Littman, D. R., Blaser, M. J., and Bonneau, R. A. (2015). Sparse and compositionally robust inference of microbial ecological networks. *PLoS Comput. Biol.* 11:e1004226. doi: 10.1371/journal.pcbi.1004226

Lan, G. Y., Yang, C., Wu, Z. X., Sun, R., Chen, B. Q., and Zhang, X. C. (2022). Network complexity of rubber plantations is lower than tropical forests for soil bacteria but not for fungi. *Soil* 8, 149–161. doi: 10.5194/soil-8-149-2022

Leff, J. W., Bardgett, R. D., Wilkinson, A., Jackson, B. G., Pritchard, W. J., De Long, J. R., et al. (2018). Predicting the structure of soil communities from plant community taxonomy, phylogeny, and traits. *ISME J.* 12, 1794–1805. doi: 10.1038/s41396-018-0089-x

Lenard, E. (2008). Habits of trees and shrubs in landscape design. *Architecture Civil Engineering Environment*. 4, 13–20.

Li, Y., Yang, Y., Wu, T. E., Zhang, H., Wei, G., and Li, Z. (2021). Rhizosphere bacterial and fungal spatial distribution and network pattern of *Astragalus mongholicus* in representative planting sites differ the bulk soil. *Appl. Soil Ecol.* 168:104114. doi: 10.1016/j.apsoil.2021.104114

Ling, N., Wang, T. T., and Kuzyakov, Y. (2022). Rhizosphere bacteriome structure and functions. Nature. *Communications* 13:8448. doi: 10.1038/s41467-022-28448-9

Liu, L. L., Huang, X. Q., Zhang, J. B., Cai, Z. C., Jiang, K., and Chang, Y. Y. (2020). Deciphering the relative importance of soil and plant traits on the development of rhizosphere microbial communities. *Soil Biol. Biochem.* 148:107909. doi: 10.1016/j.soilbio.2020.107909

Liu, S., Shi, Y., Sun, M., Huang, D., Shu, W., and Ye, M. (2023). The community assembly for understanding the viral-assisted response of bacterial community to Cr-contamination in soils. *J. Hazard. Mater.* 441:129975. doi: 10.1016/j.jhazmat.2022.129975

Lundberg, D. S., Lebeis, S. L., Paredes, S. H., Yourstone, S., Gehring, J., Malfatti, S., et al. (2012). Defining the core Arabidopsis thaliana root microbiome. *Nature* 488:86. doi: 10.1038/nature11237

McBride, J. R., and Douhovnikoff, V. (2012). Characteristics of the urban forests in arctic and near-arctic cities. *Urban For. Urban Green.* 11, 113–119. doi: 10.1016/j.ufug.2011.07.007

Miller, M.A., Pfeiffer, W., and Schwartz, T. (2010). "Creating the CIPRES science gateway for inference of large phylogenetic trees," in *Proceedings of the Gateway Computing Environments Workshop (GCE), 2010*, (New Orleans, LA: IEEE), 1–8.

Oksanen, J., Blanchet, F. G., Friendly, M., Kindt, R., Legendre, P., Mcglinn, D., et al. (2020). Package "vegan" Title Community Ecology Package Version 2.5–7. *Cran.Ism. Ac.Jp*.

Piao, S. L., Fang, J. Y., Ciais, P., Peylin, P., Huang, Y., Sitch, S., et al. (2009). The carbon balance of terrestrial ecosystems in China. *Nature* 458, 1009–1013. doi: 10.1038/nature07944

Schmid, M. W., Hahl, T., van Moorsel, S. J., Wagg, C., De Deyn, G. B., and Schmid, B. (2019). Feedbacks of plant identity and diversity on the diversity and community composition of rhizosphere microbiomes from a long-term biodiversity experiment. *Mol. Ecol.* 28, 863–878. doi: 10.1111/mec.14987

Schmitz, L., Yan, Z. C., Schneijderberg, M., de Roij, M., Pijnenburg, R., Zheng, Q., et al. (2022). Synthetic bacterial community derived from a desert rhizosphere confers salt stress resilience to tomato in the presence of a soil microbiome. *ISME J.* 16, 1907–1920. doi: 10.1038/s41396-022-01238-3

Sheldrake, M. (2020). *Entangled Life: How Fungi Make Our Worlds, Change Our Minds & Shape Our Futures. 5th ed.* New York, NY, USA: Random House.

Sheng, Y. Z., Liu, Y., Yang, J. J., Dong, H. L., Liu, B., Zhang, H., et al. (2021). History of petroleum disturbance triggering the depth-resolved assembly process of microbial communities in the vadose zone. *J. Hazard. Mater.* 402:124060. doi: 10.1016/j.jhazmat.2020.124060

Shi, Y., Dang, K. K., Dong, Y. H., Feng, M. M., Wang, B. R., Li, J. G., et al. (2020a). Soil fungal community assembly processes under long-term fertilization. *Eur. J. Soil Sci.* 71, 716–726. doi: 10.1111/ejss.12902

Shi, Y., Delgado-Baquerizo, M., Li, Y., Yang, Y., Zhu, Y.-G., Peñuelas, J., et al. (2020b). Abundance of kinless hubs within soil microbial networks are associated with high functional potential in agricultural ecosystems. *Environ. Int.* 142:105869. doi: 10.1016/j.envint.2020.105869

Shi, Y., Li, Y., Xiang, X., Sun, R., Yang, T., He, D., et al. (2018). Spatial scale affects the relative role of stochasticity versus determinism in soil bacterial communities in wheat fields across the North China plain. *Microbiome* 6:27. doi: 10.1186/s40168-018-0409-4

Shi, Y., Xiang, X., Shen, C., Chu, H., Neufeld, J. D., Walker, V. K., et al. (2015). Vegetation-associated impacts on arctic tundra bacterial and microeukaryotic communities. *Appl. Environ. Microbiol.* 81, 492–501. doi: 10.1128/AEM.03229-14

Simonin, M., Dasilva, C., Terzi, V., Ngonkeu, E. L. M., Diouf, D., Kane, A., et al. (2020). Influence of plant genotype and soil on the wheat rhizosphere microbiome: evidences for a core microbiome across eight African and European soils. *FEMS Microbiol. Ecol.* 96:67. doi: 10.1093/femsec/fiaa067

Song, Y., Wilson, A. J., Zhang, X. C., Thoms, D., Sohrabi, R., Song, S. Y., et al. (2021). FERONIA restricts pseudomonas in the rhizosphere microbiome via regulation of reactive oxygen species. *Nature Plants* 7:644. doi: 10.1038/s41477-021-00914-0

Stamatakis, A., Hoover, P., and Rougemont, J. (2008). A rapid bootstrap algorithm for the RAxML web servers. *Syst. Biol.* 57, 758–771. doi: 10.1080/10635150802429642

Stegen, J. C., Freestone, A. L., Crist, T. O., Anderson, M. J., Chase, J. M., Comita, L. S., et al. (2013a). Stochastic and deterministic drivers of spatial and temporal turnover in breeding bird communities. *Glob. Ecol. Biogeogr.* 22, 202–212. doi: 10.1111/j.1466-8238.2012.00780.x

Stegen, J. C., Lin, X. J., Fredrickson, J. K., Chen, X. Y., Kennedy, D. W., Murray, C. J., et al. (2013b). Quantifying community assembly processes and identifying features that impose them. *ISME J.* 7, 2069–2079. doi: 10.1038/ismej.2013.93

Stegen, J. C., Lin, X. J., Fredrickson, J. K., and Konopka, A. E. (2015). Estimating and mapping ecological processes influencing microbial community assembly. *Front. Microbiol.* 6:370. doi: 10.3389/fmicb.2015.00370

Stegen, J. C., Lin, X. J., Konopka, A. E., and Fredrickson, J. K. (2012). Stochastic and deterministic assembly processes in subsurface microbial communities. *ISME J.* 6, 1653–1664. doi: 10.1038/ismej.2012.22

Toju, H., Tanabe, A. S., Yamamoto, S., and Sato, H. (2012). High-coverage ITS primers for the DNA-based identification of ascomycetes and basidiomycetes in environmental samples. *PLoS One* 7:e40863. doi: 10.1371/journal.pone.0040863

Tripathi, B. M., Stegen, J. C., Kim, M., Dong, K., Adams, J. M., and Lee, Y. K. (2018). Soil pH mediates the balance between stochastic and deterministic assembly of bacteria. *ISME J.* 12, 1072–1083. doi: 10.1038/s41396-018-0082-4

Trivedi, P., Leach, J. E., Tringe, S. G., Sa, T. M., and Singh, B. K. (2020). Plant-microbiome interactions: from community assembly to plant health. *Nat. Rev. Microbiol.* 18, 607–621. doi: 10.1038/s41579-020-0412-1

van der Plas, F., Ratcliffe, S., Ruiz-Benito, P., Scherer-Lorenzen, M., Verheyen, K., Wirth, C., et al. (2018). Continental mapping of forest ecosystem functions reveals a high but unrealized potential for forest multi-functionality. *Ecol. Lett.* 21, 31–42. doi: 10.1111/ele.12868

Vieira, S., Sikorski, J., Dietz, S., Herz, K., Schrumpf, M., Bruelheide, H., et al. (2020). Drivers of the composition of active rhizosphere bacterial communities in temperate grasslands. *ISME J.* 14, 463–475. doi: 10.1038/s41396-019-0543-4

Wang, B., Huang, S., Li, Z., Zhou, Z., Huang, J., Yu, H., et al. (2022). Factors driving the assembly of prokaryotic communities in bulk soil and rhizosphere of *Torreya grandis* along a 900-year age gradient. *Sci. Total Environ.* 837:155573. doi: 10.1016/j.scitotenv.2022.155573

Webb, C. O., Ackerly, D. D., and Kembel, S. W. (2008). Phylocom: software for the analysis of phylogenetic community structure and trait evolution. *Bioinformatics* 24, 2098–2100. doi: 10.1093/bioinformatics/btn358

Whitaker, R. J., Grogan, D. W., and Taylor, J. W. (2003). Geographic barriers isolate endemic populations of hyperthermophilic archaea. *Science* 301, 976–978. doi: 10.1126/science.1086909

Xu, N., Tan, G., Wang, H., and Gai, X. (2016). Effect of biochar additions to soil on nitrogen leaching, microbial biomass and bacterial community structure. *Eur. J. Soil Biol.* 74, 1–8. doi: 10.1016/j.ejsobi.2016.02.004

Xu, H., Wang, Z. J., Li, Y., He, J. L., and Wu, X. D. (2020). Dynamic growth models for *Caragana korshinskii* shrub biomass in China. *J. Environ. Manag.* 269:110675. doi: 10.1016/j.jenvman.2020.110675

Xu, J., Zhang, Y., Zhang, P. F., Trivedi, P., Riera, N., Wang, Y. Y., et al. (2018). The structure and function of the global citrus rhizosphere microbiome. *Nat. Comm.* 9:343. doi: 10.1038/s41467-018-07343-2

Yang, Z. (2007). PAML 4: phylogenetic analysis by maximum likelihood. *Mol. Biol. Evol.* 24, 1586–1591. doi: 10.1093/molbev/msm088

Yang, Y., Li, T., Wang, Y. Q., Cheng, H., Chang, S. X., Liang, C., et al. (2021b). Negative effects of multiple global change factors on soil microbial diversity. *Soil Biol. Biochem.* 156:108229. doi: 10.1016/j.soilbio.2021.108229

Yang, T., Shi, Y., Zhu, J., Zhao, C., Wang, J. M., Liu, Z. Y., et al. (2021a). The spatial variation of soil bacterial community assembly processes affects the accuracy of source tracking in ten major Chinese cities. *Science China-Life Sciences* 64, 1546–1559. doi: 10.1007/s11427-020-1843-6

Yang, T., Tedersoo, L., Liu, X., Gao, G. F., Dong, K., Adams, J. M., et al. (2022). Fungi stabilize multi-kingdom community in a high elevation timberline ecosystem. *iMeta*, 1:e49. doi: 10.1002/imt2.49

Yang, T., Tedersoo, L., Soltis, P. S., Soltis, D. E., Gilbert, J. A., Sun, M., et al. (2019). Phylogenetic imprint of woody plants on the soil mycobiome in natural mountain forests of eastern China. *ISME J.* 13, 686–697. doi: 10.1038/s41396-018-0303-x

Yang, F., Wu, J. J., Zhang, D. D., Chen, Q., Zhang, Q., and Cheng, X. L. (2018). Soil bacterial community composition and diversity in relation to edaphic properties and plant traits in grasslands of southern China. *Appl. Soil Ecol.* 128, 43–53. doi: 10.1016/j.apsoil.2018.04.001

Yeoh, Y. K., Dennis, P. G., Paungfoo-Lonhienne, C., Weber, L., Brackin, R., Ragan, M. A., et al. (2017). Evolutionary conservation of a core root microbiome across plant phyla along a tropical soil chronosequence. *Nat. Commun.* 8:215. doi: 10.1038/s41467-017-00262-8

Yuan, Y., Dai, X., Fu, X., Kou, L., Luo, Y., Jiang, L., et al. (2020). Differences in the rhizosphere effects among trees, shrubs and herbs in three subtropical plantations and their seasonal variations. *Eur. J. Soil Biol.* 100:103218. doi: 10.1016/j.ejsobi.2020.103218

Zaneveld, J. R., McMinds, R., and Vega Thurber, R. (2017). Stress and stability: applying the Anna Karenina principle to animal microbiomes. *Nat. Microbiol.* 2:17121. doi: 10.1038/nmicrobiol.2017.121

Zhang, D. X., Chen, X. Y., Fu, G. J., Yang, Z., Song, J., and Tong, X. G. (2022). Dissimilar evolution of soil dissolved organic matter chemical properties during revegetation with arbor and shrub in desertified land of the mu Us Desert. *Sci. Total Environ.* 815:152904. doi: 10.1016/j.scitotenv.2021.152904

Zhou, J., Kang, S., Schadt, C. W., and Garten, C. T. (2008). Spatial scaling of functional gene diversity across various microbial taxa. *Proc. Natl. Acad. Sci.* 105, 7768–7773. doi: 10.1073/pnas.0709016105

frontiers | Frontiers in Microbiology

TYPE Original Research
PUBLISHED 22 March 2023
DOI 10.3389/fmicb.2023.1106888

OPEN ACCESS

EDITED BY
Jiayu Zhou,
Jiangsu Province and Chinese Academy of Sciences, China

REVIEWED BY
Sara Fareed Mohamed Wahdan,
Suez Canal University,
Egypt
Teng Yang,
Institute of Soil Science (CAS),
China

*CORRESPONDENCE
Bao-Kai Cui
✉ cuibaokai@bjfu.edu.cn

SPECIALTY SECTION
This article was submitted to Microbe and Virus Interactions with Plants, a section of the journal Frontiers in Microbiology

RECEIVED 24 November 2022
ACCEPTED 06 March 2023
PUBLISHED 22 March 2023

CITATION
Zhao W, Wang D-D, Huang K-C, Liu S, Reyila M, Sun Y-F, Li J-N and Cui B-K (2023) Seasonal variation in the soil fungal community structure of *Larix gmelinii* forests in Northeast China. *Front. Microbiol.* 14:1106888. doi: 10.3389/fmicb.2023.1106888

Seasonal variation in the soil fungal community structure of *Larix gmelinii* forests in Northeast China

Wen Zhao, Dan-Dan Wang, Kai-Chuan Huang, Shun Liu, Mumin Reyila, Yi-Fei Sun, Jun-Ning Li and Bao-Kai Cui*

School of Ecology and Nature Conservation, Beijing Forestry University, Beijing, China

Soil fungi play an indispensable role in forest ecosystems by participating in energy flow, material circulation, and assisting plant growth and development. *Larix gmelinii* is the dominant tree species in the greater Khingan Mountains, which is the only cold temperate coniferous forest in China. Understanding the variations in underground fungi will help us master the situation of *L. gmelinii* above ground. We collected soil samples from three seasons and analyzed the differences in soil fungal community structure using high-throughput sequencing technology to study the seasonal changes in soil fungal community structure in *L. gmelinii* forests. We found that the Shannon and Chao1 diversity in autumn was significantly lower than in spring and summer. The community composition and functional guild varied significantly between seasons. Furthermore, we showed that ectomycorrhizal fungi dominated the functional guilds. The relative abundance of ectomycorrhizal fungi increased dramatically from summer to autumn and was significantly negatively correlated with temperature and precipitation. Temperature and precipitation positively affect the alpha diversity of fungi significantly. In addition, pH was negatively correlated with the Chao1 diversity. Temperature and precipitation significantly affected several dominant genera and functional guilds. Among the soil physicochemical properties, several dominant genera were affected by pH, and the remaining individual genera and functional guilds were significantly correlated with total nitrogen, available phosphorus, soil organic carbon, or cation exchange capacity. For the composition of total fungal community, temperature and precipitation, as well as soil physicochemical properties except AP, significantly drove the variation in community composition.

KEYWORDS

soil fungi, *Larix gmelinii*, community structure, temporal scale, soil properties

1. Introduction

Soil fungi are important components of soil microorganisms and play a critical role in the energy flow and material cycle of forest ecosystems (Falkowski et al., 2008; Cho et al., 2017). There are some important functional groups of the soil fungi: saprophytic fungi can produce enzymes to decompose organic matter (Voříšková and Baldrian, 2013) promoting the carbon (Rousk and Frey, 2015) and nitrogen cycles (Morrison et al., 2016); mycorrhizal fungi are symbiotic with plants and assist in plant growth and development (Eldridge et al., 2021); some pathogenic fungi can also cause fungal infection of the host and affect its productivity (Maron

et al., 2011). While soil fungi can affect plant community structure directly or indirectly, plant litter and root exudates are the major sources of fungal nutrition (Broeckling et al., 2008; Nakayama et al., 2019; Hannula et al., 2021).

The diversity and composition of soil fungal communities show great spatial and temporal variability (Voříšková et al., 2014; Zhou et al., 2016a; Averill et al., 2019). Litter decomposition and phytosynthate allocation represent important factors contributing to the seasonal variation of fungal communities, while environmental conditions are important factors contributing to the geographic variation of fungal communities. The soil fungal community is sensitive to changes in the surrounding environment, and its diversity and activity are regulated by some biotic and abiotic factors such as climate factors (Hawkes et al., 2011; Tedersoo et al., 2014), soil properties (Rousk et al., 2010) and vegetation (Kivlin and Hawkes, 2016; Li et al., 2020). Therefore, observing the changes in soil fungal communities can help us understand the soil health of the ecosystem (Shi et al., 2019).

Larix gmelinii is a deciduous tree of Pinaceae with rich timber accumulation and is one of the important timber trees in Northeast China (Sun et al., 2007), which is located in a sensitive area of global warming (Li et al., 2006). As an ectomycorrhizal-associated tree species (Guo, 2012), the ectomycorrhizal fungi of *L. gmelinii* included *Cortinarius*, *Hygrophorus*, *Lactarius*, and *Suillus* (Liu et al., 2014). To date, most of the studies on the soil fungal community in *L. gmelinii* forest have focused on different forest types (Yang et al., 2017), fires (Yang T. et al., 2020), and rhizospheres (Yang Y. et al., 2020), while ignoring the understanding of the fungal community in seasonal changes on a temporal scale.

In this study, we collected 45 soil samples of *L. gmelinii* in three seasons aimed to characterize the soil fungal community in the *L. gmelinii* forest, including taxonomic composition, functional guilds, community structure and to assess the roles of environmental drivers. We hypothesized that, (i) temperature and precipitation will have significant effects on soil fungal communities, which will directly affect the living conditions and activity of fungi, (ii) considering that soil physicochemical properties vary in different seasons in the same location, pH should have an more important role on community structure compared to soil nutrient conditions.

2. Materials and methods

2.1. Study site

The study area is located in Aershan National Forest Park (47°15′17′N, 120°17′34′E, Figure 1), which is located in Aershan city, Inner Mongolia Autonomous Region, China. Aershan National Forest Park is located in the continental climate region of the Mongolian Plateau and belongs to the cold temperate humid zone. The annual average temperature is −3.2°C, the average precipitation is 452.1 mm (Li et al., 2011). The winter is long and cold, the summer is short and rainy, and the spring and autumn are cool with less precipitation (Liu et al., 2020). The plant growth period is generally 100–120 days. The dominant tree species in the forest area are *L. gmelinii* and *Betula platyphylla*, with a forest coverage rate of 80%. The study area is located in the high latitude permafrost distribution area in China (Ding et al., 2019), and the zonal soil is retisols (IUSS Working Group WRB, 2015).

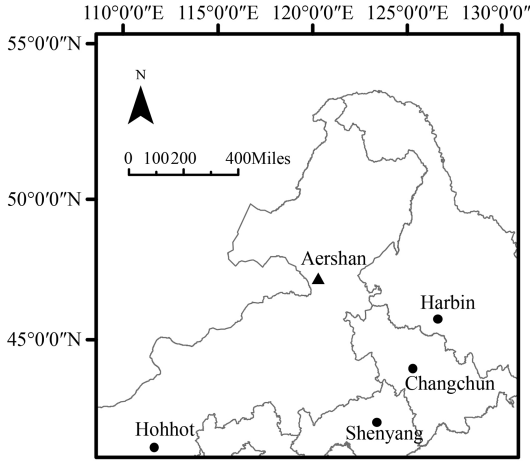

FIGURE 1
Sampling location in Aershan National Forest Park.

The *L. gmelinii* artificial forest lies at 1055 m elevation, and the slope of the study area is 12 degrees. The tree density of the forest is 2,500 stems per ha. The tree is nearly 14 m high with a stand age of 40 years. Diameter at breast height (DBH) of the selected trees ranged from 14 to 24 cm, and the average DBH of the trees is 18 cm. The main understory is various types of grass such as *Potentilla freyniana* and *Calamagrostis angustifolia*.

2.2. Soil sampling

In May, July, and October 2021, representing spring, summer and autumn respectively, soil samples were collected. Defined May to October as the growing season of *L. gmelinii*. We established three 20 m × 20 m plots at least 100 m apart, and took five soil samples from four vertices and the center as independent samples, for a total of 15 independent samples per season to represent the soil fungi in this stand. A total of 45 samples were taken for this experiment (5 independent samples × 3 plots× 3 seasons). Soil from 0–20 cm were obtained, passed through a 2 mm sieve and mixed, then filled three centrifuge tubes for DNA extraction and a ziplock bag for physicochemical property determination. The samples in centrifuge tubes were temporarily frozen in an incubator filled with dry ice and then transported to the laboratory stored at −80°C for subsequent DNA extraction, and the samples in ziplock bags were dried for determination of soil physicochemical properties. We extracted soil DNA from three separate centrifuge tubes and then mixed them into one to represent the sample.

2.3. Environmental variables

For the determination of soil properties, we referred to the method of Bao (2000). The soil in the sealed bag was dried naturally to determine its physicochemical properties: soil organic carbon (SOC) was determined by the potassium dichromate volumetric method, available phosphorus (AP) was determined by molybdenum antimony resistance colorimetry, pH was determined by the potential

method, total nitrogen (TN) was determined by Kjeldahl method, the cation exchange capacity (CEC) was determined by the ammonium acetate exchange method (Liang et al., 2015).

Climate data for each season were obtained from WorldClim[1] (accessed May 19, 2022), including monthly total precipitation (Prec), and monthly maximum and minimum temperature (Tmax and Tmin) from 2010 to 2018. Therefore, the climatic variables (Tmax, Tmin and Prec) are only three levels throughout the samples according to three seasons.

2.4. DNA extraction, amplification, and sequencing

A DNeasy Power Soil Pro Kit kit (Qiagen, Frankfurt, Germany) was used to extract the total genomic DNA of the soil samples. A NanoDrop NC2000 spectrophotometer (Thermo Fisher Scientific, Waltham, MA, United States) was used to quantify DNA; the quality of DNA was detected by 1.2% agarose gel electrophoresis. The ITS1 region of fungi was amplified, and the primers were ITS5F (5-GGAAGTAAAGTAAAAGTCGTAAAGG-3) and ITS2R (5-GCTGCGTTCTTCATCGATGC-3) (Bellemain et al., 2010), PCR system (20 μL): 2 μL (2.5 mM) dNTP. 1 μL (10 μM) forward primers and 1 μL (10 μM) reverse primers, 2 μL template DNA, 10 μL ddH2O, and 4 μL Fast pfu DNA polymerases. Circulating system: 95°C for 2 min; 30 cycles at 95°C for 30 s, 55°C for 30 s, and 72°C for 30 s; 72°C for 5 min. The PCR amplification was performed by Applied Biosystems 2,720 Thermal Cycler (Thermo Fisher Scientific, Waltham, MA, United States); the Quant-iT PicoGreen dsDNA assay was performed by a Microplate Reader FLx800 (BioTek, Burlington, Vermont, United States). PCR amplicons were purified and recovered by adding Vazyme VAHTSTM DNA Clean Beads (Vazyme, Nanjing, China) and quantified with the fluorescent reagent of Quant-iT PicoGreen dsDNA assay kit (Invitrogen, Carlsbad, CA, United States); then, amplicons were mixed in proportion to the sequencing amount, and pair-end 2 × 250 bp sequencing was performed using the Illlumina MiSeq platform with a NovaSeq 6000 SP reagent kit at Shanghai Personal Biotechnology Co., Ltd. (Shanghai, China). All raw sequencing data of this study are deposited into the NCBI database with the Short Read Archive (SRA) accession number PRJNA903950.

2.5. Sequence analysis

The early sequence processing of this experiment was based on QIIME 2–2021.2 (Bolyen et al., 2019). The Demux plug-in was used to split samples, the DADA2 plug-in was used to perform quality control, such as filtering and noise removal, position at which forward and reverse read sequences should be truncated due to decrease in quality were 222 and 232 respectively, the min and max sequence length were 230 and 438, forward and reverse reads with number of expected errors higher than 2 were be discarded. The Vsearch plug-in was used to cluster sequences into operational taxonomic units (OTUs) according to the 97% similarity principle, and the phylogeny plug-in was used to control and generate phylogenetic trees. Then, according to the fungus UNITE v.8.2 database (Nilsson et al., 2019), we used the feature classifier plug-in to annotate the species. The function guilds and trophic modes were obtained from the FUNGuild database (Nguyen et al., 2016). Finally, we used the rarefy command of the vegan package in R (R Core Team, 2022) to standardize the OTU table according to the minimum sequence number of samples, and made the rarefaction curve by rare curve command.

2.6. Statistical analysis

The data processing part was mainly completed with R 4.1.2 and SPSS 26.0 (SPSS Inc., Chicago, IL, United States), and the R part was mainly processed with the vegan package (Oksanen et al., 2020). In alpha diversity analysis, the Shannon diversity index, Chao1 richness index, and Pielou evenness index were selected for one-way analysis of variance (ANOVA) and *t*-test to compare species diversity in different seasons. To identify species and guilds enriched in seasons we employed linear statistics on relative abundance values using the R package edgeR. We grouped taxa and functions that were not identified or whose average relative abundance was less than 1% into "others," and defined dominant taxa as which relative abundance more than 1%. The beta diversity was tested by non-metric multidimensional scaling (NMDS) based on the OTU level, and the difference between the three fungal communities was tested by analysis of similarities (ANOSIM) of 999 permutations. Redundancy analysis (RDA) was used to explore the relationship between fungal community structure and soil physicochemical properties. The envfit function was used to test the significance of each physicochemical factor in RDA, and the Mantel test was conducted on community structure and soil physicochemical properties. Spearman correlation was used in Mantel test, and 999 random permutations were set to obtain the correlation R-value and the significance *p*. SPSS 26.0 was used to analyze the differences between groups of soil physicochemical properties using ANOVA, and the Spearman correlation coefficient was used to analyze the correlation between alpha diversity, dominant genera, functional guilds of fungal communities and soil physicochemical properties.

3. Results

3.1. Soil properties and climate factors

The soil total nitrogen (TN), available phosphorus (AP), and cation exchange capacity (CEC) were not significantly different among the three seasons (Table 1). Soil organic carbon (SOC) showed a significant upwards trend with seasons from spring to winter ($p < 0.05$). pH decreased in summer and increased in autumn ($p < 0.001$). Temperature and precipitation gradient showed a strong rise in summer and then decline in autumn, and the temperature and precipitation in autumn were much lower than those in spring.

3.2. Diversity of the soil fungal community

A total of 2,963,468 quality-filtered sequences were retrieved from the 45 samples. After rarefying 39,850 sequences per

1 https://www.worldclim.org/data/monthlywth.html#

TABLE 1 Soil properties and climate factors compared by ANOVA (mean values ± S.E.s).

Factor	Season	Spr.	Sum.	Aut.	*F*-value	*p*
Soil property	TN/(g/kg)	5.638 ± 0.135a	5.786 ± 0.124a	5.769 ± 0.165a	0.323	0.726
	SOC/(g/kg)	67.697 ± 1.562b	72.211 ± 1.177ab	75.560 ± 2.482a	4.678	0.015
	AP/(mg/kg)	9.206 ± 0.500a	10.591 ± 0.871a	10.045 ± 0.827a	0.863	0.429
	pH	5.612 ± 0.026b	5.022 ± 0.052c	5.815 ± 0.049a	88.849	0.000
	CEC/(cmol(+)/kg)	47.471 ± 0.435a	46.715 ± 0.385a	46.002 ± 0.572a	2.435	0.100
Climate factor	Tmax (°C)	15.730 ± 0.590b	23.130 ± 0.419a	6.415 ± 0.676c	214.579	<0.001
	Tmin (°C)	1.059 ± 0.430b	10.831 ± 0.215a	−7.928 ± 0.412c	659.990	<0.001
	Prec (mm)	47.204 ± 7.136b	140.721.646a	17.280 ± 2.607b	23.627	<0.001

SOC, soil organic carbon; AP, available phosphorus; pH, pH value; CEC, cation exchange capacity; Tmax, the monthly minimum temperature; Tmin, the monthly minimum temperature; Prec: mean monthly precipitation. Different letters indicate significant differences among different season tested by one-way ANOVA ($p < 0.05$). Soil property data were obtained from 15 replicates, and climate data were obtained from 9 years (2010–2018).

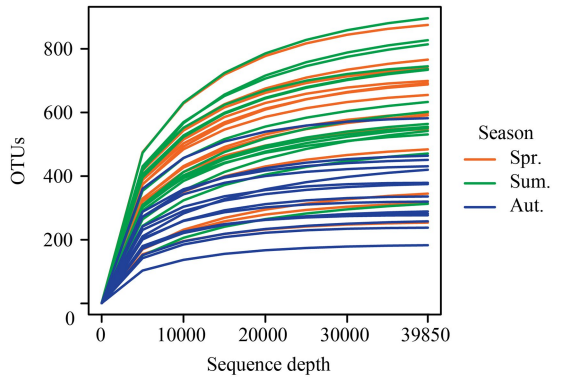

FIGURE 2
The rarefaction curves of the sequence depth and the number of OTUs from 45 samples.

sample, a total of 1,793,250 unique sequences were clustered into 5,681 operational taxonomic units (OTUs) at 97% identity. Rarefaction curves (Figure 2) of the number of OTUs with increasing sequence depth of samples, indicating that the rarefied sequence depth in our study capture most fungi members from each season.

The Shannon diversity index, Chao1 richness index, and Pielou evenness index, which represent fungal diversity (Figure 3), showed no significant difference between spring and summer, but the Shannon and Chao1 diversity in autumn was significantly lower than in spring and summer.

3.3. Community composition of the fungi

The OTUs belong to 13 phyla, 46 classes, 107 orders, 248 families, 559 genera, and 773 species after classified. There were four dominant phyla with relative abundances more than 1%: Basidiomycota was the most abundant phylum (Figure 4A), followed by Ascomycota, then Mortierellomycota and Mucoromycota. The Mortierellomycota and Mucoromycota were enriched in summer and Basidiomycota was enriched in autumn.

The dominant genera (Figure 4B) which relative abundances more than 1% of fungi were *Inocybe*, *Tomentella*, *Mortierella*, *Piloderma*, *Sebacina*, *Pseudogymnoascus*, *Trichophaea*, *Oidiodendron*, *Lactarius*, *Russula*, *Clavulina*, and *Umbelopsis*. We found that the relative abundance of *Inocybe* increased significantly in autumn, *Pilodermas* decreased significantly with seasonal changes, and the relative abundance of *Mortierella* was higher in summer. In addition, the relative abundance of *Lactarius* and *Russula* increased significantly in autumn. Mortierella and Umbelopsis were significantly enriched in summer. Moreover, Russula and Lactarius were significantly enriched in autumn.

We annotated the taxa and found that the relative abundance of ectomycorrhizal fungi (Figure 4C) was the highest among the annotated functions, followed by plant saprotroph, endophyte, undefined saprotroph, animal pathogen, dung saprotroph, plan pathogen and ericoid mycorrhizal fungi. In addition, the relative abundance of ectomycorrhizal fungi increased dramatically from summer to autumn, up to 66%. The endophyte was significantly enriched in summer. For the trophic mode (Figure 4D), the relative abundance of symbiotroph was significantly high in autumn and the relative abundance of saprotroph was highest in summer. The relative abundance of pathogenic fungi decreased with the growing season and enriched in spring.

The soil fungal community structure in different season was analyzed using nonmetric multidimensional scaling (NMDS) based on the Bray-Curtis distance. We showed that the results of NMDS analysis had some explanatory significance (stress = 0.18). There was some overlap among the three seasons (Figure 5), and there were also unique parts of each, showing the similarities and differences in the community structure of the three seasons. Analysis of similarities (ANOSIM) agreed with the NMDS in that seasonal variation caused differences in fungal community structure ($R = 0.140$, $p = 0.001$).

3.4. Environmental drivers of fungal diversity

The Shannon diversity, Chao1 richness and Pielou evenness indices of fungi significantly positively correlated with Tmax, Tmin, and Prec ($p < 0.05$, Table 2). pH was significantly negatively correlated with the Chao1 index of fungal richness ($p < 0.001$). Compared with soil physicochemical properties, climate factors had a stronger impact on fungal diversity.

10.3389/fmicb.2023.1106888

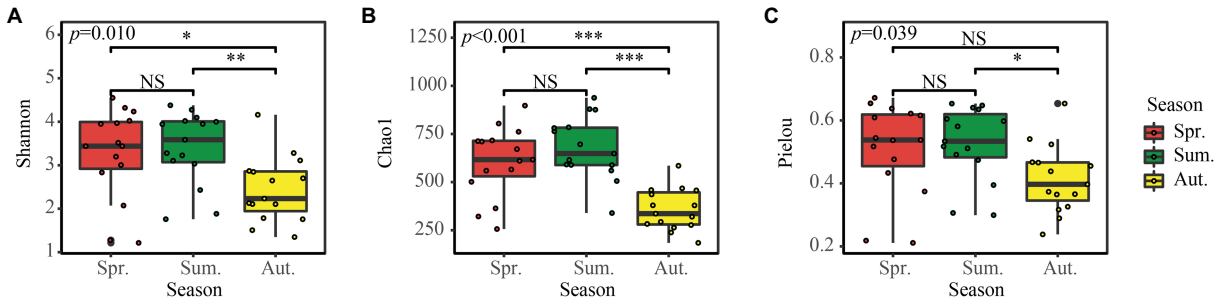

FIGURE 3
(A–C) Alpha diversity of the soil fungal community in the three seasons. NS, Not Significant; *p<0.05; **p<0.01; ***p<0.001.

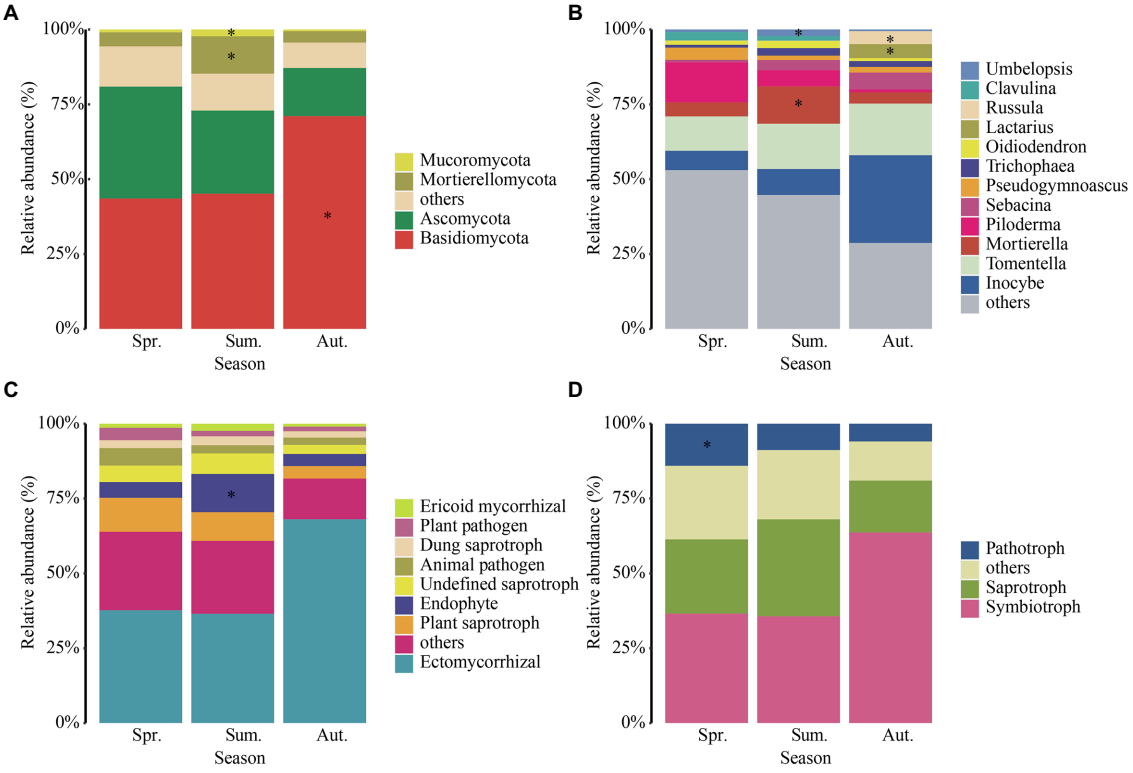

FIGURE 4
Relative abundances of dominant fungal phyla **(A)**, genera **(B)**, functional guilds **(C)**, and trophic modes **(D)** in each season. The phyla, genera, functional guilds, and trophic modes with less than 0.01of the average relative abundance are grouped into "others." Asterisks indicate significant enrichment (FDR, p<0.05).

3.5. Environmental drivers of dominant fungal genera and guilds

We conducted Spearman correlation analysis on the dominant genera of fungi and environmental factors (Table 3). We found that *Inocybe* was significantly positively correlated with pH ($p < 0.001$) and negatively correlated with climate factors ($p < 0.01$). In contrast, *Mortierella*, *Piloderma* and *Umbelopsis* were significantly negatively correlated with pH ($p < 0.01$) and positively correlated with climate factors ($p < 0.05$). *Pseudogymnoascus* was negatively correlated with AP ($p < 0.05$). *Oidiodendron* was significantly negatively correlated with SOC ($p < 0.05$). *Russula* ($p < 0.01$) was significantly negatively correlated with CEC. *Clavulina* was influenced by many factors including SOC, pH, CEC and climate factors ($p < 0.05$).

In terms of functional guilds (Table 3), ectomycorrhizal fungi were significantly negatively correlated with climate factors ($p < 0.001$), while endophyte and undefined saprotroph were significantly positively correlated with climate factors ($p < 0.001$). In addition, pH was negatively correlated with the relative abundance of endophyte and undefined saprotroph ($p < 0.01$). Moreover, plant pathogen was significantly negatively correlated with SOC ($p < 0.05$) and ericoid mycorrhizal fungi was significantly negatively correlated with TN ($p < 0.05$).

TABLE 2 Spearman correlation coefficient of alpha diversity to soil properties.

Alpha diversity	TN	SOC	AP	pH	CEC	Tmax	Tmin	Prec
Shannon	0.085	−0.142	−0.176	−0.278	0.114	0.404**	0.404**	0.404**
Chao1	0.185	−0.057	−0.036	−0.532***	0.219	0.652***	0.652***	0.652***
Pielou	0.052	−0.166	−0.205	−0.217	0.081	0.348*	0.348*	0.348**

SOC, soil organic carbon; AP, available phosphorus; pH, pH value; CEC, cation exchange capacity; Tmax, the monthly minimum temperature; Tmin, the monthly minimum temperature; Prec, mean monthly precipitation. *$p < 0.05$; **$p < 0.01$; ***$p < 0.001$.

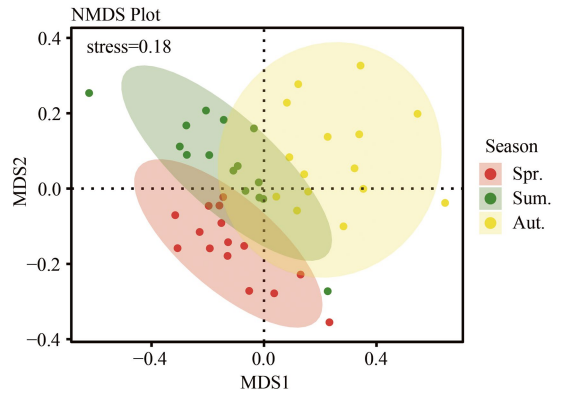

FIGURE 5
Fungal community structure based on Bray-Curtis distance, as determined by nonmetric multidimensional scaling (NMDS).

3.6. Environmental drivers of fungal community structure

To evaluate the relationship of fungal community structure with environmental variables at spatial scales, redundancy analysis (RDA) of the fungal community and the Mantel test were implemented.

The RDA result showed that the first two axes explained 9.09% of the total variation in fungi (Figure 6). Climate factors had significant effects on community structure, while only SOC and pH in soil physicochemical properties had significant effects on community structure between seasons.

Based on the Mantel test (Table 4, $p < 0.05$), the climate factor was remarkably correlated with the fungal community structure. The main factors that affected the fungal community of the soil were TN, SOC, and CEC.

In summary, whether a factor was considered separately or all environmental variables were considered, temperature and precipitation were extremely significant factors affecting the community structure, and except for AP, soil physicochemical properties had more or less influence on the community structure.

4. Discussion

4.1. Seasonal variation in soil properties and climatic factors

Temperature and precipitation are the most significant changes brought about by seasons. According to the existing research, the cold temperate zone where the Aershan National Forest Park is located in long and cold in winter (Li et al., 2011). The growing season of plants is short, and seasonal changes have a profound impact on the growth cycle of plants, which also mobilize the structural changes of fungi in the underground soil (Zhang and Fu, 2021). In this study, the temperature and precipitation increased first and then decreased, and the temperature and precipitation in autumn were much lower than those in spring, even though the lowest temperature was below zero.

In the soil physicochemical properties, TN and AP have identical change trends as the climate, while pH first decreases and then increases. SOC showed a continuous increase with the season, while CEC continued to decline with the season. Worldwide, the storage of SOC usually increases with the decrease in annual average temperature, and the carbon element in cold regions is more enriched (Stockmann et al., 2013), which is consistent with the highest content of SOC in winter in this study. Soil CEC could affect the growth and development of plants by significantly changing leaf Ca and Mg absorption, chlorophyll content, and catalase activity (Cui et al., 2021). In winter, the demand of plants for CEC decreases, which cannot drive the accumulation of CEC in the soil and may cause the loss of CEC in the soil.

4.2. The response of fungal communities to seasonal variation

Recent studies have shown that there are many factors that affect the diversity of soil fungi. Xie and Yin (2022) showed that soil fungal diversity and richness in broad-leaved forests were higher than those in conifer forests. Fungal community diversity and composition are significantly driven by soil pH, available nitrogen, available phosphorus, moisture, organic carbon, fine root biomass and root tissue density (Beauregard et al., 2010; Zhou et al., 2016b; Tauro et al., 2021). Soil pH is the dominant driver that is significantly related to fungal alpha diversity (Wang et al., 2015; Adamo et al., 2021). Seasonal climate change directly affects the diversity of soil fungi, and indirectly affects it by affecting soil properties and root variables (Xie and Yin, 2022). In neutral pH soil, soil quality decreased along the altitudinal gradient, indicating that microbial diversity was likely constrained by climatic conditions (Bayranvand et al., 2021). Climatic factors, followed by edaphic and spatial patterning, are the best predictors of soil community composition at the global scale (Tedersoo et al., 2014). In our study, the diversity of the fungal community changed with the seasons. The diversity of fungi in summer was significantly higher than that in spring and winter, which was consistent with the seasonal change in the diversity of fungi in subtropical orchard soil (Koide et al., 2005). Climate factors and soil pH significantly affect the diversity of soil fungi in *L. gmelinii* forests.

According to Lauber et al. (2008) the composition of the fungal community is most closely related to the change in soil nutrients. There was a significant correlation between the variety in fungal community composition and the availability of soil carbon and

TABLE 3 Spearman correlation coefficients of dominant fungal genera and functional guilds to soil properties.

Factor	Variable	TN	SOC	AP	pH	CEC	Tmax	Tmin	Prec
Genus	*Inocybe*	−0.106	0.060	−0.187	0.464***	−0.197	−0.436**	−0.436**	−0.436**
	Tomentella	0.050	0.112	0.045	−0.041	−0.224	−0.040	−0.04	−0.04
	Mortierella	0.132	−0.002	−0.126	−0.492***	0.048	0.597***	0.597***	0.597***
	Piloderma	−0.023	−0.145	−0.012	−0.389**	0.027	0.361*	0.361*	0.361*
	Sebacina	0.050	0.037	−0.027	−0.215	0.280	0.151	0.151	0.151
	Pseudogymnoascus	0.093	−0.125	−0.297*	0.200	0.131	−0.101	−0.101	−0.101
	Trichophaea	0.077	0.093	0.041	0.069	−0.258	0.016	0.016	0.016
	Oidiodendron	−0.220	−0.335*	0.032	−0.061	0.075	0.285	0.285	0.285
	Lactarius	−0.030	0.012	−0.167	0.172	0.060	−0.251	−0.251	−0.251
	Russula	−0.085	0.058	−0.04	0.134	−0.422**	−0.191	−0.191	−0.191
	Clavulina	−0.211	−0.317*	0.077	−0.390**	0.395**	0.393**	0.393**	0.393**
	Umbelopsis	−0.138	−0.245	0.033	−0.498***	0.098	0.634***	0.634***	0.634***
Guild	Ectomycorrhizal	0.033	0.218	0.116	0.257	−0.097	−0.474***	−0.474***	−0.474***
	Plant saprotroph	−0.115	−0.142	0.037	−0.009	0.289	0.089	0.089	0.089
	Endophyte	0.124	−0.026	−0.143	−0.471***	0.045	0.591***	0.591***	0.591***
	Undefined saprotroph	−0.009	−0.189	−0.135	−0.383**	0.225	0.497***	0.497***	0.497***
	Animal pathogen	0.138	−0.117	−0.229	0.111	0.193	0.006	0.006	0.006
	Dung saprotroph	0.127	−0.017	−0.091	0.021	−0.142	0.094	0.094	0.094
	Plant pathogen	−0.077	−0.315*	−0.145	−0.037	0.198	0.107	0.107	0.107
	Ericoid mycorrhizal	−0.22*	−0.335	0.032	−0.061	0.075	0.285	0.285	0.285

SOC, soil organic carbon; AP, available phosphorus; pH, pH value; CEC, cation exchange capacity; Tmax, the monthly minimum temperature; Tmin, the monthly minimum temperature; Prec, mean monthly precipitation. *$p < 0.05$; **$p < 0.01$; ***$p < 0.001$.

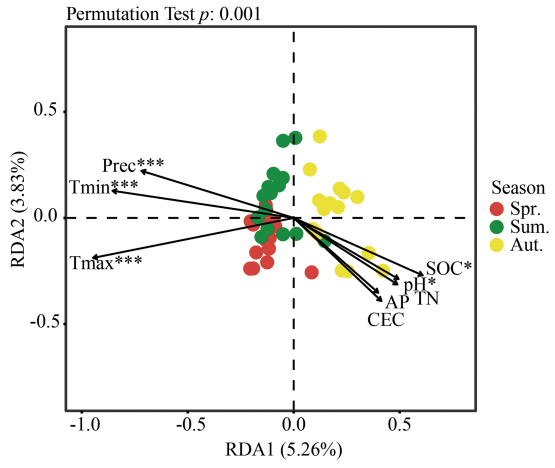

FIGURE 6
Redundancy analysis (RDA) of fungal communities at the OTU level and environmental variables. The envfit function was used to test the significance of each physicochemical factor in RDA. *$p<0.05$; ***$p<0.001$.

nitrogen (Zhang et al., 2016; Sanka Loganathachetti et al., 2017). We analyzed the correlation between dominant fungal genera and soil properties and climate factors, and the results showed that *Inocybe* and *Mortierella* among the top five dominant genera of relative abundance had a very close relationship with climate factors and pH, while *Sebacina* was significantly positively correlated with TN, SOC and CEC in soil physicochemical properties. However, in our previous study on the soil microbial community of *L. gmelinii*, the influence of soil physicochemical properties on the composition of the fungal community was not significant (Zhao et al., 2022). We thought that the difference in soil physicochemical properties in the same season was not enough to cause the difference in soil fungal diversity.

The dominant soil fungal communities could adapt and respond to climate change by altering the proportion of different dominant fungal groups by responding to moisture patterns (Huang et al., 2021). Tedersoo et al. (2014) found that climatic factors, followed by edaphic and spatial patterning, were the best predictors of soil community composition at the global scale. Variations in soil fungal community composition across seasons were attributed to their functional adaptation. Previously, soil fungi in northern coniferous forests were dominated by saprophytic fungi at the end of winter and were gradually replaced by ectomycorrhizal fungi in the growing season (Santalahti et al., 2016). The relative abundance of ectomycorrhizal fungi showed absolute dominance in all 3 months, and increased when the temperature decreased. Zeng et al. (2022) presented that ectomycorrhizal taxa dominate functional guild in subtropical evergreen broad-leaved forests. Ectomycorrhizal fungi are affected by multiple factors, and temperature and precipitation had a significant effect on them in our study. In the study of Yang T. et al. (2020), the observed decline in ectomycorrhizal fungal richness may be related to the fire-induced mortality of ectomycorrhizal plant hosts. Accordingly, we suppose that the seasonal dynamics of plants also influence the changes in the relative abundance of ectomycorrhizal fungi, except for climatic factors in this study.

TABLE 4 Correlations between fungal community structure and environmental variables assessed by Mantel tests.

Variable	TN	SOC	pH	CEC	AP	Tmax	Tmin	Prec	Total
R	0.164	0.178	−0.043	0.122	−0.076	0.184	0.101	0.101	0.176
p	0.023	0.019	0.748	0.029	0.815	0.001	0.023	0.026	0.007

SOC, soil organic carbon; AP, available phosphorus; pH, pH value; CEC, cation exchange capacity; Tmax, the monthly minimum temperature; Tmin, the monthly minimum temperature; Prec, mean monthly precipitation.

Microbial community structures were strongly affected by seasonal variations. In the study of microbial community structure at different elevations, bacterial and fungal community structures exhibited a pronounced annual cycle (Lazzaro et al., 2015; Turatsinze et al., 2021). Fungal communities differed among seasons, equivalent to the community turnover observed over thousands of kilometers in space. Climate covariates explained some spatial–temporal effects (Averill et al., 2019). According to the results of the RDA and Mantel test in this study, inter-seasonal climate factors play a core role in fungal community structure. In addition, Adamo et al. (2021) showed that soil parameters were the most important driving forces shaping soil fungal communities at the regional scale in the Mediterranean pine forests. The species richness and diversity of ectomycorrhizal fungi declined following long-term nitrogen addition in a temperate forest, while ascomycetes and saprotrophs responded positively to N enrichment (Morrison et al., 2016). SOC may affect the structure of the soil fungal community (Sul et al., 2013; Li et al., 2017), because the abundance of cellulose-degrading fungi may be linked to SOC fractions and may respond to changes in SOC fractions differently. Soil available phosphorus and nitrogen are influential factors shaping fungal communities (Tauro et al., 2021). In a previous study, the fungal community was less strongly affected by pH, because fungi generally exhibit wide pH ranges for optimal growth (Rousk et al., 2010; Wang et al., 2015). In this study, combined with RDA and Mantel test, TN, SOC, pH, CEC in soil properties and climate factors influence the structure of the soil fungal community, among which climate factors have a pivotal role.

5. Conclusion

In this study, we demonstrated that season had a strong effect on fungal community structures. This is mainly due to the impact of seasonal climate change on soil fungi. Soil properties will also cause changes in the diversity and composition of fungal communities. However, we believe that climate factors have a more significant influence on the structure of soil fungal communities than soil properties. In addition, we found that ectomycorrhizal fungi dominated the functional guilds in the *L. gmelinii* forest.

Data availability statement

The datasets presented in this study can be found in online repositories. The names of the repository/repositories and accession number(s) can be found in the article/Supplementary material.

Author contributions

B-KC designed the research. B-KC, WZ, D-DW, K-CH, SL, and MR prepared the samples. WZ conducted the molecular experiments and analyzed the data. WZ, Y-FS, J-NL, and B-KC drafted the manuscript. All authors have read and agreed to the published version of the manuscript.

Funding

The research is supported by the National Natural Science Foundation of China (nos. 32270010, U2003211, and 31870008) and Beijing Forestry University Outstanding Young Talent Cultivation Project (no. 2019JQ03016).

Acknowledgments

We would like to thank Kun Qian (Beijing Forestry University, China) for his generous help with the field sampling.

Conflict of interest

The authors declare that the research was conducted in the absence of any commercial or financial relationships that could be construed as a potential conflict of interest.

Publisher's note

Supplementary material

The Supplementary material for this article can be found online at: https://www.frontiersin.org/articles/10.3389/fmicb.2023.1106888/full#supplementary-material

References

Adamo, I., Castano, C., Bonet, J. A., Colinas, C., de Aragon, J. M., and Alday, J. G. (2021). Soil physico-chemical properties have a greater effect on soil fungi than host species in Mediterranean pure and mixed pine forests. *Soil Biol. Biochem.* 160:108320. doi: 10.1016/j.soilbio.2021.108320

Averill, C., Cates, L. L., Dietze, M. C., and Bhatnagar, J. M. (2019). Spatial vs. temporal controls over soil fungal community similarity at continental and global scales. *ISME J.* 13, 2082–2093. doi: 10.1038/s41396-019-0420-1

Bao, S. D. (2000) *Agriculture Chemical Analysis of Soil*. Beijing: China Agriculture Press.

Bayranvand, M., Akbarinia, M., Salehi Jouzani, G., Gharechahi, J., Kooch, Y., and Baldrian, P. (2021). Composition of soil bacterial and fungal communities in relation to vegetation composition and soil characteristics along an altitudinal gradient. *FEMS Microbiol. Ecol.* 97:fiaa201. doi: 10.1093/femsec/fiaa201

Beauregard, M. S., Hamel, C., and St-Arnaud, M. (2010). Long-term phosphorus fertilization impacts soil fungal and bacterial diversity but not AM fungal community in alfalfa. *Microb. Ecol.* 59, 379–389. doi: 10.1007/s00248-009-9583-z

Bellemain, E., Carlsen, T., Brochmann, C., Coissac, E., Taberlet, P., and Kauserud, H. (2010). ITS as an environmental DNA barcode for fungi: an in silico approach reveals potential PCR biases. *BMC Microbiol.* 10:189. doi: 10.1186/1471-2180-10-189

Bolyen, E., Rideout, J. R., Dillon, M. R., Bokulich, N. A., Abnet, C. C., al-Ghalith, G. A., et al. (2019). Reproducible, interactive, scalable and extensible microbiome data science using QIIME 2. *Nat. Biotechnol.* 37, 852–857. doi: 10.1038/s41587-019-0209-9

Broeckling, C. D., Broz, A. K., Bergelson, J., Manter, D. K., and Vivanco, J. M. (2008). Root exudates regulate soil fungal community composition and diversity. *Appl. Environ. Microbiol.* 74, 738–744. doi: 10.1128/AEM.02188-07

Cho, H., Kim, M., Tripathi, B., and Adams, J. (2017). Changes in soil fungal community structure with increasing disturbance frequency. *Microb. Ecol.* 74, 62–77. doi: 10.1007/s00248-016-0919-1

Cui, X., Mao, P., Sun, S., Huang, R., Fan, Y., Li, Y., et al. (2021). Phytoremediation of cadmium contaminated soils by *Amaranthus Hypochondriacus* L.: the effects of soil properties highlighting cation exchange capacity. *Chemosphere* 283:131067. doi: 10.1016/j.chemosphere.2021.131067

Ding, L. Z., Man, X. L., and Xiao, R. H. (2019). Characteristics of nitrogen content in rhizosphere soil of main tree species in northern part of Daxinganling during growing seasons. *J. Cent. South Univ. For. Technol.* 39:8. doi: 10.14067/j.cnki.1673-923x.2019.02.011

Eldridge, D. J., Travers, S. K., Val, J., Ding, J., Wang, J. T., Singh, B. K., et al. (2021). Experimental evidence of strong relationships between soil microbial communities and plant germination. *J. Ecol.* 109, 2488–2498. doi: 10.1111/1365-2745.13660

Falkowski, P. G., Fenchel, T., and Delong, E. F. (2008). The microbial engines that drive Earth's biogeochemical cycles. *Science* 320, 1034–1039. doi: 10.1126/science.1153213

Guo, L. D. (2012). Progress of microbial species diversity research in China. *Biodivers. Sci.* 20, 572–580. doi: 10.3724/SP.J.1003.2012.10129

Hannula, S. E., Heinen, R., Huberty, M., Steinauer, K., De Long, J. R., Jongen, R., et al. (2021). Persistence of plant-mediated microbial soil legacy effects in soil and inside roots. *Nat. Commun.* 12, 5686–5613. doi: 10.1038/s41467-021-25971-z

Hawkes, C. V., Kivlin, S. N., Rocca, J. D., Huguet, V., Thomsen, M. A., and Suttle, K. B. (2011). Fungal community responses to precipitation. *Glob. Chang. Biol.* 17, 1637–1645. doi: 10.1111/j.1365-2486.2010.02327.x

Huang, Q., Jiao, F., Huang, Y., Li, N., Wang, B., Gao, H., et al. (2021). Response of soil fungal community composition and functions on the alteration of precipitation in the grassland of loess plateau. *Sci. Total Environ.* 751:142273. doi: 10.1016/j.scitotenv.2020.142273

IUSS Working Group WRB (2015). "World Reference Base for soil resources 2014, update 2015 international soil classification system for naming soils and creating legends for soil maps" in *World Soil Resources Reports No. 106* (Rome: FAO), 106.

Jiang, H. Y., Yan, W., Li, X. T., and Fan, Y. J. (2010). Diversity and community structure of soil fungi in *Larix gmelinii* forest. *J. Northwest For. Univ.* 25, 100–103.

Kivlin, S. N., and Hawkes, C. V. (2016). Tree species, spatial heterogeneity, and seasonality drive soil fungal abundance, richness, and composition in Neotropical rainforests. *Environ. Microbiol.* 18, 4662–4673. doi: 10.1111/1462-2920.13342

Koide, R. T., Xu, B., Sharda, J., Lekberg, Y., and Ostiguy, N. (2005). Evidence of species interactions within an ectomycorrhizal fungal community. *New Phytol.* 165, 305–316. doi: 10.1111/j.1469-8137.2004.01216.x

Lauber, C. L., Strickland, M. S., Bradford, M. A., and Fierer, N. (2008). The influence of soil properties on the structure of bacterial and fungal communities across land-use types. *Soil Biol. Biochem.* 40, 2407–2415. doi: 10.1016/j.soilbio.2008.05.021

Lazzaro, A., Hilfiker, D., and Zeyer, J. (2015). Structures of microbial communities in alpine soils: seasonal and elevational effects. *Front. Microbiol.* 6:1330. doi: 10.3389/fmicb.2015.01330

Li, S., Huang, X., Shen, J., Xu, F., and Su, J. (2020). Effects of plant diversity and soil properties on soil fungal community structure with secondary succession in the *Pinus yunnanensis* forest. *Geoderma* 379:114646. doi: 10.1016/j.geoderma.2020.114646

Li, Y., Li, Y., Chang, S. X., Liang, X., Qin, H., Chen, J., et al. (2017). Linking soil fungal community structure and function to soil organic carbon chemical composition in intensively managed subtropical bamboo forests. *Soil Biol. Biochem.* 107, 19–31. doi: 10.1016/j.soilbio.2016.12.024

Li, J., Luo, Y. Q., Shi, J., Ma, L. Y., and Chen, C. (2011). Niche of Main understory populations of *Larix gmelinii* Rupr Forest in A'ershan area. *Forest Res.* 24, 651–658. doi: 10.13275/j.cnki.lykxyj.2011.05.013

Li, F., Zhou, G. S., and Cao, M. C. (2006). Responses of *Larix gmelinii* geographical distribution to future climate change: a simulation study. *Chin. J. Appl. Ecol.* 17, 2255–2260.

Liang, Y., Jiang, Y., Wang, F., Wen, C., Deng, Y., Xue, K., et al. (2015). Long-term soil transplant simulating climate change with latitude significantly alters microbial temporal turnover. *ISME J.* 9, 2561–2572. doi: 10.1038/ismej.2015.78

Liu, W. H., Li, Y. N., and Zhang, S. H. (2014). Isolation of ectomycorrhizal fruiting bodies of *Larix gmelinii* and screening of culture medium Inner Mongolia. *For. Invest. Des.* 37, 96–97. doi: 10.13387/j.cnki.nmld.2014.05.044

Liu, Y., Trancoso, R., Ma, Q., Yue, C., Wei, X., and Blanco, J. A. (2020). Incorporating climate effects in *Larix gmelinii* improves stem taper models in the greater Khingan Mountains of Inner Mongolia, Northeast China. *For. Ecol. Manag.* 464:118065. doi: 10.1016/j.foreco.2020.118065

Maron, J. L., Marler, M., Klironomos, J. N., and Cleveland, C. C. (2011). Soil fungal pathogens and the relationship between plant diversity and productivity. *Ecol. Lett.* 14, 36–41. doi: 10.1111/j.1461-0248.2010.01547.x

Morrison, E. W., Frey, S. D., Sadowsky, J. J., van Diepen, L. T., Thomas, W. K., and Pringle, A. (2016). Chronic nitrogen additions fundamentally restructure the soil fungal community in a temperate forest. *Fungal Ecol.* 23, 48–57. doi: 10.1016/j.funeco.2016.05.011

Nakayama, M., Imamura, S., Taniguchi, T., and Tateno, R. (2019). Does conversion from natural forest to plantation affect fungal and bacterial biodiversity, community structure, and co-occurrence networks in the organic horizon and mineral soil? *For. Ecol. Manag.* 446, 238–250. doi: 10.1016/j.foreco.2019.05.042

Nguyen, N. H., Song, Z., Bates, S. T., Branco, S., Tedersoo, L., Menke, J., et al. (2016). FUNGuild: an open annotation tool for parsing fungal community datasets by ecological guild. *Fungal Ecol.* 20, 241–248. doi: 10.1016/j.funeco.2015.06.006

Nilsson, R. H., Larsson, K. H., Taylor, A. F. S., Bengtsson-Palme, J., Jeppesen, T. S., Schigel, D., et al. (2019). The UNITE database for molecular identification of fungi: handling dark taxa and parallel taxonomic classifications. *Nucleic Acids Res.* 47, D259–D264. doi: 10.1093/nar/gky1022

Oksanen, J., Blanchet, F. G., Friendly, M., Kindt, R., Legendre, P., McGlinn, D., et al. (2020) Vegan: community ecology package. R package version 2.5-7. Available at: https://CRAN.R-project.org/package=vegan (Accessed February 10, 2023).

Põlme, S., Abarenkov, K., Henrik Nilsson, R., Lindahl, B. D., Clemmensen, K. E., Kauserud, H., et al. (2020). FungalTraits: a user-friendly traits database of fungi and fungus-like stramenopiles. *Fungal Divers.* 105, 1–16. doi: 10.1007/s13225-020-00466-2

Rousk, J., Bååth, E., Brookes, P. C., Lauber, C. L., Lozupone, C., Caporaso, J. G., et al. (2010). Soil bacterial and fungal communities across a pH gradient in an arable soil. *ISME J.* 4, 1340–1351. doi: 10.1038/ismej.2010.58

Rousk, J., and Frey, S. D. (2015). Revisiting the hypothesis that fungal-to-bacterial dominance characterizes turnover of soil organic matter and nutrients. *Ecol. Monogr.* 85, 457–472. doi: 10.1890/14-1796.1

Sanka Loganathachetti, D., Poosakkannu, A., and Muthuraman, S. (2017). Fungal community assemblage of different soil compartments in mangrove ecosystem. *Sci. Rep.* 7, 8560–8569. doi: 10.1038/s41598-017-09281-3

Santalahti, M., Sun, H., Jumpponen, A., Pennanen, T., and Heinonsalo, J. (2016). Vertical and seasonal dynamics of fungal communities in boreal scots pine forest soil. *FEMS Microbiol. Ecol.* 92:fw170. doi: 10.1093/femsec/fiw170

Shi, L., Dossa, G. G., Paudel, E., Zang, H., Xu, J., and Harrison, R. D. (2019). Changes in fungal communities across a forest disturbance gradient. *Appl. Environ. Microbiol.* 85, e00080–e00019. doi: 10.1128/AEM.00080-19

Stockmann, U., Adams, M. A., Crawford, J. W., Field, D. J., Henakaarchchi, N., Jenkins, M., et al. (2013). The knowns, known unknowns and unknowns of sequestration of soil organic carbon. *Agric. Ecosyst. Environ.* 164, 80–99. doi: 10.1016/j.agee.2012.10.001

Šťursová, M., Šnajdr, J., Cajthaml, T., Bárta, J., Šantrůčková, H., and Baldrian, P. (2014). When the forest dies: the response of forest soil fungi to a bark beetle-induced tree dieback. *Int. Soc. Microbial Ecol. J.* 8, 1920–1931. doi: 10.1038/ismej.2014.37

Sul, W. J., Asuming-Brempong, S., Wang, Q., Tourlousse, D. M., Penton, C. R., Deng, Y., et al. (2013). Tropical agricultural land management influences on soil microbial communities through its effect on soil organic carbon. *Soil Biol. Biochem.* 65, 33–38. doi: 10.1016/j.soilbio.2013.05.007

Sun, Y. J., Zhang, J., Han, A. H., Wang, X. J., and Wang, X. J. (2007). Biomass and carbon pool of *Larix gmelinii* young and middle age forest in Xing'an mountains Inner Mongolia. *Acta Ecol. Sin.* 27, 1756–1762. doi: 10.3321/j.issn:1000-0933.2007.05.011

Tauro, T. P., Mtambanengwe, F., Mpepereki, S., and Mapfumo, P. (2021). Soil fungal community structure and seasonal diversity following application of organic amendments of different quality under maize cropping in Zimbabwe. *PLoS One* 16:e0258227. doi: 10.1371/journal.pone.0258227

Team, R. C. (2022). R: A language and environment for statistical computing. *R foundation for statistical computing*, Vienna, Austria.

Tedersoo, L., Bahram, M., Põlme, S., Kõljalg, U., Yorou, N. S., Wijesundera, R., et al. (2014). Global diversity and geography of soil fungi. *Science* 346:1256688. doi: 10.1126/science.1256688

Turatsinze, A. N., Kang, B., Zhu, T., Hou, F., and Bowatte, S. (2021). Soil bacterial and fungal composition and diversity responses to seasonal deer grazing in a subalpine meadow. *Diversity* 13:84. doi: 10.3390/d13020084

Voříšková, J., and Baldrian, P. (2013). Fungal community on decomposing leaf litter undergoes rapid successional changes. *ISME J.* 7, 477–486. doi: 10.1038/ismej.2012.116

Voříšková, J., Brabcová, V., Cajthaml, T., and Baldrian, P. (2014). Seasonal dynamics of fungal communities in a temperate oak forest soil. *New Phytol.* 201, 269–278. doi: 10.1111/nph.12481

Wang, J. T., Zheng, Y. M., Hu, H. W., Zhang, L. M., Li, J., and He, J. Z. (2015). Soil pH determines the alpha diversity but not beta diversity of soil fungal community along altitude in a typical Tibetan forest ecosystem. *J. Soils Sediments* 15, 1224–1232. doi: 10.1007/s11368-015-1070-1

Xie, L., and Yin, C. (2022). Seasonal variations of soil fungal diversity and communities in subalpine coniferous and broadleaved forests. *Sci. Total Environ.* 846:157409. doi: 10.1016/j.scitotenv.2022.157409

Yang, Y., Qiu, Y. M., Wang, Z. B., and Qu, L. Y. (2020). Effect of different harvest methods on physicochemical properties and microbial community of *Larix gmelinii* rhizosphere soil. *Acta Ecol. Sin.* 40, 7621–7629. doi: 10.5846/stxb202001070053

Yang, Y., Qiu, Y., Wang, Z., Wang, H., and Qu, L. (2021). Rhizosphere soil fungal community of *Larix gmelinii* in severely burned area. *Acta Ecol. Sin.* 41, 9399–9409. doi: 10.5846/stxb202007071760

Yang, L., Sui, X., Zhu, D., Cui, F., Li, J., Song, R., et al. (2017). Study on fungal communities characteristics of different *Larix gmelinii* forest types in cold temperate zone. *J. Cent. South Univ. For. Technol.* 37, 76–84. doi: 10.14067/j.cnki.1673-923x.2017.12.013

Yang, T., Tedersoo, L., Lin, X., Fitzpatrick, M. C., Jia, Y., Liu, X., et al. (2020). Distinct fungal successional trajectories following wildfire between soil horizons in a cold-temperate forest. *New Phytol.* 227, 572–587. doi: 10.1111/nph.16531

Zeng, Q., Lebreton, A., Man, X., Jia, L., Wang, G., Gong, S., et al. (2022). Ecological drivers of the soil microbial diversity and composition in primary old-growth forest and secondary woodland in a subtropical evergreen broad-leaved forest biome in the Ailao Mountains, China. *Front. Microbiol.* 13:257. doi: 10.3389/fmicb.2022.908257

Zhang, H., and Fu, G. (2021). Responses of plant, soil bacterial and fungal communities to grazing vary with pasture seasons and grassland types, northern Tibet. *Land Degrad. Dev.* 32, 1821–1832. doi: 10.1002/ldr.3835

Zhang, T., Wang, N. F., Liu, H. Y., Zhang, Y. Q., and Yu, L. Y. (2016). Soil pH is a key determinant of soil fungal community composition in the Ny-Ålesund region, Svalbard (high Arctic). *Front. Microbiol.* 7:227. doi: 10.3389/fmicb.2016.00227

Zhao, W., Wang, D. D., Reyila, M. M., Huang, K. C., Liu, S., and Cui, B. K. (2022). Soil microbial community structure of *Larix gmelinii* forest in Aershan area. *Biodivers. Sci.* 30:22258. doi: 10.17520/biods.2022258

Zhou, J., Deng, Y. E., Shen, L., Wen, C., Yan, Q., Ning, D., et al. (2016a). Temperature mediates continental-scale diversity of microbes in forest soils. *Nat. Commun.* 7:12083. doi: 10.1038/ncomms12083

Zhou, J., Jiang, X., Zhou, B., Zhao, B., Ma, M., Guan, D., et al. (2016b). Thirty four years of nitrogen fertilization decreases fungal diversity and alters fungal community composition in black soil in Northeast China. *Soil Biol. Biochem.* 95, 135–143. doi: 10.1016/j.soilbio.2015.12.012

frontiers | Frontiers in Microbiology

TYPE Original Research
PUBLISHED 11 April 2023
DOI 10.3389/fmicb.2023.1165131

OPEN ACCESS

EDITED BY
Milan Kumar Lal,
Central Potato Research Institute (ICAR), India

REVIEWED BY
Tao Li,
Yunnan University, China
Kinga Drzewiecka,
Poznan University of Life Sciences, Poland
Nitika Kapoor,
Hans Raj Mahila Maha Vidyalaya (HRMMV), India
Jian Li,
Jiangsu University, China

*CORRESPONDENCE
Fangdong Zhan
✉ zfd97@ynau.edu.cn

SPECIALTY SECTION
This article was submitted to Microbe and Virus Interactions with Plants, a section of the journal Frontiers in Microbiology

RECEIVED 13 February 2023
ACCEPTED 16 March 2023
PUBLISHED 11 April 2023

CITATION
Wang L, Li Z, Zhang G, Liang X, Hu L, Li Y, He Y and Zhan F (2023) Dark septate endophyte *Exophiala pisciphila* promotes maize growth and alleviates cadmium toxicity. *Front. Microbiol.* 14:1165131. doi: 10.3389/fmicb.2023.1165131

Dark septate endophyte *Exophiala pisciphila* promotes maize growth and alleviates cadmium toxicity

Lei Wang[1], Zuran Li[2], Guangqun Zhang[1], Xinran Liang[1], Linyan Hu[1], Yuan Li[1], Yongmei He[1] and Fangdong Zhan[1]*

[1]College of Resources and Environment, Yunnan Agricultural University, Kunming, China, [2]College of Horticulture and Landscape, Yunnan Agricultural University, Kunming, China

Dark septate endophytes (DSE) are typical root endophytes with the ability to enhance plant growth and tolerance to heavy metals, but the underlying mechanisms are unclear. Here, the physiological and molecular mechanisms of a DSE strain, *Exophiala pisciphila*, in mitigating cadmium (Cd, 20mg/kg) toxicity in maize were investigated. Our results showed, under Cd stress, *E. pisciphila* inoculation enhanced the biomass of maize and reduced both inorganic and soluble forms of Cd (high toxicity) by 52.6% in maize leaves, which may be potentially contributing to Cd toxicity mitigation. Besides, *E. pisciphila* inoculation significantly affected the expression of genes involved in the signal transduction and polar transport of phytohormone, and then affected abscisic acid (ABA) and indole-3-acetic acid (IAA) contents in maize roots, which was the main reason for promoting maize growth. In addition, *E. pisciphila* also made a 27% increase in lignin content by regulating the expression of genes involved in the synthesis of it, which was beneficial to hinder the transport of Cd. In addition, *E. pisciphila* inoculation also activated glutathione metabolism by the up-regulation of genes related to glutathione S-transferase. This study helps to elucidate the functions of *E. pisciphila* under Cd stress, sheds light on the mechanism of detoxifying Cd and provides new insights into the protection of crops from heavy metals.

KEYWORDS

cadmium forms, phytohormone, root morphology, glutathione metabolism, lignin

1. Introduction

The heavy metal contamination of soils is a pressing issue worldwide (Marrugo-Negrete et al., 2017; Yang et al., 2018; Han et al., 2020; Qin et al., 2021). The continued increase of heavy metal levels in the soil system leads to toxicity symptoms and inhibits plant growth directly or indirectly (Jaiswal et al., 2018; Ghori et al., 2019). As a typical heavy metal, cadmium (Cd) has attracted particular concern as it is highly toxic to most organisms (Liu et al., 2018; Yang et al., 2018; Wang et al., 2021a). The rapid development of the chemical industry has exacerbated Cd pollution in the soil (Sodango et al., 2018; Zhao et al., 2019; Wang et al., 2021b). Notably, increasing amounts of Cd have entered arable soils with fertilization and wastewater irrigation (Rezapour et al., 2019; Hou, D. et al., 2020; Fu et al., 2021). Once Cd enters the arable soils, it is readily absorbed by food crops (primary producers) due to its high-water solubility, thereby causing toxicity to humans through the food chain (McLaughlin et al., 1999; Nkwunonwo et al., 2020; Suhani et al., 2021). Therefore, it is necessary to take ecological security and sustainable development approaches to reduce the accumulation of Cd in food crops.

Most plants establish symbiotic relationships with microbes in natural ecosystems (He et al., 2020; Su et al., 2021). Plant responses to environmental stresses induced by microbial symbionts have received increasing attention in recent years (Shen et al., 2020; Riaz et al., 2021; Su et al., 2021). Studies have found the association between plants and their rhizosphere microbes, particularly root-associated endophytic microbes, which reside in the internal tissues of plants, and may have positive effects on plant growth and improve the tolerance of plants to stressful environments (Rodriguez et al., 2009; Bedini et al., 2018; Zhan et al., 2018; White et al., 2019). Therefore, the endophytic microbe is considered an efficient strategy for the remediation of contaminated plants. Dark septate endophytes (DSEs) are well-known for dematiaceous septate hyphae and melanized microsclerotia, which are one of the most studied groups of root fungal endophytes (Jumpponen and Trappe, 1998). DSEs are ubiquitous colonists of plant roots in a wide range of terrestrial ecosystems and frequently distributed in stressful environments, particularly in heavy metal-polluted soils (Newsham, 2011; He et al., 2017; Hou, L. et al., 2020; Su et al., 2021).

Accumulating evidence supports that DSEs can influence the metal tolerance of plants and improve the resistance of plants to heavy metal stress (Shen et al., 2020; Wu et al., 2020; Hou, L. et al., 2020). It was demonstrated that DSE inoculation activates the glutathione (GSH) metabolism and protects the plants against heavy metal stress, because of the significant enhancement of glutathione reductase (GR) and GSH (Zhan et al., 2017). Moreover, DSE inoculation can alter the contents of various phytohormones, such as indoleacetic acid (IAA) and abscisic acid (ABA) and improve plant growth by promoting plant nutrient uptake (He et al., 2017; Wu et al., 2020; Xu et al., 2020). DSEs are closely associated with the roots of many host plants. It colonizes the root cortex of the host plants, induces changes in root traits, and promotes root growth of the host plant (e.g., root length, surface area, and biomass) (He et al., 2017). DSE inoculation can also contribute to impeding Cd transport from roots to shoots, decrease the Cd content in shoots and retain Cd in the DSE-inoculated roots (Hou, L. et al., 2020; Su et al., 2021; Xiao et al., 2021). For example, DSE has been reported to increase the root mass density (root mass per root volume), favoring the mineral nutrients storage of roots, and possibly contributing to the storage of Cd ions in the roots (Kramer-Walter et al., 2016). In addition, fungal melanin in DSE is thought to be involved in enhancing the structural rigidity of cell walls, which may contribute to the tolerance of fungus to stress (Eisenman and Casadevall, 2012; Berthelot et al., 2017). These outstanding researches have expounded the important role of DSE in improving plant tolerance from different perspectives, but there is no comprehensive investigation of it, and the corresponding molecular mechanism has not yet been elucidated.

In this study, a specific DSE strain with a high resistance to Cd stress, *Exophiala pisciphila* H93 (accession number ACCC32496, China Agricultural Culture Collection), was selected as the model DSE-association to investigate the growth, physiology, and molecular mechanisms of DSE-alleviated Cd stress in maize. The effect of DSE on the biomass, root morphological traits, phytohormone, sulfhydryl compounds, and Cd content of maize planted in Cd-contaminated soils was investigated. In addition, we applied transcriptome sequencing to explore the molecular mechanism underlying Cd detoxification by *E. pisciphila*. We focus on: (i) how *E. pisciphila* colonization reduces Cd toxicity to maize seedlings by altering morphological and physiological traits: (ii) how *E. pisciphila* colonization enhances plant tolerance of maize seedlings to Cd stress; and (iii) the transcriptomic mechanism of *E. pisciphila* associated with Cd detoxification in maize.

2. Materials and methods

2.1. Experimental design

2.1.1. Materials preparation

Exophiala pisciphila was isolated from the roots of a gramineous species (*Arundinella bengalensis*) growing naturally at an abandoned mining area in Huize County, Yunnan Province, China (103°36′ E, 26°55′ N) (Li et al., 2011). This fungus was preserved in the China Agricultural Culture Collection as accession No. ACCC32496. The *E. pisciphila* strain was cultivated in the potato dextrose agar (PDA) medium (potato 200 g, dextrose 20 g, agar 18 g, and water 1,000 mL) at 28°C for 2 weeks for its activation. A main locally cultivated maize variety, Huidan No. 4, was chosen as the host plant, which was a variety with high Cd tolerance and low Cd accumulation screened by the research group (Chen et al., 2014). The seeds were soaked in 10% sodium hypochlorite for 2 min, and 75% ethanol for 1 min for sterilization, then rinsed 3 times with sterile water and placed in a petri dish with water agar medium (agar 8 g L^{-1}) for aseptic germination (25°C for 3 days).

2.1.2. Preparation of inoculated/non-inoculated maize seedlings

Cylinder glass bottles (6.5 cm in diameter, 40 cm in height) containing 0.4 kg quartz sand (autoclaved at 121°C for 2 h) and 40 mL 50% Hoagland medium for fungal inoculation. For the treatment with *E. pisciphila* inoculation, 10 g PDA containing *E. pisciphila* and 2 maize seedlings were transferred to the bottles. During the growth of the maize seedlings, the roots attached to the *E. pisciphila* colonies, *E. pisciphila* mycelium subsequently infected the roots. For the treatment without *E. pisciphila* inoculation, 10 g PDA without *E. pisciphila* colonies and 2 maize seedlings were used. All the bottles were covered with sterile AeraSeal films (150 × 150 mm) (Mycomebio Bio-medical Science Technology Center, China) and cultivated in a glasshouse with a 10 h photoperiod (1,000–8,000 lx) at 28°C/15°C (daytime /nighttime) and 75% humidity for 14 days.

After 14 days, the *E. pisciphila*-inoculated seedlings were checked for DSE colonization by observing the presence of microsclerotia or hyphae in the root cells with a compound microscope (Olympus-BX51, Japan). Five 0.5 cm root fragments for each seedling were randomly collected and washed with deionized water, softened in a water bath with 10% (w/v) KOH at 90°C for 2 h and then stained with 0.5% acid fuchsin (Berch and Kendrick, 1982). The stained roots were pressed onto slides and observed under a compound light microscope (Olympus-BX51, 200 magnification) to determine the fungal colonization intensity with the magnified intersection method (McGonigle et al., 1990).

2.1.3. Greenhouse pot cultivation

Quartz sand (0.4 kg), 50% Hoagland medium (40 mL), and PDA (10 g) with/without *E. pisciphila* colonies were used as the culture substrate filled into cylinder glass bottles, and the Cd^{2+} ($CdCl_2 \cdot 2.5H_2O$

was added to the Hoagland medium to achieve a Cd^{2+} concentration of 200 mg/L, resulting Cd^{2+} concentration in the quartz sand was 20 mg/kg) was supplemented to half of the bottles. Based on our previous study, under 20 mg/kg Cd stress, *E. pisciphila* colonization in maize roots significantly increased maize (Huidan No. 4) biomass, plant height and Cd accumulation in the roots (He et al., 2017; Xiao et al., 2021). The four treatments were the Control (non-inoculated *E. pisciphila*, 0 mg/kg Cd^{2+}), DSE treatment (inoculated *E. pisciphila*, 0 mg/kg Cd^{2+}), Cd treatment (non-inoculated *E. pisciphila*, 20 mg/kg Cd^{2+}), Cd + DSE treatment (inoculated *E. pisciphila*, 20 mg/kg Cd^{2+}), respectively. Two non-inoculated maize seedlings of similar sizes were carefully planted in each of the glass bottles of the Control and Cd treatments, while DSE-inoculated maize seedlings were used for the DSE and Cd + DSE treatments, with 6 replicates for each treatment (half replicates were used to measure biomass, root morphology, and the other half were used for tolerance physiology and transcriptome). All inoculated treatments were successfully colonized by *E. pisciphila,* the average colonization intensity of DSE and Cd + DSE treatment was 34.80 and 42.56%, respectively, but DSE structures were not observed in noninoculated treatments. All glass bottles were placed in a glasshouse with a day temperature 28°C and night temperature 15°C for 28 days, irrigated the maize seedlings with deionized water until the plants were harvested.

2.2. Indicator determination

2.2.1. Biomass, root morphological traits and anatomical structure

The maize seedlings were divided into shoots and roots to determine the biomass and morphological traits. The roots were scanned with a scanner (Perfection V700 Photo) and analyzed the root morphological traits with the WinRHIZO Pro root system analyzer. The shoots and roots were dried at 70°C for 72 h to determine the biomass. In order to observe the root structure, root samples were prepared following the method used by Wu et al. (2018) with modifications. Root apical segments (8 mm from the root apex) were fixed in a Formalin-Aceto-Alcohol (FAA) solution (formalin: acetic acid: 70% alcohol = 1:1:16) for 24 h (Yue et al., 2019). Subsequently, the samples were dehydrated in ethanol and embedded in paraffin. Cross-sections (thick 8–12 μm) were sectioned with a Rotary Microtome (RM 2016, Leica, Germany), and stained with water-soluble safranin and fast green to detect the xylem (Wu et al., 2018). The sections were observed with a microscope (DM2000 LED, Leica, Germany), and documented using Motic Images analyzer (Motic China Group Co., Ltd.).

2.2.2. Cadmium content and chemical forms

The dried leaves and roots (0.1 g) of maize seedling were digested with a mixture of HNO_3 and $HClO_4$ (v/v 3:1) and diluted into a volumetric flask (50 mL) using 0.2% HNO_3 to measure the content of Cd by an Atomic Absorption Spectrometer (TAS-990, Beijing Puxi, China) (Zhan et al., 2015). Three replicates per treatment.

According to the methods mentioned in Luo et al. (2017) with minor modifications, 80% ethanol, 1 mol/L NaCl and 2% acetic acid were used to extract ethanol-extracted state Cd ions (F_E-Cd), sodium chloride state Cd ions (F_{NaCl}-Cd), acetic acid state Cd ions (F_{HAc}-Cd), respectively. Fresh maize sample (0.5 g) was ground into homogenate in extraction solution, then transferred to a 50 mL centrifuge tube [diluted to 1:50 (w/v)] and shaken at 25°C for 22 h. The first supernatant solution was obtained by centrifuging the homogenate at 5,000 *g* for 10 min. The sedimentation was resuspended in extraction solution and shaken for 1 h at 25°C, centrifuged at 5,000 *g* for 10 min, then the supernatants of two times suspensions and centrifugation steps were combined to obtain different chemical forms Cd. Supernatant solutions were evaporated on an electric plate at 70°C to a constant weight and digested with an acid oxidative mixture of HNO_3/$HClO_4$ (3:1, v/v) at 145°C, then determined the concentrations of Cd associated with different chemical forms by an Atomic Absorption Spectrometer (TAS-990, Beijing Puxi, China).

2.2.3. Phytohormone

Abscisic acid (ABA) and indole-3-acetic acid (IAA) contents were estimated according to double-antibody method with ELISA kits (Shanghai Huyu Biotechnology Co. Ltd., Shanghai, China) (Hedden, 1993), each sample was examined in triplicate Approximately 0.5 g of roots were ground in a mortar with 10 mL phosphate buffer solution at 4°C. Sample solution (10 μL) was added to the specificity antibody plate (40 μL of 0.15 M phosphate buffer solution per well), and conjugate reagent (50 μL with HRP labeled) was added to each well. Then the color-developing agent was added and stored in the dark for 10 min. Finally, the absorbance was measured at 450 nm after adding the stop solution (H_2SO_4) (Chen, X. et al., 2017).

2.2.4. Lignin contents and key enzymes of lignin synthesis

Root samples (0.1 g) from each treatment were used to test the lignin content, 4-coumarate CoA ligase (4CL), cinnamyl-alcohol dehydrogenase (CAD), and peroxidase (POD) activities, determined using commercial kits (Suzhou Grace Bio-technology Co. Ltd., Suzhou, China) according to the previous methods (Cheng et al., 2020). The lignin was determined by the acetylation method, the acetylated lignin had a characteristic absorption peak at 280 nm, and the absorbance value at 280 nm was recorded to calculate the lignin content (Fan et al., 2021). 4CL can catalyze 4-coumarate and CoA to generate 4-coumarate CoA, and the 4CL activity can be reflected by measuring the 4-coumarate CoA generation rate at 333 nm. CAD can catalyze Cinnamyl alcohol to generate Cinnamic aldehyde, and then react with a specific chromogen, and calculate the CAD enzyme activity by detecting the increased rate of colored substances. Under the catalysis of peroxidase, H_2O_2 oxidizes specific substrates with maximum light absorption at 470 nm, and the POD activity is determined by measuring the change of absorbance at 470 nm.

2.2.5. Sulfhydryl compounds

The homogenate was centrifuged at 10,000 × *g* at 4°C for 20 min to obtain a supernatant. The glutathione synthetase (GSS), γ-glutamyl cysteine synthetase (γ-GCS), glutathione reductase (GR) and glutathione (GSH) contents were assessed using the methods described in the commercial assay kits from Nanjing Jiancheng Bioengineering Institute (Nanjing, China) according to the previous methods (Zhan et al., 2017). The γ-GCS and GR assay kit was designed using principles described by Seelig and Meister (1985) and Foster and Hess (1980), respectively. NADH and NADPH oxidation were assessed by measuring the decrease in absorbance at 340 nm at 37°C. The activity of γ-GCS was determined as the amount of enzyme

necessary for the consumption of 1 μ mol of NADH per minute, while the activity of GR was defined as the oxidation of 1 nmol of NADPH per minute (Zhan et al., 2017). The content of glutathione (GSH) was determined using a colorimetric microplate assay following the instructions provided by Nanjing Jiancheng Bioengineering Institute. After washing the plant tissue with pre-cooled PBS, the supernatant obtained from centrifugation was used to measure the absorbance values at 405 nm, which were then used to determine the GSH content. GSS activities were determined by measuring the ATP-dependent formation of -glutamyl hydroxamate from L-glutamate and hydroxylamine in the supernatant. GSS activity was defined as nmol of -glutamyl hydroxamate produced per second with absorbance measured at 550 nm at 37°C (Yajun et al., 2008).

2.3. Transcriptome sequencing

Three root sub-samples (0.5 g) for RNA extraction were obtained from well-growing roots of maize seedling, each treatment was examined in triplicate. Total RNA was extracted by Trizol-extraction methods with TRIzol RNA reagent (Invitrogen Inc., United States). The RNA concentration and integrity were determined and assessed using the Qubit 2.0 Fluorometer (Thermo Fisher Scientific Inc., United States) and Agilent 2100 Bioanalyzer Instrument (Agilent Technologies, Inc., United States, only RNA Integrity Number ≥ 7 was used for RNA-Seq analysis). Genes with false discovery rate (FDR) < 0.05 and absolute fold change ≥2 were defined as differentially expressed genes (DEGs), transcripts were considered significantly differentially expressed. For details, please refer to the section 1 of Supplementary material. Four genes were randomly selected to confirm the accuracy of RNA-Seq through qRT-PCR. There was a significant correlation between the RNA-Seq and qPCR data ($p < 0.001$; Supplementary Figure S1).

2.4. Statistical analyses

All data analyses were performed in R version 3.6.1 (Team, 2020) and SPSS 25.0 (SPSS, Inc.), the data were log-transformed when needed. The *t*-test was performed in SPSS 25.0 to test the differences in Cd accumulation and chemical forms between Cd and Cd + DSE treatments. One-way analysis of variance was used to test the responses of maize traits to DSE inoculation and Cd stress ("multcomp" package, Tukey's HSD, checking for homogeneity of variances with Levene's test). Plots were generated using GraphPad Prism 8.0. DEGs for each pairwise comparison was analyzed with the "edgeR" package. Visualization of GO terms were generated by using the "REVIGO" web service.

3. Results

3.1. Biomass and root morphological traits of maize seedlings

In this study, *E. pisciphila* inoculation (without Cd stress) induced a significant increase in the shoot biomass of maize seedlings by 43.2%, relative to the control. The shoot biomass under Cd stress treatment (non-inoculated *E. pisciphila*) did not demonstrate any significant differences from the control, however, the root biomass exhibited significant decreases by 39.3%. In addition, Cd stress inoculated with *E. pisciphila* (Cd + DSE treatment) significantly increased shoot and root biomass of maize seedlings by 68.8 and 16.8%, respectively, relative to the biomass under Cd stress (Figure 1A). In addition, the root length, volume, and surface area of DSE treatment (*E. pisciphila* inoculation only) significantly increased by 76.4%, 35.2% and 34.0% relative to the control, respectively, but the average diameter exhibited a significant decrease of 13.3% on average (Figures 1B–E). Cd stress with *E. pisciphila* inoculation resulted in a significant increase in the root length, volume, and surface area relative to the Cd stress treatment by 24.4%, 9.5%, and 9.5%, respectively. However, there was a significant decrease in the average diameter by an average of 12.7% (Figures 1B–E).

3.2. Cd content and chemical forms of maize seedlings

As the *E. pisciphila* was inoculated (Cd + DSE treatment), the Cd contents of both the leaves and roots of the maize significantly decreased by 23.6 and 35.3% relative to the Cd stress (Cd treatment, Figure 2A). Compared with the Cd treatment, the Cd stress with *E. pisciphila* inoculation (Cd + DSE treatment) significantly increased the F_{HAc}-Cd and F_{NaCl}-Cd contents of the maize leaves by 98.8 and 14.5%, respectively, but significantly reduced the F_E-Cd contents by 52.6% (Figures 2B–D).

3.3. Phytohormone contents, lignin content, sulfhydryl compounds and related enzyme activities of maize seedlings

In the current study, with DSE inoculation (without Cd stress), the content of ABA showed a significant increase relative to the control by 65.2% (Figure 3A). The ABA content significant increased by 60.1%, while IAA content significantly decreased by 22.3% with the Cd treatment, relative to the control. Moreover, compared with the Cd stress, DSE inoculation under Cd stress (Cd + DSE treatment) resulted in a significant increase in the IAA content, with an average increase of 51.5%, whereas ABA content was significantly decreased by 37.4% (Figures 3A,B). Compared with the control, Cd treatment, DSE treatment and Cd stress with DSE inoculation (Cd + DSE) treatments resulted in a significant increase in lignin content, 4CL, CAD, and POD activities (Figures 3C–F). Moreover, compared with the Cd treatment, DSE inoculation under Cd stress (Cd + DSE) resulted in a significant increase in the lignin content by 27.7%, as well as the 4CL, CAD and POD activities by 27.1, 68.2 and 28.8%. In the present study, we found that the GR and γ-GCS activities in the maize leaves increased significantly under Cd treatment (Figures 4C,D). Moreover, DSE inoculation resulted in a significant increase in the GSH content, GSS, and GR activities in the leaves of maize under Cd stress (Cd + DSE, Figures 4A–C).

3.4. Transcriptome sequencing

DSE treatment resulted in differences in 433 differentially expressed genes (DEGs). More specifically, 287 DEGs were

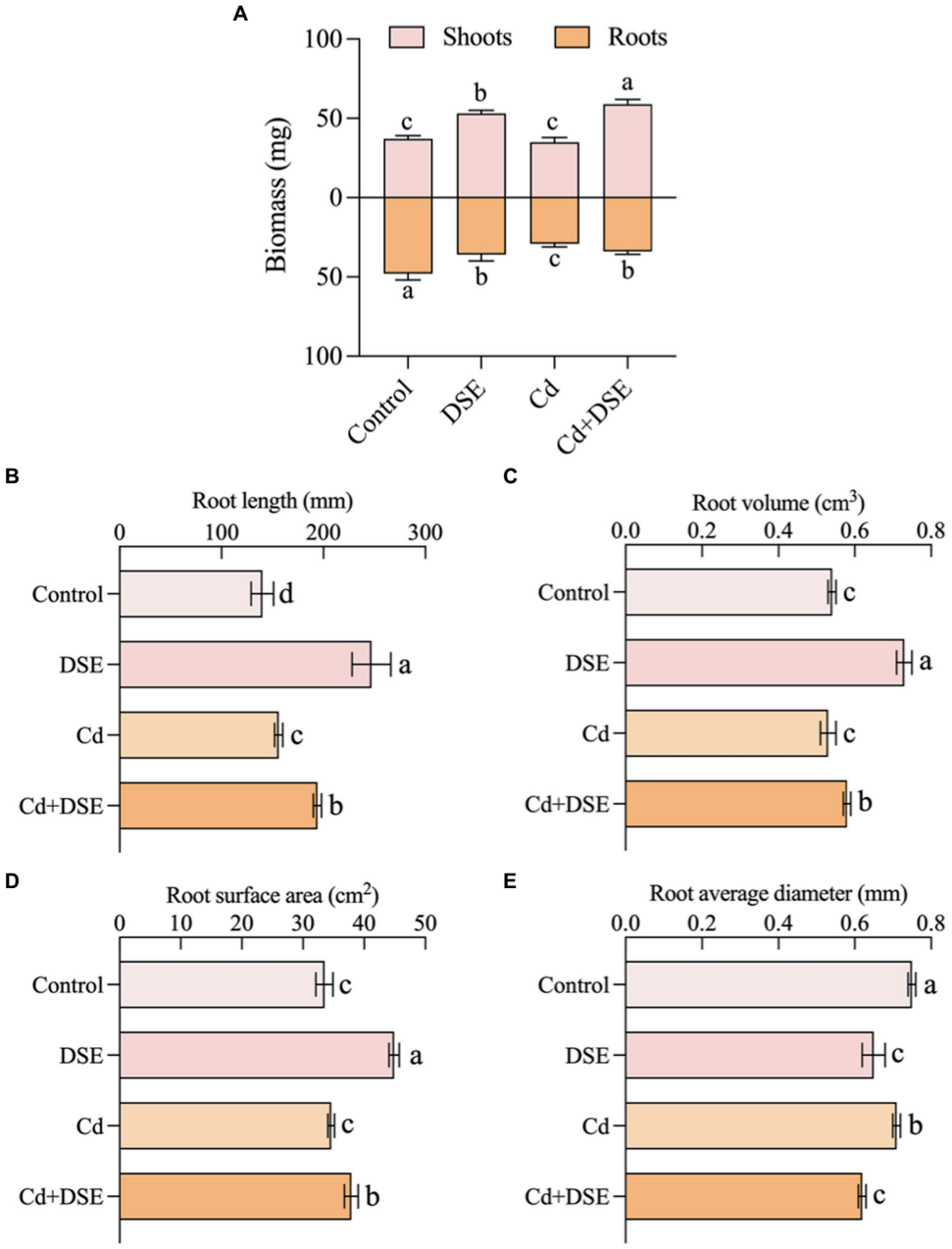

FIGURE 1
Responses of shoots and roots biomass **(A)** and morphological traits, including root length **(B)**, root volume **(C)**, root surface area **(D)** and root average diameter **(E)** of maize to *E. pisciphila* inoculation and Cd stress. Data were mean values ($n = 3$) and error bars represent the standard deviation. Different letters indicate significant differences between treatments.

up-regulated and 146 DEGs were down-regulated, relative to the control. In addition, compared with the Cd stress treatment, 948 DEGs were different after DSE inoculation, among which 529 DEGs were up-regulated and 419 DEGs were down-regulated (Supplementary Table S1). A higher number of GO enriched biological process (BPs) was recognized in the 'Cd versus Cd + DSE.' Among these, the most significant BPs (FDR < 0.01) were the hydrogen peroxide catabolic process, the hydrogen peroxide metabolic process, the reactive oxygen species metabolic process, the oxidation–reduction process and response to oxidative stress (FDR < 0.01, Figure 5A). GO enriched BPs in 'Control versus DSE' included the nicotianamine metabolic process, the nicotianamine biosynthetic process, the tricarboxylic acid biosynthetic process, transmembrane transport and the oxidation–reduction process (FDR < 0.01, Figure 5B). Among the enriched KEGG pathways of 'Cd versus Cd + DSE', the most significant pathways were identified as phenylpropanoid biosynthesis, biosynthesis of secondary metabolites, metabolic pathways, sesquiterpenoid and triterpenoid biosynthesis, and the nitrogen metabolism (Figure 6A). The enriched KEGG pathways of 'Control versus DSE' included the nitrogen metabolism, thiamine metabolism, cutin, suberine and wax biosynthesis, zeatin biosynthesis and biosynthesis of unsaturated fatty acids (Figure 6B).

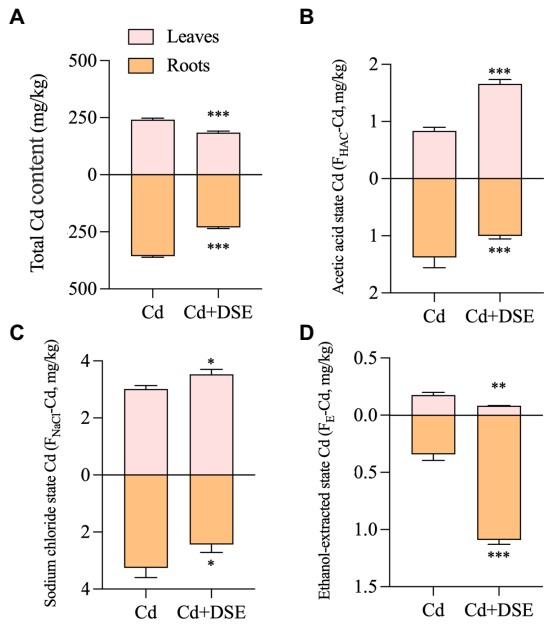

FIGURE 2
Responses of Cd accumulation **(A)** and chemical forms, including acetic acid state Cd **(B)**, sodium chloride state Cd **(C)** and ethanol-extracted state Cd **(D)** of maize to *E. pisciphila* inoculation. Data were mean values (n=3) and error bars represent the standard deviation. "NS," "*," "**," and "***" mean no significance, $p < 0.05$, $p < 0.01$, and $p < 0.001$, respectively.

The transcriptomic analysis revealed that the expression of early auxin-responsive genes such as *IAA24* and *GH3.6* in the plant hormone signal transduction pathway were significantly reduced under Cd stress with DSE inoculation compared with Cd stress (Figure 7 and Supplementary Table S3). Moreover, DSE inoculation significantly down-regulated the gene expression in *E3 ubiquitin-protein ligase* (regulate the ubiquitination of IAA) under Cd stress. DSE inoculation under Cd stress significantly up-regulated the expression of ABA-responsive genes (*Abscisic acid stress ripening*), as well as ABA-related protein genes (*Pathogenesis-related protein*) (Figure 7 and Supplementary Table S4), which regulated ABA content in maize. In addition, transcriptomic analysis revealed that DSE inoculation under Cd stress significantly affected the synthesis of p-hydroxyphenyl (H), guaiacyl (G), and syringyl (S) lignin in the phenylpropanoid biosynthesis pathway (Figure 7). DSE inoculation under Cd stress also led to the up-regulation of glutathione S-transferase related genes in the Glutathione metabolism pathway (Figure 7).

4. Discussion

In the present study, maize seedlings were subjected to Cd stress, and those treated with *E. pisciphila* inoculation exhibited a significant increase in both shoot and root biomass. The results are consistent with those reported by Wu et al. (2020), Su et al. (2021), and Xiao et al. (2021), who found that the shoot and root biomass of maize, rice, and blueberry seedlings increased after inoculation with DSE. In addition, with *E. pisciphila* inoculation, the root length, surface area, and volume of the maize seedlings were significantly increased regardless of the presence of Cd stress. Hou, L. et al. (2020) also reported that DSE inoculation enhanced the root length and surface area of *Medicago sativa*, which facilitated plant growth and improved Cd tolerance. Ban et al. (2017) found that DSE inoculation increased the root length of maize seedlings subjected to stress induced by exposure to different Pb concentrations, indicating that DSE inoculation can improve the growth of maize roots. Thus, the research indicates that *E. pisciphila* inoculation affects the root morphological traits of maize seedlings in such a way that is conducive to plant growth.

In addition to the above results, we also observed a significant shift in the chemical forms of Cd in the *E. pisciphila*-colonized maize. We argue that these chemical forms of Cd are closely related to their biological toxicity, as they determine their reactivity and solubility. Among the various chemical forms of Cd, the Cd-phosphate complex extracted by 2% acetic acid (F_{HAc}-Cd) is important for plant tolerance to Cd due to its insolubility, low mobility, and low toxicity (Qiu et al., 2011). Compared with Cd stress without inoculation, Cd stress with DSE inoculation significantly increased the F_{HAc}-Cd and F_{NaCl}-Cd contents of the maize leaves but reduced their F_E-Cd contents. Similarly, studies on *Poa pratensis* and *Festuca arundinacea* have shown that an increased level of undissolved Cd-phosphate complexes (extracted by 2% acetic acid, F_{HAc}-Cd) favored Cd tolerance (Xu and Wang, 2013). The inorganic, water-soluble form of Cd (FE-Cd, which can be extracted with 80% ethanol) has a greater negative effect on plants than the effect caused by Cd complexed with phosphate and undissolved (FHAc-Cd, extracted with 2% acetic acid). Wang et al. (2016) found that DSE increased the amount of inactive Cd in maize and reduced both the soluble and inorganic content of Cd, however, there were no similar effects noted in the maize roots. In this study, *E. pisciphila* inoculation reduced the F_E-Cd content in maize leaves, which helped to alleviate the toxicity of Cd to plants.

Phytohormones are important regulators of heavy metal tolerance in plants, which enhance plant adaptation to environmental stress by regulating adaptive responses. In the current study, *E. pisciphila* inoculation prior to Cd stress resulted in a significant increase in the IAA content and decreased the ABA content in plant roots compared with the Cd stress without inoculation. This finding is consistent with those reported by He et al. (2017), whereby DSE inoculation significantly increase in the IAA content in maize exposed to a Cd concentration of 20 mg/kg, whereas ABA content significantly decreased under the same treatment. Similarly, Khan and Lee (2013) found that root colonization by endophytes resulted in a significant decrease in the ABA content of *Glycine max* L. under heavy metal stress. Furthermore, increased root volume may be associated with the activation of the IAA in the roots of maize, which is induced by *E. pisciphila* colonization. IAA can effectively stimulate the growth of host plant roots, improve nutrient uptake, and promote plant growth (Khan et al., 2012; Chen, B. et al., 2017). Furthermore, studies have shown that endophytic bacteria can promote plant growth under Cd stress by producing IAA and directly regulating the expression of genes involved in Cd uptake and transport and that IAA may help plants alleviate the toxicity of Cd to cells (Sukumar et al., 2013; Chen, B. et al., 2017). Therefore, *E. pisciphila* can improve plant growth by regulating the phytohormone contents in response to Cd stress.

As the outer barrier of plants, the Casparian strip functions as a physiological fence and valve, which can control the entry of water and mineral ions into vascular tissues, protect against abiotic stress, and defend against the infiltration of toxic compounds. Lignin,

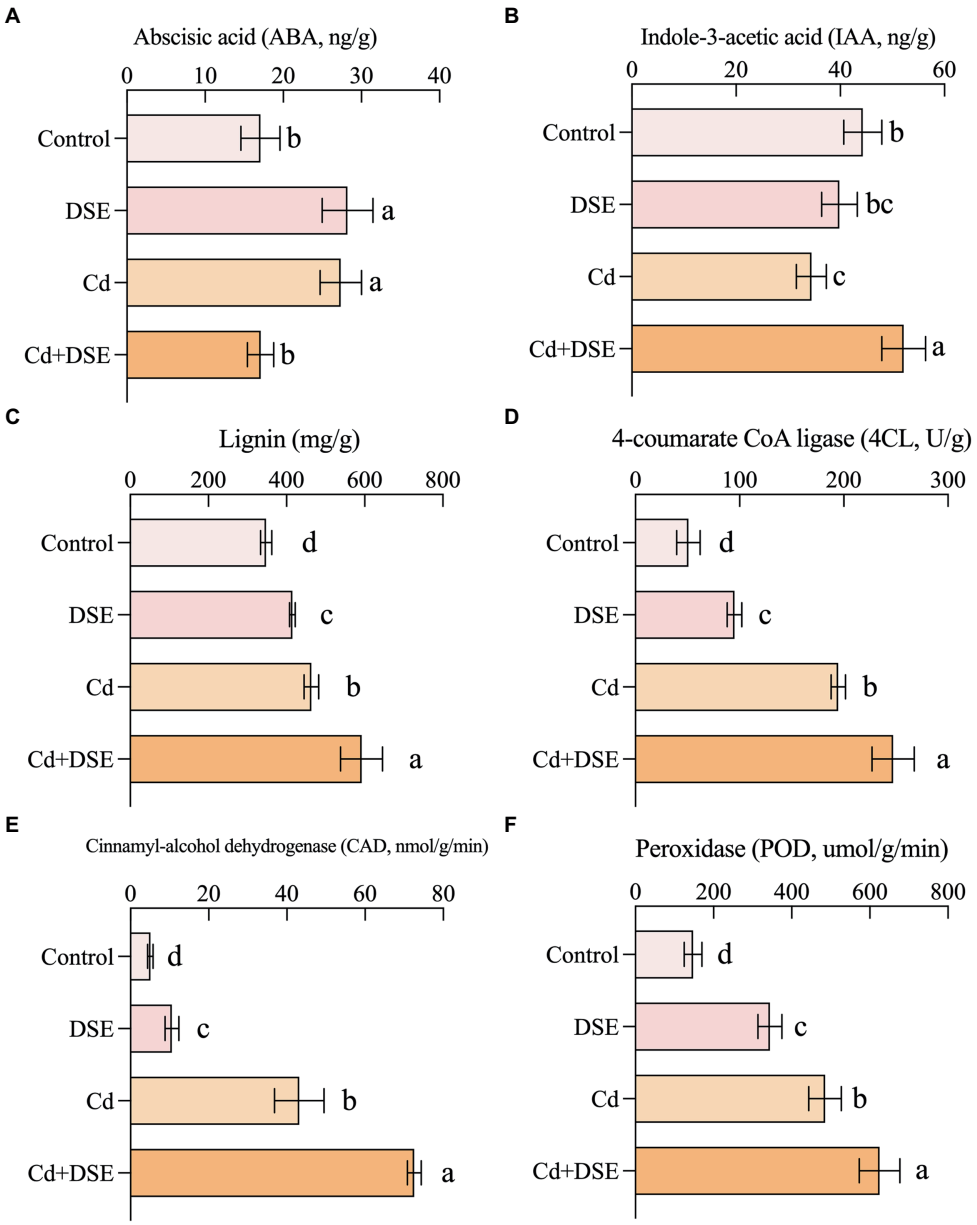

FIGURE 3
Responses of phytohormone and lignin contents and related enzyme activities of maize roots to *E. pisciphila* inoculation and Cd stress. **A**: abscisic acid, **B**: Indole-3-acetic acid, **C**: Lignin; **D**: 4-coumarate CoA ligase, **E**: Cinnamyl-alcohol dehydrogenase, **F**: Peroxidase. Data were mean values ($n = 3$) and error bars represent the standard deviation. Different letters indicate significant differences between treatments.

which is the main component of the Casparian strip, was found to be significantly increased under Cd stress both with and without *E. pisciphila* inoculation. Líška et al. (2016) demonstrated that Cd exposure resulted in the asymmetric development of the exodermis and endodermis structures of maize roots, while the cell wall of the exodermis was significantly thickened to reduce the uptake and transport of harmful ions by the roots. Moreover, compared with maize subjected to Cd stress, those treated with *E. pisciphila* inoculation prior to Cd stress exhibited a significant increase in the lignin content as well as the activities of 4CL, CAD and POD, which were positively associated with lignin synthesis. Additionally, lignin is reported to be an ideal site for metal ion binding *via* the various functional groups (Guo et al., 2008). Our results showed, under Cd stress of DSE-inoculated maize promoted the Cd tolerance of host, including the Cd compartmentation by Casparian strip. We argue that *E. pisciphila* can significantly increase the lignin content, inhibit the migration of Cd from the cortex into the central column, and hinder the transport of Cd.

Sulfhydryl compounds play an important role in the response of plants to heavy metal stress. Among the various heavy metal tolerance mechanisms employed by plants, sulfhydryl compounds act by chelating heavy metal ions to form low-toxicity products (Wang et al., 2019; Chen et al., 2021). In the present study, under Cd stress, the activities of GR and γ-GCS activities in the maize leaves significantly increased. Similarly, the activity of GR was significantly increased in two mustard cultivars after exposure to Cd stress (Iqbal et al., 2010).

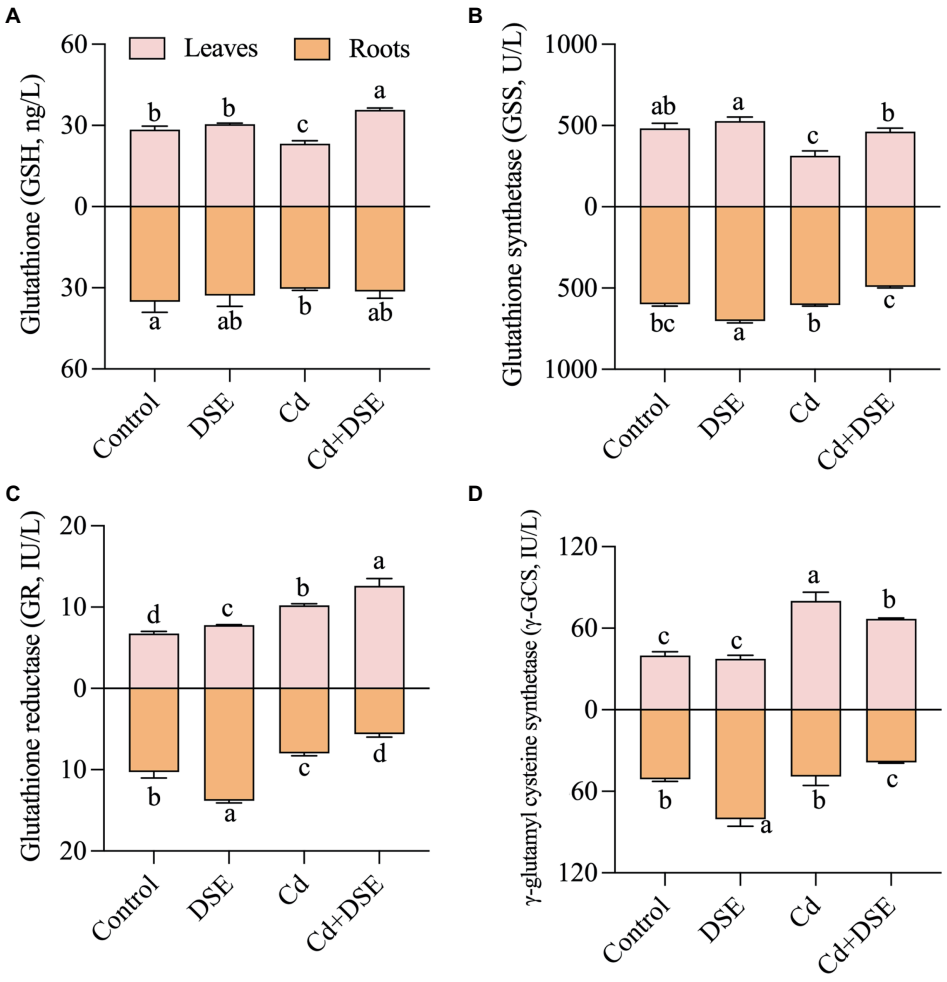

FIGURE 4
Responses of sulfhydryl compounds of maize leaves and roots to *E. pisciphila* inoculation and Cd stress. **A**: glutathione, **B**: glutathione synthetase, **C**: glutathione reductase; **D**: γ-glutamyl cysteine synthetase. Data were mean values ($n = 3$) and error bars represent the standard deviation. Different letters indicate significant differences between treatments.

Moreover, under Cd stress, the GSH content, GSS activity, and GR activity in the leaves of maize increased significantly following *E. pisciphila* inoculation. Similar to our results, DSE colonization increased the GSH content and enhanced the GR activity of maize under the Cd treatment, while also decreasing the Cd content in maize leaves (Zhan et al., 2017). Pan et al. (2016) also determined the positive effects conferred by endophytic inoculation and observed an increase in the GSH concentration, Cd tolerance, and accumulation of Cd in the roots of *Sedum alfredii*. Studies on tobacco have also shown that endophytes significantly increased the expression of genes related to the GSH metabolism and promoted the retention of Cd in tobacco roots (Hui et al., 2015). These results suggest that sulfhydryl compounds and enzymes respond positively to Cd stress and tolerance.

The transcriptome was analyzed to explore the underlying mechanisms of the above results. Under Cd stress, gene expression related to the early auxin- response and the ubiquitination of IAA were significantly downregulated following *E. pisciphila* inoculation compared to the condition of Cd stress non-inoculation, which are crucial for maintaining IAA homeostasis in plants (Yue et al., 2016; Li et al., 2017). *E. pisciphila* inoculation also significantly upregulated the genetic expression of ABA-responsive and ABA-related proteins, which regulated ABA content in maize. In addition, under Cd stress, *E. pisciphila* inoculation significantly affected the expression of genes related to the synthesis of lignin. This is attributed to the significant changes in the expression of 4CL, CAD, and POD induced by *E. pisciphila*. *E. pisciphila* inoculation under Cd stress also led to the upregulation of glutathione S-transferase-related genes in the glutathione metabolism pathway. This indicates that the phytohormones, lignin content, sulfhydryl compounds and related enzymes may be involved in the promotion of plant growth induced by *E. pisciphila* inoculation.

In this study, the biological function and molecular mechanism of the DSE strain *E. pisciphila* in mitigating Cd toxicity in maize were investigated. The results demonstrated that *E. pisciphila* inoculation induced a significantly upregulated tolerance to Cd, with a significant decrease in phytotoxicity and an increase in maize root and shoot biomass. *E. pisciphila* promoted maize growth by regulating the expression of phytohormone-related genes to affect phytohormone contents in maize roots, alleviating Cd toxicity by regulating the expression of genes related to lignin synthesis and glutathione S-transferase, increasing lignin contents, and activating glutathione

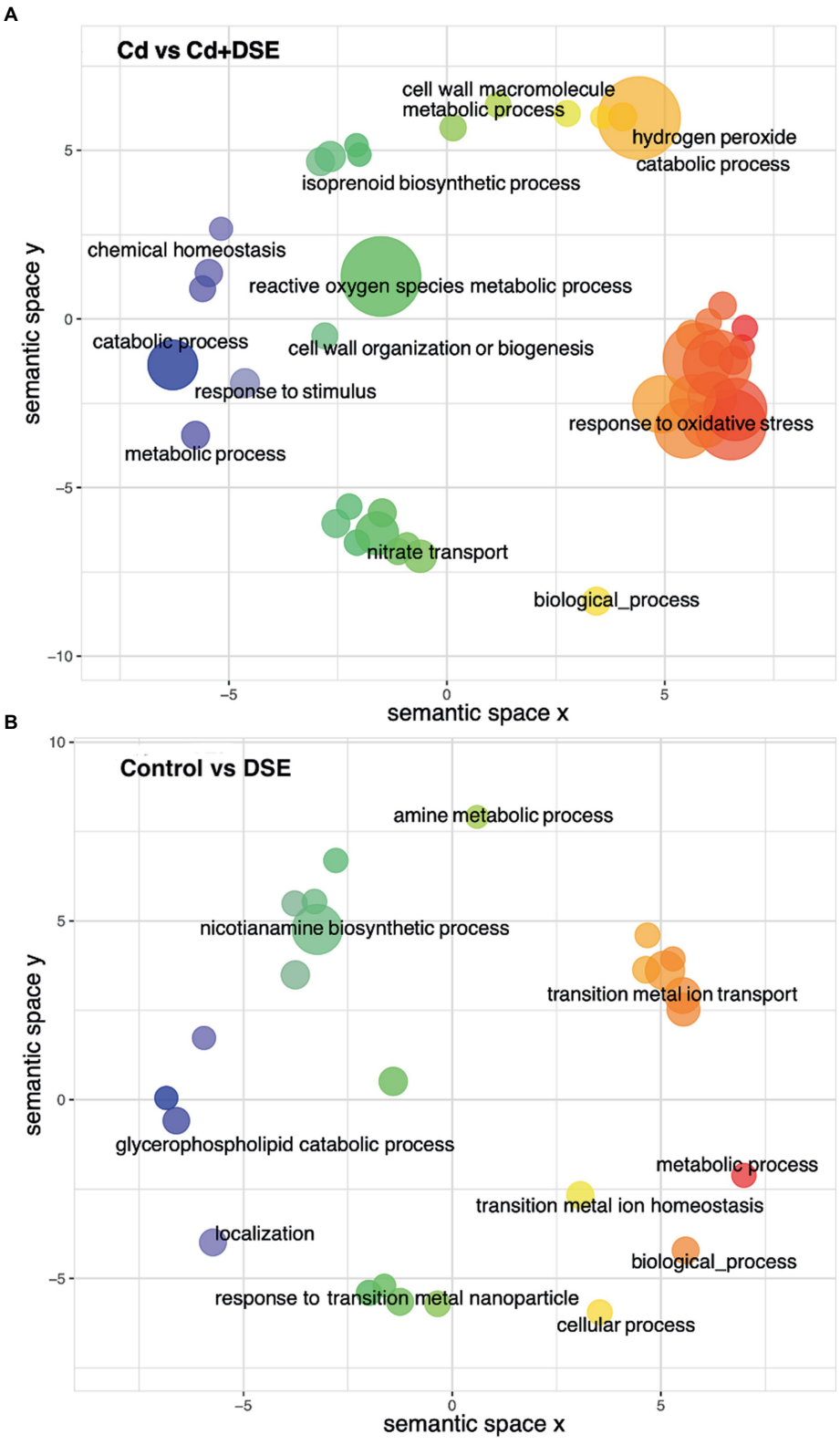

FIGURE 5
Graphical depiction of enriched GO-BPs in **(A)** Cd vs. Cd+DSE and **(B)** Control vs. DSE (FDR<0.05). GO-BP terms are colored by semantic similarity to other GO terms and bubble size reflects the abs_log10_pvalue of the GO-term in the Fisher test. The two-dimensional semantic space was generated by the REVIGO web service.

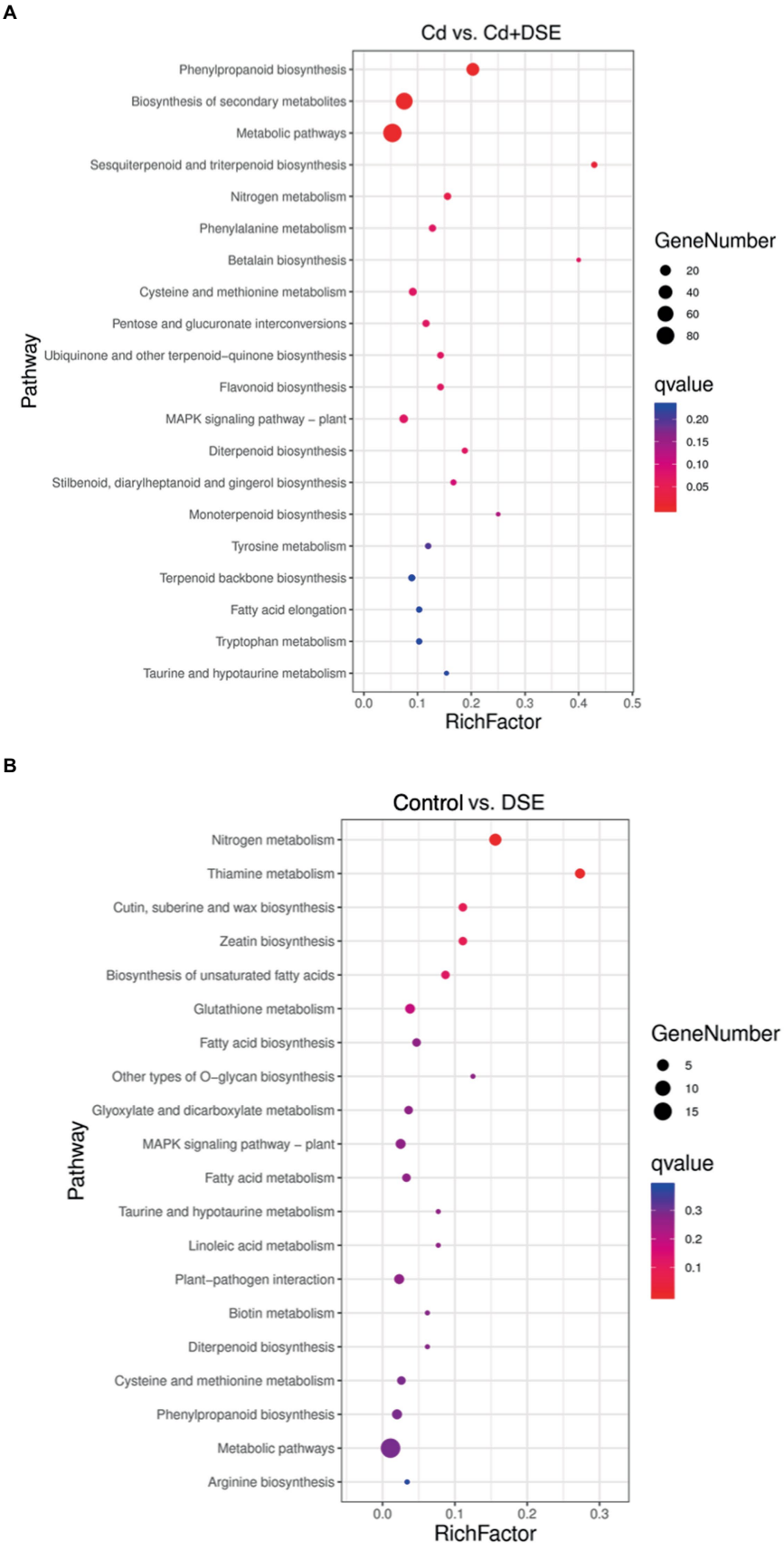

FIGURE 6
Top 20 of KEGG enrichment pathway in **(A)** Cd vs. Cd+DSE and **(B)** Control vs. DSE treatments.

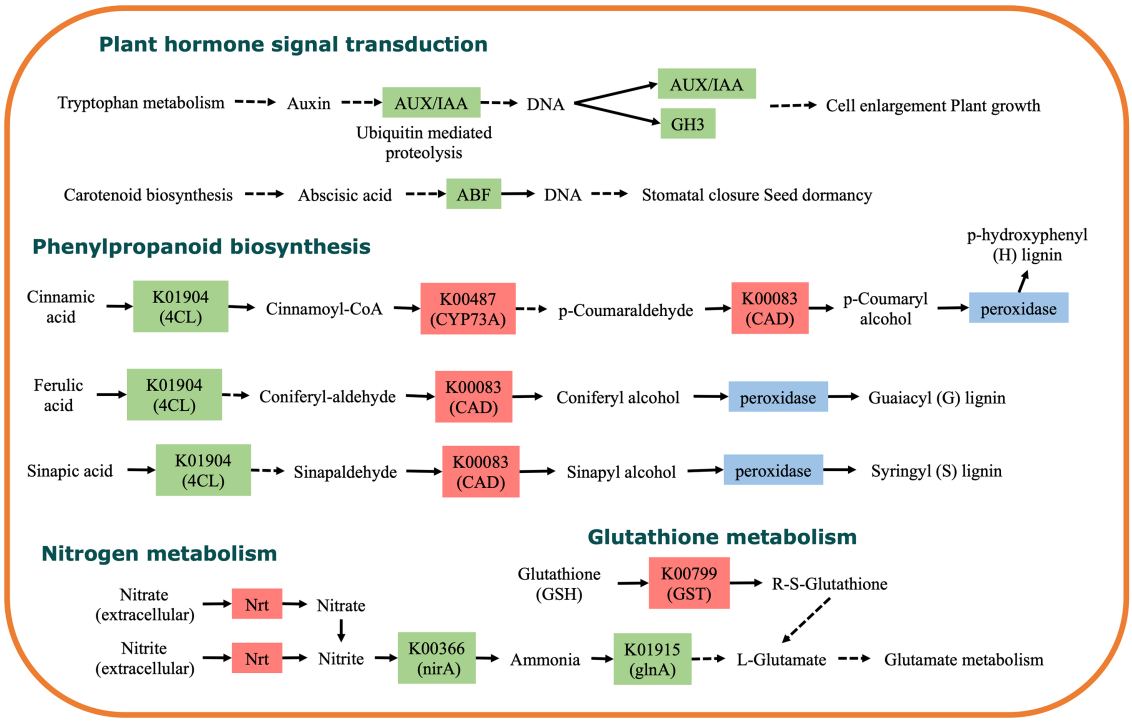

FIGURE 7
KEGG pathway enriched by differentially expressed genes between Cd and Cd+DSE treatments. Colors indicate significant differential expression, red represents up-regulation, green represents down-regulation, and blue represents both up-regulation and down-regulation.

metabolism to reduce the levels of highly toxic forms of Cd. The results of this study help to elucidate the mechanism by which *E. pisciphila* colonization enhances heavy metal resistance in plants and provide a basis for improving plant growth performance at the morphological, physiological, toxicological, and transcriptional levels.

Data availability statement

The datasets presented in this study can be found in online repositories. The names of the repository/repositories and accession number(s) can be found at: https://www.ncbi.nlm.nih.gov/- PRJNA936425.

Author contributions

FZ and GZ conceived and designed the experiments. GZ, LH, XL, and ZL performed the experiments. LW analyzed the data and wrote the manuscript. FZ, YL, and YH provided editorial advice. All authors read and approved the final manuscript.

Funding

This study was financially supported by the National Natural Science Foundation of China (No. 41877130), the Key Project of Yunnan Agricultural Foundation (2017FG001-014), and the Reserve Talents Fund for Young and Middle-Aged Academic and Technological Leaders in Yunnan Province (No 202005AC160038).

Conflict of interest

The authors declare that the research was conducted in the absence of any commercial or financial relationships that could be construed as a potential conflict of interest.

Publisher's note

Supplementary material

The Supplementary material for this article can be found online at: https://www.frontiersin.org/articles/10.3389/fmicb.2023.1165131/full#supplementary-material

References

Ban, Y., Xu, Z., Yang, Y., Zhang, H., Chen, H., and Tang, M. (2017). Effect of dark septate endophytic fungus *Gaeumannomyces cylindrosporus* on plant growth, photosynthesis and Pb tolerance of maize (*Zea mays* L.). *Pedosphere* 27, 283–292. doi: 10.1016/S1002-0160(17)60316-3

Bedini, A., Mercy, L., Schneider, C., Franken, P., and Lucic-Mercy, E. (2018). Unraveling the initial plant hormone signaling, metabolic mechanisms and plant defense triggering the endomycorrhizal symbiosis behavior. *Front. Plant Sci.* 9:1800. doi: 10.3389/fpls.2018.01800

Berch, S. M., and Kendrick, B. (1982). Vesicular-arbuscular mycorrhizae of southern Ontario ferns and fern-allies. *Mycologia* 74, 769–776. doi: 10.1080/00275514.1982.12021584

Berthelot, C., Perrin, Y., Leyval, C., and Blaudez, D. (2017). Melanization and ageing are not drawbacks for successful agro-transformation of dark septate endophytes. *Fungal Biol.* 121, 652–663. doi: 10.1016/j.funbio.2017.04.004

Chen, Q. Y., Liu, L., Yang, L., Dong, B., Wen, Y. Z., Zhang, Z., et al. (2021). Response of sulfhydryl compounds in subcells of *Cladophora rupestris* under Pb stress. *Environ. Sci. Pollut. Res.* 28, 13112–13123. doi: 10.1007/s11356-020-11577-3

Chen, B., Luo, S., Wu, Y., Ye, J., Wang, Q., Xu, X., et al. (2017). The effects of the endophytic bacterium *Pseudomonas fluorescens* Sasm05 and IAA on the plant growth and cadmium uptake of *Sedum alfredii* Hance. *Front. Microbiol.* 8:2538. doi: 10.3389/fmicb.2017.02538

Chen, X., Qiu, L., Guo, H., Wang, Y., Yuan, H., Yan, D., et al. (2017). Spermidine induces physiological and biochemical changes in southern highbush blueberry under drought stress. *Braz. J. Bot.* 40, 841–851. doi: 10.1007/s40415-017-0401-4

Chen, J., Yu, W., Zu, Y., and Li, Y. (2014). Variety difference of Cd accumulation and translocation in *Zea mays*. *Ecol. Environ. Sci.* 23, 1671–1676. doi: 10.16258/j.cnki.1674-5906.2014.10.012

Cheng, B., Raza, A., Wang, L., Xu, M., Lu, J., Gao, Y., et al. (2020). Effects of multiple planting densities on lignin metabolism and lodging resistance of the strip intercropped soybean stem. *Agronomy* 10:1177. doi: 10.3390/agronomy10081177

Eisenman, H. C., and Casadevall, A. (2012). Synthesis and assembly of fungal melanin. *Appl. Microbiol. Biotechnol.* 93, 931–940. doi: 10.1007/s00253-011-3777-2

Fan, F., Zhou, Z., Qin, H., Tan, J., and Ding, G. (2021). Exogenous brassinosteroid facilitates xylem development in *Pinus massoniana* seedlings. *Int. J. Mol. Sci.* 22:7615. doi: 10.3390/ijms22147615

Foster, J. G., and Hess, J. L. (1980). Responses of superoxide dismutase and glutathione reductase activities in cotton leaf tissue exposed to an atmosphere enriched in oxygen. *Plant Physiol.* 66, 482–487. doi: 10.1104/pp.66.3.482

Fu, Y., Li, F., Guo, S., and Zhao, M. (2021). Cadmium concentration and its typical input and output fluxes in agricultural soil downstream of a heavy metal sewage irrigation area. *J. Hazard. Mater.* 412:125203. doi: 10.1016/j.jhazmat.2021.125203

Ghori, N. H., Ghori, T., Hayat, M. Q., Imadi, S. R., Gul, A., Altay, V., et al. (2019). Heavy metal stress and responses in plants. *Int. J. Environ. Sci. Technol.* 16, 1807–1828. doi: 10.1007/s13762-019-02215-8

Guo, X., Zhang, S., and Shan, X. Q. (2008). Adsorption of metal ions on lignin. *J. Hazard. Mater.* 151, 134–142. doi: 10.1016/j.jhazmat.2007.05.065

Han, R., Zhou, B., Huang, Y., Lu, X., Li, S., and Li, N. (2020). Bibliometric overview of research trends on heavy metal health risks and impacts in 1989–2018. *J. Clean. Prod.* 276:123249. doi: 10.1016/j.jclepro.2020.123249

He, Y. M., Fan, X. M., Zhang, G. Q., Li, B., Li, T. G., Zu, Y. Q., et al. (2020). Effects of arbuscular mycorrhizal fungi and dark septate endophytes on maize performance and root traits under a high cadmium stress. *S. Afr. J. Bot.* 134, 415–423. doi: 10.1016/j.sajb.2019.09.018

He, Y., Yang, Z., Li, M., Jiang, M., Zhan, F., Zu, Y., et al. (2017). Effects of a dark septate endophyte (DSE) on growth, cadmium content, and physiology in maize under cadmium stress. *Environ. Sci. Pollut. Res.* 24, 18494–18504. doi: 10.1007/s11356-017-9459-6

Hedden, P. (1993). Modern methods for the quantitative analysis of plant hormones. *Annu. Rev. Plant Biol.* 44, 107–129. doi: 10.1146/annurev.pp.44.060193.000543

Hou, D., O'Connor, D., Igalavithana, A. D., Alessi, D. S., Luo, J., Tsang, D. C., et al. (2020). Metal contamination and bioremediation of agricultural soils for food safety and sustainability. *Nat. Rev. Earth Environ.* 1, 366–381. doi: 10.1038/s43017-020-0061-y

Hou, L., Yu, J., Zhao, L., and He, X. (2020). Dark septate endophytes improve the growth and the tolerance of *Medicago sativa* and *Ammopiptanthus mongolicus* under cadmium stress. *Front. Microbiol.* 10:3061. doi: 10.3389/fmicb.2019.03061

Hui, F., Liu, J., Gao, Q., and Lou, B. (2015). *Piriformospora indica* confers cadmium tolerance in *Nicotiana tabacum*. *J. Environ. Sci.* 37, 184–191. doi: 10.1016/j.jes.2015.06.005

Iqbal, N., Masood, A., Nazar, R., Syeed, S., and Khan, N. A. (2010). Photosynthesis, growth and antioxidant metabolism in mustard (*Brassica juncea* L.) cultivars differing in cadmium tolerance. *Agric. Sci. China* 9, 519–527. doi: 10.1016/S1671-2927(09)60125-5

Jaiswal, A., Verma, A., and Jaiswal, P. (2018). Detrimental effects of heavy metals in soil, plants, and aquatic ecosystems and in humans. *J. Environ. Pathol. Toxicol. Oncol.* 37, 183–197. doi: 10.1615/JEnvironPatholToxicolOncol.2018025348

Jumpponen, A., and Trappe, J. M. (1998). Dark septate endophytes: a review of facultative biotrophic root–colonizing fungi. *New Phytol.* 140, 295–310. doi: 10.1046/j.1469-8137.1998.00265.x

Khan, A. L., Hamayun, M., Kang, S. M., Kim, Y. H., Jung, H. Y., Lee, J. H., et al. (2012). Endophytic fungal association via gibberellins and indole acetic acid can improve plant growth under abiotic stress: an example of *Paecilomyces formosus* LHL10. *BMC Microbiol.* 12, 1–14. doi: 10.1186/1471-2180-12-3

Khan, A. L., and Lee, I. J. (2013). Endophytic *Penicillium funiculosum* LHL06 secretes gibberellin that reprograms *Glycine max* L. growth during copper stress. *BMC Plant Biol.* 13, 86–14. doi: 10.1186/1471-2229-13-86

Kramer-Walter, K. R., Bellingham, P. J., Millar, T. R., Smissen, R. D., Richardson, S. J., and Laughlin, D. C. (2016). Root traits are multidimensional: specific root length is independent from root tissue density and the plant economic spectrum. *J. Ecol.* 104, 1299–1310. doi: 10.1111/1365-2745.12562

Li, P., Cao, W., Fang, H., Xu, S., Yin, S., Zhang, Y., et al. (2017). Transcriptomic profiling of the maize (*Zea mays* L.) leaf response to abiotic stresses at the seedling stage. *Front. Plant Sci.* 8:290. doi: 10.3389/fpls.2017.00290

Li, T., Liu, M. J., Zhang, X. T., Zhang, H. B., Sha, T., and Zhao, Z. W. (2011). Improved tolerance of maize (*Zea mays* L.) to heavy metals by colonization of a dark septate endophyte (DSE) *Exophiala pisciphila*. *Sci. Total Environ.* 409, 1069–1074. doi: 10.1016/j.scitotenv.2010.12.012

Líška, D., Martinka, M., Kohanová, J., and Lux, A. (2016). Asymmetrical development of root endodermis and exodermis in reaction to abiotic stresses. *Ann. Bot.* 118, 667–674. doi: 10.1093/aob/mcw047

Liu, L., Li, J., Yue, F., Yan, X., Wang, F., Bloszies, S., et al. (2018). Effects of arbuscular mycorrhizal inoculation and biochar amendment on maize growth, cadmium uptake and soil cadmium speciation in Cd-contaminated soil. *Chemosphere* 194, 495–503. doi: 10.1016/j.chemosphere.2017.12.025

Luo, N., Li, X., Chen, A. Y., Zhang, L. J., Zhao, H. M., Xiang, L., et al. (2017). Does arbuscular mycorrhizal fungus affect cadmium uptake and chemical forms in rice at different growth stages? *Sci. Total Environ.* 599-600, 1564–1572. doi: 10.1016/j.scitotenv.2017.05.047

Marrugo-Negrete, J., Pinedo-Hernández, J., and Díez, S. (2017). Assessment of heavy metal pollution, spatial distribution and origin in agricultural soils along the Sinú River Basin, Colombia. *Environ. Res.* 154, 380–388. doi: 10.1016/j.envres.2017.01.021

McGonigle, T. P., Miller, M. H., Evans, D. G., Fairchild, G. L., and Swan, J. A. (1990). A new method which gives an objective measure of colonization of roots by vesicular-arbuscular mycorrhizal fungi. *New Phytol.* 115, 495–501. doi: 10.1111/j.1469-8137.1990.tb00476.x

McLaughlin, M. J., Parker, D. R., and Clarke, J. M. (1999). Metals and micronutrients–food safety issues. *Field Crop Res.* 60, 143–163. doi: 10.1016/S0378-4290(98)00137-3

Newsham, K. K. (2011). A meta-analysis of plant responses to dark septate root endophytes. *New Phytol.* 190, 783–793. doi: 10.1111/j.1469-8137.2010.03611.x

Nkwunonwo, U. C., Odika, P. O., and Onyia, N. I. (2020). A review of the health implications of heavy metals in food chain in Nigeria. *Sci. World J.* 2020, 1–11. doi: 10.1155/2020/6594109

Pan, F., Meng, Q., Wang, Q., Luo, S., Chen, B., Khan, K. Y., et al. (2016). Endophytic bacterium *Sphingomonas* SaMR12 promotes cadmium accumulation by increasing glutathione biosynthesis in *Sedum alfredii* Hance. *Chemosphere* 154, 358–366. doi: 10.1016/j.chemosphere.2016.03.120

Qin, G., Niu, Z., Yu, J., Li, Z., Ma, J., and Xiang, P. (2021). Soil heavy metal pollution and food safety in China: Effects, sources and removing technology. *Chemosphere* 267:129205. doi: 10.1016/j.chemosphere.2020.129205

Qiu, Q., Wang, Y., Yang, Z., and Yuan, J. (2011). Effects of phosphorus supplied in soil on subcellular distribution and chemical forms of cadmium in two Chinese flowering cabbage (*Brassica parachinensis* L.) cultivars differing in cadmium accumulation. *Food Chem. Toxicol.* 49, 2260–2267. doi: 10.1016/j.fct.2011.06.024

Rezapour, S., Atashpaz, B., Moghaddam, S. S., Kalavrouziotis, I. K., and Damalas, C. A. (2019). Cadmium accumulation, translocation factor, and health risk potential in a wastewater-irrigated soil-wheat (*Triticum aestivum* L.) system. *Chemosphere* 231, 579–587. doi: 10.1016/j.chemosphere.2019.05.095

Riaz, M., Kamran, M., Fang, Y., Wang, Q., Cao, H., Yang, G., et al. (2021). Arbuscular mycorrhizal fungi-induced mitigation of heavy metal phytotoxicity in metal contaminated soils: A critical review. *J. Hazard. Mater.* 402:123919. doi: 10.1016/j.jhazmat.2020.123919

Rodriguez, R. J., White, J. F., Arnold, A. E., and Redman, R. S. (2009). Fungal endophytes: diversity and functional roles. *New Phytol.* 182, 314–330. doi: 10.1111/j.1469-8137.2009.02773.x

Seelig, G. F., and Meister, A. (1985). Glutathione biosynthesis; γ-glutamylcysteine synthetase from rat kidney. *Method. Enzymol.* 113, 379–390. doi: 10.1016/S0076-6879(85)13050-8

Shen, M., Schneider, H., Xu, R., Cao, G., Zhang, H., Li, T., et al. (2020). Dark septate endophyte enhances maize cadmium (Cd) tolerance by the remodeled host cell walls

and the altered Cd subcellular distribution. *Environ. Exp. Bot.* 172:104000. doi: 10.1016/j.envexpbot.2020.104000

Sodango, T. H., Li, X., Sha, J., and Bao, Z. (2018). Review of the spatial distribution, source and extent of heavy metal pollution of soil in China: impacts and mitigation approaches. *J. Health Pollut.* 8, 53–70. doi: 10.5696/2156-9614-8.17.53

Su, Z. Z., Dai, M. D., Zhu, J. N., Liu, X. H., Li, L., Zhu, X. M., et al. (2021). Dark septate endophyte *Falciphora oryzae*-assisted alleviation of cadmium in rice. *J. Hazard. Mater.* 419:126435. doi: 10.1016/j.jhazmat.2021.126435

Suhani, I., Sahab, S., Srivastava, V., and Singh, R. P. (2021). Impact of cadmium pollution on food safety and human health. *Curr. Opin. Toxicol.* 27, 1–7. doi: 10.1016/j.cotox.2021.04.004

Sukumar, P., Legue, V., Vayssieres, A., Martin, F., Tuskan, G. A., and Kalluri, U. C. (2013). Involvement of auxin pathways in modulating root architecture during beneficial plant–microorganism interactions. *Plant Cell Environ.* 36, 909–919. doi: 10.1111/pce.12036

Team, R. C. (2020). *R Core Team R: a language and environment for statistical computing*. Foundation for Statistical Computing.

Wang, L., Gao, Y., Jiang, W., Chen, J., Chen, Y., Zhang, X., et al. (2021b). Microplastics with cadmium inhibit the growth of *Vallisneria natans* (Lour.) Hara rather than reduce cadmium toxicity. *Chemosphere* 266:128979. doi: 10.1016/j.chemosphere.2020.128979

Wang, L., Gao, Y., Wang, X., Qin, Z., Liu, B., Zhang, X., et al. (2021a). Warming enhances the cadmium toxicity on macrophyte *Myriophyllum aquaticum* (Vell.) Verd. seedlings. *Environ. Pollut.* 268:115912. doi: 10.1016/j.envpol.2020.115912

Wang, J. L., Li, T., Liu, G. Y., Smith, J. M., and Zhao, Z. W. (2016). Unraveling the role of dark septate endophyte (DSE) colonizing maize (*Zea mays*) under cadmium stress: physiological, cytological and genic aspects. *Sci. Rep.* 6, 1–12. doi: 10.1038/srep22028

Wang, W., Meng, M., and Li, L. (2019). Arsenic detoxification in Eucalyptus: subcellular distribution, chemical forms, and sulfhydryl substances. *Environ. Sci. Pollut. Res.* 26, 24372–24379. doi: 10.1007/s11356-019-05701-1

White, J. F., Kingsley, K. L., Zhang, Q., Verma, R., Obi, N., Dvinskikh, S., et al. (2019). Endophytic microbes and their potential applications in crop management. *Pest Manag. Sci.* 75, 2558–2565. doi: 10.1002/ps.5527

Wu, F. L., Li, Y., Tian, W., Sun, Y., Chen, F., Zhang, Y., et al. (2020). A novel dark septate fungal endophyte positively affected blueberry growth and changed the expression of plant genes involved in phytohormone and flavonoid biosynthesis. *Tree Physiol.* 40, 1080–1094. doi: 10.1093/treephys/tpaa047

Wu, Q., Tang, Y., Dong, T., Liao, Y., Li, D., He, X., et al. (2018). Additional AM fungi inoculation increase *Populus cathayana* intersexual competition. *Front. Plant Sci.* 9:607. doi: 10.3389/fpls.2018.00607

Xiao, Y., Dai, M. X., Zhang, G. Q., Yang, Z. X., He, Y. M., and Zhan, F. D. (2021). Effects of the dark septate endophyte (DSE) *Exophiala pisciphila* on the growth of root cell wall polysaccharides and the cadmium content of *Zea mays* L. under cadmium stress. *J. Fungi.* 7:1035. doi: 10.3390/jof7121035

Xu, R., Li, T., Shen, M., Yang, Z. L., and Zhao, Z. W. (2020). Evidence for a dark septate endophyte (*Exophiala pisciphila*, H93) enhancing phosphorus absorption by maize seedlings. *Plant Soil* 452, 249–266. doi: 10.1007/s11104-020-04538-9

Xu, P., and Wang, Z. (2013). Physiological mechanism of hypertolerance of cadmium in Kentucky bluegrass and tall fescue: chemical forms and tissue distribution. *Environ. Exp. Bot.* 96, 35–42. doi: 10.1016/j.envexpbot.2013.09.001

Yajun, H., Wangzhen, G., Xinlian, S., and Tianzhen, Z. (2008). Molecular cloning and characterization of a cytosolic glutamine synthetase gene, a fiber strength-associated gene in cotton. *Planta* 228, 473–483. doi: 10.1007/s00425-008-0751-z

Yang, Q., Li, Z., Lu, X., Duan, Q., Huang, L., and Bi, J. (2018). A review of soil heavy metal pollution from industrial and agricultural regions in China: Pollution and risk assessment. *Sci. Total Environ.* 642, 690–700. doi: 10.1016/j.scitotenv.2018.06.068

Yue, L., Chen, F., Yu, K., Xiao, Z., Yu, X., Wang, Z., et al. (2019). Early development of apoplastic barriers and molecular mechanisms in juvenile maize roots in response to La_2O_3 nanoparticles. *Sci. Total Environ.* 653, 675–683. doi: 10.1016/j.scitotenv.2018.10.320

Yue, R., Lu, C., Qi, J., Han, X., Yan, S., Guo, S., et al. (2016). Transcriptome analysis of cadmium-treated roots in maize (*Zea mays* L.). *Front. Plant Sci.* 7:1298. doi: 10.3389/fpls.2016.01298

Zhan, F., He, Y., Li, Y., Li, T., Yang, Y. Y., Toor, G. S., et al. (2015). Subcellular distribution and chemical forms of cadmium in a dark septate endophyte (DSE), *Exophiala pisciphila*. *Environ. Sci. Pollut. Res.* 22, 17897–17905. doi: 10.1007/s11356-015-5012-7

Zhan, F., Li, B., Jiang, M., Qin, L., Wang, J., He, Y., et al. (2017). Effects of a root-colonized dark septate endophyte on the glutathione metabolism in maize plants under cadmium stress. *J. Plant Interact.* 12, 421–428. doi: 10.1080/17429145.2017.1385868

Zhan, F., Li, B., Jiang, M., Yue, X., He, Y., Xia, Y., et al. (2018). Arbuscular mycorrhizal fungi enhance antioxidant defense in the leaves and the retention of heavy metals in the roots of maize. *Environ. Sci. Pollut. Res.* 25, 24338–24347. doi: 10.1007/s11356-018-2487-z

Zhao, X., Huang, J., Lu, J., and Sun, Y. (2019). Study on the influence of soil microbial community on the long-term heavy metal pollution of different land use types and depth layers in mine. *Ecotox. Environ. Safe.* 170, 218–226. doi: 10.1016/j.ecoenv.2018.11.136

frontiers | Frontiers in Microbiology

TYPE Original Research
PUBLISHED 14 April 2023
DOI 10.3389/fmicb.2023.1160631

OPEN ACCESS

EDITED BY
Xiancan Zhu,
Anhui Normal University, China

REVIEWED BY
Tao Zhang,
Northeast Normal University, China
Xu Liu,
Institute of Soil Science (CAS), China

*CORRESPONDENCE
Hongwei Yu
✉ hongweiyu1990@126.com
Jianqing Ding
✉ jding@henu.edu.cn

SPECIALTY SECTION
This article was submitted to Microbe and Virus Interactions with Plants, a section of the journal Frontiers in Microbiology

RECEIVED 07 February 2023
ACCEPTED 28 March 2023
PUBLISHED 14 April 2023

CITATION
Chen L, Wang M, Shi Y, Ma P, Xiao Y, Yu H and Ding J (2023) Soil phosphorus form affects the advantages that arbuscular mycorrhizal fungi confer on the invasive plant species, *Solidago canadensis*, over its congener. *Front. Microbiol.* 14:1160631. doi: 10.3389/fmicb.2023.1160631

Soil phosphorus form affects the advantages that arbuscular mycorrhizal fungi confer on the invasive plant species, *Solidago canadensis*, over its congener

Li Chen[1], Mengqi Wang[1], Yu Shi[1], Pinpin Ma[2], Yali Xiao[3], Hongwei Yu[1]* and Jianqing Ding[1]*

[1]State Key Laboratory of Crop Stress Adaptation and Improvement, School of Life Sciences, Henan University, Kaifeng, China, [2]College of Life Sciences, Jiangxi Science and Technology Normal University, Nanchang, China, [3]School of Life Sciences and Agricultural Engineering, Nanyang Normal University, Nanyang, China

Interactions between plants and arbuscular mycorrhizal fungi (AMF) are strongly affected by soil phosphorus (P) availability. However, how P forms impact rhizosphere AMF diversity, community composition, and the co-occurrence network associated with native and invasive plants, and whether these changes in turn influence the invasiveness of alien species remain unclear. In this work, we performed a greenhouse experiment with the invasive species *Solidago canadensis* and its native congener *S. decurrens* to investigate how different forms of P altered the AMF community and evaluate how these changes were linked with the growth advantage of *S. canadensis* relative to *S. decurrens*. Plants were subjected to five different P treatments: no P addition (control), simple inorganic P (sodium dihydrogen phosphate, NaP), complex inorganic P (hydroxyapatite, CaP), simple organic P (adenosine monophosphate, AMP) and complex organic P (myo-inositol hexakisphosphate, PA). Overall, invasive *S. canadensis* grew larger than native *S. decurrens* across all P treatments, and this growth advantage was strengthened when these species were grown in CaP and AMP treatments. The two *Solidago* species harbored divergent AMF communities, and soil P treatments significantly shifted AMF community composition. In particular, the differences in AMF diversity, community composition, topological features and keystone taxa of the co-occurrence networks between *S. canadensis* and *S. decurrens* were amplified when the dominant form of soil P was altered. Despite significant correlations between AMF alpha diversity, community structure, co-occurrence network composition and plant performance, we found that alpha diversity and keystone taxa of the AMF co-occurrence networks were the primary factors influencing plant growth and the growth advantage of invasive *S. canadensis* between soil P treatments. These results suggest that AMF could confer invasive plants with greater advantages over native congeners, depending on the forms of P in the soil, and emphasize the important roles of multiple AMF traits in plant invasion.

KEYWORDS

Glomeraceae, keystone taxa, microbial diversity, nutrient form, plant invasion, plant-fungal interaction

Introduction

Plant invasions are a serious threat to biodiversity and ecosystem functions, particularly in recent decades due to globalization (Livingstone et al., 2020; Rai and Singh, 2020). The invasive success of exotic species is complex to predict and depends on a range of biotic and abiotic conditions (Enders et al., 2020). Of all the factors affecting the success of plant invasions, plant association with soil mutualistic microbes contributes greatly to the performance of exotic species by promoting nutrient absorption and tolerance to stressors (Reinhart and Callaway, 2006; Lamit et al., 2022). However, the magnitude and direction of symbiotic associations between plants and soil microbes are frequently affected by soil nutrients (Chen et al., 2020, 2021). Thus, greater attention should be paid to soil nutrient mediated interactions between invasive plants and mutualistic microbes. Insights into soil mutualistic microbes associated with invasive plants under various nutrient conditions could help improve understanding of the microbiome-related mechanisms underlying invasion success.

Arbuscular mycorrhizal fungi (AMF) establish symbiotic relationships with most terrestrial plants and provide multiple benefits to host plants (Basu et al., 2018; Mathur et al., 2019; Cao et al., 2020). Consequently, shifts in the AMF community and their interconnections may influence plant growth and fitness (Liang et al., 2019; Schröder et al., 2019). For example, a higher AMF richness or greater abundance of specific AMF taxa may enhance plant productivity and promote plant diversity (Vogelsang et al., 2006), and plant species that harbor distinct AMF communities have been shown to exhibit heterogenous growth responses (Sheng et al., 2022). Moreover, the effects conferred by mycorrhiza may vary between native and invasive species. Awaydul et al. (2019) found that mycorrhizal networks increased nutrient acquisition in invasive plants compared with native plants. Therefore, variations in AMF diversity, community structure, and co-occurrence networks could potentially affect plant growth and the invasiveness of exotic plants. Although a growing number of studies have highlighted the importance of AMF to invasion success of exotic plants (Majewska et al., 2017; Yu et al., 2022), the roles of AMF taxa, community assembly, and their relative contributions to the success of plant invasions are still poorly understood.

Phosphorus (P) is a growth-limiting nutrient in many natural ecosystems, playing important roles in plant and AMF growth and metabolism. For example, soil P can affect invasive plant performance by changing functional traits or photosynthesis (Esterhuizen et al., 2020). P can also significantly mediate AMF spore growth (UI Haq et al., 2022), colonization rate (Grman and Robinson, 2013), hyphal length (Xiang et al., 2014) and community structure (Wang et al., 2022). Thus, the key role of soil P availability in mediating the invasive plant-AMF interaction is well accepted (Chen et al., 2020). However, soil P exists in a range of inorganic and organic compounds (Song et al., 2007; Azene et al., 2022), and different forms of P differ distinctly in their efficacy on invasive plant growth and AMF metabolism and functions (Yang et al., 2020; Qi et al., 2022; Zhang et al., 2022). Additionally, existing evidence regarding soil nutrient-modulated plant-AMF interactions has typically focused on mycorrhizal colonization or hyphal density (Chen et al., 2020; Ma et al., 2020), while ignoring mycorrhizal response may also depend on complex microbial interactions (Chaudhary et al., 2022). Therefore, investigating the effect of different forms of P on AMF communities and identifying the essential components of mycorrhizal traits that enhance invasive plant performance could provide mechanistic insights into soil nutrient-regulated plant-fungal interactions, which are crucial to the management of invasive plants.

Solidago canadensis, one of the most notorious invasive plants in the world, was introduced into China in the 1930s (Dong et al., 2006a). In the introduced range, *S. canadensis* was characterized by rapid growth and high reproductive capacity (Dong et al., 2006b) and formed strong mutualistic interactions with AMF (Yu and He, 2022), which helped it outcompete the native species. Invasive *Solidago* can maintain its dominance across a range of soil nutrient environments (Dong et al., 2006a), including inorganic P-dominant and organic P-dominant habits (Yang et al., 2020). Although previous studies found that *S. canadensis* can benefit more from organic than inorganic P (Yang et al., 2020; Zhang et al., 2022) and perform better compared with the native species *S. decurrens* under diverse nutrient conditions (Yu and He, 2022), few studies have explicitly tested whether this is associated with AMF community.

In this study, we conducted a greenhouse experiment to examine the impacts of different forms of P in the soil on the AMF community, and evaluate their effects on the growth and growth advantage of *S. canadensis*. We hypothesized that: (1) native and invasive species would respond differently to different forms of P in terms of AMF diversity, community structure, co-occurrence network, and plant performance; (2) differences in AMF traits conferred by different soil P environments contribute differently to plant growth and growth advantage in *S. canadensis*. Our work provides clear evidence that soil P conditions alter multiple mycorrhizal traits, which is linked to enhanced invasive plant performance.

Materials and methods

Study species

Solidago canadensis L., native to North America, is a perennial forb propagated by seeds and rhizomes. Since its introduction into China in 1935 (Dong et al., 2006a), *S. canadensis* has invaded large areas and diverse habitats in southern China (Dong et al., 2006a; Yu and He, 2022). *Solidago decurrens* L., a native congener perennial forb, occurs commonly in the range that was invaded by *S. canadensis* in China. We collected *S. canadensis* and *S. decurrens* seeds from natural populations and used them for the following experiment.

Experimental design

The experiment was conducted in a greenhouse from May to August at Henan University campus, Kaifeng, China (34°49′13″ N, 114°18′ 18″ E). We collected soil from barren land and sieved it through 2 mm mesh to remove roots and other debris. To prepare the growth medium, we mixed the soil with an equal volume of sand to minimize the potential adverse effects of excessive P in the soil. The basic properties of this growth medium were as follows: $11.5 \pm 0.13\ g{\cdot}kg^{-1}$ carbon, $0.1 \pm 0.01\ g{\cdot}kg^{-1}$ total nitrogen, $3.8 \pm 0.21\ mg{\cdot}kg^{-1}$ available nitrogen, $1.4 \pm 0.15\ mg{\cdot}kg^{-1}$ available phosphorus, and pH of 7.9 ± 0.01. The growth medium was divided into 2 kg portions in individual 2 l pots (11 cm × 16 cm × 14 cm).

To investigate the effects of different P sources on plant performance and rhizosphere AMF communities, we set up five P treatments: control (no P addition), sodium dihydrogen phosphate (NaH_2PO_4, simple inorganic P, NaP), hydroxyapatite [$Ca_5(OH)(PO_4)_3$, complex inorganic P, CaP], adenosine monophosphate ($C_{10}H_{14}N_5O_7P$, simple organic P, AMP), and myo-inositol hexakisphosphate ($C_6H_{18}O_{24}P_6$, complex organic P, PA). We designed these P treatments based on previous research (Pearse et al., 2007; Yang et al., 2020; Qi et al., 2022). The P concentration was supplied at 20 mg kg^{-1} soil, roughly corresponding to the medium soil P content in areas invaded by invasive plants (Chen et al., 2020). We supplemented the four P sources to pots and mixed them with growth medium thoroughly.

Seeds of *S. canadensis* and *S. decurrens* were surface-sterilized with 2% NaClO for 2 min, then germinated in trays filled with 25 kGy gamma-irradiation sterilized vermiculite. When seedlings reached the three-leaf stage, similar size seedlings were transplanted into the pots as described above. All the pots were positioned randomly in the greenhouse and rotated each week to avoid the potential effects of microsite variability. The growth conditions in the greenhouse were as follows: 16 h light (day) and 8 h dark (night), 25°C during the day and 18°C during the night at a relative humidity of 60%. To avoid other nutrient limitations on plant growth, we supplemented equivalent modified P-free Hoagland's nutrient solution to each pot during the course of experiments. Plants were watered daily to ensure that all plants had sufficient water for growth. Each treatment was replicated eight times, resulting in 80 pots in total.

Plant harvest, soil sampling, and calculation of relative change in biomass

After 70 days growth, the experimental plants were harvested, dried at 60°C for 72 h, and weighed to determine whole-plant biomass. To evaluate difference in plant performance between native and invasive species, we calculated the growth advantage (GA) of invasive *S. canadensis* over its native conger *S. decurrens* according to the following equation:

$$GA = \left[(Sc - Sd) / Sd \right] \times 100\%$$

where Sc and Sd are the biomass of *S. canadensis* and *S. decurrens*, respectively, grown in a given P treatment. The growth advantage can signify an invader's potential invasiveness, and a high GA value indicates high plant invasiveness.

Rhizosphere soil samples were collected when the plants were harvested. At harvest, we removed the whole plant from the soil, gently shook the plant to remove the loosely adhering soil around the roots, and collected the tightly adhering soil around the root (rhizosphere soil) by manually brushing (Shi et al., 2022). In total, 80 rhizosphere soil samples were collected. All of these samples were frozen at −80°C for DNA extraction within 2 weeks.

DNA extraction, polymerase chain reaction amplification, and bioinformatic analyzes

Soil microbial DNA was extracted from 0.25 g soil of each soil sample using Magabio Soil and Feces Genomic DNA Purification Kit (Bioer Technology, Zhejiang, China) according to the manufacturer's instructions; DNA concentration and purity were then assessed using a NanoDrop One (Thermo Fisher Scientific, MA, United States). The small subunit rRNA (SSU rRNA) region was amplified using the primer set AMV4.5NF (5′-AAGCTCGTAGTTGAATTTCG-3′) and AMDGR (5′-CCCAACTATCCCTATTAATCAT-3′) (Lumini et al., 2010). The polymerase chain reaction (PCR) reactions, containing 25 µl 2x Premix Taq, 1 µl each forward and reverse primer (10 µM), and 3 µl DNA template (20 ng/µl) in a volume of 50 µl, were amplified by thermocycling: 5 min at 94°C for initialization; 30 cycles of 30 s denaturation at 94°C, 30 s annealing at 52°C, and 30 s extension at 72°C; and 10 min final elongation at 72°C. PCR products were quality-checked using 1% agarose gel electrophoresis, and purified with E.Z.N.A. Gel Extraction Kit (Omega, USA). Finally, equimolar concentrations of amplified samples were pooled and sequenced using an Illumina Nova 6000 platform at Magigene Biotechnology Co., Ltd. (Guangzhou, China).

QIIME2 (Bolyen et al., 2019) was used to process paired-end sequence reads. Using the q2-dada2 plugin, raw sequence data were quality-filtered and de-replicated, chimeras were removed, and sequences were grouped into amplicon sequence variations (ASVs) (Callahan et al., 2016). For taxonomic classification, representative sequences were blasted against the MaarjAM database using the q2-feature-classifier plugin, with at least 95% query coverage and 97% sequence identity (Frew, 2022). Non-AMF sequences and singletons were excluded prior to the analysis. The resultant dataset was rarefied at the minimum number of sequences across all samples, and the data were used for the downstream analysis. All sequence data were archived in the NCBI Sequence Read Archive (SRA) database under accession number PRJNA922727.

Arbuscular mycorrhizal fungi co-occurrence network construction

Network analyzes of the AMF ASVs in the two *Solidago* species under different P treatments were conducted individually. Co-occurrence networks were constructed using the SparCC method on the iNAP platform through the publicly available pipeline[1] (Feng et al., 2022). Based on 20 iterations and 100 bootstraps, pair-wise ASVs with strong correlations ($r > 0.5$ and $p < 0.05$) were retained to construct the networks. Based on the within-module connectivity (*Zi*) and among-module connectivity (*Pi*) values, we divided the nodes in each network into four categories: peripherals ($Zi < 2.5$ and $Pi < 0.62$, nodes with few links and play a negligible role in the network), connectors ($Zi < 2.5$ and $Pi > 0.62$, link modules and crucial to network coherence), module hubs ($Zi > 2.5$ and $Pi < 0.62$, link nodes within a module that are vital to the module) and network hubs ($Zi > 2.5$ and $Pi > 0.62$, link nodes both within and among modules that are important to the network). This allowed us to evaluate potential topological roles of taxa in the networks. Nodes serving as hubs or connectors in a network were defined as keystone species in the network. The topological properties were analyzed and the networks were visualized using Gephi v0.9.3 (Bastian et al., 2009).

1 http://mem.rcees.ac.cn:8081

Statistical analysis

All statistical analyzes were performed using R v4.1.2 (R Core Team, 2022) using the agricolae, (Mendiburu, 2021) vegan (Oksanen et al., 2022), and plspm (Sanchez et al., 2017) packages. A two-way analysis of variance (ANOVA) was conducted to evaluate the effects of plant species and P treatments on plant biomass, alpha diversity, and relative abundance of AMF families. One-way ANOVA with least significant difference (LSD) *post-hoc* tests were implemented when significant differences among treatments were detected. Independent *t*-tests were further used to examine the difference in biomass and alpha diversity between native and invasive *Solidago* species under the same P treatment. Data were square root or natural log transformed to meet the assumption of normality. To assess variation in AMF community composition, principal coordinate analysis (PCoA) based on Bray–Curtis distance matrices and permutational multivariate analysis of variance (PERMANOVA) were used to describe the significance of plant species and P forms on microbial composition. Pairwise comparisons were used to compare differences between different P treatments on AMF community composition. Venn analysis was performed to identify the number of unique and shared ASVs among the five P treatments in the native and invasive *Solidago*. Relationships between AMF variables (i.e., alpha diversity, relative abundance at the family level, and abundance of keystone species in the networks) and plant performance (i.e., biomass and the growth advantage of *S. canadensis*) were evaluated using Pearson correlation.

Partial least squares path modeling (PLS-PM) was performed to quantify the influence of P treatments on plant growth and the growth advantage of *S. canadensis* conferred by the AMF. PLS-PM analyzes were carried out according to previously published methods (Sanchez, 2013). We defined P treatments, alpha diversity, community structure, keystone species, total biomass, and growth advantage as latent variables, and assumed that P treatments affected total biomass or growth advantage *via* alpha diversity, community structure, and keystone species in the co-occurrence networks. Only variables with significant relationships to biomass were included in the models. Based on biomass, we defined and descended the P treatments as integers from 5 to 1. Dillon-Goldstein's rho was used to evaluate how well a block of indicators described their corresponding latent construct. Loadings reflected the correlations between a latent variable and its indicators. The Dillon-Goldstein's rho and loadings greater than 0.7 were defined as acceptable (Supplementary Table S1). To evaluate the quality of the model, goodness-of-fit (GoF) and R^2 determination coefficients were calculated. Moreover, we assessed the relative contribution of each latent variable to the R^2 of total biomass and the growth advantage of *S. canadensis* using the following equation:

$$R^2(\%) = \beta_j cor(y, x_j) / \sum_j \beta_j cor(y, x_j)$$

where j is the number of latent variables, β is the path coefficient, and cor(y, x_j) is the correlation between explanatory and response variables (Tenenhaus et al., 2005; Yu and He, 2017).

Results

Effects of different forms of P on plant performance

Overall, the invasive *S. canadensis* grew larger than the native *S. decurrens* across all treatments (4.10 ± 0.32 g vs. 1.93 ± 0.15 g; $F_S = 128.51$, $p < 0.001$). P treatments, as well as their interactions with the plant species, exerted significant effects on whole-plant biomass (all $p < 0.001$, Figure 1A). Specifically, NaP and PA increased whole-plant biomass in the native *S. decurrens* while the supplementation of NaP, AMP, and PA promoted the growth of the invasive *S. canadensis* (Figure 1A). Compared with *S. decurrens*, *S. canadensis* had greater biomass under each of the five P treatments, leading to a substantial growth advantage for invasive *Solidago*. However, the growth advantage of *S. canadensis* varied with P forms ($F_P = 16.01$, $p < 0.001$) and was enhanced with application of CaP and AMP (Figure 1B).

Arbuscular mycorrhizal fungi diversity and its relationship with plant performance

In total, 1,568,984 high-quality AMF sequence reads were produced before rarefication, with 528 ASVs identified from all soil samples. After rarefication, the AMF alpha diversity was strongly influenced by plant species and P treatments. Across all treatments, *S. canadensis* had a greater richness ($F_S = 33.57$, $p < 0.001$) and Shannon index ($F_S = 26.77$, $p < 0.001$) than *S. decurrens* (Figures 2A,B). Richness and Shannon index were similar between the two species in the control treatment (Figures 2A,B). However, there were clear differences in alpha diversity between the two *Solidago* species when P was added to the soil, with the invasive *Solidago* showing a higher response to resource fluctuations in terms of microbial diversity (Figures 2A,B). Of all P treatments, AMP treatment resulted in the highest richness and Shannon index for both species (Figures 2A,B). Furthermore, the whole-plant biomass and the growth advantage of *S. canadensis* increased with the increasing alpha diversity (Figures 2C–F).

Arbuscular mycorrhizal fungi community structure and its relationship with plant performance

PCoA of Bray–Curtis distances revealed that AMF communities were delineated by plant species and forms of P (Figures 3A–C). In general, *S. decurrens* and *S. canadensis* harbored distinct AMF communities (Figure 3A; Supplementary Table S2). Adding P, except CaP, altered the AMF community structure of both *S. decurrens* and *S. canadensis* compared with the control treatment (Figures 3B,C; Supplementary Table S3). Moreover, the difference in AMF community composition between *S. decurrens* and *S. canadensis* intensified when the dominant P form in the soil changed (Supplementary Table S4). In addition, Venn plots showed that AMF communities in the two *Solidago* species had a greater proportion of common ASVs among different P forms (Figures 3D,E).

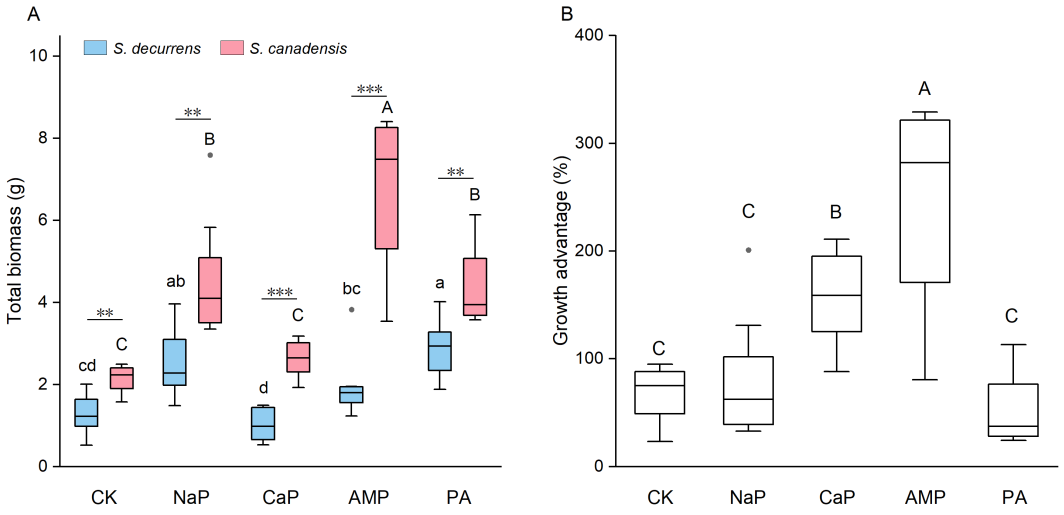

FIGURE 1
(A) Total biomass of *S. decurrens* and *S. canadensis* grown under five P treatments. CK: no P addition; NaP: sodium dihydrogen phosphate; CaP: hydroxyapatite; AMP: adenosine monophosphate; PA: myo-inositol hexakisphosphate. The line in the box represents the median value, box boundaries indicate the value in the 25–75th percentile range, whiskers indicate the 95% confidence intervals. The different lower-case letters among *S. decurrens* and different upper-case letters among *S. canadensis* denote significant differences at $p<0.05$. The asterisks denote difference between *S. decurrens* and *S. canadensis* in the same P treatment. *$p<0.05$, **$p<0.01$, ***$p<0.001$. **(B)** The growth advantage of *S. canadensis* over *S. decurrens* under five P treatments. Different upper-case letters above the boxes indicate significant differences at $p<0.05$.

ASVs detected in the rhizosphere soil were classified into six genera within six families. At the family level, the AMF communities were dominated by Glomeraceae (45.6%), followed by Claroideoglomeraceae (28.3%), Diversisporaceae (15.0%), Acaulosporaceae (10.8%), Gigasporaceae (0.27%) and Paraglomeraceae (0.05%) (Figure 4A). Overall, *S. decurrens* had higher relative abundances of Claroideoglomeraceae and Diversisporaceae and a lower relative abundance of Acaulosporaceae than *S. canadensis* (Figure 4A; Supplementary Table S5). P treatments resulted in distinct variations in AMF community structure between *S. decurrens* and *S. canadensis* (Table 1). For example, the applications of NaP and AMP increased Claroideoglomeraceae abundance but reduced Acaulosporaceae abundance relative to the control in *S. decurrens* (Figure 4A; Supplementary Table S5). AMP addition increased the relative abundance of Glomeraceae while decreasing the abundances of Diversisporaceae and Acaulosporaceae in *S. canadensis* (Figure 4A; Supplementary Table S5). Variations in AMF abundance were strongly correlated with plant performance. The relative abundance of Diversisporaceae was negatively correlated with whole-plant biomass (Figure 4B; Supplementary Table S6). The relative abundances of Glomeraceae were positively correlated with the growth advantage of *S.canadensis* over *S. decurrens* (Figure 4C; Supplementary Table S6), while those of Diversisporaceae and Acaulosporaceae were negatively correlated with the growth advantage of *S.canadensis* over *S. decurrens* (Figures 4D,E; Supplementary Table S6).

Arbuscular mycorrhizal fungi co-occurrence network and its relationship with plant performance

The AMF co-occurrence networks in *S. decurrens* and *S. canadensis* had distinct patterns with different P treatments (Figure 5; Table 2). In the control treatment, the average degree, average clustering coefficient, and complexity in the co-occurrence network of *S. decurrens* were greater than those of *S. canadensis* (Table 2). Adding P decreased average degree and complexity in the network of *S. decurrens*, while the opposite pattern was observed for *S. canadensis*, apart from with NaP (Table 2). Variations in complexity were positively correlated with the growth advantage of *S. canadensis* (Figure 5D).

P treatment also had a significant impact on keystone species of the AMF co-occurrence networks (Supplementary Figure S1). The keystone species mainly belonged to the Glomeraceae, with a higher proportion in *S. canadensis* networks (76%) than those of *S. decurrens* (56%) (Supplementary Table S7). Relative to control, the number of keystone species decreased with inorganic P (i.e., NaP and CaP) but increased with organic P (i.e., AMP and PA) in the networks of *S. decurrens*. In contrast, the number of keystone species in *S. canadensis* networks was higher with all P treatments compared to the control, with the highest number of keystone species in the AMP treatment (Table 2). There was a strong correlation between the abundance of most keystone species and plant biomass and growth advantage of *S. canadensis* (Table 3). Interestingly, the ASVs that were positively correlated with plant biomass and growth advantage of *S. canadensis* all belonged to Glomeraceae, and the ASV that was negatively correlated with growth advantage of *S. canadensis* belonged to Claroideoglomeraceae (Table 3).

Pathways linking P treatment and plant performance

Overall, P treatments had a significant effect on plant performance *via* the modification of multiple AMF traits. P treatments favored plant species growth primarily through increasing alpha diversity of AMF (Figure 6A), which accounted for 59% of the total variance in

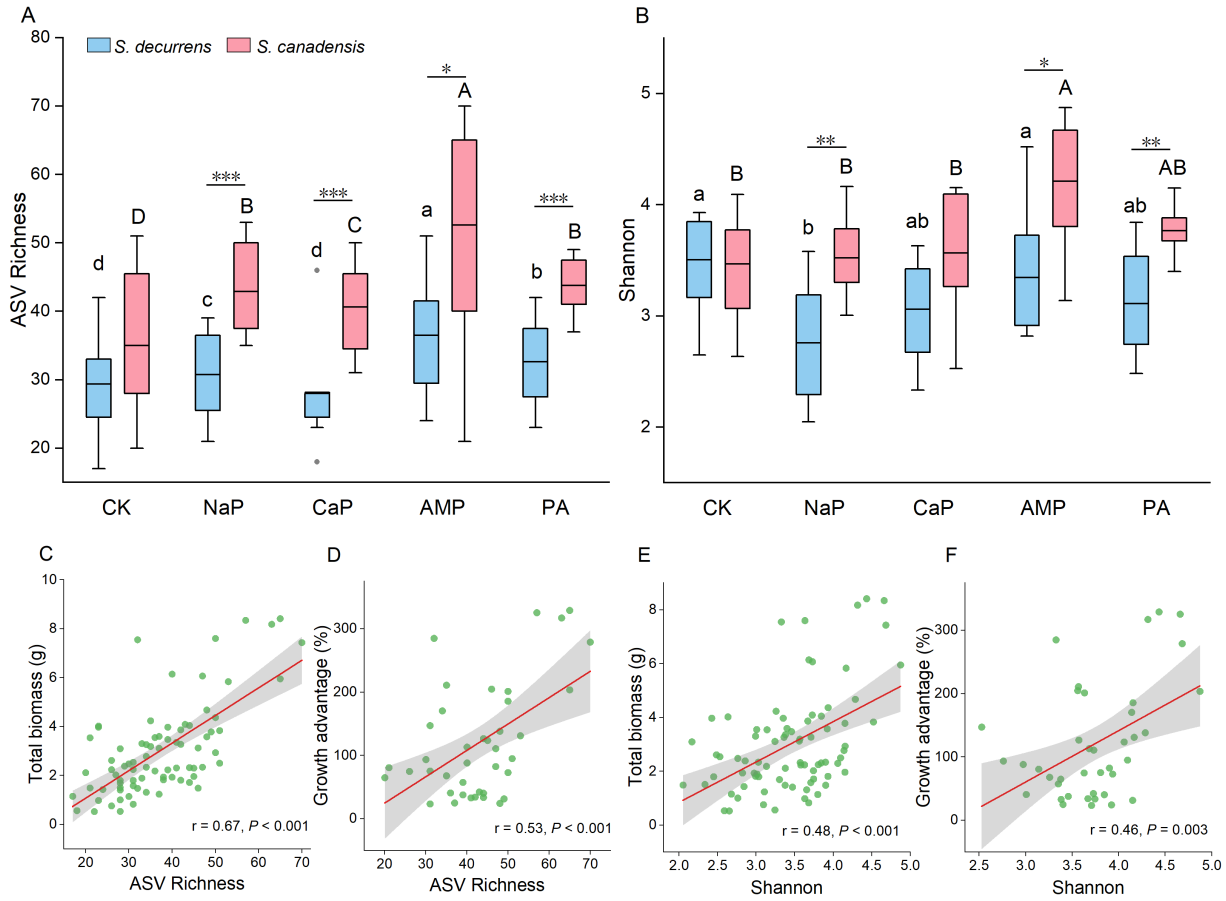

FIGURE 2
The variation of arbuscular mycorrhizal fungi (AMF) **(A)** ASV richness and **(B)** Shannon index in the rhizosphere soil of *S. decurrens* and *S. canadensis* under five P treatments. CK: no P addition; NaP: sodium dihydrogen phosphate; CaP: hydroxyapatite; AMP: adenosine monophosphate; PA: myo-inositol hexakisphosphate. The line in the box represents the median value, box boundaries indicate values in the 25–75th percentile range, whiskers indicate the 95% confidence intervals. The different lower-case letters among *S. decurrens* and different upper-case letters among *S. canadensis* denote significant differences at $p<0.05$. The asterisks denote difference between *S. decurrens* and *S. canadensis* in the same P treatment. *$p<0.05$, **$p<0.01$, ***$p<0.001$. Pearson correlations between ASV richness and **(C)** plant growth, **(D)** growth advantage of *S. canadensis* over *S. decurrens*, Shannon index and **(E)** plant growth, **(F)** growth advantage of *S. canadensis* over *S. decurrens*. The gray ribbons represent the 95% confidence intervals.

plant biomass (Figure 6C). P treatments also enhanced the growth advantage of *S. canadensis* over *S. decurrens* through alterations in keystone species (Figure 6B); this factor had a greater impact on growth advantage than alpha diversity and community structure (Figure 6D).

Discussion

Associations with AMF can influence host plants nutrient absorption and resistance to abiotic stress, further determining the invasion success of exotic plants (Zhang et al., 2017; Awaydul et al., 2019; Yu and He, 2022). In this study, by manipulating P in soils, we found that AMF diversity, community structure, and co-occurrence networks associated with native and invasive *Solidago* species responded distinctly to various P forms, indicating that soil nutrients are important drivers of symbiotic plant-fungal interactions in invasion ecology. P treatments may also affect the growth and invasiveness of invasive *Solidago*, as indicated by its growth advantage, through influencing alpha diversity and keystone taxa in the co-occurrence network of AMF. Together, our results suggest that differences in soil P may result in different interactions between AMF and native and invasive plants, and that multiple AMF traits play a vital role in enhancing *S. canadensis* invasion.

Variations in plant–AMF interactions induced by soil P forms

Soil nutrients mediate interactions between symbiotic fungi and host plants (Qi et al., 2022; Wang et al., 2022), thus variations in the quality and quantity of soil nutrients may modify multiple AMF traits, consequently influencing plant performance. As expected, in this study, increased soil P availability affected the AMF community and promoted plant biomass, and this effect was strongly sensitive to P forms. Our results suggest that organic P facilitated greater AMF diversity and plant biomass than inorganic P for both native and invasive *Solidago* species. Moreover, even at the same level of P for a given species, multiple AMF characteristics, including diversity, certain AMF taxa, and topological features of the network varied

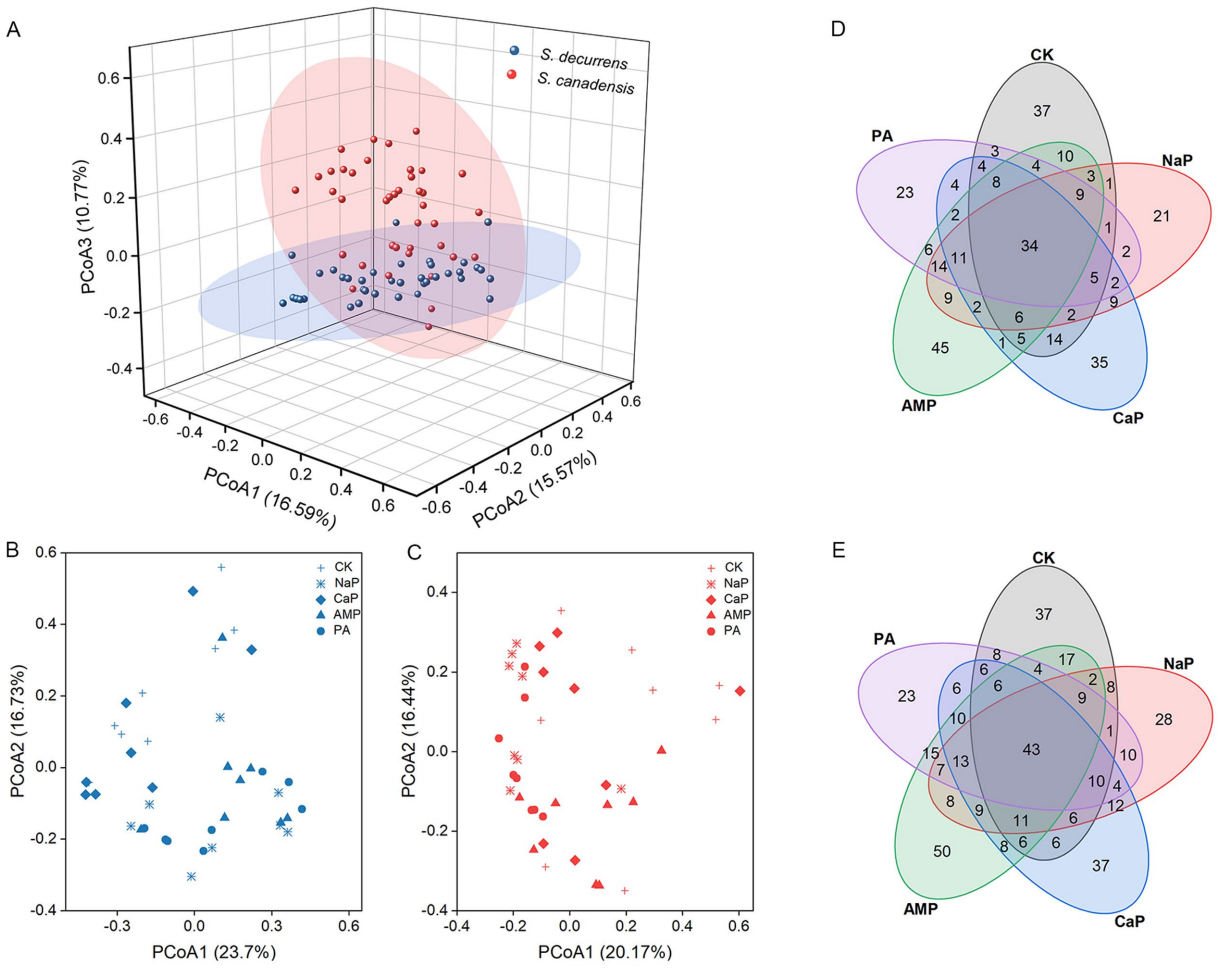

FIGURE 3
(A) Principal coordinates analysis (PCoA) based on the Bray–Curtis distance showing the differences in AMF community structure of *S. decurrens* and *S. canadensis*. Principal coordinates analysis (PCoA) based on the Bray–Curtis distance showing the difference in AMF community structure among five P treatments in **(B)** *S. decurrens* and **(C)** *S. canadensis*. CK: no P addition; NaP: sodium dihydrogen phosphate; CaP: hydroxyapatite; AMP: adenosine monophosphate; PA: myo-inositol hexakisphosphate. Venn diagrams showing the number of shared and unique ASVs among five P treatments in **(D)** *S. decurrens* and **(E)** *S. canadensis*. CK: no P addition; NaP: sodium dihydrogen phosphate; CaP: hydroxyapatite; AMP: adenosine monophosphate; PA: myo-inositol hexakisphosphate.

distinctly to different organic and inorganic P forms. These results support our first hypothesis and the prevailing opinion that plant-fungal interactions are highly context-dependent.

Previous studies showed that plant-AMF interactions were either independent of invasive status (Bunn et al., 2015) or were greater (Sheng et al., 2022; Yu et al., 2022) or weaker (Vogelsang and Bever, 2009) in invaders than natives. In this study, we found that differences in plant-AMF interactions between *S. decurrens* and *S. canadensis* were amplified with greater P availability. Compared with *S. decurrens*, the AMF associated with *S. canadensis* responded to various P sources with greater plasticity in terms of diversity and community composition, potentially allowing *S. canadensis* to maintain a constant growth advantage across a variety of environments. We proposed a couple of scenarios to account for the divergence. First, native and invasive species exhibit a preference for different AMF taxa due to evolutionary and host filtering (Lekberg et al., 2013; Zhang et al., 2017), and may preferentially reward (e.g., provide carbohydrate or fatty acids) more beneficial microbial partners when faced with fluctuating soil nutrients, resulting in shifts in AMF communities (Johnson, 2010). Second, native and invasive plants grown in soil containing heterogeneous forms of P may differ in their plasticity to adjust root architecture and allocation (Yang et al., 2020; Zhang et al., 2022), which both govern interactions with AMF (Bergmann et al., 2020). Third, invasive species may also release greater concentrations of root chemical signaling compounds, such as flavonoids and strigolactones than native species, enhancing communications with mycorrhizal fungi (Inderjit et al., 2021; Yu et al., 2022).

Linkages between AMF traits and plant performance

Microbial alpha diversity, a proxy for functional diversity, is susceptible to soil nutrients (Lang et al., 2022; Wang et al., 2022). In this study, we found a clear increase in AMF richness for *S. canadensis* grown in soil with AMP; these plants also had the highest biomass and growth advantage across all treatments. A greater AMF diversity normally means a stronger functional complementarity, such as

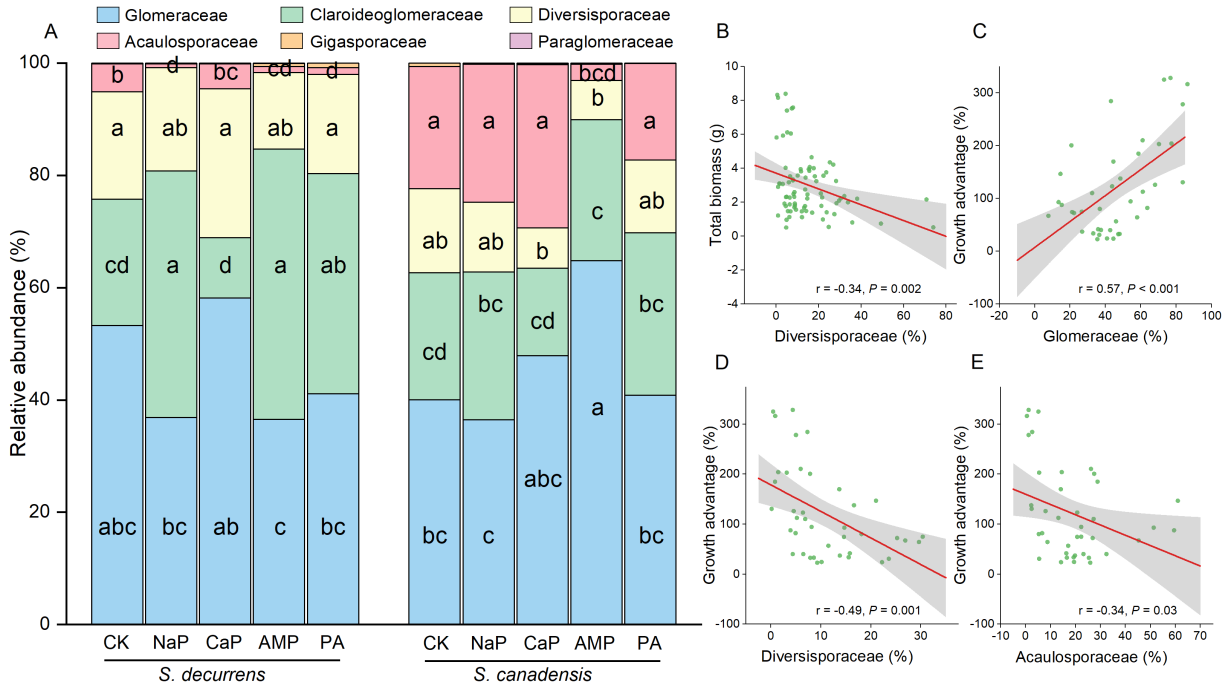

FIGURE 4
(A) Relative abundance of AMF at the family level of *S. decurrens* and *S. canadensis* under five P treatments. CK: no P addition; NaP: sodium dihydrogen phosphate; CaP: hydroxyapatite; AMP: adenosine monophosphate; PA: myo-inositol hexakisphosphate. The different lower-case letters among *S. decurrens* and *S. canadensis* denote significant differences at $p<0.05$. **(B)** Pearson correlations between the relative abundance of Diversisporaceae and plant growth. Pearson correlations between the relative abundance of **(C)** Glomeraceae, **(D)** Diversisporaceae, and **(E)** Acaulosporaceae and the growth advantage of *S. canadensis* over *S. decurrens*. The gray ribbons represent the 95% confidence intervals.

TABLE 1 Two-way analysis of variance (ANOVA) on the effects of plant species and P treatments on relative abundance of AMF at the family level.

Relative abundance (%)	Species (S)		Phosphorous (P)		S×P	
	F	*p*	*F*	*p*	*F*	*p*
Glomeraceae	0.03	0.87	1.59	0.19	2.34	0.06
Claroideoglomeraceae	**8.67**	**0.00**	**8.46**	**<0.001**	**2.82**	**0.03**
Diversisporaceae	**7.79**	**0.01**	1.02	0.41	1.05	0.39
Acaulosporaceae	**129.63**	**<0.001**	**10.80**	**<0.001**	**6.21**	**<0.001**
Gigasporaceae	0.00	0.99	0.38	0.82	1.70	0.16
Paraglomeraceae	0.08	0.78	0.89	0.48	0.86	0.49

Significant effects are shown in bold ($p<0.05$).

occupying a broader resource niche (Loreau and Hector, 2001), and higher community-level soil acid phosphatase and alkaline phosphatase activity (Wang et al., 2014), allowing host plants to use resources more efficiently. In addition, diverse AMF can also enhance communication and cooperation with other microbes, such as phosphate-solubilizing bacteria and diazotrophs (Zhang et al., 2016; Zhu et al., 2018), which may increase P mineralization and nitrogen fixation. These benefits to host plants may determine the positive relationship between AMF diversity and plant growth. Moreover, our path analysis showed that AMF alpha diversity had a greater impact on plant performance than community structure or keystone species in the networks. Together, these results suggest that AMF alpha diversity could be a good predictor of plant growth and invasiveness for *S. canadensis* in a range of soil P environments.

Although there was an association between AMF diversity and plant performance, it should be noted that the non-negligible roles of certain AMF taxa on invasive plant-AMF interactions. For example, Sheng et al. (2022) found that a higher abundance of Glomeraceae in non-native *Conyza canadensis* enhanced their growth in invasive populations to a greater extent than native populations, suggesting specific AMF taxa play important roles in influencing the invasiveness of exotic species. Our results revealed that variations in abundance of Glomeraceae, the predominant taxon in the AMF families, exhibited positive relationship with the growth advantage of *S. canadensis* compared with Diversisporaceae and Acaulosporaceae. Normally, different AMF families have distinct functional traits, which can affect the amount and quality of benefits to their host plants. Previous studies found that Glomeraceae can colonize roots more rapidly, acquire and transport P to host plants more efficiently (de la Providencia et al., 2005; Voets et al., 2006), and grant better protection from pathogens (Powell et al., 2009) than other AMF families. This may partially explain why Glomeraceae appear to contribute

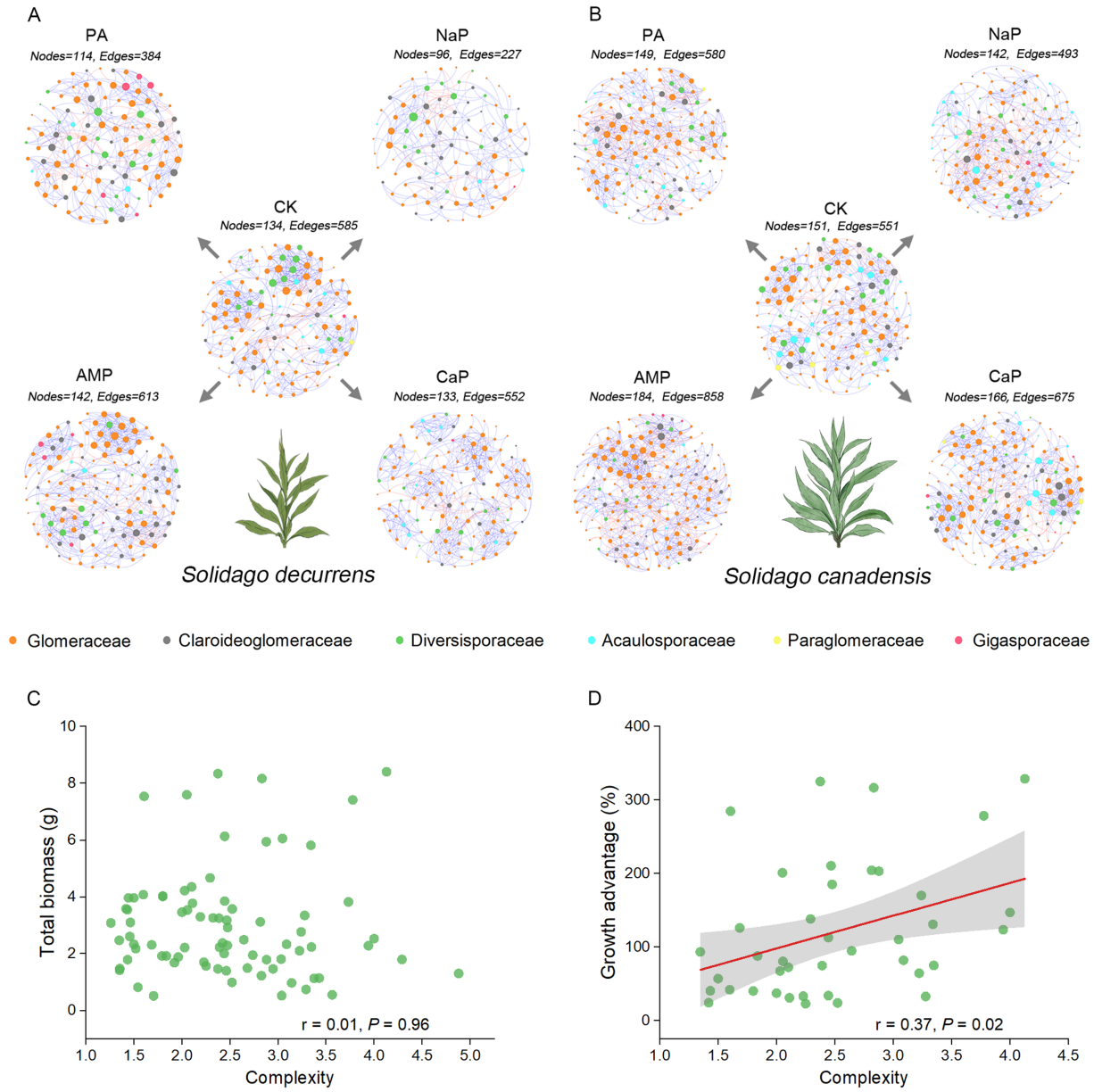

FIGURE 5
The AMF co-occurrence networks of **(A)** *S. decurrens* and **(B)** *S. canadensis* under five P treatments were visualized to show the significant associations (r>0.50, p<0.05) between AMF ASVs. CK: no P addition; NaP: sodium dihydrogen phosphate; CaP: hydroxyapatite; AMP: adenosine monophosphate; PA: myo-inositol hexakisphosphate. Each node represents an ASV, different colors represent different families, the node size represents the degree of the node, and edges denote significant correlations between ASVs (blue: positive correlation; red: negative correlation). Pearson correlations between the complexity of AMF co-occurrence networks and **(C)** plant growth, **(D)** growth advantage of *S. canadensis* over *S. decurrens*. The gray ribbons represent the 95% confidence intervals.

substantially to the invasiveness of *S. canadensis*. Future works involving multiple pairs of invasive and native congeners are needed to better understand how Glomeraceae interact with invasive plants.

Soil microbes rarely exist independently; instead, they are connected to form complex ecological networks that may have a greater influence on plant performance and ecosystem functions than univariate diversity or composition metrics (Chen et al., 2022; Tian et al., 2022). This study demonstrated a positive correlation between AMF network complexity and growth advantage of *S. canadensis*; this is in accordance with a previous study reporting that mycorrhizal networks increased growth and nutrient acquisition of *S. canadensis* over that of native (Awaydul et al., 2019). This indicates that highly connected AMF co-occurrence networks favor invasive species over native species. In addition to network complexity, keystone species in the networks, identified using network topological features, also play an important role in maintaining greater AMF mutualisms on *S. canadensis* than *S. decurrens*. We found that keystone species positively linked to plant biomass occurred more frequently in the AMF network of *S. canadensis* compared to native species. Moreover, the significant relationship between keystone species and growth advantage of *S. canadensis* remained robust when the confounding factors (i.e.,

TABLE 2 Topological features of the AMF co-occurrence network of two *Solidago* species under five P treatments.

Topological features	CK	NaP	CaP	AMP	PA
S. decurrens					
Nodes	134	96	133	142	114
Edge	585	227	552	613	384
Average degree	8.73	4.73	8.3	8.63	6.74
Average clustering coefficient	0.65	0.42	0.65	0.54	0.52
Positive correlations (%)	91.62	83.26	93.48	89.07	84.11
Negative correlations (%)	8.38	16.74	6.52	10.93	15.89
Density	0.07	0.05	0.06	0.06	0.06
Modularity	0.75	0.65	0.77	0.73	0.69
Complexity	4.37	2.36	4.15	4.32	3.37
Number of keystone species	4	3	2	5	9
S. canadensis					
Nodes	151	142	166	184	149
Edge	551	493	675	858	580
Average degree	7.30	6.94	8.13	9.33	7.79
Average clustering coefficient	0.53	0.48	0.54	0.52	0.55
Positive correlations (%)	91.10	77.28	87.41	78.09	73.97
Negative correlations (%)	8.89	22.72	12.59	21.91	26.03
Density	0.05	0.05	0.05	0.05	0.05
Modularity	0.74	0.64	0.73	0.66	0.70
Complexity	3.65	3.47	4.07	4.66	3.89
Number of keystone species	2	7	7	9	8

CK, no P addition; NaP, sodium dihydrogen phosphate; CaP, hydroxyapatite; AMP, adenosine monophosphate; PA, myo-inositol hexakisphosphate.

TABLE 3 Pearson correlations between keystone species abundance and plant growth, growth advantage of *S. canadensis*.

ASVID	Family	Total biomass		Growth advantage	
		r	*p*	*r*	*p*
ASV307	Glomeraceae	**0.30**	**0.01**	-	-
ASV721	Glomeraceae	**0.25**	**0.03**	-	-
ASV28	Glomeraceae	**0.44**	**<0.001**	**0.50**	**<0.001**
ASV95	Glomeraceae	**0.26**	**0.02**	0.19	0.25
ASV160	Glomeraceae	**0.26**	**0.02**	0.24	0.14
ASV240	Glomeraceae	**0.49**	**<0.001**	**0.47**	**0.002**
ASV354	Glomeraceae	**0.30**	**0.01**	**0.50**	**<0.001**
ASV609	Glomeraceae	**0.42**	**<0.001**	**0.32**	**0.045**
ASV830	Glomeraceae	**0.40**	**<0.001**	**0.42**	**0.008**
ASV1668	Glomeraceae	**0.28**	**0.01**	0.13	0.41
ASV63	Claroideoglomeraceae	−0.05	0.66	**−0.45**	**0.004**

Significant correlations are shown in bold ($p < 0.05$).

alpha diversity and community structure) were controlled for in the path analysis. In addition, all the keystone species that were positively correlated with plant biomass and growth advantage in *S. canadensis* belonged to Glomeraceae, an AMF family that has been reported to enhance invasive plant growth previously (Sheng et al., 2022). Thus, the more substantial effects of keystone species on the growth advantage in *S. canadensis*, relative to other AMF traits, implies that the symbiotic fungus-mediated invasiveness of exotic species is likely enhanced by key individual taxa rather than the whole community.

Together, these findings supported our second hypothesis that a variety of AMF traits induced by different soil P sources contribute differently to plant growth and growth advantage in *S. canadensis*. However, it should be noted that other mycorrhizal traits, such as mycorrhizal colonization and hyphal length density, may also contribute to the superior performance of invasive species. Thus, our work highlights the necessity to disentangle the effects of multiple mycorrhizal traits on plant invasion in further studies. Furthermore, although this study focused primarily on the effect of different forms of P on invasive plant-AMF interactions, the soil nutrient availability may also have a role (Chen et al., 2020). Notwithstanding these points, our findings may have some implications for exotic species management strategies, and could improve understanding of the microbiome-related mechanisms underpinning the invasion success of exotic plants for a number of reasons. First, P fractions vary by ecosystem (Song et al., 2007; Azene et al., 2022). We found that organic P facilitated growth of the invasive *Solidago* to a greater extent than inorganic P, which is in accordance with previous studies (Yang et al., 2020; Zhang et al., 2022). Accordingly, ecosystems with higher organic P might carry a higher risk of plant invasion. Second, microbial-based invasive plant management has been suggested as a novel tool for controlling invasive plants (Shahrtash and Brown, 2021). In this study, keystone species had the strongest effect on the growth advantage of *S. canadenis*, which means keystone species play a potential functional role in plant invasion. This is consistent with a recent study that reported keystone species contributed to invader tolerance to biotic stressors (Xu et al., 2022). Therefore, identifying keystone species that disrupt nutrient absorption and facilitate disease development in invasive plants could enable a microbial invasive plant management strategy. Finally, AMF enable a better performance of invader over congeneric native species through multiple dimension traits, which previous studies have not investigated. Future studies should address the correlations between different AMF traits and plant invasions.

In summary, our results show that plant growth, growth advantage of invasive species, and AMF traits vary with the form of soil P. Furthermore, differences in AMF traits with different sources of P have different effects on plant growth and growth advantage of *S. canadensis*. These results indicate that the AMF community mediates plant growth and growth advantage under different nutrient conditions, highlighting the importance of environmental context on plant invasions. They also emphasize the relative contribution of microbial community composition and their interconnections in enhancing the environmental adaptability of invasive plants. A more detailed understanding of the mechanism by which AMF communities are altered depending on the P forms in the soil will help guide invasive plant management. Future experiments that simultaneously consider AMF community, mycorrhizal association and hyphal density will contribute to a

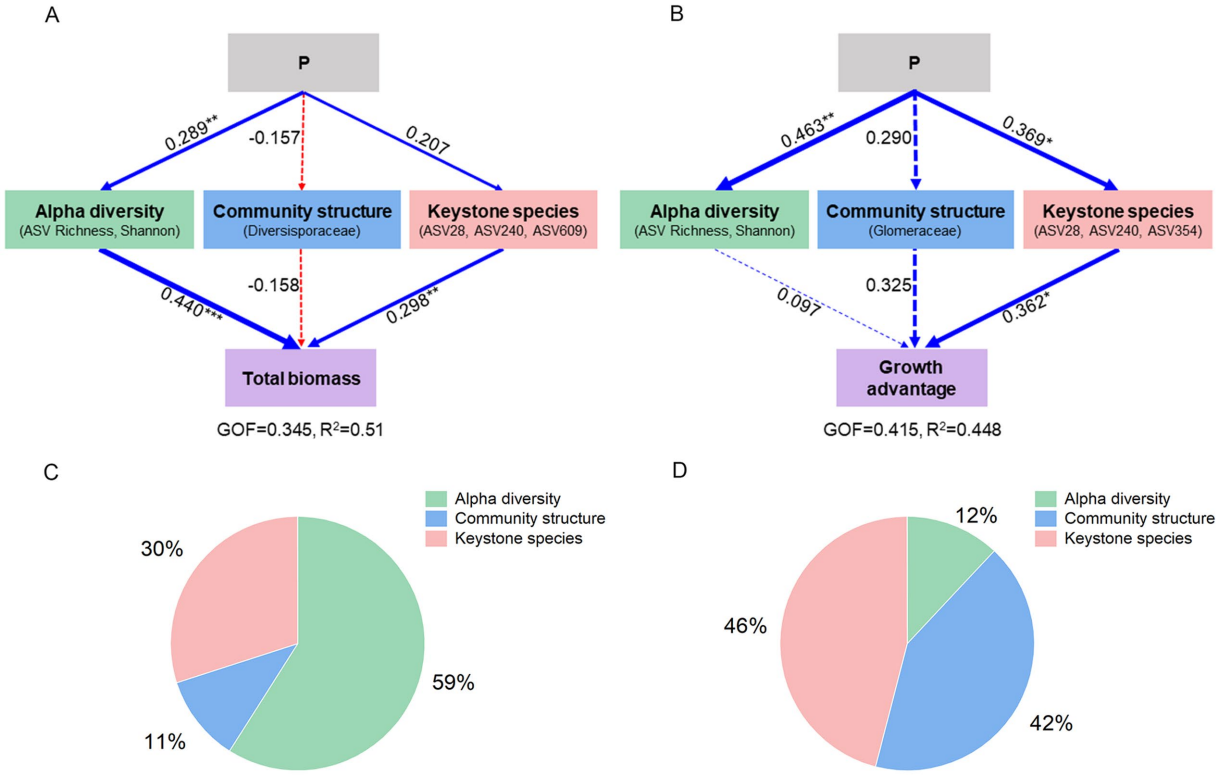

FIGURE 6
Path models showing the effects of P treatments on **(A)** plant growth and **(B)** growth advantage of *S. canadensis* over *S. decurrens* through alpha diversity, community structure and keystone species of the AMF. The line size represents the value of the path coefficient. The solid and dash lines represent significant and non-significant relationship. Blue lines represent positive effects, red lines represent negative effects. The asterisks denote the significance of path coefficient. *p<0.05, **p<0.01, ***p<0.001. The final models fit the data well, as assessed using GOF and R^2. The relative contribution of AMF latent variables to global explained observed variability (R^2) of the **(C)** total biomass of two *Solidago* species and **(D)** growth advantage of *S. canadensis* over *S. decurrens*.

better understanding of the role of soil microbes and nutrients in invasion success of exotic species.

Data availability statement

The datasets presented in this study can be found in online repositories. The names of the repository/repositories and accession number(s) can be found at: https://www.ncbi.nlm.nih.gov/, PRJNA922727.

Author contributions

HY designed the study. LC, MW, PM, and YX conducted the experiments. LC and HY analyzed the data and wrote the manuscript. JD and YS revised the manuscript. All authors discussed the results and approved the final manuscript.

Funding

This work was supported by the National Natural Science Foundation of China (32001233 and U21A20190), and the China Postdoctoral Science Foundation (2019 M662526).

Acknowledgments

We are grateful for the assistance of all staff members in the Biotic Interaction and Biosecurity Laboratory, Henan University at Kaifeng, Henan, China.

Conflict of interest

The authors declare that the research was conducted in the absence of any commercial or financial relationships that could be construed as a potential conflict of interest.

Publisher's note

Supplementary material

The Supplementary material for this article can be found online at: https://www.frontiersin.org/articles/10.3389/fmicb.2023.1160631/full#supplementary-material

References

Awaydul, A., Zhu, W. Y., Yuan, Y. G., Xiao, J., Hu, H., Chen, X., et al. (2019). Common mycorrhizal networks influence the distribution of mineral nutrients between an invasive plant, *Solidago canadensis*, and a native plant, *Kummerowia striata*. *Mycorrhiza* 29, 29–38. doi: 10.1007/s00572-018-0873-5

Azene, B., Qiu, P., Zhu, R. H., Pan, K. W., Sun, X. M., Nigussie, Y., et al. (2022). Response of soil phosphorus fractions to land use change in the subalpine ecosystems of southeast margin of Qinghai-Tibet plateau, Southwest China. *Ecol. Indic.* 144:109432. doi: 10.1016/j.ecolind.2022.109432

Bastian, M., Heymann, S., and Jacomy, M. (2009). Gephi: An open source software for exploring and manipulating networks. *Proc. Int. AAAI Conf. Web Soc. Med.* 3, 361–362. doi: 10.1609/icwsm.v3i1.13937

Basu, S., Rabara, R. C., and Negi, S. (2018). AMF: the future prospect for sustainable agriculture. *Physiol. Mol. Plant Pathol.* 102, 36–45. doi: 10.1016/j.pmpp.2017.11.007

Bergmann, J., Weigelt, A., Plas, F., Laughlin, D. C., and Mommer, L. (2020). The fungal collaboration gradient dominates the root economics space in plants. *Sci. Adv.* 6:eaba3756. doi: 10.1101/2020.01.17.908905

Bolyen, E., Rideout, J. R., Dillon, M. R., Bokulich, N. A., Abnet, C. C., Al-Ghalith, G. A., et al. (2019). Reproducible, interactive, scalable and extensible microbiome data science using QIIME 2. *Nat. Biotechnol.* 37, 852–857. doi: 10.1038/s41587-019-0209-9

Bunn, R. A., Ramsey, P. W., and Lekberg, Y. (2015). Do native and invasive plants differ in their interactions with arbuscular mycorrhizal fungi? A meta-analysis. *J. Ecol.* 103, 1547–1556. doi: 10.1111/1365-2745.12456

Callahan, B. J., McMurdie, P. J., Rosen, M. J., Han, A. W., Johnson, A. J. A., and Holmes, S. P. (2016). DADA2: high resolution sample inference from Illumina amplicon data. *Nat. Methods* 13, 581–583. doi: 10.1038/nmeth.3869

Cao, Y. P., Wu, X. F., Zhukova, A., Tang, Z. H., Weng, Y., Li, Z. X., et al. (2020). Arbuscular mycorrhizal fungi (AMF) species and abundance exhibit different effects on saline-alkaline tolerance in *Leymus chinensis*. *J. Plant Interact.* 15, 266–279. doi: 10.1080/17429145.2020.1802524

Chaudhary, V. B., Holland, E. P., Charman-Anderson, S., Guzman, A., Bell-Dereske, L., Cheeke, T. E., et al. (2022). What are mycorrhizal traits? *Trends Ecol. Evol.* 37, 573–581. doi: 10.1016/j.tree.2022.04.003

Chen, E. J., Liao, H. X., Chen, B. M., and Peng, S. L. (2020). Arbuscular mycorrhizal fungi are a double-edged sword in plant invasion controlled by phosphorus concentration. *New Phytol.* 226, 295–300. doi: 10.1111/nph.16359

Chen, W. Q., Wang, J. Y., Chen, X., Meng, Z. X., Xu, R., Duoji, D. Z., et al. (2022). Soil microbial network complexity predicts ecosystem function along elevation gradients on the Tibetan plateau. *Soil Biol. Biochem.* 172:108766. doi: 10.1016/j.soilbio.2022.108766

Chen, Q., Wu, W. W., Qi, S. S., Cheng, H., Li, Q., Ran, Q., et al. (2021). Arbuscular mycorrhizal fungi improve the growth and disease resistance of the invasive plant *Wedelia trilobata*. *J. Appl. Microbiol.* 130, 582–591. doi: 10.1111/jam.14415

de la Providencia, I. E., de Souza, F. A., Fernández, F., Delmas, N. S., and Declerck, S. (2005). Arbuscular mycorrhizal fungi reveal distinct patterns of anastomosis formation and hyphal healing mechanisms between different phylogenic groups. *New Phytol.* 165, 261–271. doi: 10.1111/j.1469-8137.2004.01236.x

Dong, M., Lu, J. Z., Zhang, W. J., Chen, J. K., and Li, B. (2006a). Canada goldenrod (*Solidago canadensis*): an invasive alien weed rapidly spreading in China. *Acta Phytotaxon. Sin.* 44, 72–85. doi: 10.1360/aps050068

Dong, M., Lu, B. R., Zhang, H. B., Chen, J. K., and Li, B. (2006b). Role of sexual reproduction in the spread of an invasive clonal plant *Solidago canadensis* revealed using intersimple sequence repeat markers. *Plant Species Biol.* 21, 13–18. doi: 10.1111/j.1442-1984.2006.00146.x

Enders, M., Havemann, F., Ruland, F., Bernard-Verdier, M., Catford, J. A., Gómez-Aparicio, L., et al. (2020). A conceptual map of invasion biology: integrating hypotheses into a consensus network. *Glob. Ecol. Biogeogr.* 29, 978–991. doi: 10.1111/geb.13082

Esterhuizen, N., Forrester, J., Esler, K. J., Wigley-Coetzee, C., and Valentine, A. J. (2020). Nitrogen and phosphorus influence *Acacia saligna* invasiveness in the fynbos biome. *Plant Ecol.* 221, 309–320. doi: 10.1007/s11258-020-01010-7

Feng, K., Peng, X., Zhang, Z., Gu, S. S., He, Q., Shen, W. L., et al. (2022). iNAP: an integrated network analysis pipeline for microbiome studies. *iMeta* 1:e13. doi: 10.1002/imt2.13

Frew, A. (2022). Root herbivory reduces species richness and alters community structure of root-colonising arbuscular mycorrhizal fungi. *Soil Biol. Biochem.* 171:108723. doi: 10.1016/j.soilbio.2022.108723

Grman, E., and Robinson, T. M. P. (2013). Resource availability and imbalance affect plant–mycorrhizal interactions: a field test of three hypotheses. *Ecology* 94, 62–71. doi: 10.1890/12-0385.1

Inderjit, S. D., Kaur, H., Kalisz, S., and Bezemer, T. M. (2021). Novel chemicals engender myriad invasion mechanisms. *New Phytol.* 232, 1184–1200. doi: 10.1111/nph.17685

Johnson, N. C. (2010). Resource stoichiometry elucidates the structure and function of arbuscular mycorrhizas across scales. *New Phytol.* 185, 631–647. doi: 10.1111/j.1469-8137.2009.03110.x

Lamit, L. J., Giovati, A. S., Jo, I., Frank, D. A., and Fridley, J. D. (2022). Woody invaders are more highly colonized by arbuscular mycorrhizal fungi than congeneric native species. *Am. J. Bot.* 109, 655–663. doi: 10.1002/ajb2.1839

Lang, M., Zhang, C. Y., Su, W. H., Chen, X. X., Zou, C. Q., and Chen, X. P. (2022). Long-term P fertilization significantly altered the diversity, composition and mycorrhizal traits of arbuscular mycorrhizal fungal communities in a wheat-maize rotation. *Appl. Soil Ecol.* 170:104261. doi: 10.1016/j.apsoil.2021.104261

Lekberg, Y., Gibbons, S., Rosendahl, S., and Ramsey, P. W. (2013). Severe plant invasions can increase mycorrhizal fungal abundance and diversity. *ISME J.* 7, 1424–1433. doi: 10.1038/ismej.2013.41

Liang, J. F., An, J., Gao, J. Q., Zhang, X. Y., Song, M. H., and Yu, F. H. (2019). Interactive effects of biochar and AMF on plant growth and greenhouse gas emissions from wetland microcosms. *Geoderma* 346, 11–17. doi: 10.1016/j.geoderma.2019.03.033

Livingstone, S. W., Isaac, M. E., and Cadotte, M. W. (2020). Invasive dominance and resident diversity: unpacking the impact of plant invasion on biodiversity and ecosystem function. *Ecol. Monogr.* 90:e01425. doi: 10.1002/ecm.1425

Loreau, M., and Hector, A. (2001). Partitioning selection and complementarity in biodiversity experiments. *Nature* 412, 72–76. doi: 10.1038/35083573

Lumini, E., Orgiazzi, A., Borriello, R., Bonfante, P., and Bianciotto, V. (2010). Disclosing arbuscular mycorrhizal fungal biodiversity in soil through a land-use gradient using a pyrosequencing approach. *Environ. Microbiol.* 12, 2165–2179. doi: 10.1111/j.1462-2920.2009.02099.x

Ma, X. C., Geng, Q. H., Zhang, H. G., Bian, C. Y., Chen, H. Y. Y., Jiang, D. L., et al. (2020). Global negative effects of nutrient enrichment on arbuscular mycorrhizal fungi, plant diversity and ecosystem multifunctionality. *New Phytol.* 229, 2957–2969. doi: 10.1111/nph.17077

Majewska, M. L., Rola, K., and Zubek, S. (2017). The growth and phosphorus acquisition of invasive plants *Rudbeckia laciniata* and *Solidago gigantea* are enhanced by arbuscular mycorrhizal fungi. *Mycorrhiza* 27, 83–94. doi: 10.1007/s00572-016-0729-9

Mathur, S., Tomar, R. S., and Jajoo, A. (2019). Arbuscular mycorrhizal fungi (AMF) protects photosynthetic apparatus of wheat under drought stress. *Photosyn. Res.* 139, 227–238. doi: 10.1007/s11120-018-0538-4

Mendiburu, F. (2021). *Agricolae: Statistical Procedures for Agricultural Research*. R Package Version 1.3.5. Available at: https://CRAN.R-project.org/package=agricolae (Accessed October 30, 2022).

Oksanen, J., Simpson, G., Bianchet, F., Kindt, R., Legendre, P., Minchin, P., et al. (2022). *Vegan: Community Ecology Package*. R Package Version 2.6.2. Available at: https://CRAN.R-project.org/package=vegan (Accessed October 30, 2022).

Pearse, S. J., Veneklaas, E. J., Cawthray, G., Bolland, M. D. A., and Lambers, H. (2007). Carboxylate composition of root exudates does not relate consistently to a crop species' ability to use phosphorus from aluminium, iron or calcium phosphate sources. *New Phytol.* 173, 181–190. doi: 10.1111/j.1469-8137.2006.01897.x

Powell, J. R., Parrent, J. L., Hart, M. M., Klironomos, J. N., Rillig, M. C., and Maherali, H. (2009). Phylogenetic trait conservatism and the evolution of functional trade-offs in arbuscular mycorrhizal fungi. *Proc. R. Soc. Biol. Sci.* 276, 4237–4245. doi: 10.1098/rspb.2009.1015

Qi, S. S., Wang, J. H., Wan, L. Y., Dai, Z. C., da Silva Matos, D. M., Du, D. L., et al. (2022). Arbuscular mycorrhizal fungi contribute to phosphorous uptake and allocation strategies of *Solidago canadensis* in a phosphorous-deficient environment. *Front. Plant Sci.* 13:831654. doi: 10.3389/fpls.2022.831654

R Core Team. (2022). *R: A Language and Environment for Statistical Computing*. Vienna, Austria: R Foundation for Statistical Computing. Available at: https://www.R-project.org.

Rai, P. K., and Singh, J. S. (2020). Invasive alien plant species: their impact on environment, ecosystem services and human health. *Ecol. Indic.* 111:106020. doi: 10.1016/j.ecolind.2019.106020

Reinhart, K. O., and Callaway, R. M. (2006). Soil biota and invasive plants. *New Phytol.* 170, 445–457. doi: 10.1111/j.1469-8137.2006.01715.x

Sanchez, G. (2013). *PLS Path Modeling with R*. Trowchez Editions, Berkeley

Sanchez, G., Trinchera, L., and Russolillo, G. (2017). *Plspm: Tools for Partial Least Squares Path Modeling (PLS–PM)*. R Package Version 0.9. Available at: https://cran.r-project.org/src/contrib/Archive/plspm/ (Accessed October 30, 2022).

Schröder, R., Mohri, M., and Kiehl, K. (2019). AMF inoculation of green roof substrate improves plant performance but reduces drought resistance of native dry grassland species. *Ecol. Eng.* 139:105583. doi: 10.1016/j.ecoleng.2019.105583

Shahrtash, M., and Brown, S. P. (2021). A path forward: promoting microbial-based methods in the control of invasive plant species. *Plan. Theory* 10:943. doi: 10.3390/plants10050943

Sheng, M., Rosche, C., Al-Gharaibeh, M., Bullington, L. S., Callaway, R. M., Clark, T., et al. (2022). Acquisition and evolution of enhanced mutualism—an underappreciated mechanism for invasive success? *ISME J.* 16, 2467–2478. doi: 10.1038/s41396-022-01293-w

Shi, Y., Zhang, K. P., Ma, T. T., Zhang, Z. Y., Li, P., Xing, Z. L., et al. (2022). Foliar herbivory reduces rhizosphere fungal diversity and destabilizes the co-occurrence network. *Front. Microbiol.* 13:846332. doi: 10.3389/fmicb.2022.846332

Song, C., Han, X. Z., and Tang, C. (2007). Changes in phosphorus fractions, sorption and release in udic Mollisols under different ecosystems. *Biol. Fertil. Soils* 44, 37–47. doi: 10.1007/s00374-007-0176-z

Tenenhaus, M., Esposito, V., Chatelin, Y. M., and Lauro, C. (2005). PLS path modeling. *Comput. Stat. Data Anal.* 48, 159–205. doi: 10.1016/j.csda.2004.03.005

Tian, B. L., Zhu, M. K., Pei, Y. C., Ran, G. Y., Shi, Y., and Ding, J. Q. (2022). Climate warming alters the soil microbial association network and role of keystone taxa in determining wheat quality in the field. *Agric. Ecosyst. Environ.* 326:107817. doi: 10.1016/j.agee.2021.107817

UI Haq, J., Sharif, M., Ali Akbar, W., Ur Rahim, H., Ahmad Mian, I., Ahmad, S., et al. (2022). Arbuscular mycorrhiza fungi integrated with single super phosphate improve wheat-nitrogen-phosphorus acquisition, yield, root infection activity, and spore density in alkaline-calcareous soil. *Gesunde Pflanz.* 1–10. doi: 10.1007/s10343-022-00718-y

Voets, L., de la Providencia, I. E., and Declerck, S. (2006). Glomeraceae and Gigasporaceae differ in their ability to form hyphal networks. *New Phytol.* 172, 185–188. doi: 10.2307/4091488

Vogelsang, K. M., and Bever, J. D. (2009). Mycorrhizal densities decline in association with nonnative plants and contribute to plant invasion. *Ecology* 90, 399–407. doi: 10.1890/07-2144.1

Vogelsang, K. M., Reynolds, H. L., and Bever, J. D. (2006). Mycorrhizal fungal identity and richness determine the diversity and productivity of a tallgrass prairie system. *New Phytol.* 172, 554–562. doi: 10.1111/j.1469-8137.2006.01854.x

Wang, Q., Bao, Y. Y., Liu, X. W., and Du, G. X. (2014). Spatio-temporal dynamics of arbuscular mycorrhizal fungi associated with glomalin-related soil protein and soil enzymes in different managed semiarid steppes. *Mycorrhiza* 24, 525–538. doi: 10.1007/s00572-014-0572-9

Wang, G. Z., Koziol, L., Foster, B. L., and Bever, J. D. (2022). Microbial mediators of plant community response to long-term N and P fertilization: evidence of a role of plant responsiveness to mycorrhizal fungi. *Glob. Chang. Biol.* 28, 2721–2735. doi: 10.1111/gcb.16091

Xiang, D., Verbruggen, E., Hu, Y. J., Veresoglou, S. D., Rillig, M. C., Zhou, W. P., et al. (2014). Land use influences arbuscular mycorrhizal fungal communities in the farming-pastoral ecotone of northern China. *New Phytol.* 204, 968–978. doi: 10.1111/nph.12961

Xu, Z. W., Guo, X., Allen, W. J., Li, M. Y., and Guo, W. H. (2022). Native tree root exudates promote tolerance of simulated herbivory of an invasive tree via altered functional traits. *Plant Soil* 479, 389–404. doi: 10.1007/s11104-022-05528-9

Yang, J. X., Peng, Y., and He, W. M. (2020). Organic and inorganic phosphorus differentially influence invasive forbs. *Flora* 263:151532. doi: 10.1016/j.flora.2019.151532

Yu, H. W., and He, W. M. (2017). Negative legacy effects of rainfall and nitrogen amendment on leaf lifespan of steppe species. *J. Plant Ecol.* 10, rtw090–rtw838. doi: 10.1093/jpe/rtw090

Yu, H. W., and He, W. M. (2022). Arbuscular mycorrhizal fungi compete asymmetrically for amino acids with native and invasive *Solidago*. *Microb. Ecol.* 84, 131–140. doi: 10.1007/s00248-021-01841-5

Yu, H. W., He, Y. Y., Zhang, W., Chen, L., Zhang, J. L., Zhang, X. B., et al. (2022). Greater chemical signaling in root exudates enhances soil mutualistic associations in invasive plants compared to natives. *New Phytol.* 236, 1140–1153. doi: 10.1111/nph.18289

Zhang, F. J., Li, Q., Chen, F. X., Xu, H. Y., Inderjit, I., and Wan, F. H. (2017). Arbuscular mycorrhizal fungi facilitate growth and competitive ability of an exotic species *Flaveria bidentis*. *Soil Biol. Biochem.* 115, 275–284. doi: 10.1016/j.soilbio.2017.08.019

Zhang, Z., Pan, M. X., Zhang, X., and Liu, Y. J. (2022). Responses of invasive and native plants to different forms and availability of phosphorus. *Am. J. Bot.* 109, 1560–1567. doi: 10.1002/ajb2.16081

Zhang, L., Xu, M. G., Liu, Y., Zhang, F. S., Hodge, A., and Feng, G. (2016). Carbon and phosphorus exchange may enable cooperation between an arbuscular mycorrhizal fungus and a phosphate-solubilizing bacterium. *New Phytol.* 210, 1022–1032. doi: 10.1111/nph.13838

Zhu, C., Tian, G. L., Luo, G. W., Kong, Y. L., Guo, J. J., Wang, M., et al. (2018). N-fertilizer-driven association between the arbuscular mycorrhizal fungal community and diazotrophic community impacts wheat yield. *Agric. Ecosyst. Environ.* 254, 191–201. doi: 10.1016/j.agee.2017.11.02

frontiers | Frontiers in Microbiology

TYPE Original Research
PUBLISHED 02 June 2023
DOI 10.3389/fmicb.2023.1131797

OPEN ACCESS

EDITED BY
Kai Sun,
Nanjing Normal University, China

REVIEWED BY
Xin Qian,
Fujian Agriculture and Forestry University, China
Xianan Xie,
South China Agricultural University, China
Jesús Muñoz-Rojas,
Meritorious Autonomous University of Puebla, Mexico

*CORRESPONDENCE
Furong Gui
furonggui18@sina.com

†These authors share first authorship

RECEIVED 26 December 2022
ACCEPTED 15 May 2023
PUBLISHED 02 June 2023

CITATION
Du E, Chen Y, Li Y, Li Y, Sun Z, Hao R and Gui F (2023) Effects of *Septoglomus constrictum* and *Bacillus cereus* on the competitive growth of *Ageratina adenophora*. *Front. Microbiol.* 14:1131797. doi: 10.3389/fmicb.2023.1131797

Effects of *Septoglomus constrictum* and *Bacillus cereus* on the competitive growth of *Ageratina adenophora*

Ewei Du[1†], Yaping Chen[1†], Yang Li[2], Yahong Li[3], Zhongxiang Sun[1], Ruoshi Hao[4] and Furong Gui[1,2*]

[1]State Key Laboratory for Conservation and Utilization of Bioresources in Yunnan, College of Plant Protection, Yunnan Agricultural University, Kunming, China, [2]Graduate School, Yunnan Agricultural University, Kunming, China, [3]Yunnan Plant Protection and Quarantine Station, Kunming, China, [4]Yunnan Plateau Characteristic Agriculture Industry Research Institute, Kunming, China

Beneficial microorganisms play a pivotal role in the invasion process of exotic plants, including arbuscular mycorrhizal fungi (AMF) and *Bacillus*. However, limited research exists on the synergistic influence of AMF and *Bacillus* on the competition between both invasive and native plants. In this study, pot cultures of *Ageratina adenophora* monoculture, *Rabdosia amethystoides* monoculture, and *A. adenophora* and *R. amethystoides* mixture were used to investigate the effects of dominant AMF (*Septoglomus constrictum*, SC) and *Bacillus cereus* (BC), and the co-inoculation of BC and SC on the competitive growth of *A. adenophora*. The results showed that inoculation with BC, SC, and BC+SC significantly increased the biomass of *A. adenophora* by 14.77, 112.07, and 197.74%, respectively, in the competitive growth between *A. adenophora* and *R. amethystoides*. Additionally, inoculation with BC increased the biomass of *R. amethystoides* by 185.07%, while inoculation with SC or BC+SC decreased *R. amethystoides* biomass by 37.31 and 59.70% compared to the uninoculated treatment. Inoculation with BC significantly increased the nutrient contents in the rhizosphere soil of both plants and promoted their growth. Inoculation with SC or SC+BC notably increased the nitrogen and phosphorus contents of *A. adenophora*, therefore enhancing its competitiveness. Compared with single inoculation, dual inoculation with SC and BC increased AMF colonization rate and *Bacillus* density, indicating that SC and BC can form a synergistic effect to further enhance the growth and competitiveness of *A. adenophora*. This study reveals the distinct role of *S. constrictum* and *B. cereus* during the invasion of *A. adenophora*, and provide new clues to the underlying mechanisms of interaction between invasive plant, AMF and *Bacillus*.

KEYWORDS

***Ageratina adenophora*, arbuscular mycorrhizal fungi, *Bacillus*, synergistic inoculation, competitive advantage**

1. Introduction

The invasion of exotic plants has resulted in a rapid decline in global biodiversity (Powell et al., 2013), with severe implications on the functioning of the whole ecosystem function (Richardson and Pyšek, 2012) and incurring significant economic losses. Thus, understanding the invasion mechanisms of these plants has emerged as a pressing and pragmatic concern (Sol et al., 2012; Anna et al., 2020). The spreading capacity in their new habitat is at least partly influenced by their association with symbiotic microorganisms (Fahey and Stephen, 2022).

Beneficial symbiotic microorganisms regulate competitive growth between invasive and native plants (Abbott et al., 2015; Dawson et al., 2016). The Enhanced Mutualisms Hypothesis (EMP) suggests that invasive plants facilitate positive soil feedback by enriching their associated beneficial symbiotic microbes, thereby promoting their own growth and expansion (D'Antonio et al., 2017; Zhang et al., 2020). In contrast, the Degraded Mutualisms Hypothesis (DMP) proposes that exotic plants can weaken the symbiotic relationship between beneficial microbes and native plants, creating a competitive disadvantage for the latter and facilitating the successful invasion of invasive plants (Vogelsang and Bever, 2009).

Arbuscular mycorrhizal fungi (AMF) can form a mutualistic symbiosis with most terrestrial plants to adapt better to limited nutrient supply conditions (Smith and Smith, 2011). In most nutrient-poor soils, the low availability of nitrogen and phosphorus is often the main limiting factor affecting plant growth (Xu et al., 2012). AMF is reported to dominate the uptake of phosphate, ammonium and nitrate nitrogen uptake in symbiotic plants (Fan et al., 2020; Wang et al., 2020; Xie et al., 2022). Accumulating evidence suggests that AMF can develop symbiosis with invasive plants, which greatly contributes to the successful invasion of invasive plants (Lekberg et al., 2013; Aslani et al., 2019). AMF enhances the resistance of invasive plants to biotic and abiotic stresses, thus promoting the establishment of invasive plants in their new habitats (Dickie et al., 2017; Qi et al., 2022). The exotic plants affect AMF abundance and richness (Zhang et al., 2017; Kong et al., 2022). When invasive plants grow alongside native plants, the mycorrhizal colonization rate of the invasive plants increases while that of the native plants decreases, giving invasive plants a competitive advantage over native plants (Zhang et al., 2018). AMF forms a common mycorrhizal network (CMN) that allows the plant-to-plant transfer of carbon and mineral nutrients between native plants and alien plants (Weremijewicz et al., 2018; Awaydul et al., 2019). Therefore, AMFs are more beneficial to invasive plants than native species, which may be a key factor in the successful invasion of exotic plants.

Bacillus is an important plant growth-promoting rhizobacteria (PGPR). Most *Bacillus* have many beneficial effects on plants and can promote plant growth by activating soil nutrients and producing phytohormones (Fan et al., 2018; Saxena et al., 2020), which also protects plants from biotic stresses by directly inhibiting plant pathogens and inducing plants to acquire systemic resistance (Stefany et al., 2021; Kurniawan and Chuang, 2022). *Bacillus* diversity and abundance differed in the rhizosphere soil of invasive and native plants. Chen et al. (2022) found that *Bacillus* diversity differed in the rhizosphere soil of the exotic (*Flaveria bidentis*) and native plants (*Setaria viridis*). The relative abundance of *Brecibacterium frigoritolerans* was higher in the *F. bidentis* rhizosphere than in the *S. viridis* rhizosphere. Additionally, the dominant *Bacillus* in the *F. bidentis* rhizosphere promoted *F. bidentis* competitive growth by elevating soil nitrogen and phosphorus levels. These studies indicate that *Bacillus* is also crucial for the successful invasion of exotic plants. As previously evidenced, AMF and PGPR can mutually promote their own growth and development, forming a synergistic effect to further enhance plant growth and promote their tolerance to diverse stresses (Krishnamoorthy et al., 2016; Hidri et al., 2019). However, few studies have examined whether combinations of AMF and *Bacillus* would contribute to the successful invasion of invasive plants. Therefore, understanding the effects of AMF, *Bacillus* and their combinations in the rhizosphere soil on the competitiveness of invasive plants with native plants is conducive to exploring the ecological role of two functional rhizosphere microorganisms in plant invasion.

Ageratina adenophora (Spreng.), a perennial herbaceous plant of the Asteraceae family, originates from Mexico and Costa Rica. Due to its strong reproductive and dispersal capabilities, morphological plasticity and stress tolerance, it has invaded many countries across Asia, Africa, and Oceania (Poudel et al., 2019; Tang et al., 2019; Gu et al., 2021). Since its first introduction from Myanmar into the Yunnan Province of China in the 1940s, *A. adenophora* has spread widely across southwestern and central China, becoming a dominant and invasive plant in China (Wang and Wang, 2006; Gui et al., 2009). *A. adenophora*'s colonization in southwestern China expanded considerably, with its suitable habitat distribution rapidly advancing eastward and northward (Li W. T. et al., 2022). The invasion of this plant has resulted in the destruction of native biodiversity, alteration of ecological community structures, and posed a severe threat to the development of agriculture, forestry and livestock industries, resulting in enormous economic and ecological losses (Song et al., 2017; Wang et al., 2017; Ren et al., 2021). *A. adenophora* has been shown to selectively aggregate functional microbes that mediate soil nutrient cycling to form a favorable soil microenvironment in the invasive habitats that facilitate its invasion (Niu et al., 2007; Zhao et al., 2007; Li Q. et al., 2022). In contrast to native plant rhizosphere soil, *A. adenophora* rhizosphere soil exhibits a remarkably higher abundance of nitrogen-fixing bacteria, phosphorus-solubilizing bacteria, and IAA-producing bacteria (Xu et al., 2012; Fang et al., 2019). Our previous studies demonstrated that *Bacillus cereus* has a high abundance in the rhizosphere soil of *A. adenophora* and *R. amethystoides* and exerted a positive feedback effect on *A. adenophora* (Sun et al., 2021; Du et al., 2022a). The AM fungus *Septoglomus constrictum* was also identified in the rhizosphere soil of *A. adenophora* and *R. amethystoides*, which improved the growth of *A. adenophora* and its resistance to *A. gossypii* feeding (Yu et al., 2012; Li et al., 2016; Du et al., 2022b). However, the relationship between AMF and *Bacillus* in the rhizosphere of *A. adenophora* and *R. amethystoides* and the effects of this relationship on the competitive growth between the two plants remain unknown.

To address this knowledge gap, we hypothesized that a synergistic interaction between *B. cereus* and *S. constrictum* might enhance the competitive growth of *A. adenophora*. To test this hypothesis, we compared the effects of single inoculation with AMF or *Bacillus* and co-inoculation of two kinds of microorganisms on the AMF colonization rate and *Bacillus* density of *A. adenophora* to explore whether both microorganisms form a synergistic effect. To illustrate the impact and reasons of microorganisms on plant growth, we compared their biomass, relative competitiveness, root growth characteristics, and nutrient content, as well as the soil's available nutrient content.

2. Materials and methods

2.1. Microbial inoculation preparation

The spores of *S. constrictum* were isolated from the rhizosphere soil of *A. adenophora* in our previous study (Du et al., 2022b). The mycorrhizal inoculum, consisting of fragments of colonized roots, spores, and hyphae of *S. constrictum,* was propagated using maize as the host plant. The spore density (20 spores/100 g of soil) was

determined based on the quantity of *S. constrictum* spores in the rhizosphere soil of *A. adenophora* in the field and used for subsequent analyses.

The *B. cereus* strain A20 (GenBank accession: OM149794) was isolated from *A. adenophora* and *R. amethystoides* rhizosphere soil (Du et al., 2022a). The strain's organic phosphate-solubilizing ability, inorganic phosphate-solubilizing ability, potassium-solubilizing ability, nitrogen-fixing ability, and IAA-producing ability were 53.66, 92.38, 51.33, 23.67, 61.55 mg/L, respectively. The siderophores-producing ability of the strain was 0.48, according to the methodology of Payne (1994). The strain was separately cultured on nutrient agar plates at 37°C for 8–12 h to obtain single colonies. The colonies of activated *Bacillus* were selected using an aseptic toothpick and incubated in 1 mL of nutrient liquid medium culture in a 1.5 mL centrifuge tube. After shaking at 180 rpm for 24 h at 37°C, the liquid was transferred into a triangular flask containing 100 mL of nutrient liquid broth medium and shaken at 180 rpm for 24 h at 37°C. The *Bacillus* suspension was then expanded to a concentration of 10^8 CFU/mL (Sun et al., 2022).

2.2. Plants and soil preparation

The soils and seeds of the exotic and native plants were purchased from Yunnan Agricultural University (Kunming, China; 25°08′30″ N, 102°45′13″ E, altitude 1964 m). Before sowing, the seeds were surface disinfected for 10 min in a 5% sodium hypochlorite solution. Next, the seeds were washed 5 times using sterile water, followed by 1 min soaking in 75% alcohol and rinsing 5 times in sterile water. The soil was crushed, sieved (2 mm), then mixed with vermiculite (v/v = 1:1) $[(Mg, Fe, Al)_3[(Si,Al)_4O_{10}(OH)_2]. 4H_2O]$ (Dounan Plant and Flower Co., Ltd., Kunming, China). The properties of the soil were as follows: pH = 6.25, 15.502 g/kg organic matter, 0.899 g/kg total nitrogen, 0.351 g/kg total phosphorus, 40.03 g/kg total potassium, 20.28 μg/g available nitrogen, 5.089 μg/g available phosphorus (AP), and 32.32 mg/kg available potassium (AK). Lastly, the mixtures were subjected to 2 h heating (121°C) in an autoclave.

2.3. Experiment design

The impact of AMF and *Bacillus* on competitive *A. adenophora* and *R. amethystoides* growth was investigated by conducting a greenhouse experiment at the Yunnan Agricultural University. The experiment considered two factors: (1) Plant type: *A. adenophora*, *R. amethystoides*, *A. adenophora* and *R. amethystoides*, and (2) inoculum treatments: C (uninoculated treatment), BC (inoculated with *B. cereus*), SC (inoculated with *S. constrictum*), and BC + SC (dual-inoculation with *B. cereus* and *S. constrictum*). Following the design of Gibson et al. (1999) and Zhang et al. (2018), the planting included a monoculture of *A. adenophora* and *R. amethystoides*, and *A. adenophora* and *R. amethystoides* mixture, with two plants per pot for monoculture treatment, and one *A. adenophora* and one *R. amethystoides* per pot for mixture treatment. Before starting the experiment, 1 kg soil in the pots was used for sowing the seeds of *A. adenophora* and/or *R. amethystoides* and inoculums of *S. constrictum* (20 per/100 g of soil) and/or *B. cereus* (10 mL 10^8 CFU/mL). For the non-AMF treatment, we added the same amount of sterilized inoculum and the filtrate (<20 mm) of the AMF inoculum, while for the non-*Bacillus* treatment, we added 10 mL of the sterilized bacterial suspension. The study was conducted using a randomized design comprising 10 repetitions per treatment (3 planting treatments × 4 inoculation treatments × 10 replicates = 120 pots). The plants were watered with sterile water once every 2 days, and the seeds were grown in a controlled environment in a greenhouse at a temperature of 25°C with 10 h light/14 h dark.

2.4. Measurement

2.4.1. Biomass and corrected index of relative competition intensity

Ageratina adenophora and *Rabdosia amethystoides* were collected under different treatments following germination for 120 days. The soil in the roots and shoots was collected to measure their biomass. All roots and shoots were dried (80°C, 72 h), and the growth index data were obtained. The total biomass (aboveground and belowground biomass) was measured. The plant competitiveness was quantified using CRCI, calculated following the methodology of Oksanen et al. (2006):

$$CRCI = \arcsin [(X - Y) / \max (X, Y)],$$

where X and Y represent individual plant biomass in intraspecific and interspecific competition, respectively; CRCI value >0 represents the negative effect, whereas CRCI value <0 represents the positive effect of the competition on the target plant.

2.4.2. Root growth characteristics

The roots were washed, cut, and evenly distributed in a scanning tray filled with water. They were scanned using a root scanner (Epson Expression 10000XL; Epson, Long Beach, CA, United States) and analyzed using the WinRhizo software (Regent Instruments Inc., Québec City, QC, Canada) and their root length (RL), root surface area (RS), root diameter (RD), and root volume (RV) were calculated.

2.4.3. Total nitrogen, phosphorus and potassium concentration

The dried plants were ground with a high-throughput Tissuelyser-48 grinder (Shanghai Jingxin Industrial Development Co., Ltd. Shanghai, China). C concentration was determined using 20 mg plant powder via the potassium dichromate-concentrated sulfuric acid oxidation method (K2Cr2O7-H2SO4) (Kong et al., 2022). The plant samples (2 g powder) were digested in a concentrated perchloric and nitric acids mixture (v:v = 1: 6) to measure the N, P, and K concentrations. Nitrogen and phosphorus content was analyzed separately using the micro-Kjeldahl method (Nelson and Sommers, 1973) and inductively coupled plasma spectroscopy (Isaac and Johnson, 1983). Six replicates were set up for each treatment.

2.4.4. Colonization of AMF

After rinsing in 10% KOH, the roots were acidified with 2% HCl and stained with 0.1% acid fuchsin solution. Then, the mycorrhizal root colonization percentage was determined by visually observing fungal colonization (Zhang et al., 2017). The magnified intersections method was used for analyzing AMF colonization in the *A. adenophora*

and *R. amethystoides* roots (Giovannetti and Mosse, 1980; Biermann and Linderman, 1981). Two hundred root segments for each replicate were analyzed using the Olympus BX43 compound microscope (Olympus, Tokyo, Japan), and six replicates per treatment were conducted. The colonization percentage of each segment was measured by colonization (presence of hyphae, vesicles, or arbuscules) in that region. AMF colonization was calculated by combining the percentage colonization of the 200 root segments.

2.4.5. Density of *Bacillus cereus*

The density of *B. cereus* in each soil sample was analyzed to investigate different treatment impacts on their growth on nutrient agar medium plates using the suspension dilution method (Yang et al., 2012; Du et al., 2020; Sun et al., 2022). Briefly, 1 g rhizosphere soil with 9 mL of sterile water was incubated at 200 r/min, heated at 90°C for 10 min, and serially diluted. Then, 0.1 mL of 10^{-3} supernatant was added to nutrient agar plates and cultured for 18 h at 37°C. Colonies were counted as the colony-forming units/ per gram of dry soil (CFU/g) according to volume dilution. Six replicates were conducted for each treatment.

2.5. Statistical analysis

The variables are expressed as mean ± standard error ($n = 6$). The SPSS v21.0 (IBM, Armonk, New York) software was used for statistical analyses. The Shapiro–Wilk test was used for testing data normality. All data conformed to normality distribution. A two-way ANOVA (Tuckey test) was conducted to determine inoculum effects on the biomass, root growth characteristics, total N, P, and K concentrations, and soil characteristics in the monoculture and mixture treatment. Differences among different inoculums (C, BC, SC, and BC + SC) in these variables above were determined using multiple comparisons (Tuckey test). A one-way ANOVA (Tuckey test) was conducted to determine inoculum effects on CRCI, AMF colonization rate, and *Bacillus* density in the monoculture and mixture treatment. Monoculture and the mixture influence on plant growth were evaluated using Student's *t*-test. Pearson's rank correlation coefficient was used to analyze the correlation between AMF colonization and plant growth parameters. All graphics were created by Excel and Origin 2019 (OriginLab, United States).

3. Results

3.1. Impacts of competition and inoculum on *Ageratina adenophora* and *Rabdosia amethystoides* biomass

The present study investigates the impact of competition on the biomass of two plant species, *A. adenophora* and *R. amethystoides*, and the effect of inoculation treatments on their growth (Figure 1 and Supplementary Table S1). Our results demonstrate that competition has an opposite effect on the two species. *A. adenophora* exhibited a significantly higher biomass in the presence of other plants [C: $F_{(1,10)} = 0.288$; BC: $F_{(1,10)} = 2.164$; SC: $F_{(1,10)} = 3.501$; BC + SC: $F_{(1,10)} = 21.928$; all $p < 0.001$], whereas *R. amethystoides* showed a higher biomass in monoculture [C: $F_{(1,10)} = 1.173$; BC: $F_{(1,10)} = 5.483$; SC: $F_{(1,10)} = 2.564$; BC + SC: $F_{(1,10)} = 1.342$; all $p < 0.001$]. The inoculation treatments significantly increased the biomass of both species, regardless of the presence [$F_{(3,20)} = 124.773$, $p < 0.001$] or absence of competition [$F_{(3,20)} = 113.963$, $p < 0.001$]. In particular, the BC + SC treatment showed the greatest positive impact, increasing *A. adenophora* biomass by 197.74 and 116.39% in the mixture and monoculture treatments, respectively. Interestingly, the effect of inoculation treatments varied depending on the presence of competition. The biomass of *R. amethystoides* in the mixture treatment was significantly reduced by the SC and BC + SC treatments, while the BC treatment led to a remarkable increase. In contrast, all inoculation treatments positively impacted the biomass of *R. amethystoides* in the monoculture treatment. These results suggest that competition may modulate the response of plants to inoculation treatments.

3.2. Impacts of inoculum on the corrected index of relative competition intensity of *Ageratina adenophora* and *Rabdosia amethystoides*

Our results demonstrate that interspecific competition has a significant positive effect on *A. adenophora* growth [$F_{(3,20)} = 31.547$, $p < 0.001$] and a significant negative effect on *R. amethystoides* growth [$F_{(3,20)} = 492.927$, $p < 0.001$] in both non-inoculation and inoculation treatments (Figure 2). Additionally, inoculation with BC reduced the positive effect of interspecific competition on *A. adenophora* ($p = 0.251$), while inoculation with SC and BC + SC enhanced the positive effect on *A. adenophora* (SC: $p = 0.001$; SC + BC: $p < 0.001$). Inoculation of BC treatment alleviated the negative effect on *R. amethystoides* growth when grown with *A. adenophora* in comparison with the control ($p < 0.001$), while inoculation with SC and BC + SC treatments enhanced this negative effect (SC: $p < 0.001$; SC + BC: $p < 0.001$).

3.3. Impacts of competition and inoculum on root growth characteristics of *Ageratina adenophora* and *Rabdosia amethystoides*

The effect of competition on root length, root surface area, root diameter and root volume of *A. adenophora* and *R. amethystoides* were consistent with the biomass trend (Figure 3 and Supplementary Table S1). Monoculture treatment of *A. adenophora* led to significantly lower root growth characteristics than mixture treatment [C: root length: $F_{(1,10)} = 3.478$; root surface area: $F_{(1,10)} = 2.822$; root diameter: $F_{(1,10)} = 3.451$; root volume: $F_{(1,10)} = 0.074$; BC: root length: $F_{(1,10)} = 0.564$; root surface area: $F_{(1,10)} = 0.277$; root diameter: $F_{(1,10)} = 5.739$; root volume: $F_{(1,10)} = 0.542$; SC: root length: $F_{(1,10)} = 0.645$; root surface area: $F_{(1,10)} = 0.065$; root diameter: $F_{(1,10)} = 0.273$; all $p < 0.001$; root volume: $F_{(1,10)} = 3.259$, $p = 0.009$; BC + SC: root length: $F_{(1,10)} = 1.695$, $p < 0.001$; root surface area: $F_{(1,10)} = 6.935$, $p = 0.001$; root diameter: $F_{(1,10)} = 1.291$, $p = 0.002$; root volume: $F_{(1,10)} = 0.089$, $p = 0.001$], while monoculture treatment of *R. amethystoides* was associated with significantly higher root growth characteristics compared to mixture treatment [C: root length: $F_{(1,10)} = 1.127$, $p < 0.001$; root surface area: $F_{(1,10)} = 1.217$, $p < 0.001$; root diameter: $F_{(1,10)} = 1.135$, $p = 0.049$; root volume: $F_{(1,10)} = 2.646$; BC: root length: $F_{(1,10)} = 13.136$; root surface area:

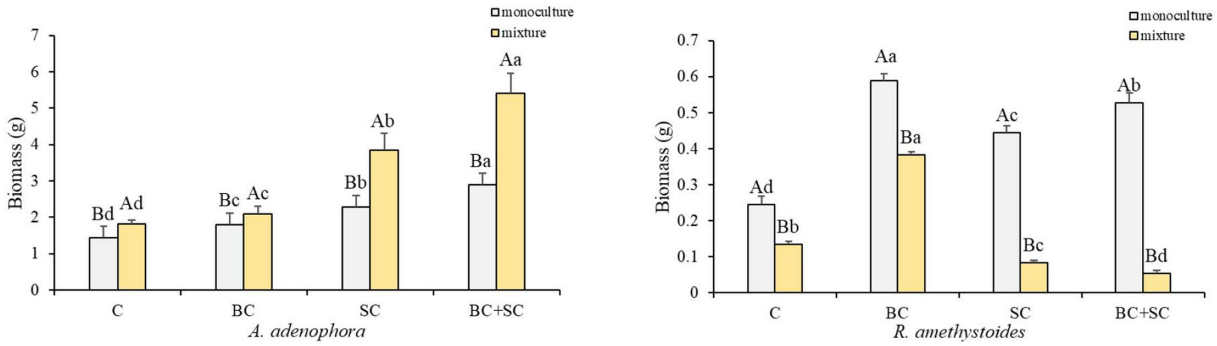

FIGURE 1
Effect of competition and inoculum on *A. adenophora* and *R. amethystoides* biomass. C, control; BC, inoculated with *B. cereus*; SC, inoculated with *S. constrictum*; BC+SC, inoculated with *B. cereus* and *S. constrictum*. Different lowercase letters in lower case indicate significant differences between the four treatments at $p<0.05$. Different uppercase letters indicate significant differences between the monoculture or mixture at $p<0.05$. Error bars represent±SE of mean ($n=6$).

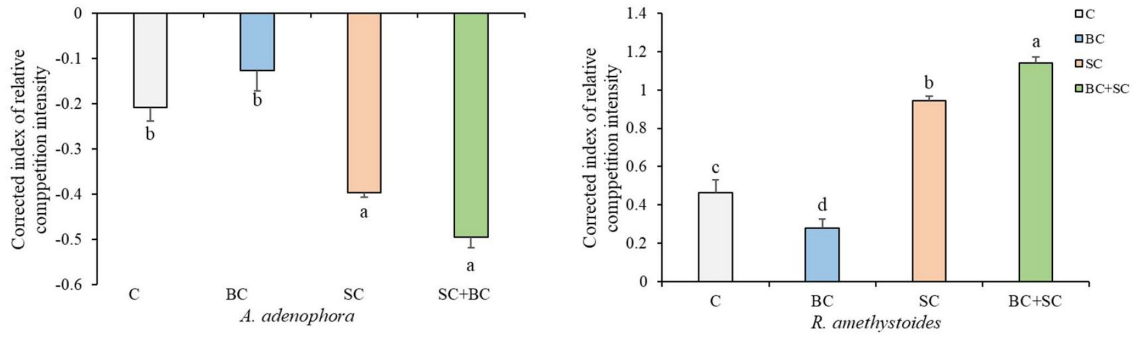

FIGURE 2
Effect of inoculum on *A. adenophora* and *R. amethystoides* CRCI. C, control; BC, inoculated with *B. cereus*; SC, inoculated with *S. constrictum*; BC+SC, inoculated with *B. cereus* and *S. constrictum*. Different lowercase letters in lower case indicate significant differences between the four treatments at $p<0.05$. Error bars represent±SE of mean ($n=6$).

$F_{(1,10)}=11.633$; root diameter: $F_{(1,10)}=0.178$; root volume: $F_{(1,10)}=4.546$; SC: root length: $F_{(1,10)}=1.483$; root surface area: $F_{(1,10)}=1.348$; root diameter: $F_{(1,10)}=2.248$; root volume: $F_{(1,10)}=1.613$; BC+SC: root length: $F_{(1,10)}=1.839$; root surface area: $F_{(1,10)}=1.938$; root diameter: $F_{(1,10)}=2.170$; root volume: $F_{(1,10)}=12.570$; all $p<0.001$]. For *A. adenophora*, the root growth characteristics were significantly increased by inoculation treatment both in monoculture and mixture treatment, among which the root growth characteristics of BC+SC treatment were significantly higher ($p<0.05$). Additionally, inoculation treatment of *R. amethystoides* in monoculture and mixture treatments with BC exhibited a significant increase in the root growth characteristics ($p<0.05$), while inoculation treatments with SC and BC+SC resulted in a significant decrease in the root growth characteristics of *R. amethystoides* ($p<0.05$).

3.4. Effects of competition and inoculum on *Ageratina adenophora* and *Rabdosia amethystoides* nutrient concentrations

Competition effects on total N, P and K concentrations of *A. adenophora* and *R. amethystoides* were consistent with the trend in biomass (Figure 4 and Supplementary Table S1). *A. adenophora* in monoculture treatment showed significantly higher nitrogen, phosphorus and potassium concentrations than in mixture treatment [C: N: $F_{(1,10)}=1.285$; P: $F_{(1,10)}=11.400$; K: $F_{(1,10)}=1.556$; all $p<0.001$; BC: N: $F_{(1,10)}=0.010$, $p=0.005$; P: $F_{(1,10)}=1.560$, $p<0.001$; K: $F_{(1,10)}=0.890$, $p<0.001$; SC: N: $F_{(1,10)}=0.109$, $p=0.032$; P: $F_{(1,10)}=2.822$, $p<0.001$; K: $F_{(1,10)}=0.632$, $p<0.001$; BC+SC: N: $F_{(1,10)}=0.509$, $p=0.001$; P: $F_{(1,10)}=2.822$, $p<0.001$; K: $F_{(1,10)}=0.068$, $p<0.001$], while *R. amethystoides* in monoculture treatment had significantly increased nutrient concentrations than those in mixture treatment [C: N: $F_{(1,10)}=3.491$, $p<0.001$; P: $F_{(1,10)}=0.872$, $p=0.001$; K: $F_{(1,10)}=1.101$; BC: N: $F_{(1,10)}=1.649$; P: $F_{(1,10)}=4.085$; K: $F_{(1,10)}=0.039$; SC: N: $F_{(1,10)}=1.574$; P: $F_{(1,10)}=3.467$; K: $F_{(1,10)}=1.337$; BC+SC: N: $F_{(1,10)}=0.434$; P: $F_{(1,10)}=2.778$; K: $F_{(1,10)}=0.448$; all $p<0.001$]. For *A. adenophora*, inoculation treatment significantly increased N, P, and K concentrations in monoculture and mixture treatments ($p<0.001$). The nutrient contents of BC+SC treatment were significantly increased compared to other treatments ($p<0.001$), and the N, P and K concentrations were increased by 41.47, 30.56, and 34.09% in monoculture treatment and 35.97, 43.26, and 28.61% in mixture treatment, respectively. For *R. amethystoides*, inoculation with BC treatment significantly enhanced N, P, and K concentrations

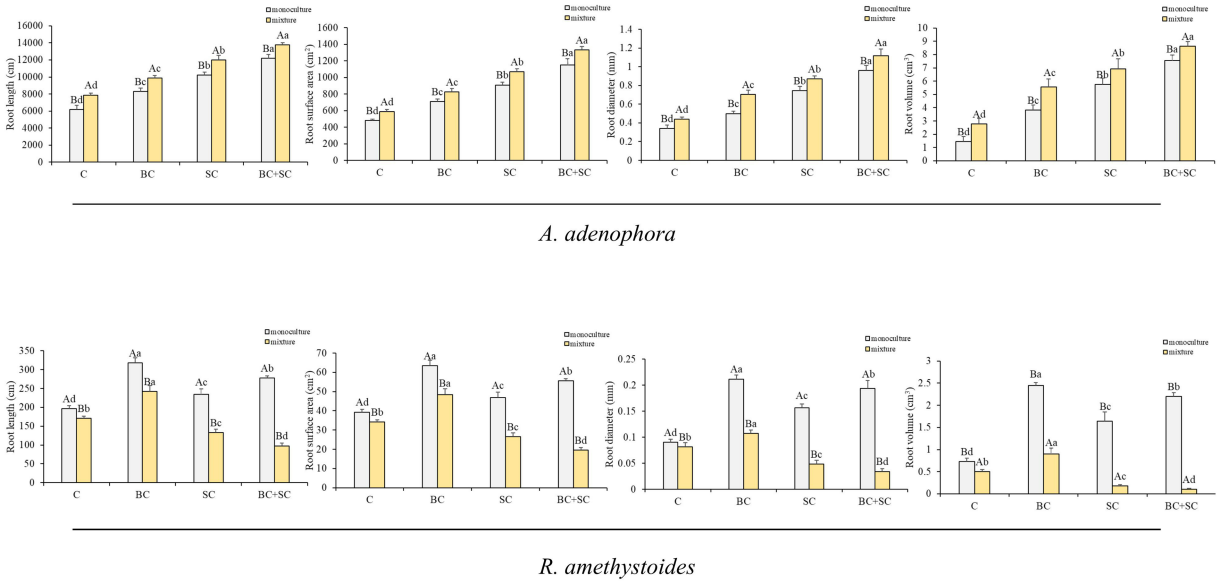

FIGURE 3
Effect of competition and inoculum on the root growth characteristics of *A. adenophora* and *R. amethystoides*. C, control; BC, inoculated with *B. cereus*; SC, inoculated with *S. constrictum*; BC+SC, inoculated with *B. cereus* and *S. constrictum*. Different lowercase letters significant differences between the four treatments at $p<0.05$. Different uppercase letters indicate significant differences between the monoculture or mixture at $p<0.05$. Error bars represent±SE of mean ($n=6$).

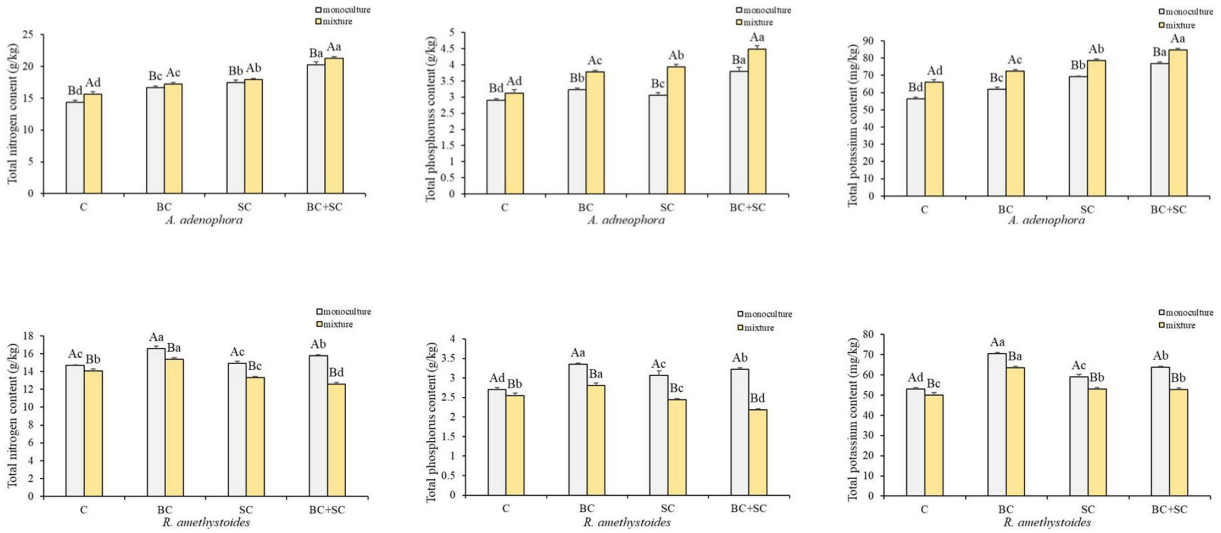

FIGURE 4
Effect of competition and inoculum on the nutrient concentrations of *A. adenophora* and *R. amethystoides*. C, control; BC, inoculated with *B. cereus*; SC, inoculated with *S. constrictum*; BC+SC, inoculated with *B. cereus* and *S. constrictum*. Different lowercase letters in lower case indicate significant differences between the four treatments at $p<0.05$. Different uppercase letters indicate significant differences between the monoculture or mixture at $p<0.05$. Error bars represent±SE of mean ($n=6$).

in both monoculture and mixture treatments ($p<0.001$), while inoculation of SC and BC + SC significantly increased the nutrient concentrations in monoculture treatment ($p<0.001$) but decreased N and P concentrations in mixture treatment ($p<0.001$). Inoculation with SC treatment reduced the N and P concentrations by 5.42 and 4.47%, and inoculation with BC + SC treatment reduced the N and P by 10.78 and 14.41% in mixture treatment, respectively.

3.5. Effects of competition and inoculum on AMF colonization and *Bacillus* density of *Ageratina adenophora* and *Rabdosia amethystoides*

Ageratina adenophora had a higher colonization rate than *R. amethystoides* in treatments with SC and BC + SC (Figure 5).

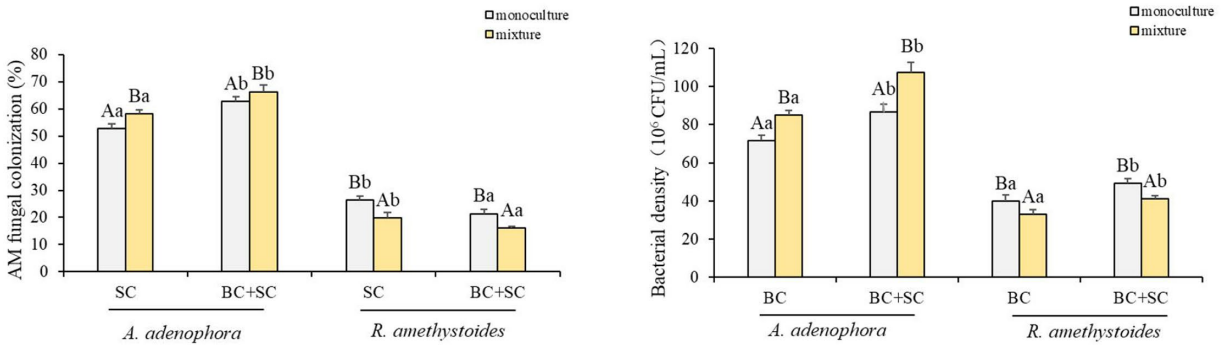

FIGURE 5
Effect of competition and inoculum on the AMF colonization and Bacterial density of *A. adenophora* and *R. amethystoides*. C, control; BC, inoculated with *B. cereus*; SC, inoculated with *S. constrictum*; BC+SC, inoculated with *B. cereus* and *S. constrictum*. Different lowercase letters in lower case indicate significant differences between the four treatments at $p<0.05$. Different uppercase letters indicate significant differences between the monoculture or mixture at $p<0.05$. Error bars represent±SE of mean ($n=6$).

Competition differentially affected the AMF colonization of the two plants. *A. adenophora* in mixture treatment showed a remarkably higher AMF colonization rate than that in monoculture treatment [SC: $F_{(1,10)}=0.003$; BC+SC: $F_{(1,10)}=1.104$; both $p<0.001$], while *R. amethystoides* in mixture treatment had a significantly lower AMF colonization rate than that in monoculture treatment [SC: $F_{(1,10)}=0.064$; BC+SC: $F_{(1,10)}=2.844$; both $p<0.001$]. *A. adenophora* inoculated with BC+SC had a significantly higher AMF colonization rate than that inoculated with SC in both monoculture and mixture treatments [monoculture: $F_{(3,20)}=102.150$; mixture: $F_{(3,20)}=48.412$, both $p<0.001$]. However, *R. amethystoides* inoculated with SC had a significantly higher AMF colonization rate than that inoculated with SC in both monoculture and mixture treatment [monoculture: $F_{(3,20)}=32.194$; mixture: $F_{(3,20)}=18.654$; both $p<0.001$].

Bacillus density in *A. adenophora* rhizosphere soil was significantly higher than in *R. amethystoides* rhizosphere soil in all treatments (Figure 5). In addition, the *Bacillus* density was significantly higher in *A. adenophora* rhizosphere soil in mixture treatment than that in monoculture treatment [BC: $F_{(1,10)}=0.363$; BC+SC: $F_{(1,10)}=0.630$; both $p<0.001$]. However, *Bacillus* density was significantly higher in *R. amethystoides* rhizosphere soil in monoculture treatment than that in mixture treatment [BC: $F_{(1,10)}=1.875$; BC+SC: $F_{(1,10)}=0.870$; both $p<0.001$]. Further, the *Bacillus* density in rhizosphere soil of *A. adenophora* and *R. amethystoides* in BC+SC treatment was significantly increased relative to that with BC treatment [*A. adenophora*: monoculture: $F_{(3,20)}=58.615$; mixture: $F_{(3,20)}=90.504$; *R. amethystoides*: monoculture: $F_{(3,20)}=34.690$; mixture: $F_{(3,20)}=38.400$; all $p<0.001$].

3.6. Impact of competition and inoculum on soil characteristic

For *A. adenophora* monoculture treatment and *A. adenophora* and *R. amethystoides* mixture treatment, inoculation significantly increased nitrate-nitrogen (NO_3^--N) and AP content in rhizosphere soil [Am: NO_3^--N: $F_{(3,20)}=353.767$; AP: $F_{(3,20)}=158.065$; A+R: NO_3^--N: $F_{(3,20)}=211.638$; AP: $F_{(3,20)}=294.625$; all $p<0.001$, Table 1, and Supplementary Table S1]. Among them, NO_3^--N and AP contents in the rhizosphere soil of BC inoculated treatment were significantly increased ($p<0.001$). For *R. amethystoides* monoculture treatment, NO_3^--N, AP, ammonium N (NH_4^+-N) and AK contents were significantly increased by the inoculation treatment [NO_3^--N: $F_{(3,20)}=179.125$; AP: $F_{(3,20)}=28.439$; NH_4^+-N: $F_{(3,20)}=213.247$; AK: $F_{(3,20)}=47.405$; all $p<0.001$], among which the available nutrient content of the rhizosphere soil of BC inoculation treatment was significantly increased ($p<0.001$).

3.7. Correlation of AMF colonization rate and the density of *Bacillus* with plant growth indicator and soil characteristics

Here, we investigated the impact of monoculture and mixed cropping of *A. adenophora* with *R. amethystoides* on the colonization rate of *S. constrictum* and *B. cereus*, as well as their correlation with various growth parameters and nutrient concentrations in two different soil types, SC and BC+SC. Our findings indicated that *S. constrictum* colonization rate was positively correlated with biomass, total N, P and K concentrations, root growth characteristics, NO_3^--N, and AP, but a negatively correlated with NH_4^+-N contents (except in SC inoculated monoculture treatment) and AK contents (Figure 6). In the mixture treatment of *A. adenophora* with *R. amethystoides* in SC and BC+SC treatment, *S. constrictum* colonization rate in *R. amethystoides* was negatively associated with biomass, total N and P concentrations and root growth characteristics, but positively correlated with total K concentration and soil characteristics (Figure 6).

In both the monoculture and mixture treatments of *A. adenophora* with *R. amethystoides* in BC and BC+SC treatment, the density of *B. cereus* showed a significantly positive correlation with biomass, total N, P and K concentrations, root growth characteristics, NO_3^--N and AP contents, but a negative correlation with NH_4^+-N and AK contents (Figure 7). In the mixture treatment with *A. adenophora* in BC+SC treatment, the density of *B. cereus* showed a significantly negative correlation with biomass, total N and P concentration and root growth characteristics but a positive correlation with total K concentration and soil characteristics (Figure 7).

10.3389/fmicb.2023.1131797

TABLE 1 Soil characteristics under different treatments.

Treatments		NO_3^--N (μg/g)	NH_4^+-N (μg/g)	Available P (μg/g)	Available K (mg/g)
Am	C	13.190 ± 0.109 Bd	3.540 ± 0.103Ba	4.365 ± 0.086Ad	29.093 ± 1.327ABa
	BC	15.289 ± 0.714Aa	3.620 ± 0.106Ba	5.838 ± 0.190Aa	28.595 ± 1.618Ba
	SC	13.837 ± 0.179Ac	3.550 ± 0.070Ba	4.881 ± 0.090Ac	28.347 ± 1.543Aa
	BC + SC	14.343 ± 0.066Bb	3.515 ± 0.040Ba	5.155 ± 0.076Ab	28.117 ± 0.897Ba
A + R	C	13.652 ± 0.162Ac	3.732 ± 0.077Aa	4.337 ± 0.071Ad	29.713 ± 0.951Aa
	BC	15.518 ± 0.202Aa	3.708 ± 0.069Ba	6.012 ± 0.083Aa	30.015 ± 0.662ABa
	SC	13.847 ± 0.110Ac	3.542 ± 0.149Ba	4.923 ± 0.129Ac	28.645 ± 1.435Aa
	BC + SC	14.930 ± 0.102Ab	3.558 ± 0.152Ba	5.253 ± 0.106Ab	29.167 ± 1.285ABa
Rm	C	12.630 ± 0.092Cd	3.620 ± 0.164ABc	4.313 ± 0.085Ad	28.103 ± 0.571Bc
	BC	14.682 ± 0.269Ba	4.208 ± 0.078Aa	5.143 ± 0.058Ba	31.338 ± 0.269Aa
	SC	13.037 ± 0.120Bc	4.000 ± 0.078Ab	4.559 ± 0.049Bc	29.568 ± 0.459Ab
	BC + SC	14.302 ± 0.185Bb	3.990 ± 0.107Ab	4.933 ± 0.050Bb	30.330 ± 0.576Ab

C, control; BC, inoculated with *B. cereus*; SC, inoculated with *S. constrictum*; BC + SC, inoculated with *B. cereus* and *S. constrictum*; Am, *A. adenophora* monoculture; A + R: *A. adenophora* and R, amethystoides mixture; Rm, R. amethystoides monoculture. Different letters in lower case indicate significant differences between the four treatments at $p < 0.05$. Different uppercase letters indicate significant differences between the monoculture or mixture at $p < 0.05$.

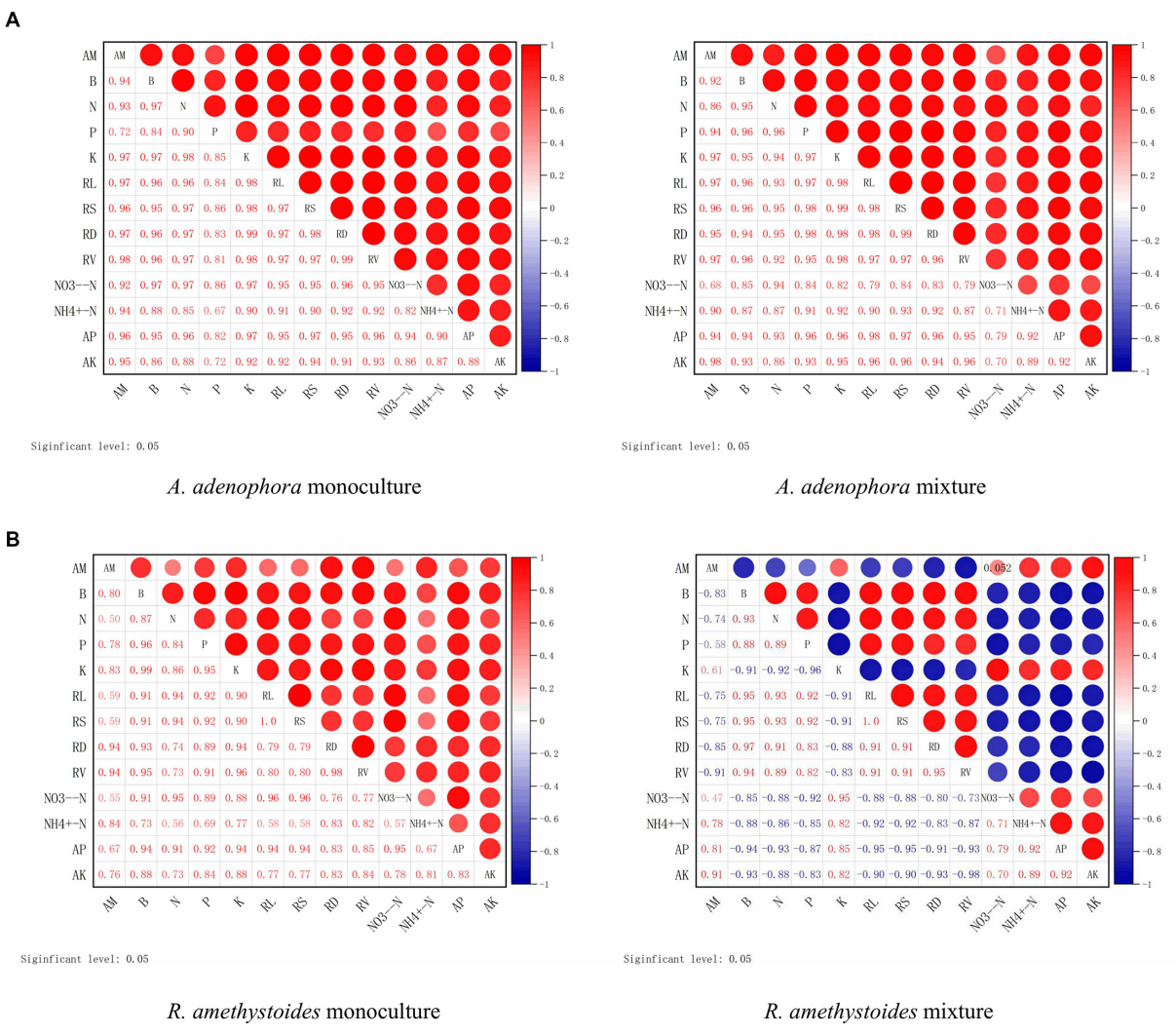

FIGURE 6
Correlation between root colonization by an arbuscular mycorrhizal fungus, *S. constrictum*, and plant growth indicators of *A. adenophora* **(A)** and *R. amethystoides* **(B)**. AM, AM colonization; B, biomass; RL, root length; RS, root surface area; RD, root diameter; RV, root volume. Red circles represent a positive correlation between root colonization and plant growth indicators. Larger circles represent a stronger correlation.

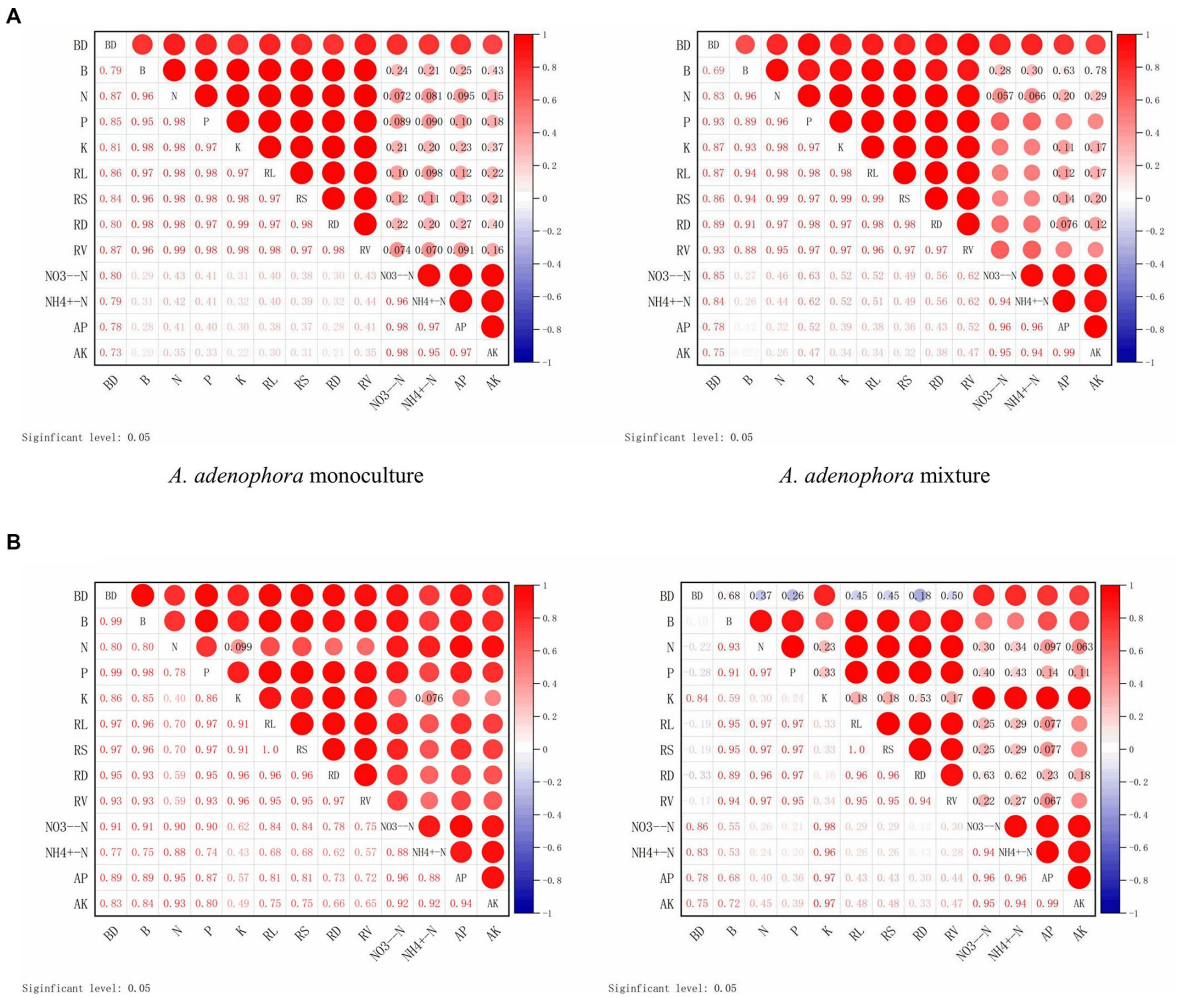

FIGURE 7
Correlation between the density of *B. cereus* (BC) and plant growth indicators of *A. adenophora* **(A)** and *R. amethystoides* **(B)**. AM, AM colonization; B, biomass; RL, root length; RS, root surface area; RD, root diameter; RV; root volume. Blue circles represent a negative correlation and red circles represent a positive correlation between root colonization and plant growth indicators. Larger circles represent a stronger correlation.

4. Discussion

When invasive plants establish themselves in a new habitat, they tend to accumulate beneficial microorganisms (mainly comprising AMF and *Bacillus*) in their rhizosphere to promote their growth and facilitate their invasion in response to abiotic factors (i.e., nutrient deficiencies) and biotic factors (i.e., feeding by generalist insects) (Meisner et al., 2013; Fu et al., 2017; Mohanty et al., 2018). In this present study, we investigated the common AMF and *Bacillus* present in the rhizosphere soil of both the invasive plant (*A. adenophora*) and native plant (*R. amethystoides*) and the explored the effect of single microbes versus co-culture on the competitive growth of the two plants. We found that *S. constrictum* and *B. cereus* exerted different effects on the two plants. Compared with the control treatment, inoculation with *S. constrictum* enhanced *A. adenophora*'s competitive growth but inhibited that of *R. amethystoides*, while inoculation with *B. cereus* inhibited *A. adenophora* growth but facilitated that of *R. amethystoides* growth (Figure 2). *S. constrictum* and *B. cereus* significantly increased the AM fungal colonization rate in the root and *Bacillus* density in the rhizosphere of *A. adenophora* (Figure 5) and further improved its competitiveness (Figure 2). These results supported our hypothesis that *S. constrictum* and *B. cereus* can form a synergistic effect that further promotes *A. adenophora* competitiveness and invasion.

AMF is critical for the successful invasion of some exotic species (Bunn et al., 2015; Reinhart et al., 2017). AMF affects the competition of invasive species with native species by changing nutrient uptake (Zhang et al., 2017, 2018). In this study, the competitive ability of inoculated *S. constrictum* to *A. adenophora* was significantly increased, while that of *R. amethystoides* was significantly decreased compared with the control treatment, indicating that *S. constrictum* increased *A. adenophora* competition to *R. amethystoides* (Figure 2). Relative to the monoculture treatment, the N, P and K concentrations of *A. adenophora* were significantly increased, and those of *R. amethystoides* were concomitantly decreased when the two plant species were in interspecific competition (Figure 4). Our results were concordant with Shen et al. (2020), who found that AMF improved the competitive ability of *A. adenophora* against the native *A. annua*

by significantly enhancing the N and P of the former. Therefore, AMFcan enhance *A. adenophora*'s competitiveness by providing more nutrients, which may be attributed to their different AMF colonization rates (Waller et al., 2016; Xia et al., 2021). Compared to monoculture treatment, the AMF colonization rate of *R. amethystoides* was significantly decreased, while the AMF colonization rate of *A. adenophora* was significantly increased when the two plant species were in interspecific competition. Chen et al. (2020) also found that competition reduced the AM colonization of native plants *Sesbania cannabina* and *Eupatorium chinense* by more than half when grown together with the invasive plants *Bidens pilosa* and *Eupatorium catarium*. AMF affects the competitiveness of both invasive and native species by altering their capacities for soil nutrient acquisition (Vogelsang and Bever, 2009; Pinzone et al., 2018). The correlation analysis results showed that in the mixture treatment, the increase in biomass, plant N, P, and K concentration and root growth characteristics of *A. adenophora*, as well as the decrease in biomass, plant N and P concentration and root growth characteristics of *R. amethystoides*, were significantly associated with AMF colonization rate when grown in the mixture treatment (Figure 6). These indicate that the colonization of roots by AMF can promote plant growth (Kong et al., 2022). Taken together, AMF contributes to *A. adenophora* out-competing native *R. amethystoides* through *S. constrictum*, which provides more nutrients to *A. adenophora* than to *R. amethystoides* with higher colonization in *A. adenophora*.

Bacillus is one of the rhizosphere-promoting bacteria for plants (Gupta et al., 2015; Gouda et al., 2018). It can directly release plant hormones, siderophores and ammonia, which provide soil nutrients through fixing N, and solubilizing P and K, thereby promoting plant growth (Ding et al., 2015; Khan et al., 2019). Moreover, it can also indirectly produce antimicrobial compounds to alleviate the inhibition of diverse pathogens in the plant (Alina et al., 2015; Khan et al., 2019). Our results also revealed that inoculation with *B. cereus* could significantly increase the nitrate nitrogen and AP contents in *A. adenophora* and *R. amethystoides* rhizosphere soil for plant growth (Table 1). Sun et al. (2021) showed that as the density of *B. cereus* increased, the soil available nutrient contents also increased. Roots directly affect the growth of aboveground parts and overall plant growth and development, with root growth and structure playing a key role in water and nutrient absorption (Comas et al., 2013; Ma et al., 2018). Here, *B. cereus* inoculation enhanced the root growth and nutrient absorption capacity of *A. adenophora* (Figure 3), thus increasing the N, P and K concentrations in the plants (Figure 4). A similar trend was also found in *R. amethystoides*. N and P have a positive synergistic effect, thus increasing the photosynthetic rate and improving the growth of plants (Schleuss et al., 2020). Our study also revealed that inoculation with *B. cereus* weakened the positive effect of interspecific competition on *A. adenophora* and alleviated the negative effect on *R. amethystoides* growth but did not change the competitive relationship between *A. adenophora* and *R. amethhystoides* (Figure 2). We also found that *B. cereus* inoculation led to significantly greater promotion on *R. amethystoides* biomass than *A. adenophora*, which may be due to the different effect of root exudates from the two plants on the growth-promoting effect of *Bacillus* (Sun et al., 2021, 2022). To understand the potential mechanisms, future studies may conduct a comparative analysis of the secondary metabolites of *A. adenophora* and *R. amethystoides* and their effect on *Bacillus*'s ability to solubilize phosphorus and fix nitrogen.

The combination of AMF and *Bacillus* is not only helpful to plant growth and resistance to various stresses but also benefits each other (Sangwan and Prasanna, 2021). In this present study, co-inoculation with *B. cereus* and *S. constrictum* treatments significantly increased the density of *B. cereus* in *A. adenophora* and *R. amethystoides* rhizosphere soil when the two species were grown in monoculture or together. Many *Bacillus* can be used as mycorrhizal helper bacteria (MHB), which is positively associated with root colonization and hyphal development of AMF. AMF can provide a habitat for bacteria and secrete mycelial secretions to promote the growth and development of PGPR (Zhang et al., 2018; Wang et al., 2022). Zhang et al. (2018) demonstrated that the hyphal exudates of AMF not only served as a carbon source for bacterial growth but also played a signaling role in triggering the bacteria-mediated organic phosphate mineralization process, which stimulated the expression of phosphatase genes in bacteria and released phosphatase. We revealed that inoculation with *B. cereus* isolated from the soil of mixture treatment of *A. adenophora* and *R. amethystoides* could increase soil nutrients in monoculture or mixture treatment, thereby increasing the N and P contents of both plants (Table 1). Several studies have shown that a suitable combination of inoculants with AMF and PGPR significantly affects plant growth compared with inoculations of the two alone (Zhang et al., 2014; Krishnamoorthy et al., 2016; Hidri et al., 2019). We found that the biomass, root growth characteristics, and nutrient contents of two plants with *B. cereus* and *S. constrictum* inoculation were significantly higher than those with single inoculation in *A. adenophora* or *R. amethystoides* monoculture. AMF mycelium recruits many bacteria, which provide functions that are absent from the AMF, thus further promoting the plant growth (Zhou et al., 2020; Jiang et al., 2021). In comparison with the monoculture, the AMF colonization rate of *A. adenophora* in the mixture of co-inoculation with *B. cereus* and *S. constrictum* treatments was significantly increased, while the AMF colonization rate of *R. amethystoides* was significantly reduced, which are consistent with the results of changes in nutrient content and growth in their respective plants. *B. cereus* inoculation increased the AMF colonization rate in *A. adenophora* rhizosphere soil in the SC + BC treatment and transported more activated nutrients for the plants. Meanwhile, the AMF colonization rate of *R. amethystoides* decreased when *A. adenophora* competed with *R. amethystoides*, which weakened the transport of available nutrients and inhibited the growth of *R. amethystoides*. Du et al. (2020) reported that AMF and *Bacillus* co-inoculation provided more N for *F. bidentis*, which enhanced the competitive advantage of *F. bidentis* over native *E. prostrata*. These results indicated that different functional microbial communities are involved in the underlying invasion mechanism, in which AMF may play a major role in the interspecific competition between invasive and native plants, and that *B. cereus*, as a mycorrhizal helper bacterial, promotes hyphal development and colonization of plant roots, thus helping the alien plant to compete over the native plant. Due to the few microbial species used in this study, the generality of our conclusion should be further tested by including more species. Moreover, it is necessary to continue to test the effects of AMF and *Bacillus* on the invasion ability of *A. adenophora* with various environmental factors in the future, such as non-sterile soil and different nutrient concentrations.

5. Conclusion

Our finding revealed that the symbiotic association of AMF and *Bacillus* with high content in the inter-rhizosphere soil of *A. adenophora* and *R. amethystoides* increased the competitive advantage of *A. adenophora*. However, *S. constrictum* and *B. cereus* played different roles in the invasion of *A. adenophora*. *S. constrictum* provided competitive advantages with different AM fungal colonization rates in the roots of *A. adenophora* and *R. amethystoides*, which resulted in more nutrient supply to invasive plants, while *B. cereus* may have activated more soil nutrients and promoted the hyphal development and colonization of plant roots. Overall, these findings enhanced our understanding on the role of AMF and bacteria in invasion by *A. adenophora*.

Data availability statement

The original contributions presented in the study are included in the article/Supplementary material, further inquiries can be directed to the corresponding author.

Author contributions

FG, ED, and YC designed the research. YL and RH collected the samples. ED and YHL performed the experiments. ZS and YHL performed bioinformatic and statistical analyses. ED and YC wrote the first draft. ZS and FG reviewed the manuscript. All authors contributed to the article and approved the submitted version.

Funding

This work was supported by the Yunnan Eco-Friendly Food International Cooperation Research Center (YEFICRC) Project of Yunnan Provincial of Yunnan Provincial Key Program (Grant No. 2019ZG00910), National Key Research and Development Program of China (2021YFD1400200), and Scientific Research Foundation of Education Department of Yunnan Province (2022Y224).

Conflict of interest

The authors declare that the research was conducted in the absence of any commercial or financial relationships that could be construed as a potential conflict of interest.

Publisher's note

Supplementary material

The Supplementary material for this article can be found online at: https://www.frontiersin.org/articles/10.3389/fmicb.2023.1131797/full#supplementary-material

References

Abbott, K. C., Karst, J., Biederman, L. A., Borrett, S. R., Hastings, A., Walsh, V., et al. (2015). Spatial heterogeneity in soil microbes alters outcomes of plant competition. *PLoS One* 10:e0125788. doi: 10.1371/journal.pone.0125788

Alina, S. O., Constantinscu, F., and Petruta, C. C. (2015). Biodiversity of *Bacillus subtilis* group and beneficial traits of *Bacillus* species useful in plant protection. *Rom. Biotechnol. Lett.* 20, 10737–10750.

Anna, A., Pavlína, K., and Zuzana, M. (2020). Plant–soil feedback contributes to predicting plant invasiveness of 68 alien plant species differing in invasive status. *Oikos* 129, 1257–1270. doi: 10.1111/oik.07186

Aslani, F., Juraimi, A. S., Ahmad-Hamdani, M. S., Alam, M. A., Hasan, M. M., Hashemi, F. S. G., et al. (2019). The role of arbuscular mycorrhizal fungi in plant invasion trajectory. *Plant Soil* 441, 1–14. doi: 10.1007/s11104-019-04127-5

Awaydul, A., Zhu, W. Y., Yuan, Y. G., Xiao, J., Hu, H., Chen, X., et al. (2019). Common mycorrhizal networks influence the distribution of mineral nutrients between an invasive plant, *Solidago canadensis*, and a native plant, *Kummerowa striata*. *Mycorrhiza* 29, 29–38. doi: 10.1007/s00572-018-0873-5

Biermann, B., and Linderman, R. G. (1981). Quantifying vesicular-arbuscular mycorrhizas: a proposed method towards standardization. *New Phytol.* 87, 63–67. doi: 10.1111/j.1469-8137.1981.tb01690.x

Bunn, R. A., Ramsey, P. W., and Lekberg, Y. (2015). Do native and invasive plants differ in their interactions with arbuscular mycorrhizal fungi? A meta-analysis. *J ecol*. 103, 1547–1556. doi: 10.1111/1365-2745.12456

Chen, X., Li, Q., Wang, Y., Chen, F. X., Zhang, X. Y., and Zhang, F. J. (2022). *Bacillus* promotes invasiveness of exotic *Flaveria bidentis* by increasing its nitrogen and phosphorus uptake. *J. Plant Ecol.* 15, 596–609. doi: 10.1093/jpe/rtab046

Chen, E. J., Liao, H. X., Chen, B. M., and Peng, S. L. (2020). Arbuscular mycorrhizal fungi are a double-edged sword in plant invasion controlled by phosphorus concentration. *New Phytol.* 226, 295–300. doi: 10.1111/nph.16359

Comas, L. H., Becker, S. R., Cruz, V. M. V., Byrne, P. F., and Dierig, D. A. (2013). Root traits contributing to plant productivity under drought. *Front. Plant Sci.* 4:442. doi: 10.3389/fpls.2013.00442

D'Antonio, C. M., Yelenik, S. G., and Mack, M. C. (2017). Ecosystem vs. community recovery 25 years after grass invasions and fire in a subtropical woodland. *J. Ecol.* 105, 1462–1474. doi: 10.1111/1365-2745.12855

Dawson, W., Schrama, M., and Austin, A. (2016). Identifying the role of soil microbes in plant invasions. *J. Ecol.* 104, 1211–1218. doi: 10.1111/1365-2745.12619

Dickie, I. A., Bufford, J. L., Cobb, R. C., Desprez-Loustau, M. L., Grelet, G., Hulme, P. E., et al. (2017). The emerging science of linked plant–fungal invasions. *New Phytol.* 215, 1314–1332. doi: 10.1111/nph.14657

Ding, X., Peng, X. J., Jin, B. S., Xiao, M., Chen, J. K., Li, B., et al. (2015). Spatial distribution of bacterial communities driven by multiple environmental factors in a beach wetland of the largest freshwater lake in China. *Front. Microbiol.* 6:129. doi: 10.3389/fmicb.2015.00129

Du, E. W., Chen, X., Li, Q., Chen, F. X., Xu, H. Y., and Zhang, F. J. (2020). *Rhizoglomus intraradices* and associated *Brevibacterium frigoritolerans* enhance the competitive growth of *Flaveria bidentis*. *Plant Soil* 453, 281–295. doi: 10.1007/s11104-020-04594-1

Du, E. W., Chen, Y. P., Li, Y. H., Sun, Z. X., and Gui, F. R. (2022a). Rhizospheric *Bacillus*-facilitated effects on the growth and competitive ability of the invasive plant *Ageratina adenophora*. *Front. Plant Sci.* 13:882255. doi: 10.3389/fpls.2022.882255

Du, E. W., Chen, Y. P., Li, Y. H., Zhang, F. J., Sun, Z. X., Hao, R. S., et al. (2022b). Effect of arbuscular mycorrhizal fungi on the responses of *Ageratina adenophora* to *Aphis gossypii* herbivory. *Front. Plant Sci.* 13:1015947. doi: 10.3389/fpls.2022.1015947

Fahey, C., and Stephen, L. F. (2022). Soil microbes alter competition between native and invasive plants. *J. Ecol.* 110, 404–414. doi: 10.1111/1365-2745.13807

Fan, X. N., Che, X. R., Lai, W. Z., Wang, S. J., Hu, W. T., Chen, H., et al. (2020). The auxin-inducible phosphate transporter AsPT5 mediates phosphate transport and is indispensable for arbuscule formation in Chinese milk vetch at moderately high phosphate supply. *Environ. Microbiol.* 22, 2053–2079. doi: 10.1111/1462-2920.14952

Fan, B., Wang, C., Song, X., Ding, X., Wu, L., Wu, H., et al. (2018). *Bacillus velezensis* FZB42 in 2018: the gram-positive model strain for plant growth promotion and biocontrol. *Front. Microbiol.* 9:2491. doi: 10.3389/fmicb.2018. 02491

Fang, K., Wang, Y. Z., and Zhang, H. B. (2019). Different effects of plant growth-promoting bacteria on invasive plants. *S. Afr. J. Bot.* 124, 94–101. doi: 10.1016/j.sajb.2019.04.007

Fu, W., Wang, N., Pang, F., Huang, Y. L., Wu, J., Qi, S. S., et al. (2017). Soil microbiota and plant invasions: current and future. *Biodivers. Sci.* 25, 1295–1302. doi: 10.17520/biods.2017071

Gibson, D. J., Connolly, J., and Weidenhamer, H. (1999). Designs for greenhouse studies of interactions between plants. *J. Ecol.* 87, 1–16. doi: 10.1046/j.1365-2745.1999.00321.x

Giovannetti, M., and Mosse, B. (1980). An evaluation of techniques for measuring vesicular arbuscular mycorrhizal infection in roots. *New Phytol.* 84, 489–500. doi: 10.2307/2432123

Gouda, S., Kerry, R. G., Das, G., Paramithiotis, S., and Patra, J. K. (2018). Revitalization of plant growth promoting rhizobacteria for sustainable development in agriculture. *Microbiol. Res.* 206, 131–140. doi: 10.1016/j.micres.2017.08.016

Gu, C. J., Tu, Y. L., Liu, L. S., Wei, B., Zhang, Y. L., Yu, H. B., et al. (2021). Predicting the potential global distribution of *Ageratina adenophora* under current and future climate change scenarios. *Ecol. Evol.* 11, 12092–12113. doi: 10.1002/ece3.7974

Gui, F. R., Wan, F. H., and Guo, J. Y. (2009). Determination of the population genetic structure of the invasive weed *Ageratina adenophora* using ISSR-PCR markers. *Russ. J. Plant Physiol.* 56, 410–416. doi: 10.1134/S1021443709030157

Gupta, G., Parihar, S. S., Ahirwar, N. K., Snehim, S. K., and Singh, V. (2015). Plant growth promoting rhizobacteria (PGPR): current and future prospects for development of sustainable agriculture. *J. Microb. Biochem. Technol.* 7, 96–102. doi: 10.4172/1948-5948.1000188

Hidri, R., Mahmoud, O. M., Farhat, N., Cordero, I., Pueyo, J. J., Debez, A., et al. (2019). Arbuscular mycorrhizal fungus and rhizobacteria affect the physiology and performance of *Sulla coronaria* plants subjected to salt stress by mitigation of ionic imbalance. *J. Plant Nutr. Soil Sci.* 182, 451–462. doi: 10.1002/jpln.201800262

Isaac, R. A., and Johnson, W. C. (1983). High speed analysis of agricultural samples using inductively coupled plasma-atomic emission spectroscopy. *Spectrochim. Acta B* 38, 277–282. doi: 10.1016/0584-8547(83)80124-4

Jiang, F. Y., Zhang, L., Zhou, J. C., George, T., and Feng, G. (2021). Arbuscular mycorrhizal fungi enhance mineralization of organic P by carrying bacteria along their extraradical hyphae. *New Phytol.* 230, 304–315. doi: 10.1111/nph.17081

Khan, N., Bano, A., Rahman, M. A., Guo, J., Kang, Z. Y., and Babar, M. A. (2019). Comparative physiological and metabolic analysis reveals a complex mechanism involved in drought tolerance in chickpea (*Cicer arietinum* L.) induced by PGPR and PGRs. *Sci. Rep.* 9:2019. doi: 10.1038/s41598-019-38702-8

Kong, L. J., Chen, X., Yerger, E. H., Li, Q., Chen, F. X., Xu, H. Y., et al. (2022). Arbuscular mycorrhizal fungi enhance the growth of the exotic species *Ambrosia artemisiifolia*. *J. Plant Ecol.* 15, 581–595. doi: 10.1093/jpe/rtab087

Krishnamoorthy, R., Kim, K., Subramanian, P., Senthilkumar, M., and Anandham, R. (2016). Arbuscular mycorrhizal fungi and associated bacteria isolated from salt-affected soil enhances the tolerance of maize to salinity in coastal reclamation soil. *Agric. Ecosyst. Environ.* 231, 233–239. doi: 10.1016/j.agee.2016.05.037

Kurniawan, A., and Chuang, H. W. (2022). Rhizobacterial *Bacillus mycoides* functions in stimulating the antioxidant defence system and multiple phytohormone signalling pathways to regulate plant growth and stress tolerance. *J. Appl. Microbiol.* 132, 1260–1274. doi: 10.1111/jam.15252

Lekberg, Y., Gibbons, S. M., Rosendahl, S., and Ramsey, P. W. (2013). Severe plant invasions can increase mycorrhizal fungal abundance and diversity. *ISME J.* 7, 1424–1433. doi: 10.1038/ismej.2013.41

Li, L. Q., Zhang, M. S., Liang, Z. P., Xiao, B., Wan, F. H., and Liu, W. X. (2016). Arbuscular mycorrhizal fungi enhance invasive plant, Ageratina adenophora growth and competition wih native plants. *Chin. J, Ecol.* 35, 79–86. doi: 10.13292/j.1000-4890.201601.011

Li, Q., Wan, F., and Zhao, M. (2022). Distinct soil microbial communities under *Ageratina adenophora* invasions. *Plant Biol.* 24, 430–439. doi: 10.1111/plb.13387

Li, W. T., Zheng, Y. L., Wang, R. F., Wang, Z. Y., Liu, Y. M., Shi, X., et al. (2022). Shifts in chemical and microbiological properties belowground of invader *Ageratina adenophora* along an altitudinal gradient. *J. Plant Ecol.* 15, 561–570. doi: 10.1093/jpe/rtac003

Ma, Z. Q., Guo, D. L., Xu, X. I., Lu, M., Bardgett, R. D., Bardgett, R. D., et al. (2018). Evolutionary history resolves global organization of root functional traits. *Nat. Int. Weekly J. Sci.* 570:E25. doi: 10.1038/s41586-019-1214-3

Meisner, A., De Deyn, G. B., De Boer, W., and Van Der Putten, W. H. (2013). Soil biotic legacy effects of extreme weather events influence plant invasiveness. *Proc. Natl. Acad. Sci. U. S. A.* 110, 9835–9838. doi: 10.1073/pnas.13009 22110

Mohanty, S. K., Arthikala, M. K., Nanjareddy, K., and Lara, M. (2018). Plant-symbiont interactions: the functional role of expansions. *Symbiosis* 74, 1–10. doi: 10.1007/s13199-017-0501-8

Nelson, D. W., and Sommers, L. E. (1973). Determination of Total nitrogen in plant material. *Agron. J.* 65, 109–112. doi: 10.2134/agronj1973.00021962006500010033x

Niu, H. B., Liu, W. X., Wan, F. H., and Liu, B. (2007). An invasive aster (*Ageratina adenophora*) invades and dominates forest understories in China: altered soil microbial communities facilitate the invader and inhibit natives *Plant Soil.* 294, 73–85. doi: 10.1007/s11104-007-9230-8

Oksanen, L., Sammul, M., and Magi, M. (2006). On the indices of plant-plant competition and their pitfalls. *Oikos* 112, 149–155. doi: 10.1111/j.0030-1299.2006.13379.x

Payne, S. M. (1994). Detection, isolation, and characterization of siderophores. *Methods Enzymol.* 235, 329–344. doi: 10.1016/0076-6879(94)35151-1

Pinzone, P., Potts, D., Pettibone, G., and Warren, R. (2018). Do novel weapons that degrade mycorrhizal mutualisms promote species invasion? *Plant Ecol.* 219, 539–548. doi: 10.1007/s11258-018-0816-4

Poudel, A. S., Jha, P. K., Shrestha, B. B., Muniappan, R., and Novak, S. (2019). Biology and management of the invasive weed *Ageratina adenophora* (Asteraceae): current state of knowledge and future research needs. *Weed Res.* 59, 79–92. doi: 10.1111/wre.12351

Powell, K. I., Chase, J. M., and Knight, T. M. (2013). Invasive plants have scale-dependent effects on diversity by altering species-area relationships. *Science* 339, 316–318. doi: 10.1126/science.1226817

Qi, S. S., Wang, J. H., Wan, L. Y., Dai, Z. C., Da Silva Matos, D. M., Du, D. L., et al. (2022). Arbuscular mycorrhizal fungi contribute to phosphorous uptake and allocation strategies of *Solidago canadensis* in a phosphorous-deficient environment. *Front. Plant Sci.* 13:831654. doi: 10.3389/fpls.2022.831654

Reinhart, K. O., Lekberg, Y., Klironomos, J., and Maherali, H. (2017). Does responsiveness to arbuscular mycorrhizal fungi depend on plant invasive status? *Ecol. Evol.* 7, 6482–6492. doi: 10.1002/ece3.3226

Ren, Z. H., Okyere, S. K., Wen, J., Xie, L., Cui, Y. J., Wang, S., et al. (2021). An overview: the toxicity of *Ageratina adenophora* on animals and its possible interventions. *Int. J. Mol. Sci.* 22:11581. doi: 10.3390/ijms222111581

Richardson, D. M., and Pyšek, P. (2012). Naturalization of introduced plants: ecological drivers of biogeographical patterns. *New Phytol.* 196, 383–396. doi: 10.1111/j.1469-8137.2012.04292.x

Sangwan, S., and Prasanna, R. (2021). Mycorrhizae helper bacteria: unlocking their potential as bioenhancers of plant - arbuscular mycorrhizal fungal associations. *Microb. Ecol.* 84, 1–10. doi: 10.1007/s00248-021-01831-7

Saxena, A. K., Kumar, M., Chakdar, H., Anuroopa, N., and Bagyaraj, D. J. (2020). *Bacillus* species in soil as a natural resource for plant health and nutrition. *J. Appl. Microbiol.* 128, 1583–1594. doi: 10.1111/jam.14506

Schleuss, P. M., Widdig, M., Heintz-Buschart, A., Kirkman, K., and Spohn, M. (2020). Interactions of nitrogen and phosphorus cycling promote P acquisition and explain synergistic plant-growth responses. *Ecology* 101:e03003. doi: 10.1002/ecy.3003

Shen, K., Cornelissen, J. H. C., Wang, Y., Wu, C., He, Y., Ou, J., et al. (2020). AM fungi alleviate phosphorus limitation and enhance nutrient competitiveness of invasive plants via mycorrhizal networks in karst areas. *Front. Ecol. Evol.* 8:125. doi: 10.3389/fevo.2020.00125

Smith, S. E., and Smith, F. A. (2011). Roles of arbuscular mycorrhizas in plant nutrition and growth: new paradigms from cellular to ecosystem scales. *Annu. Rev. Plant Biol.* 62, 227–250. doi: 10.1146/annurev-arplant-042110-103846

Sol, D., Maspons, J., Vall-llosera, M., Bartomeus, I., Garcia-Pea, G. E., Piol, J., et al. (2012). Unraveling the life history of successful invaders. *Science* 337, 580–583. doi: 10.1126/science.1221523

Song, X. Y., Hogan, J. A., Brown, C., Cao, M., and Yang, J. (2017). Snow damage to the canopy facilitates alien weed invasion in a subtropical montane primary forest in South-Western China. *For. Ecol. Manag.* 391, 275–281. doi: 10.1016/j.foreco.2017.02.031

Stefany, C., Claudia, P., Giuliana, D., Fabrizio, D. P., Alessio, C., Marco, M., et al. (2021). Plant growth promotion function of *Bacillus* sp. strains isolated from salt-Pan rhizosphere and their biocontrol potential against *Macrophomina phaseolina*. *Int. J. Mol. Sci.* 22:3324. doi: 10.3390/ijms22073324

Sun, C. F., Li, Q., Han, L. L., Chen, X., and Zhang, F. J. (2022). The effects of allelochemicals from root exudates of *Flaveria bidentis* on two *Bacillus* species. *Front. Plant Sci.* 13:1001208. doi: 10.3389/fpls.2022.1001208

Sun, Y. Y., Zhang, Q. X., Zhao, Y. P., Diao, Y. H., Gui, F. R., and Yang, G. Q. (2021). Beneficial rhizobacterium provides positive plant–soil feedback effects to *Ageratina adenophora*. *J. Integr. Agric.* 20, 1327–1335. doi: 10.1016/S2095-3119(20)63234-8

Tang, S. C., Pan, Y. M., Wei, C. Q., Li, X. Q., and Lü, S. H. (2019). Testing of an integrated regime for effective and sustainable control of invasive crofton weed (*Ageratina adenophora*) comprising the use of natural inhibitor species, activated charcoal, and fungicide. *Weed Biol. Manage.* 19, 9–18. doi: 10.1111/wbm.12171

Vogelsang, K. M., and Bever, J. D. (2009). Mycorrhizal densities decline in association with nonnative plants and contribute to plant invasion. *Ecology* 90, 399–407. doi: 10.1890/07-2144.1

Waller, L. P., Callaway, R. M., Klironomos, J. N., Ortega, Y. K., Maron, J. L., and Shefferson, R. (2016). Reduced mycorrhizal responsiveness leads to increased competitive tolerance in an invasive exotic plant. *J. Ecol.* 104, 1599–1607. doi: 10.1111/1365-2745.12641

Wang, S. S., Chen, A. Q., Xie, K., Yang, X. F., Luo, Z. Z., Chen, J. D., et al. (2020). Functional analysis of the OsNPF4.5 nitrate transporter reveals a conserved mycorrhizal pathway of nitrogen acquisition in plants. *Proc. Natl. Acad. Sci. U. S. A.* 117, 16649–16659. doi: 10.1073/pnas.2000926117

Wang, Y. H., Hou, L. L., Wu, X. Q., Zhu, M. L., Dai, Y., and Zhao, Y. J. (2022). Mycorrhiza helper bacterium *Bacillus pumilus* HR10 improves growth and nutritional status of *Pinus thunbergii* by promoting mycorrhizal proliferation. *Tree Physiol.* 42, 907–918. doi: 10.1093/treephys/tpab139

Wang, C., Lin, H. L., Feng, Q. S., Jin, C. Y., Cao, A. C., and He, L. (2017). A new strategy for the prevention and control of *Eupatorium adenophorum* under climate change in China. *Sustainability* 9:11. doi: 10.3390/su9112037

Wang, R., and Wang, Y. Z. (2006). Invasion dynamics and potential spread of the invasive alien plant species *Ageratina adenophora* (Asteraceae) in China. *Divers. Distrib.* 12, 397–408. doi: 10.1111/j.1366-9516.2006.00250.x

Weremijewicz, J., Sternberg, L. D. S. L. O., and Janos, D. P. (2018). Arbuscular common mycorrhizal networks mediate intra-and interspecific interactions of two prairie grasses. *Mycorrhiza* 28, 71–83. doi: 10.1007/s00572-017-0801-0

Xia, Y., Dong, M. H., Yu, L., Kong, L. D., Seviour, R., and Kong, Y. H. (2021). Compositional and functional profiling of the rhizosphere microbiomes of the invasive weed *Ageratina adenophora* and native plants. *PeerJ* 9:e10844. doi: 10.7717/peerj.10844

Xie, X. N., Lai, W. Z., Che, X. R., Wang, S. J., Ren, Y., Hu, W. T., et al. (2022). A SPX domain-containing phosphate transporter from *Rhizophagus irregularis* handles phosphate homeostasis at symbiotic interface of arbuscular mycorrhizas. *New Phytol.* 234, 650–671. doi: 10.1111/nph.17973

Xu, C. W., Yang, M. Z., Chen, Y. J., Chen, L. M., Zhang, D. Z., Mei, L., et al. (2012). Changes in non-symbiotic nitrogen-fixing bacteria inhabiting rhizosphere soils of an invasive plant *Ageratina adenophora*. *Appl. Soil Ecol.* 54, 32–38. doi: 10.1016/j.apsoil.2011.10.021

Yang, X., Zhang, L. H., Zhang, C., Zhang, J. L., Han, J. M., and Dong, J. G. (2012). Effects of *Flaveria bidentis* invasion on soil microbial communities, enzyme activities and nutrients. *Plant Nutr. Fert. Sci.* 18, 907–914. doi: 10.11674/zwy.2012.11499

Yu, W. Q., Liu, W. X., Gui, F. R., Liu, W. Z., Wan, F. H., and Zhang, L. L. (2012). Invasion of exotic *Ageratina adenophora* alters soil physical and chemical characteristics and arbuscular mycorrhizal fungus community. *Acta Ecol. Sin.* 32, 7027–7035. doi: 10.5846/stxb201110091468

Zhang, L., Fan, J. Q., Ding, X. D., He, X. H., Zhang, F. S., and Feng, G. (2014). Hyphosphere interactions between an arbuscular mycorrhizal fungus and a phosphate solubilizing bacterium promote phytate mineralization in soil. *Soil Biol. Biochem.* 74, 177–183. doi: 10.1016/j.soilbio.2014.03.004

Zhang, L., Feng, G., and Declerck, S. (2018). Signal beyond nutrient, fructose, exuded by an arbuscular mycorrhizal fungus triggers phytate mineralization by a phosphate solubilizing bacterium. *ISME J.* 12, 2339–2351. doi: 10.1038/s41396-018-0171-4

Zhang, H. Y., Goncalves, P., Copeland, E., Qi, S. S., Dai, Z. C., Li, G. L., et al. (2020). Invasion by the weed *Conyza canadensis* alters soil nutrient supply and shifts microbiota structure. *Soil Biol. Biochem.* 143:107739. doi: 10.1016/j.soilbio.2020.107739

Zhang, F. J., Li, Q., Chen, F. X., Xu, H. Y., Inderjit, , and Wan, F. H. (2017). Arbuscular mycorrhizal fungi facilitate growth and competitive ability of an exotic species *Flaveria bidentis*. *Soil Biol. Biochem.* 115, 275–284. doi: 10.1016/j.soilbio.2017.08.019

Zhang, F. J., Li, Q., Yerger, E. H., Chen, X., Shi, Q., and Wan, F. H. (2018). AM fungi facilitate the competitive growth of two invasive plant species, *Ambrosia artemisiifolia* and *Bidens pilosa*. *Mycorrhiza* 28, 703–715. doi: 10.1007/s00572-018-0866-4

Zhao, L., Meng, L., and Li, B. (2007). Effects of fertilization on the relative competitive ability of *Eupatorium adenophorum* and *Lolium perenne* at their seedling stage. *Chin. J. Ecol.* 26, 1743–1747. doi: 10.13292/j.1000-4890.2007

Zhou, J. C., Chai, X. F., Zhang, L., George, T. S., Wang, F., and Feng, G. (2020). Different arbuscular mycorrhizal fungi cocolonizing on a single plant root system recruit distinct microbiomes. *mSystems* 5:e00929. doi: 10.1128/mSystems.00929-20

Frontiers in Microbiology

Explores the habitable world and the potential of microbial life

The largest and most cited microbiology journal which advances our understanding of the role microbes play in addressing global challenges such as healthcare, food security, and climate change.

Discover the latest Research Topics

See more →

Frontiers

Avenue du Tribunal-Fédéral 34
1005 Lausanne, Switzerland
frontiersin.org

Contact us

+41 (0)21 510 17 00
frontiersin.org/about/contact